

ORNL-1318  
Progress

80A

MARTIN MARIETTA ENERGY SYSTEMS LIBRARIES



3 4456 0353047 2

LABORATORY RECORDS  
1954



HOMOGENEOUS REACTOR PROJECT

QUARTERLY PROGRESS REPORT

FOR PERIOD ENDING JULY 1, 1952

CENTRAL RESEARCH LIBRARY  
DOCUMENT COLLECTION

**LIBRARY LOAN COPY**

**DO NOT TRANSFER TO ANOTHER PERSON**

If you wish someone else to see this document,  
send in name with document and the library will  
arrange a loan.



OAK RIDGE NATIONAL LABORATORY  
OPERATED BY  
CARBIDE AND CARBON CHEMICALS COMPANY  
A DIVISION OF UNION CARBIDE AND CARBON CORPORATION



POST OFFICE BOX P  
OAK RIDGE, TENNESSEE

[REDACTED]

**DECLASSIFIED**

ORNL-1318

This document consists of 184 pages.

CLASSIFICATION CHANGED TO:

BY A

BY:

BY DE: TID-1148  
G. Merman 7/22/57

Copy 80 of 195 copies. Series A.

Contract No. W-7405-eng-26

**HOMOGENEOUS REACTOR PROJECT**  
**QUARTERLY PROGRESS REPORT**  
**for Period Ending July 1, 1952**

J. A. Swartout, Acting Project Director  
C. H. Secoy, Project Chemist  
C. E. Winters, Project Engineer

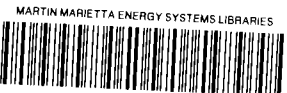
Compiled by W. E. Thompson

DATE ISSUED

SEP 2 1952

**OAK RIDGE NATIONAL LABORATORY**  
operated by  
**CARBIDE AND CARBON CHEMICALS COMPANY**  
A Division of Union Carbide and Carbon Corporation  
Post Office Box P  
Oak Ridge, Tennessee

[REDACTED]



3 4456 0353047 2

[REDACTED]

INTERNAL DISTRIBUTION

- G. T. Felbeck (C&CCC)
- 2-3. Chemistry Library
  4. Physics Library
  5. Health Physics Library
  6. Metallurgy Library
  - 7-8. Reactor Experimental Engineering Library
  - 9-10. Training School Library
  - 11-20. Central Files
  21. R. E. Aven
  22. S. E. Beall
  23. E. P. Blizard
  24. E. G. Bohlmann
  25. G. E. Boyd
  26. W. M. Breazeale
  27. R. C. Briant
  28. R. B. Briggs
  29. F. R. Bruce
  30. J. H. Buck
  31. A. D. Callihan
  32. D. W. Cardwell
  33. C. E. Center
  34. G. H. Clewett
  35. D. D. Cowen
  36. J. L. English
  37. D. E. Ferguson
  38. W. R. Gall
  39. J. P. Gill
  40. R. J. Goldstein
  41. C. B. Graham
  42. J. C. Griess
  43. J. H. Gross
  44. C. S. Harrill
  45. P. N. Haubenrich
  46. C. G. Heisig
  47. A. Hollaender
  48. A. S. Householder
  49. W. B. Humes (K-25)
  50. G. R. Jenkins (C&CCC, South Charleston)
  51. C. P. Keim
  52. M. T. Kelley
  53. E. M. King
  54. A. S. Kitzes
  55. J. A. Lane
  56. C. E. Larson
  57. L. B. Emlet (Y-12)
  58. S. C. Lind
  59. R. S. Livingston
  60. R. N. Lyon
  61. W. L. Marshall
  62. H. F. McDuffie
  63. J. R. McWherter
  64. E. C. Miller
  65. K. Z. Morgan
  66. E. J. Murphy
  67. P. M. Reyling
  68. H. C. Savage
  69. C. H. Secoy
  70. C. L. Segaser
  71. E. D. Shipley
  72. A. H. Snell
  73. F. L. Steahly
  74. C. D. Stano
  75. J. A. Swainout
  76. E. H. Taylor
  77. W. E. Thompson
  78. M. Tobias
  79. S. Visner
  80. A. M. Weinberg
  81. T. A. Welton
  82. E. P. Wigner (consultant)
  83. C. E. Winters
  84. F. C. VonderLage
  85. F. C. Zapp
  86. P. C. Zmola

[REDACTED]

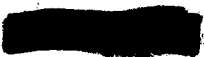
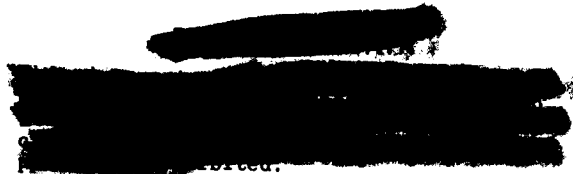
EXTERNAL DISTRIBUTION

- 87-97. Argonne National Laboratory
- Armed Forces Special Weapons Project (Sandia)
- 99-106. Atomic Energy Commission, Washington
- 107. Battelle Memorial Institute
- 108-110. Brookhaven National Laboratory
- 111. Bureau of Ships
- 112-113. California Research and Development Company
- 114-119. Carbide and Carbon Chemicals Company (Y-12 Area)
- 120. Chicago Patent Group
- 121. Chief of Naval Research
- 122-126. duPont Company
- 127-129. General Electric Company (ANPP)
- 130-133. General Electric Company, Richland
- 134. Hanford Operations Office
- 135-141. Idaho Operations Office
- 142. Iowa State College
- 143-146. Knolls Atomic Power Laboratory
- 147-149. Los Alamos
- 150. Massachusetts Institute of Technology (Kaufmann)
- 151. Massachusetts Institute of Technology (Benedict)
- 152-154. Mound Laboratory
- 155. National Advisory Committee for Aeronautics, Cleveland
- 156. National Advisory Committee for Aeronautics, Washington
- 157-158. New York Operations Office
- 159-160. North American Aviation, Inc.
- 161. Nuclear Development Associates (NDA)
- 162. Patent Branch, Washington
- 163. Rand Corporation
- 164. Savannah River Operations Office, Augusta
- 165. Savannah River Operations Office, Wilmington
- 166-167. University of California Radiation Laboratory
- 168. Vitro Corporation of America
- 169-172. Westinghouse Electric Corporation
- 173-180. Wright Air Development Center
- 181-195. Technical Information Service, Oak Ridge



Reports previously issued in this series are as follows:

ORNL-527	Date Issued, December 28, 1949
ORNL-630	Period Ending February 28, 1950
ORNL-730	Feasibility Report - Date Issued, July 6, 1950
ORNL-826	Period Ending August 31, 1950
ORNL-925	Period Ending November 30, 1950
ORNL-990	Period Ending February 28, 1951
ORNL-1057	Period Ending May 15, 1951
ORNL-1121	Period Ending August 15, 1951
ORNL-1221	Period Ending November 15, 1951
ORNL-1280	Period Ending March 15, 1952



[REDACTED]

## SUMMARY

### PART I

#### HOMOGENEOUS REACTOR EXPERIMENT

##### Status of the HRE

In March, subcritical testing of the HRE with a natural uranium fuel solution at 250°C and 1000 psi showed that the reactor system, together with its auxiliary components, was performing according to expectations except for minor leaks that developed in a section of the high-pressure piping and in the pulsafeeder pump diaphragm. The causes for the leaks were remedied by design changes.

After the tests were completed, the system was dismantled and inspected with particular attention to corrosion. No evidence of unusual corrosion was found, but minor mechanical failures were discovered. After the failures were repaired, the system was re-assembled with the high-pressure portion isolated (except for an emergency fuel dump line) so that critical experiments could be performed in the simplest possible system.

After a final test of the system showed no leaks or other failures, 1418 lb of D<sub>2</sub>O was added to the reflector system and enriched uranium to the fuel system. On April 15, 1952 criticality was reached at 30°C with the D<sub>2</sub>O reflector full, the shim

and safety rods out, the control rod one-third withdrawn, and with a fuel concentration of 24.9 g of U<sup>235</sup> per kilogram of H<sub>2</sub>O. The concentration that had been calculated for criticality under these conditions was 25.1 g of U<sup>235</sup> per kilogram of H<sub>2</sub>O.

During the low-power (< 10 milliwatts), low-temperature, critical experiments the following values were obtained for the effectiveness of components of the control system at temperatures between 30 and 105°C:

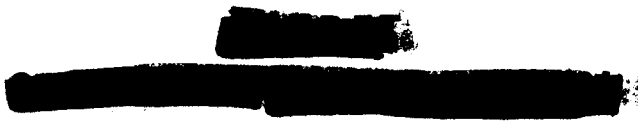
Control, shim, and safety plates	1.4% $k_{eff}$ at 30°C (calculated value 2.6%)
Reflector effectiveness	6.6% $k_{eff}$ in going from full to empty
Temperature coefficient	$4.1 \times 10^{-4}$ $k_{eff}/^{\circ}\text{C}$ at 30°C $5.4 \times 10^{-4}$ $k_{eff}/^{\circ}\text{C}$ at 100°C

The low-temperature experiments were completed on May 22, 1952, and the low-pressure system was then reconnected in preparation for experiments at higher temperatures. A multiplication experiment performed on the dump tanks showed no measurable multiplication with the entire fuel charge (4.5 kg of U<sup>235</sup>) in the dump tanks.

At the end of June, low-power, high-temperature experiments were under

[REDACTED]

[REDACTED]



way. It has been determined that operation of the fuel pulsafeeder pump, addition of oxygen, and pressurization with steam do not influence criticality, individually or collectively.

#### Engineering Studies of Components

Four pulsafeeder pump diaphragm leaks caused by metal chips under the diaphragm have led to the design and fabrication of new pump heads that incorporate strainers to exclude the damaging particles. The new pump head is assembled by a special technique that gives a stronger mechanical seal on the edges of the diaphragm by weld shrinkage. The mechanical seal with a seal weld to back it up appears to be a promising, leak-tight arrangement. Additional improvements in pump performance have been obtained by shortening the hydraulic lines in the pulsafeeder system.

Alternate types of fuel feed pumps to replace the pulsafeeder in subsequent reactor systems are being studied. A multistage, centrifugal pump and a piston type of pump have been selected as the most promising alternatives. The major problems associated with pumps of these types are leakage and maintenance, both of which must be essentially eliminated if the pumps are to be attractive for reactor use.

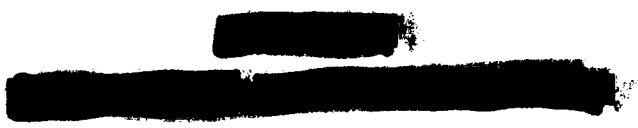
#### HRE Design

With the completion of the design of apparatus for withdrawing a sample of fuel solution from the HRE system and for handling the radioactive solution in the chemistry laboratory during analysis, the final design of the HRE is complete. A design manual has been written in rough-draft form and should be finished during the next quarter.

With the exception of the top shielding plug and a satisfactory isolation valve, the fuel sampling and handling apparatus has been fabricated and found to perform satisfactorily. Equipment for handling the samples in the chemistry laboratory is being fabricated. Improved high-pressure valves that will withstand the 1000-psi pressure drop and the corrosive fuel solution are being tested.

#### Controls and Instrumentation

Several refinements have been made in the HRE instrumentation to improve the operating characteristics of the controls. A new coaxial valve for regulating oxygen flow into the reactor fuel system has been developed and tested with satisfactory results. In the development of a means for measuring concentration of uranium in



[REDACTED]

the fuel solution, emphasis is now being placed on a spectrophotometric method. The main problem associated with this method is that of finding a material for the cell windows so that they do not corrode, change characteristics because of radiation, or break under pressure. To date, synthetic sapphires and spinels are promising materials.

### Corrosion

*Experimental Corrosion Studies.* An effect of oxygen pressure on the corrosion of type 347 stainless steel by uranyl sulfate solution containing 300 g of uranium per liter has been observed. Corrosion rates were lower by a factor of 2 at 50-psi oxygen pressure than those observed at 100 psi and higher pressures. A study of the effectiveness of molybdenum as a corrosion inhibitor indicated that it did not help appreciably. Corrosion rates as a function of pH were studied by using solutions containing uranium trioxide or sulfuric acid in addition to the uranyl sulfate. The data indicate that corrosion is lowest at the pH of stoichiometric uranyl sulfate and suggest that the decrease in acidity resulting from the addition of uranium trioxide will not decrease corrosion as anticipated.

*Dynamic Corrosion and Solution Stability.* Emphasis during this quarter has been placed on finding a

combination of fuel solution, container material, and operating conditions suitable for reliable service over long periods. The addition of copper (6.4 g of  $\text{CuSO}_4$  per liter), which might be desirable to give a homogeneous, hydrogen-oxygen recombination catalyst, apparently increases the rate of attack of type 347 stainless steel uranyl sulfate solution containing 40 g of uranium per liter at  $250^\circ\text{C}$ . The addition of uranium trioxide to high-concentration uranyl sulfate solutions as a means of decreasing hydrogen ion concentration gave no significant improvement in corrosion rates and confirmed the indications in the static tests. In at least two cases (uranyl sulfate solutions containing 5 and 40 g of uranium per liter) a small precipitate of uranium trioxide was observed after operation at  $250^\circ\text{C}$  even though none had been added to the loops.

The severity of erosion-assisted attack at sharp corners and in other regions of high turbulence has been demonstrated in several loops in which the development of leaks or of badly corroded local areas has been experienced. The effects of velocity and turbulence on this type of attack are being studied in two loops containing crosses, tees, angles, and bends of various radii, all in 1/2-, 1-, and 1 1/2-in. pipe sizes.

Corrosion tests of various types of stainless steel have been carried

[REDACTED]

contents

[REDACTED]

[REDACTED]

out in the 100-gpm loops by using small, pin samples. These tests indicate that at 250°C in uranyl sulfate solutions containing from 5 to 300 g of uranium per liter, type 321 stainless steel is attacked least, although types 347 and 316 stainless steel are not appreciably poorer except in the presence of copper. At 100 and 150°C in the same solution, type 309 columbium-stabilized stainless steel is superior to types 347 and 304 stainless steel, which are only slightly more susceptible to attack.

Titanium continues to show excellent corrosion resistance under all conditions to which it has been subjected. Parts for a complete loop of titanium are now being assembled; a titanium impeller for a Westinghouse Model 100A pump is being fabricated. A loop containing a section of titanium pipe and several titanium inserts is being fabricated.

During this quarter three pump failures have occurred that have been attributed to stress corrosion of the Inconel can around the rotor. Type 347 stainless steel cans will be substituted for the Inconel cans even though this will reduce the electrical efficiency of the pump. It has been shown that a wrought, stainless steel impeller is superior, corrosionwise, to one of cast stainless steel.

*Static Corrosion Studies.* In the study of the effect of oxygen and

uranyl sulfate concentrations on corrosion, the final corrosion rates determined by defilmed weight losses and dissolved nickel contents in uranyl sulfate containing 40, 100, and 300 g of uranium per liter with 125 to 3700 ppm of dissolved oxygen were between 0.15 and 0.45 mpy after 10.5 to 11 weeks of exposure in static bombs at 250°C. An increase in corrosion rate with increased oxygen concentration was noted in uranyl sulfate solutions containing 100 g of uranium per liter but not in solutions containing 300 g of uranium per liter.

Preconditioning of stainless steel by exposure to dilute uranyl sulfate at 250°C prior to exposure to more concentrated solutions has been found to give a slight reduction in corrosion rates, but the effect is so minor that no further investigation is planned. A study of the effectiveness of pre-treating stainless steel with dry, oxygen gas at 250°C gave very encouraging results for producing thin, adherent surface films and for reducing corrosion rates when samples were subsequently exposed to uranyl sulfate at 250°C. This study is being continued.

**Radiation Stability**

Long-term irradiation tests of uranyl sulfate solutions contained in chromate-pretreated type 347 stainless steel are now in their twelfth week of

[REDACTED]

[REDACTED]

[REDACTED]

[REDACTED]

exposure in the LITR at an average flux of  $3.5 \times 10^{12}$ , without solution failure. Comparisons of oxygen consumption in and out of radiation suggest that radiation may increase the corrosion rate.

The decomposition of hydrogen peroxide in various samples of uranyl sulfate solutions has been studied from room temperature to 100°C. Large differences among the observed first-order reaction rate constants for decomposition are attributed to small amounts of catalytically active impurities present in the solutions. The effect of peroxide concentration upon the formation and precipitation of uranium peroxide has been examined, and attempts have been made to determine the maximum concentration of peroxide that can be tolerated without precipitation of uranium peroxide. Consideration of the decomposition rate and the tolerable concentration leads to predictions of allowable power densities for reactor operation. For example, based on the characteristics of un-enriched fuel taken from the HRE after operation at 250°C, it is conservatively predicted that the HRE can be run at a total power of at least 41 kw at a temperature of 100°C without precipitation of uranium peroxide.

## PART II

### BOILING REACTOR AND SLURRY STUDIES

#### Boiling Reactor Research

Calculations of the decrease in boiling reactor fuel density as a

function of power level have been extended. Steam separators to discourage the recirculation of bubbles that have reached the top of the liquid are being studied, and they appear promising for boiling reactor application.

Nuclear calculations of critical mass, control rod kinetics, stability of the reactor, and the buildup of fission products in the proposed Teapot boiling reactor experiment have been completed.

#### Slurry Fuel Studies

*Chemical and Engineering Studies.* Although the rod, platelet, and bipyramid crystal forms of uranium trioxide appear to be stable indefinitely upon standing or with mild agitation at 250°C, mechanically broken particles, after digestion at 250°C, form platelets. Therefore it appears likely that the uranium trioxide present in an aqueous reactor slurry fuel would be in the platelet crystal form.

A method of preparing uranium trioxide from uranyl acetate was studied and found to have no significant advantages over the uranyl nitrate, peroxide precipitation method now used.

Data on crystal growth indicate that although initial growth of small uranium trioxide particles at 250°C is rapid, a type of equilibrium is soon reached, and the growth rates become much slower. The "stable" particle sizes for rods and platelets at

[REDACTED]

[REDACTED]

[REDACTED]

[REDACTED]

equilibrium are 3.9 and 7.8  $\mu$  (equivalent spherical diameter), respectively.

In-reactor tests of uranium trioxide slurry indicate that caking and corrosion may be increased by radiation effects. Some reduction of uranium(VI) and an increase in uranium solubility were observed during the experiments. Further study of the factors contributing to caking and corrosion is planned.

A laboratory test assembly for observing the boiling, foaming, caking, and heat transfer properties of slurries has been set up and placed in operation. The experimental slurry boiler installation has a 4-kw heater and is designed to operate at 250°C and 600-psi pressure.

*Slurry Pumping Studies.* A slurry containing 78 g of uranium per liter as  $UO_3 \cdot H_2O$  has been circulated in a 100-gpm, type 347 stainless steel loop for 100 hr at 250°C. No visible evidence of corrosion or erosion was found after this period. The uranium trioxide particles, which were originally rod shaped, had broken down into nearly spherical particles, and although these particles circulated through the pump bearings, no evidence of bearing wear was observed.

### PART III

## GENERAL HOMOGENEOUS REACTOR STUDIES

### ISHR Design

Conceptual design of an intermediate-scale homogeneous reactor is proceeding upon the bases that the fuel may be either solution or slurry, the operating temperature may be 250°C or some lower temperature, the power level will be about 50 megawatts, the core diameter will be 6 ft, and the circulation rate variable will be in the range of 5,000 to possibly 20,000 gpm. A flowsheet that has been developed for the ISHR is similar in many respects to the HRE flowsheet, but it differs in that the decomposition gases are separated in an external separator rather than in the core and are recombined at high pressure. The main circulating system consists of the reactor vessel, an external, centrifugal, gas separator, a shell-and-tube heat exchanger, and a circulating pump. It is planned to duplicate, where possible, the equipment that might be used in a full-scale reactor. Designs for pumps and heat exchangers are being developed by manufacturers. The core vessel and gas separators have been studied, and a preliminary arrangement for the high-pressure recombiner has been worked out.

[REDACTED]

[REDACTED]

[REDACTED]



**Engineering Studies of Components**

*4000-gpm Pump Test Loop.* Delivery of all material for the loop is anticipated by November 1952.

*HRP Main Circulating Pumps.* The Allis Chalmers Mfg. Co. is now preparing the final design of a 20,000-gpm, totally enclosed, canned-rotor pump. A contract is being negotiated with the Worthington Corporation for design of a 20,000-gpm centrifugal pump that has a pressure breakdown on the shaft followed by a low-pressure mechanical seal to enable a standard electric motor to be used. A tentative proposal for the Byron Jackson Company to design a high-pressure shaft seal that can be used on a conventional type of pump is being considered.

*Fuel Feed Pump Development.* The use of multistage, centrifugal pumps to supply about 10 gpm against a 1000-psi head is being considered. Tentative service requirements and design criteria have been specified, and pump manufacturers have been contacted with regard to design, development, and fabrication.

*Isolation Valves.* Negotiations with the Crane Co. for a predesign study of 20-in. isolation valves have been started. The purpose of the study is to establish fundamental design concepts and feasibility.

*Large Heat Exchangers.* The Lummus Co. has completed the predesign of a

heat exchanger to remove 200 megawatts of heat from 20,000 gpm of reactor fuel. The design appears feasible and within the limits of industrial practice.

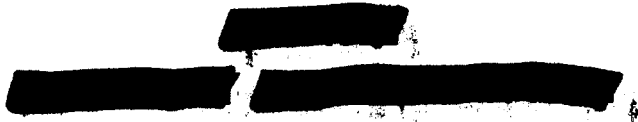
*Core Development Studies.* The study of flow distribution and pressure drop in various types of core configurations has made use of approximately 12-in. core models to investigate rotating and straight-through flow. A larger model with an 8-ft sphere and 50,000-gpm flow rates is under construction. Mathematical relationships for computing velocities and pressure drops have been developed and are being tested in the hope of finding a method of extrapolating data from the small models to apply to large-scale reactor cores.

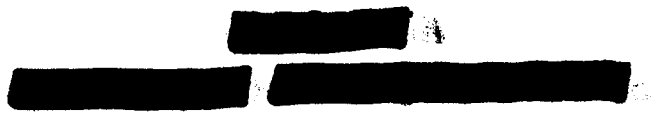
**Fundamental Radiation Chemistry Studies**

Studies of gas production from fissioning solutions have been extended to cover uranyl nitrate and uranium(IV) sulfate.

Studies of the recombination of hydrogen and oxygen have been extended to include heterogeneous catalysts of the platinum group. Such catalysts offer some promise for use at temperatures of 100 to 150°C.

Active consideration is being given to the development of small-scale dynamic corrosion tests that could be used ultimately in experimental holes in the LITR and the X-10 graphite





reactor to provide rapid surveys of the effects of changing environmental conditions.

### Solution Chemistry

A study of the effects of radiation on the valence state of plutonium has shown that the tendency of plutonium(III) and plutonium(VI) to return to plutonium(IV) is greatly enhanced by radiation.

Measurements of the conductivity of uranyl sulfate solutions are being extended to solutions at 200 and 250°C. A study of the effect of uranium trioxide on the conductivity of uranyl sulfate solutions indicates that, since a U-to-SO<sub>4</sub> ratio of 1.2 gives little difference in conductivity, the corrosiveness of uranyl sulfate solutions containing uranium trioxide should change little.

Vapor pressures of saturated uranyl sulfate solutions have been determined between 50 and 100°C.

Determinations of the solubilities of fission products in uranyl sulfate solutions indicate that most fission products are about an order of magnitude more soluble in uranyl sulfate than in water. Data are reported for silver sulfate and barium sulfate. The solubility of uranium trioxide in

uranyl sulfate solutions at 250°C has also been determined. The effect of uranium trioxide on the two-liquid phase transition temperatures of uranyl sulfate solutions has been studied; uranium trioxide reduces the temperature at which the transition occurs.

Further studies of the use of the Ag,Ag<sub>2</sub>SO<sub>4</sub> electrode as a high-temperature reference electrode for measuring the potential of the film on stainless steel in uranyl sulfate solutions at 250°C show the electrode to be satisfactory and quite sensitive.

### Static Corrosion Tests of Alternate Systems

*Corrosion of Titanium in Uranyl Sulfate Solutions.* The corrosion rates of titanium samples exposed to uranyl sulfate solutions containing 40 and 300 g of uranium per liter in static bombs at 250°C are uniformly low, that is, considerably less than 0.05 mpy.

*Uranyl Fluoride Corrosion Studies.* Investigations on the effects of oxygen and uranium concentrations on the corrosion of type 347 stainless steel by uranyl fluoride at 250°C have shown that the corrosion rates are strongly affected by dissolved oxygen concentration and to a lesser degree by uranium concentration.



[REDACTED]

### Metallurgy

A study of methods and techniques for the assembly of a titanium pump impeller led to the conclusion that either welded or riveted fastenings would be acceptable, with riveting being preferred. A program of study on the properties of titanium has been established. The major fields of interest at present are: transition temperature studies, hydrogen embrittlement, effects of reactor solutions and conditions on impact specimens, and effects of radiation on impact specimens. Currently, effort is being devoted to the preparation of iodide-titanium impact specimens.

### Chemical Processing

*Plutonium Chemistry.* Partial pressures of oxygen above about 40 psi have been shown to stabilize plutonium in the hexavalent state. At 200 psi the ratio of plutonium(VI) to plutonium(IV) at various plutonium concentrations was always about 33:1 after 48 hr of heating. The solubility of plutonium(IV) in 1.0 M uranyl sulfate at 100°C was found to be about 0.01 mg/ml, compared with 0.003 mg/ml at 250°C. Based upon laboratory

tests, the amount of plutonium that would be adsorbed on a 15-ft-dia spherical reactor core vessel of stainless steel was calculated to be 175 grams.

*Solvent Extraction.* The behavior of neptunium in various solvent extraction processes has been studied. It appears that neptunium(V) is the most stable form, and studies of its behavior in the Purex process have been started. Preliminary investigations of the effects of radiation on the extraction processes have also been started.

*Economic Comparison of UF<sub>6</sub> Distillation and TBP Extraction for Processing Uranyl Sulfate Fuel.* The results of an economic study indicate that UF<sub>6</sub> distillation compares favorably with TBP extraction as a method of decontaminating uranium from a uranyl sulfate reactor fuel. The saving indicated for dry fluoride processing is about one dollar per gram of plutonium produced. However, these conclusions are based on a comparatively untested, dry-fluoride flowsheet and are valid only insofar as the assumptions made in preparing the flowsheet are realistic.

[REDACTED]

[REDACTED]

1. The first part of the document discusses the importance of maintaining accurate records of all transactions.

2. The second part of the document discusses the importance of maintaining accurate records of all transactions.

3. The third part of the document discusses the importance of maintaining accurate records of all transactions.

[REDACTED]

## TABLE OF CONTENTS

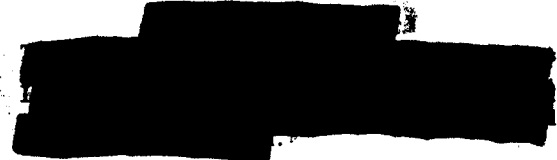
	PAGE
PART I. HOMOGENEOUS REACTOR EXPERIMENT	1
STATUS OF THE HRE	3
Initial Critical Experiment	4
Calibration of Rods	4
Calibration of Reflector Level	4
Pressure Coefficient of Reactivity at 25°C	5
Temperature Coefficient of Reactivity	5
Inhour Curves at 25°C	6
Present Status	6
Possible Operation at Temperatures Below 150°C	9
 ENGINEERING STUDIES OF COMPONENTS	 9
Pulsafeeder Pump Development	9
Mechanical design	9
Effect of fluid inertia on the pump suction	11
Positive-Displacement Pump Development	12
 HRE DESIGN	 13
Fuel Solution Sampling Apparatus	13
Fuel Sampler Installation in the Chemistry Laboratory	17
Operation of HRE at 100°C	18
 CONTROLS AND INSTRUMENTATION	 19
Process Instrumentation	19
Concentration Measurement	20
 CORROSION	 22
Experimental Corrosion Studies	22
Effect of oxygen pressure on the attack of type 347 stainless steel by uranyl sulfate and sulfuric acid	23

Effect of different acid solutions on the attack of type 347 stainless steel	25
Effectiveness of molybdenum as an inhibitor	30
Discussion	33
Dynamic Corrosion and Solution Stability	36
Solution variables	36
Flow tests	38
Materials tests	39
Westinghouse Model 100A pump	40
Static Corrosion Studies	41
Uranyl sulfate corrosion studies	41
Reflector corrosion studies	56
<b>RADIATION STABILITY</b>	<b>56</b>
Long-Term Irradiations at High Temperature and High Flux	56
Solution stability	57
Corrosion in and out of radiation	58
Kinetics of the Decomposition of Hydrogen Peroxide in Uranyl Sulfate Solutions	59
Determination of decomposition rates	59
Solubility of uranyl peroxide	61
Reactor operation as governed by peroxide decomposition	64
Plans for future work	64
<b>PART II. BOILING REACTOR AND SLURRY STUDIES</b>	<b>67</b>
<b>BOILING REACTOR RESEARCH</b>	<b>69</b>
Power Removal from a Boiling Reactor	69
Nucleation by Fission Fragments	69
Physics of the Teapot Reactor	70
Critical mass	70
Central thimble and control rod	70
Fission-product poisons	70
Inherent stability	70
Teapot Reactor Auxiliaries	75

	[REDACTED]	
	[REDACTED]	
SLURRY FUEL STUDIES		76
Chemical and Engineering Studies		76
UO <sub>3</sub> chemistry		77
Radiation chemistry		84
Slurry engineering studies		86
Slurry Pumping Studies		88
Loop test at 250°C		88
Thorium loop test at 150°C		90
Bearing tests with UO <sub>3</sub> ·H <sub>2</sub> O slurry		90
Crystal growth		90
Criticality experiments		91
	PART III. GENERAL HOMOGENEOUS REACTOR STUDIES	93
ISHR DESIGN		95
Flowsheets		95
Equipment Layouts		98
Design of Reactor Vessel		102
Pumps		105
Heat Exchanger		105
Gas Separator		107
High-Pressure Recombination System		108
Criticality Calculations for Reactor		108
Criticality Calculations for Dump Tanks		110
Power and Pressure Surges		110
ENGINEERING STUDIES OF COMPONENTS		112
4000-gpm Pump Test Loop		112
HRP Main Circulating Pumps		112
Allis-Chalmers pump development		112
Worthington Corporation pump development		113
Byron Jackson Company shaft seal development		114
Fuel Feed Pump Development		115
Isolation Valves		116
Large Heat Exchangers		118
	[REDACTED]	



Core Development Studies	118
Small-scale rotating-flow models	119
Intermediate-scale rotating-flow models	122
Small-scale straight-through models	123
Intermediate-scale straight-through models	125
Gas Separators	125
FUNDAMENTAL RADIATION CHEMISTRY STUDIES	127
Gas Production from Uranium Solutions	127
Uranyl nitrate	127
Uranous sulfate	127
Catalytic Solution Recombination of Hydrogen and Oxygen at 100°C	129
Catalysis by rhodium	130
Catalysis by ruthenium	130
Catalysis by palladium	130
Catalysis by osmium	130
Catalysis by platinum	130
Effects of Radiation on Corrosion	131
SOLUTION CHEMISTRY	133
Plutonium Solubility in $UO_3-H_3PO_4-H_2O$ Solutions	133
Influence of Radiation on the Valence of Plutonium	133
Conductivity of Uranyl Sulfate in Aqueous Solution	135
Vapor Pressures of Aqueous Uranyl Sulfate Solutions	138
Solubility of Silver Sulfate in 1.26 M and 0.126 M Uranyl Sulfate	142
Solubility of Barium Sulfate in Uranyl Sulfate Solutions at 250°C	142
Solubility of Uranium Trioxide in Uranyl Sulfate Solutions at 250°C	143
Further Studies of Two-Liquid Phase Temperatures for $UO_3-UO_2SO_4-H_2O$ Systems	147
Experiments with High-Temperature Electrodes	147
STATIC CORROSION TESTS OF ALTERNATE SYSTEMS	149
Corrosion of Titanium in Uranyl Sulfate Solutions	149
Uranyl Fluoride Corrosion Studies	149



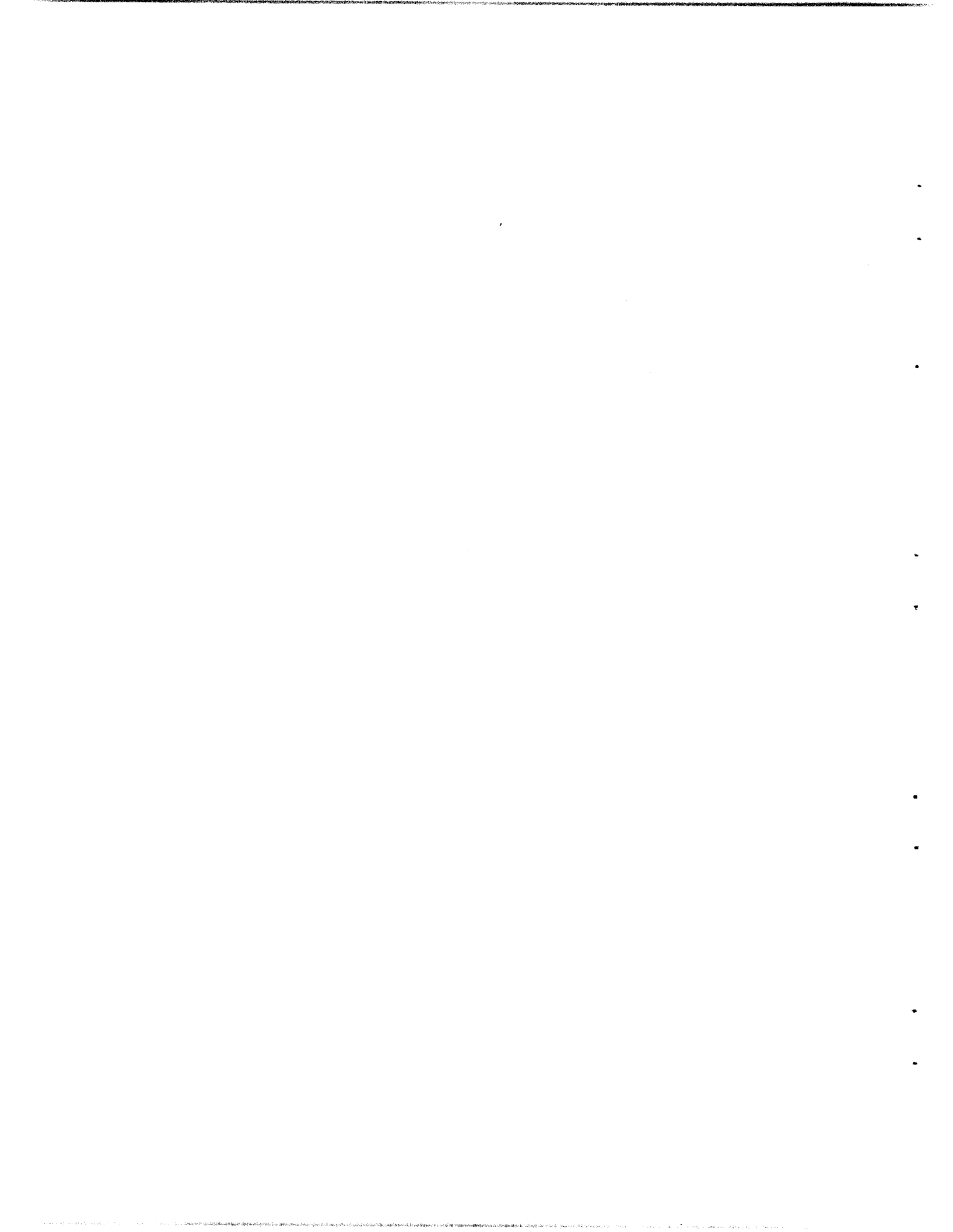


METALLURGY	153
Corrosion Metallurgy	153
Specifications and Fabrication	154
Properties of Titanium	155
Nondestructive Testing	157
Radiation Damage Studies	157
CHEMICAL PROCESSING	158
Plutonium Chemistry	158
Effect of varying oxygen pressure on the behavior of hexavalent plutonium at 250°C	158
Effect of plutonium concentration on the behavior of plutonium in 1 M uranyl sulfate solutions	158
Solubility of tetravalent plutonium in 1 M uranyl sulfate solution at 100°C	159
Adsorption of plutonium on stainless steel	159
Solvent Extraction	160
Extraction of neptunium by tributyl phosphate	161
Dibutyl butylphosphonate as an extractant for uranium from uranyl sulfate solutions	162
Radiation damage on solvent extraction	162
Economic Comparison of UF <sub>6</sub> Distillation and TBP Extraction for Processing Uranyl Sulfate Fuel	163



**Part I**

**HOMOGENEUS REACTOR EXPERIMENT**



# HRP QUARTERLY PROGRESS REPORT

## STATUS OF THE HRE

S. E. Beall, Section Chief

W. S. Brown	J. A. Ransohoff
J. J. Harriston	M. Richardson
J. W. Hill, Jr.	L. W. Thacker
S. I. Kaplan	T. H. Thomas
T. H. Mauney	S. Visner
V. K. Paré	R. Van Winkle

P. M. Wood

At the beginning of this quarter (March 15) the HRE was operating continuously at the designed conditions of 1000-psi pressure at 250°C and with a fuel solution of 30 g of natural uranium sulfate per kilogram of water so that engineering testing could be completed and the nuclear experiments started.

Two runs of nine days' duration that were made to obtain a material balance on the entire fuel system provided evidence that water and uranium balances can be made to an accuracy of  $\pm 2\%$ . Afterwards, hydrogen and oxygen gases were fed into the reactor core to simulate normal power operation in which these gases appear as decomposition products. Over an 18-hr period of continuous gas addition at flow rates from 0.1 to 15 cfm it was possible to observe the satisfactory performance of the fuel off-gas system, including the let-down heat exchanger and valve, the flame and catalytic recombiners, and the charcoal adsorption beds. However, a high-pressure piping rupture occurred because of fatigue failure in a machined reducing coupling on the fuel-oxygenation chamber. Examination showed that a slight imperfection at a sharp corner of the fitting was gradually enlarged through the wall thickness by repeated vibrational stress caused by the operation of the

pulsafeeder pump. It was also discovered at the end of the run that the inner (fuel) pulsafeeder pumping diaphragm had been punctured by very small (about 1/64 in. dia) grains of metal that may have accumulated from weld repairs or from the micro-metallic filter in the fuel inlet line. In an effort to prevent similar diaphragm failures the fuel pulsafeeder has been modified to include a filtering screen over the inlet and exit ports of the diaphragm.

Following completion of the engineering experiments on April 4, the high-pressure fuel system was dismantled and inspected with particular attention to corrosion, but no evidence of excessive corrosion was visible. The Westinghouse, Model 100A, fuel-circulating pump had a cracked rear bearing and embrittled tantalum labyrinth rings, so it was necessary to replace these parts. During this shutdown period, several valves (the fuel dump valve, the let-down valve, and the pressurizer bleed valve) that had indicated leakage past the seat were replaced by new valves with flanges to allow remote removal. Other revisions dictated by the accumulation of several months of operating experience included water cooling of the pressurizer bleed line, replacement of the fuel dump tank level indicator, modification of the 1-gph pulsafeeder

## HRP QUARTERLY PROGRESS REPORT

flow indicator, and reworking of the fuel-sampling arrangement.

The reactor piping was then re-assembled for the performance of the low-temperature nuclear experiments. In the interest of reducing the number of variables affecting reactivity, the high-pressure fuel-circulating system was isolated from the low-pressure system, except for the fuel dump line. Reactor instrumentation was also temporarily revised as necessary for the experiments. The reflector system was dried to an exit-gas dew point of  $-35^{\circ}\text{C}$  by using a vacuum pump in conjunction with heat application to low points of the system. Drying was followed by the addition of 1418 lb of heavy water on April 10, which completed all preparations so that the first critical experiment could be started on April 11.

### INITIAL CRITICAL EXPERIMENT

The initial critical experiment on the homogeneous reactor was completed on April 15, 1952, at which time the reactor was critical at  $30^{\circ}\text{C}$  and fully reflected with  $\text{D}_2\text{O}$ , the shim and safety rods were out, the control rod was one-third withdrawn, and the fuel concentration was 24.9 g of  $\text{U}^{235}$  per kilogram of  $\text{H}_2\text{O}$ . This concentration is within 1% of the predicted value of 25.1 grams. Only the high-pressure system that consisted essentially of the core, main heat exchanger, and circulating pump was used. Subsequently, additional experiments were performed on the same system between the temperatures of 20 and  $105^{\circ}\text{C}$  at power levels below 10 megawatts to evaluate the various reactivity controls.

### CALIBRATION OF RODS

The shim and control rod curves were calibrated by means of reactor period data and also by changes in fuel con-

centration. The theoretical factor used for converting concentration data to reactivity is 0.0149 units of  $k_{eff}$  for each gram of  $\text{U}^{235}$  per kilogram of  $\text{H}_2\text{O}$ . The period data were interpreted by means of an inhour curve based on a delayed-neutron normalization of 0.75% with a contribution of photoneutrons from the  $\text{D}_2\text{O}$ . As shown in Figs. 1 and 2, the agreement between the two types of data is within the experimental error. It was demonstrated that the safety plate has the same effectiveness as the shim plate. However, the total value of the control, shim, and safety plates at room temperature is only 1.4% in  $k_{eff}$  as compared with the calculated value of 2.6%. The calibration of the rods at  $100^{\circ}\text{C}$  by changes in concentration is not significantly different from that at room temperature.

### CALIBRATION OF REFLECTOR LEVEL

The effectiveness of the  $\text{D}_2\text{O}$  reflector at room temperature was evaluated from 100% full, corresponding to 12 in. above the top of the core, to a point 11 in. below the top, or 7 in. from the bottom of the core. The results are shown in Fig. 3, in

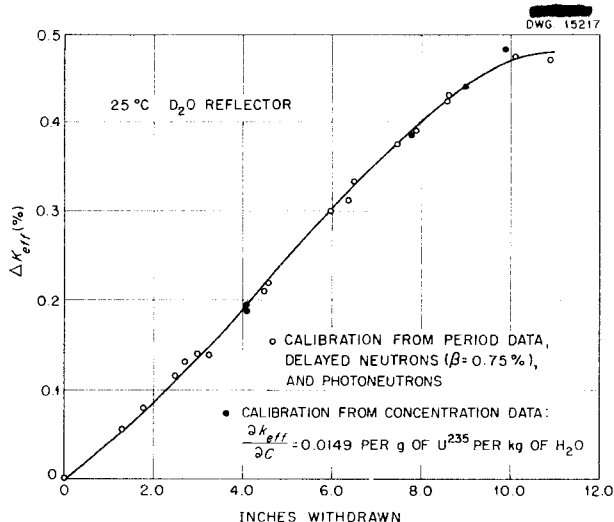
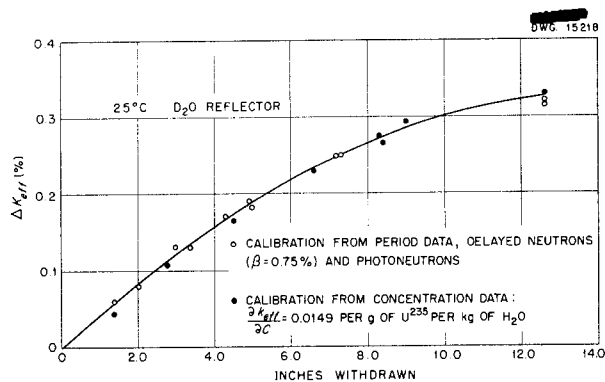


Fig. 1. HRE Shim Rod Calibration.

which it is apparent that the extrapolation of the experimental results to obtain the effectiveness of the entire reflector is in good agreement with the theoretical value of 6.6% in  $k_{eff}$ .

**PRESSURE COEFFICIENT OF REACTIVITY AT 25°C**

The experimental points in Fig. 4, obtained with the pressure balanced



**Fig. 2. HRE Control Rod Calibration.**

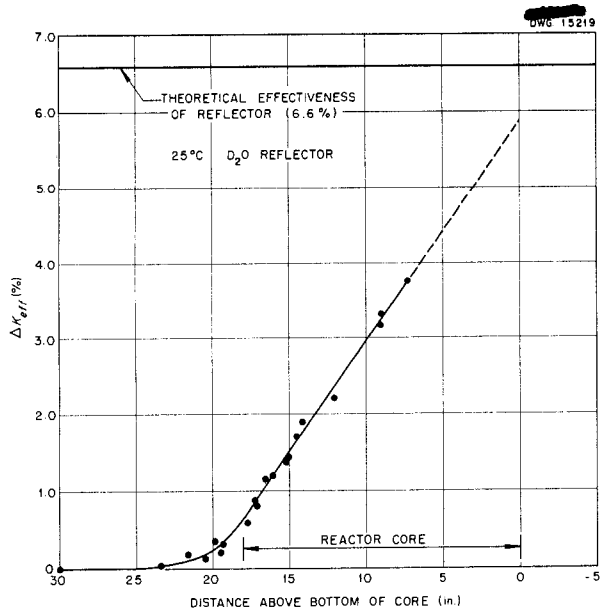


**Fig. 3. Calibration of Reflector Level for HRE.**

across the core, agree with the pressure coefficient of reactivity calculated from theory, that is, 0.16% in  $k_{eff}$  for 1000 psi. An additional 0.02% in  $k_{eff}$  is obtained from stretching the core by maintaining a pressure differential of 900 psi.

**TEMPERATURE COEFFICIENT OF REACTIVITY**

The critical concentrations at temperatures from 20 to 105°C, with and without operation of the circulating pump, are plotted in Fig. 5. At 30°C, the temperature coefficient of reactivity is  $4.1 \times 10^{-4} k_{eff}/^{\circ}\text{C}$ ,

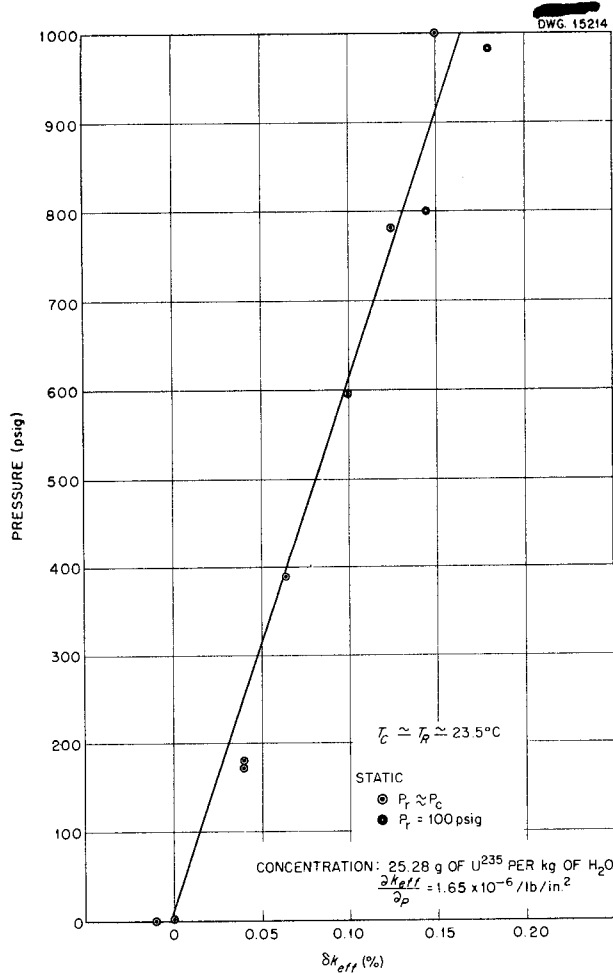


**Fig. 4. Pressure Coefficient of Reactivity for HRE.**

# HRP QUARTERLY PROGRESS REPORT

DWG. 15598R1

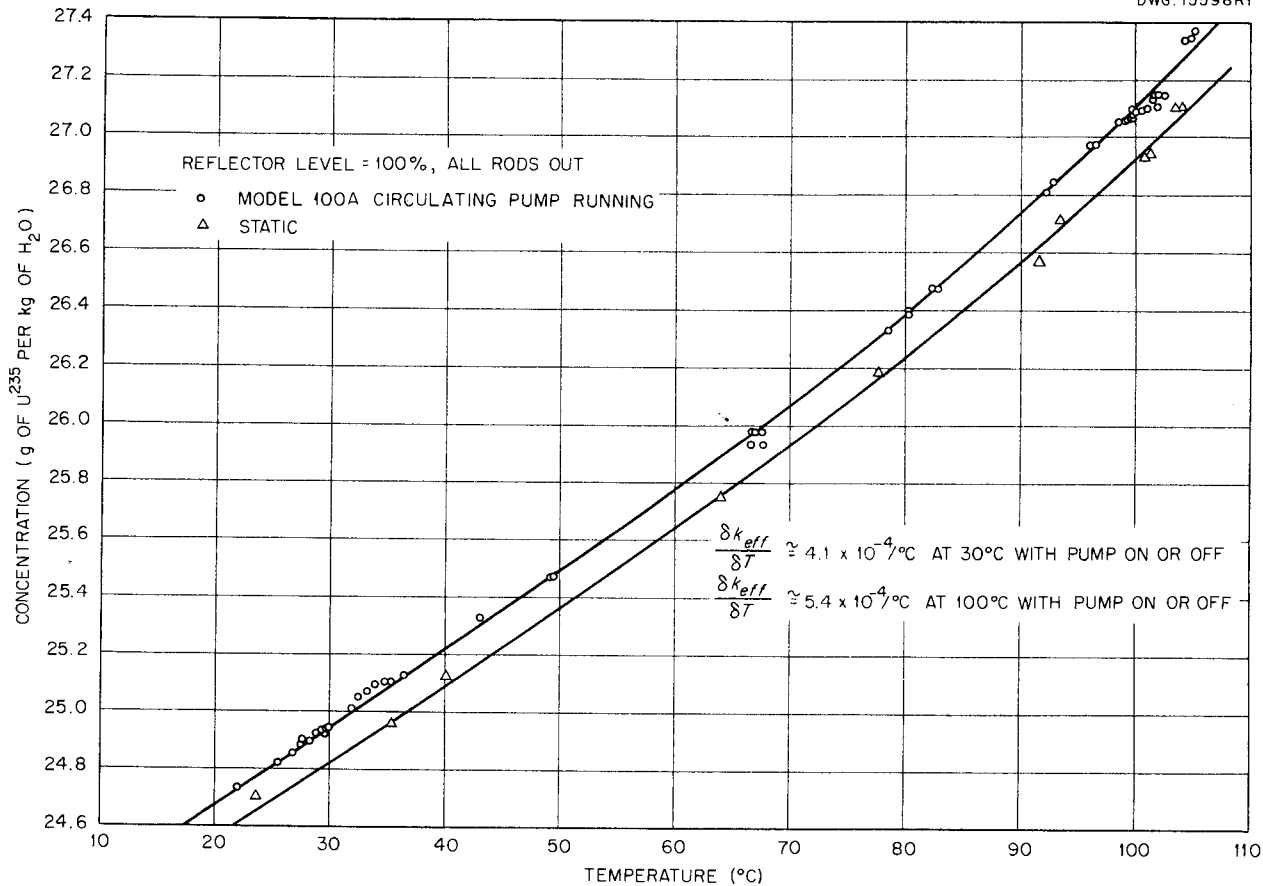


Fig. 5. Critical Concentration vs. Temperature of D<sub>2</sub>O-Reflected HRE.

as compared with a theoretical value of  $2.5 \times 10^{-4}$ . The value of the coefficient at 100°C is  $5.4 \times 10^{-4}$ , which compares favorably with a theoretical estimate of  $5.5 \times 10^{-4} k_{eff}/^\circ\text{C}$ .

## IN HOUR CURVES AT 25°C

The experimentally determined reactor periods are plotted in Fig. 6 as a function of excess reactivity for the static reactor and also for the full circulation of 120 gpm. The calculated curves based on a delayed neutron contribution of 0.75% in addition to photoneutrons from the D<sub>2</sub>O are also shown for comparison. The curve for full circulation takes into

account the loss of delayed neutrons that are emitted outside the reactor core<sup>(1)</sup> but is based on the approximations that the production of precursors is uniform throughout the core and that the value of a delayed neutron is independent of the point of emission within the core. These approximations may account for the apparent discrepancy at short periods.

## PRESENT STATUS

After the low-temperature experiments were completed on May 22, the

(1) R. E. Aven, *Delayed Neutrons and Their Reactivity Contribution to the Homogeneous Reactor*, ORNL CF-51-12-1 (Dec. 4, 1951).

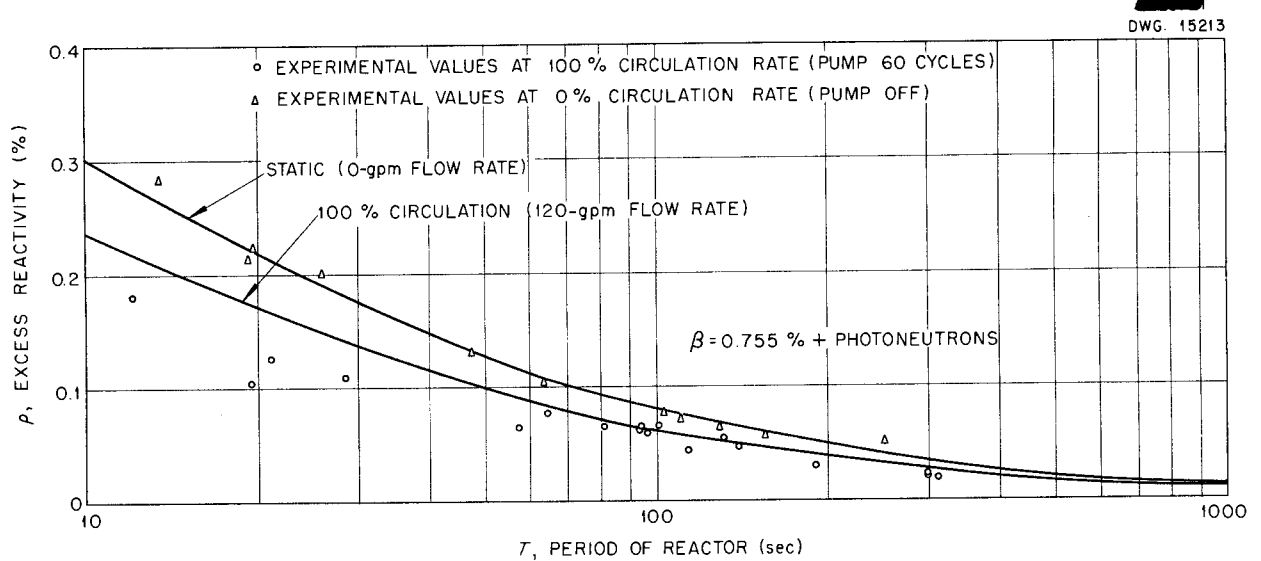


Fig. 6. Inhour Curves for the HRE.

high-pressure fuel system was re-connected to the low-pressure system, which contains the dump tanks, concentration control equipment, and off-gas system. Several temporary connections required in the instrumentation and control circuitry for operation with the low-pressure system were removed. The few remaining unfinished portions of the shield were completed so that access to the cells can now be gained only by removing the top plugs. Also, the front and rear flanges of the Westinghouse, Model 100A fuel pump were welded closed without damage to the pump.

During the shutdown a multiplication experiment was performed in the fuel dump tanks to ensure that no hazard would result from draining the entire available fuel charge of 4.5 kg of  $U^{235}$  into the dump tanks. No multiplication within the error limits of the neutron detection equipment was measurable; that is, multiplication was not greater than about 1.2.

Before continuing the nuclear experiments, the high-pressure fuel and  $D_2O$  piping was pressure tested at 1200 psi at room temperature; then the reactor was heated to  $250^\circ C$  and examined for leaks. After allowing the equipment to cool, nuts and bolts on all flanges were retightened and the temperature was raised to  $250^\circ C$  once more. No leaks were found, either visually or with the leak detector system.

With confidence that the reactor was free of leaks, experimentation was resumed and the reactor was loaded with 2.8 kg of  $U^{235}$  and about 220 liters of water. The variables associated with operation of the low-pressure fuel system, that is, fuel pulsafeder pump operation, oxygen addition, and finally pressurization with steam, were introduced one at a time. None of these factors appear to influence the criticality of the reactor. Operation for a short time near  $250^\circ C$  is planned to obtain the temperature coefficient

# HRP QUARTERLY PROGRESS REPORT

UNCLASSIFIED  
DWG. 15599A

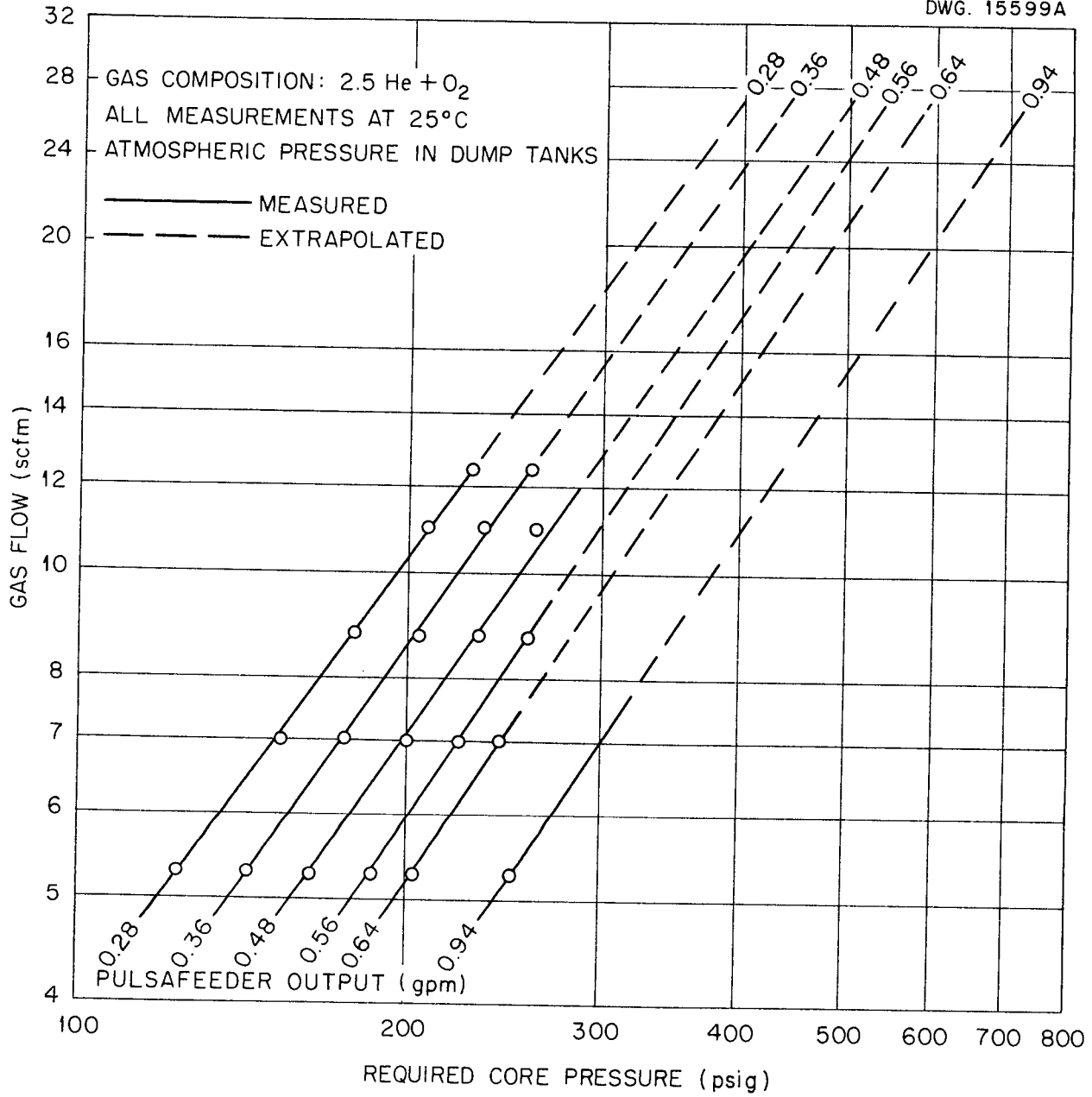


Fig. 7. Capacity of Let-down System for Gas at Reduced Core Pressures and Liquid Flows.

of reactivity and to evaluate the control mechanisms before increasing the power level for the remainder of the experimental program, as outlined in the previous quarterly report.<sup>(2)</sup>

#### POSSIBLE OPERATION AT TEMPERATURES BELOW 150°C

In view of recent corrosion data gathered in the experimental loops, it appears desirable to operate the HRE for extended periods at temperatures below 150°C. Furthermore, the pressurizer temperature has been arbitrarily limited to a maximum of 250°C, which would permit a fuel system pressure of about 500 psi. Since operation of the let-down system at one-half the designed pressure appeared questionable, it was

<sup>(2)</sup>S. Visner, V. K. Paré, and P. M. Wood, *Homogeneous Reactor Project Quarterly Progress Report for Period Ending March 15, 1952*, ORNL-1280, p. 11.

decided to test the fuel off-gas system at pressures below 500 psi. A mixture of helium and oxygen of average molecular weight equivalent to stoichiometric hydrogen and oxygen was used for the test. The data plotted in Fig. 7 are the results of gas flow measurements at several pressures and at several liquid flow rates at 25°C. Although this temperature is perhaps 75°C lower than the average temperature of the let-down gas when the core is operated at 150°C, even after correcting the volumes to the higher temperature, it appears that there should be no difficulty in handling decomposition gases at the lower pressures if the pulsafeder flow rate is kept below 1 gpm and the gas evolution does not exceed the 11.25 cfm expected at 1000 kw. These results are in fair agreement with the earlier, less accurate measurements at higher pressures and temperatures reported in the previous quarterly report.

### ENGINEERING STUDIES OF COMPONENTS

C. B. Graham, Section Chief  
J. S. Culver            C. W. Keller  
L. F. Goode            D. Toomb

#### PULSAFEEDER PUMP DEVELOPMENT

**Mechanical Design.** Four pulsafeder pump heads have failed because of leaks in the diaphragm. Examination has shown all failures to be the result of metal chips that worked their way into the head and punctured the diaphragm. Since it is practically impossible to eliminate all foreign particles from a system as complex as the HRE, strainers are now being built into the pulsafeder pump heads to exclude any particles large enough to damage the diaphragm. A section of the new design incorporating the strainers is

shown in Fig. 8. Accumulation of very small particles under the diaphragm could lead to fatigue failure, but examination of the diaphragms after periods of operation has indicated that the particles are pumped out and do not accumulate.

Two recently rebuilt heads developed leaks in the diaphragm seal weld during the final pressure test. One head that was cut apart lacked the usual evidence of pressure from the flanges bearing on the diaphragm. The initial compression of the flanges on the

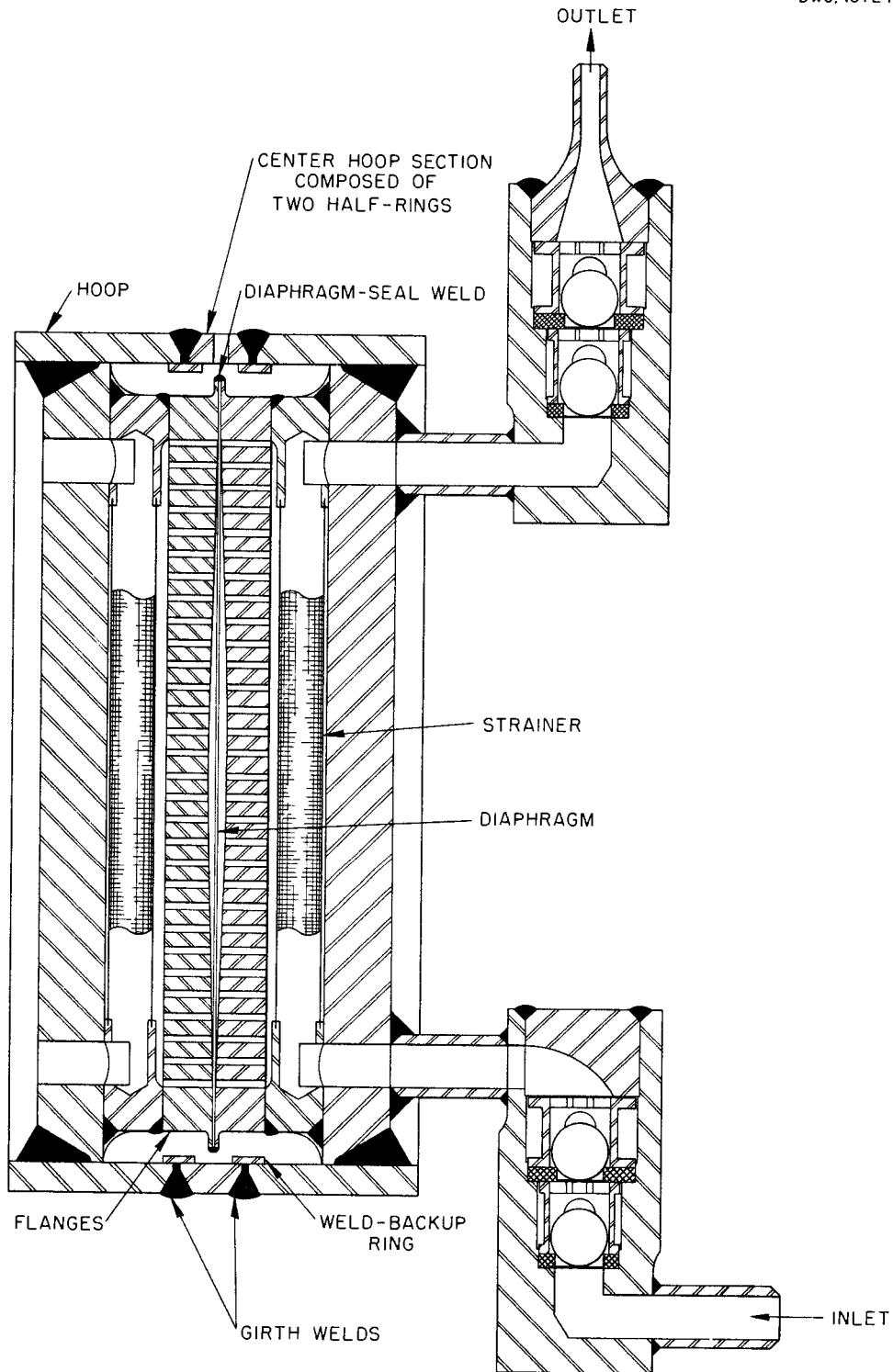


Fig. 8. Pulsafeeder Head Assembly.

diaphragm is normally obtained by heating the hoop prior to final welding so that on cooling the hoop contracts and compresses the flanges on the diaphragm and makes a seal to resist the hydrostatic pressures encountered during operation. It is essential that the flanges be compressed to prevent movement of the edge of the diaphragm and consequent breaking of the seal weld during operation.

A study showed that it is impossible to determine whether tension exists in the hoop after welding. The welding sequence employed on the pulsafeder pump head that failed left the seal weld vulnerable to shearing due to differential expansion between the flanges. In an attempt to correct the difficulty, the hoop was redesigned as shown in Fig. 8. The center section is composed of two half rings that are welded in after the seal weld is completed and tested, thus heating of the flanges during final welding is minimized and the desired tension in the hoop is provided by weld shrinkage. To demonstrate the effectiveness of the girth weld in drawing the flanges together, one of the heads with a leaking seal weld was sent to the shop and a 60-deg V groove was cut all the way through the hoop on its centerline. The groove was then filled with weld metal, and the head was pressure tested and found tight despite the fact that the seal weld leak had not been repaired.

Because of the success of this test, another head was assembled without a seal weld. The two half hoops were first welded to the two flanges and trimmed for girth welding. After inserting the diaphragm the girth weld was made. Pressure testing showed a possible leak that has not been confirmed but leaves some doubt as to the safety of omitting the seal weld if radioactive substances are to be handled.

These two experiments demonstrate that a mechanical seal can be made by proper fabrication technique.

The new fuel-pumping head for the reactor is being built with a seal weld, as shown in Fig. 8, which backs up the mechanical seal between the flanges and the diaphragm. Two other experimental pumping heads, without seal welds, are operating satisfactorily in the mockup.

**Effect of Fluid Inertia on the Pump Suction.** When the D<sub>2</sub>O pulsafeder pump on the HRE was started, it operated poorly in comparison with the fuel pump. It was noisy, had low and erratic output, and was very prone to collect air in the oil system. An analysis of the effect of inertia of the fluid in the lines during the suction stroke provided information on the problem and suggested a remedy.

At the start of the suction stroke the fluid flow in the lines between the piston and dump tanks must accelerate. The driving force for this acceleration is the difference in pressure between the dump tank and the oil in the piston less any static and friction head in the line. The oil pump is provided with a suction valve that will permit oil to flow into the system at the piston end if the pressure is reduced more than 10 in. Hg below atmospheric pressure. Because of the long lines, the high density of the fluorocarbon oil (1.8), and the relatively high acceleration requirements, the pump takes in large quantities of oil at each stroke. This reduces the D<sub>2</sub>O capacity and requires oil discharge through the relief valve at the end of each stroke. Because of the momentary subatmospheric pressure at the piston during the suction stroke, air is drawn in through the packing gland. Since the packing on the piston pump is a Chevron type of seal

## HRP QUARTERLY PROGRESS REPORT

intended for pressure use, it frequently lets air into the oil system and materially reduces output. "O" rings have been installed to eliminate air leakage.

To reduce these effects the oil pumps on both fuel and D<sub>2</sub>O systems will be moved to new positions alongside the pits where the heads are located. This change results in shorter hydraulic lines. At the same time the D<sub>2</sub>O intermediate heads will be installed in the pit to decrease the large fluorocarbon head now existing.

It is expected that a material increase in output will be achieved due to a larger volume-intake stroke and to decreased compressibility losses. These gains may allow a lower operating speed, which will further decrease acceleration in both the suction and discharge lines and result in quieter operation, longer pump life, and less critical adjustment.

### POSITIVE-DISPLACEMENT PUMP DEVELOPMENT

Effort has been expended to gain additional information on pulsafeeder pumps because the feed pump (pulsafeeder) is an essential part of the HRE and because it appears that pumps of high head and low capacity will be needed for future reactors. Although it now appears that the pump being used for the HRE will be adequate, the possibility of additional trouble remains. Studies have been made of several pumps but each seems to lack some of the desirable features of the pulsafeeder, for example, complete freedom from leaks and maintenance requirements in the radioactive regions.

A multistage centrifugal pump and a modified positive-displacement (plunger-type) pump of the triplex or

Milton Roy variety have been selected for further study.

The multistage centrifugal pump is discussed in Part III of this report under the heading "Engineering Studies of Components." A year or longer would be required for the design, construction, and testing of a pump of this type.

A plunger pump is frequently used in industrial applications of this type. However, if used for fuel or heavy water it would be necessary to overcome the problem of reducing the leakage to almost zero without the use of grease and without frequent adjustment of the seals. Leakage may be diminished by reducing the pressure drop across the seal to a minimum by allowing a small amount of the pumped fluid to leak along the plunger to a low-pressure region and then returning it to the pump by suction. Two seals with low-pressure water between them would be located between the low-pressure region and the atmosphere. The water between the seals would be maintained at a slightly higher pressure than that of the pump suction, and as a result a slight in-leakage to the pump would be maintained; any leakage to the atmosphere would be water. It would also be necessary for the materials of construction to be moderately resistant to radiation and fuel.

A number of materials and designs have been suggested for the high-pressure breakdown and seals, and considerable testing will be required to determine which are satisfactory or preferable. A triplex pump and a Milton Roy pump have been installed for testing.

Difficulty in maintaining adequate alignment of the high-pressure breakdown is anticipated if a close fitting

Stellite piston is operated against a Stellite or Graphitar cylinder wall, and it is believed that a Chevron seal may prove more satisfactory. Graphite-asbestos packings are being tested as a possibility for the outer seals. The Garlock Packing Company manufactures Chevron seals of Nylon-,

Neoprene-, and Teflon-impregnated asbestos lubricated with graphite that are reputed to operate for periods up to one year with little leakage and no attention. Several of these seals have been ordered for testing, and these may prove to be more satisfactory than the packing.

---

## HRE DESIGN

R. B. Briggs, Section Chief  
C. L. Segaser                      F. C. Zapp

With the completion of the design of an apparatus for withdrawing a sample of fuel solution from the reactor system and equipment for handling the radioactive solution in the chemistry laboratory during the analysis, the work of the design group on the HRE is considered complete. A design manual has been written in rough draft form and should be finished in the next quarter. A pictorial assembly drawing of the entire HRE facility has been made for inclusion in the design manual. The drawing is reproduced here as Fig. 9.

Figure 10 is a revised, pictorial, assembly drawing of the pressure vessel, core tank, top flange, control thimbles, pressurizer, and piping as installed in the HRE. It is essentially the same as the drawing shown in Fig. 3 of the quarterly report for the period ending May 15, 1951.<sup>(1)</sup> However, since that time the internal basket type of catalytic recombiner in the reflector vessel has been replaced by an external circulating type of high-pressure catalytic recombiner. Also, the regulating plate, formerly a comparatively narrow strip

of sheathed Boral, has been replaced by a much wider plate containing approximately eight times the area of the previous plate for more effective control.

## FUEL SOLUTION SAMPLING APPARATUS

The design of a device for extracting approximately 0.5 cc of solution from the reactor system was described in the previous report. With the exception of the top shielding plug and a satisfactory isolation valve, all the items required for installation of this device in the reactor shield have been fabricated. The isolation chamber, indexing table, and manipulator have been assembled on a wooden framework for testing. Mechanical functioning of the device has been satisfactory.

Difficulty has been experienced in obtaining satisfactory high-pressure valves for separating the sampling equipment from the reactor circulating system. No standard commercial valves satisfied all of the design and materials requirements. Kerotest diaphragm valves appeared to satisfy the design requirements but could not be obtained in the necessary materials. The major factor in favor of the Kerotest valve was its use of a

---

<sup>(1)</sup> *Homogeneous Reactor Project Quarterly Progress Report for Period Ending May 15, 1951, ORNL-1057, p. 10.*

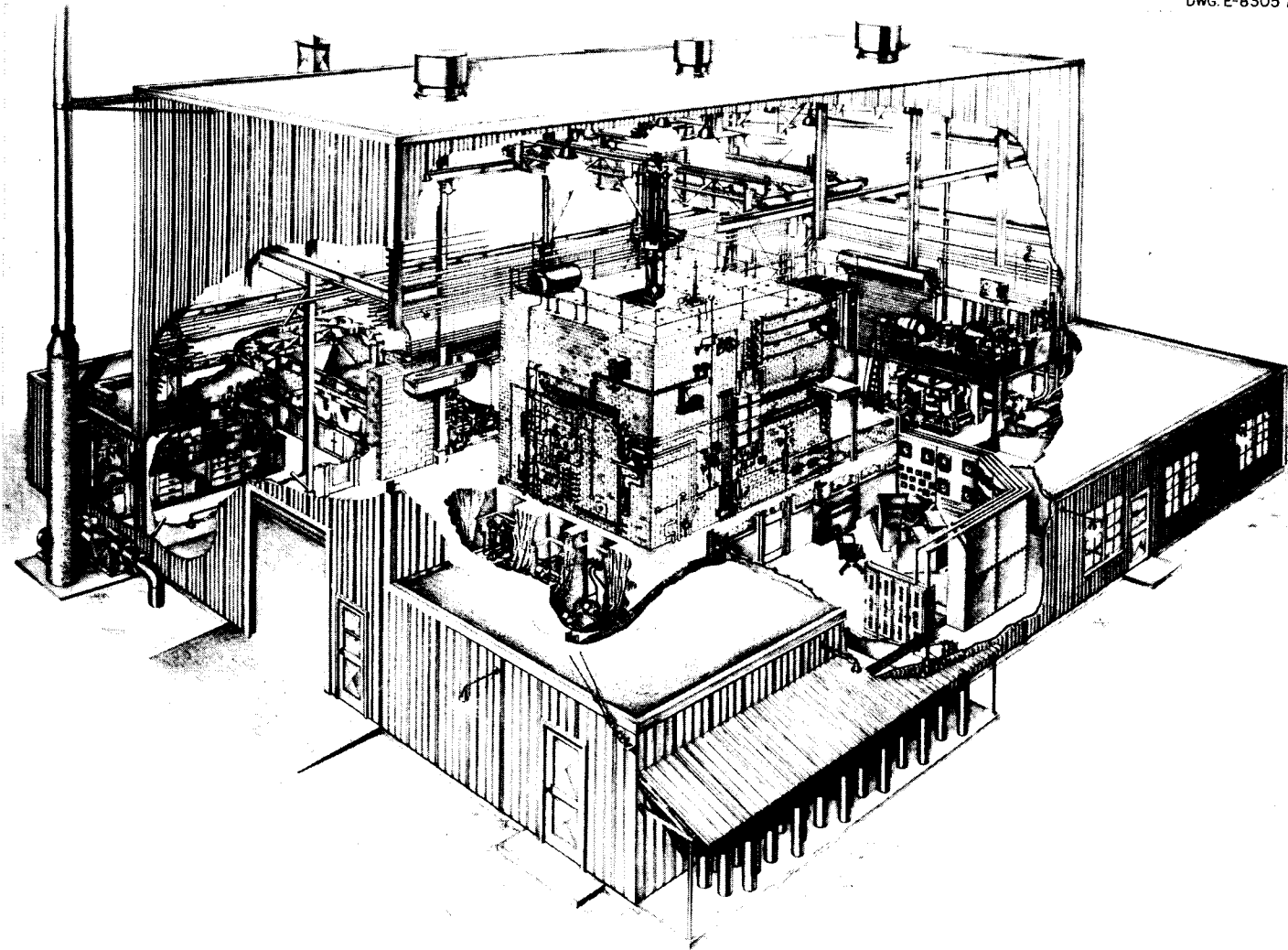


Fig. 9. The Homogeneous Reactor Experiment.

DWG. D-9065 A

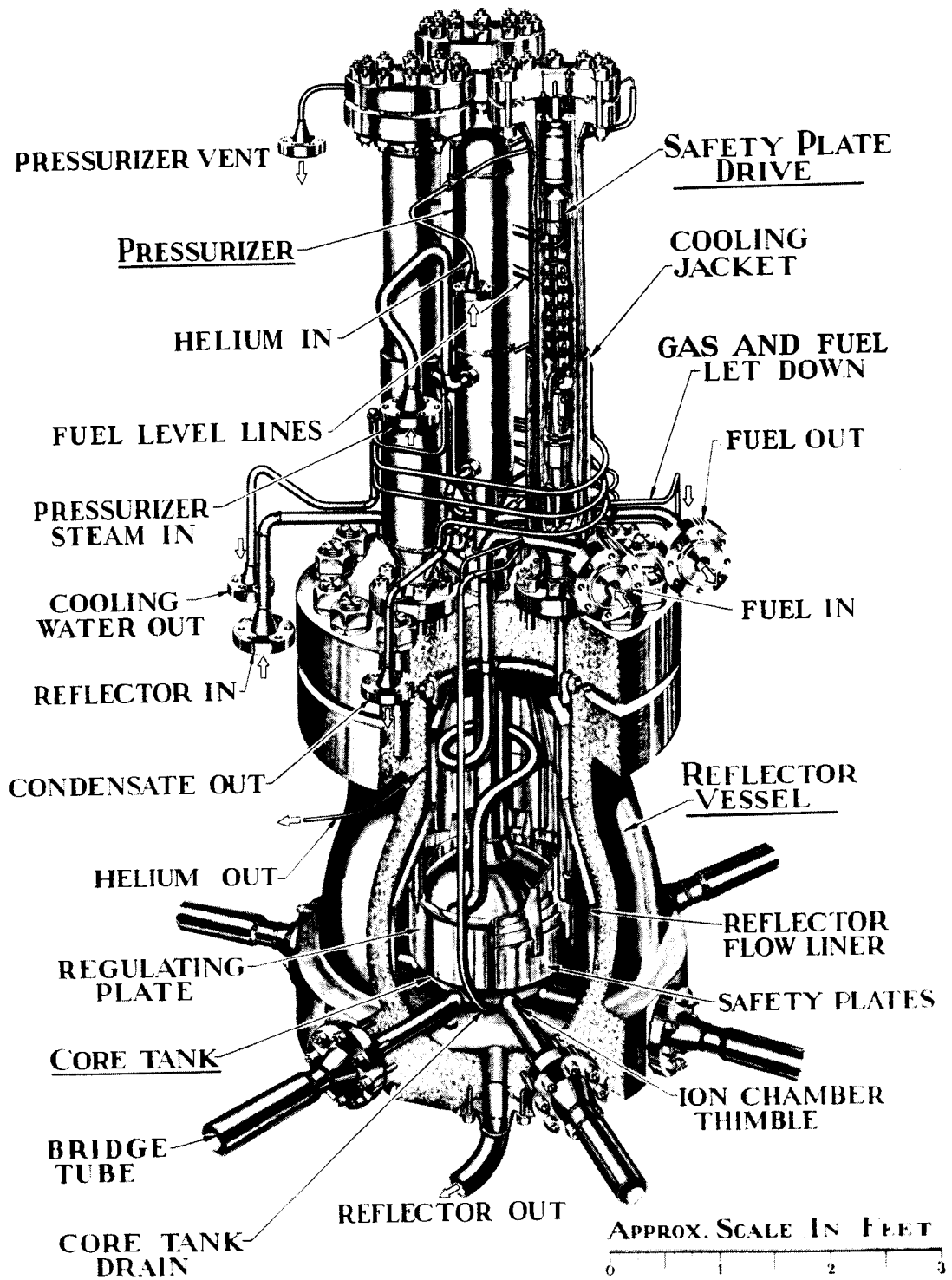


Fig. 10. Reactor Tank Assembly.

## HRP QUARTERLY PROGRESS REPORT

diaphragm to eliminate the packing and the possibility of leakage around the stem.

Because Kerotest valves could not be obtained in the necessary materials, a similar valve was designed for fabrication in the ORNL shops. A ball was substituted for the poppet assembly used in Kerotest valves to reduce the machining required. A drawing of the valve is presented in Fig. 11. Three valves have been made for tests of materials and valve operation.

The first valve, made with a Stellite ball as the poppet on a Stellite seat, was tested hydrostatically at 1500 psi to determine the effectiveness of the Stellite ball and seat and the diaphragm seal. This valve leaked at a rate of one drop every 10 to 15 sec at 1500 psi, possibly because of slight imperfections in the surface finish of the ball and the valve seat and a slight eccentricity of the ball.

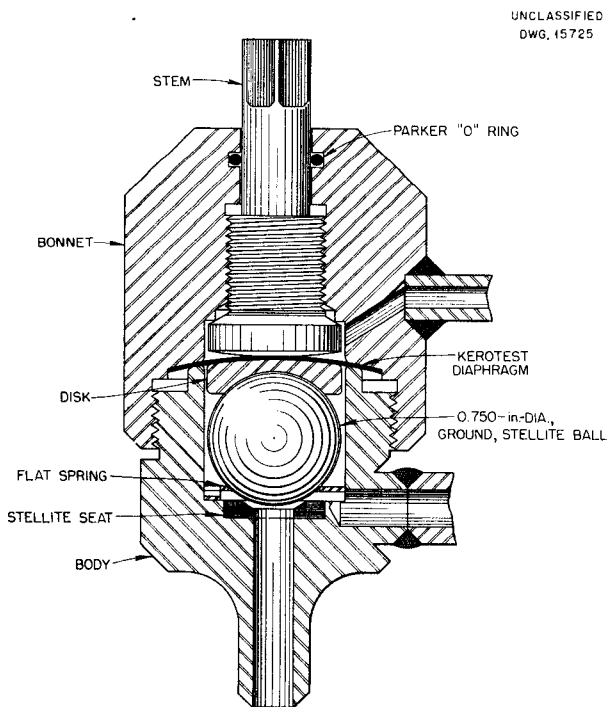


**Fig. 11. High-pressure Isolation Valve.**

A type 303 stainless steel ball was then substituted for the Stellite ball and the valve was again tried. This combination held under a hydrostatic test at 1500 psi, showing no perceptible leakage after several cycles. The valve was tested under simulated service conditions on one of the corrosion study loops for four days, during which time it was cycled every 2 hours. After each cycle, the valve held under 1000 psi at 250°C, but after the fourth day a perceptible leak was observed. The valve was then removed and examined. There was some corrosion of the seat and there were ring grooves in the ball where it contacted the seat. It appeared that the leakage resulted from a combination of the corrosion of the seat and the shifting of the ball in such a way that seating marks crossed and permitted the solution to leak through the crossed grooves.

The second valve tested contained a Stellite ball on a type 347 stainless steel seat, and the third valve had a type 303 stainless steel ball on a titanium seat. These valves, which sealed satisfactorily when tested at a pressure of 1500 psi, were installed in series in a corrosion loop so that uranyl sulfate solution containing 40 g of uranium per liter could be circulated through them continuously at 250°C and 1000-psi pressure. There was a pressure drop of 40 psi across the assembly of valves.

When the loop was started, the valves sealed satisfactorily at 100°C. However, neither valve would seal after solution was permitted to flow through them for 5 min at 100 to 125°C. Although they would not seal, the valves were left in place with solution flowing through them continuously for 253 hr at 250°C. Visual examination of the valves after 253 hr revealed the following facts.

1. The diaphragm seals and stainless steel bodies were in good condition.

2. The Stellite ball was badly corroded at the area of the seat and the corrosion products adhered to the seat.

3. The titanium seat appeared in excellent condition with no visible signs of corrosion. The stainless steel ball had contacted this seat in two places, which indicated that the ball had rotated during operation. One of the seated depressions in the ball was not a complete ring. There was no serious corrosion of the ball.

It is evident, as was to be expected, that Stellite cannot be used in the high-temperature solution. It is believed that the failure of the valve containing the titanium seat and stainless steel ball to seal properly resulted from the valve being mounted horizontally. The seat was not designed to guide the ball back into place after it dropped slightly out of alignment when the valve was opened.

The valve containing the stainless steel ball and titanium seat is being subjected to further testing. Because the titanium fared so well, a fourth valve (Fig. 12) is being fabricated with the core poppet and seat both made of titanium.

#### FUEL SAMPLER INSTALLATION IN THE CHEMISTRY LABORATORY

After a sample of solution is removed from the reactor system, the problem remains of safely transporting it to the analytical laboratory and withdrawing aliquots for analysis. In brief, the procedure visualized is to transfer the cylindrical shield containing the sample from the top of the reactor to a dolly on the operating

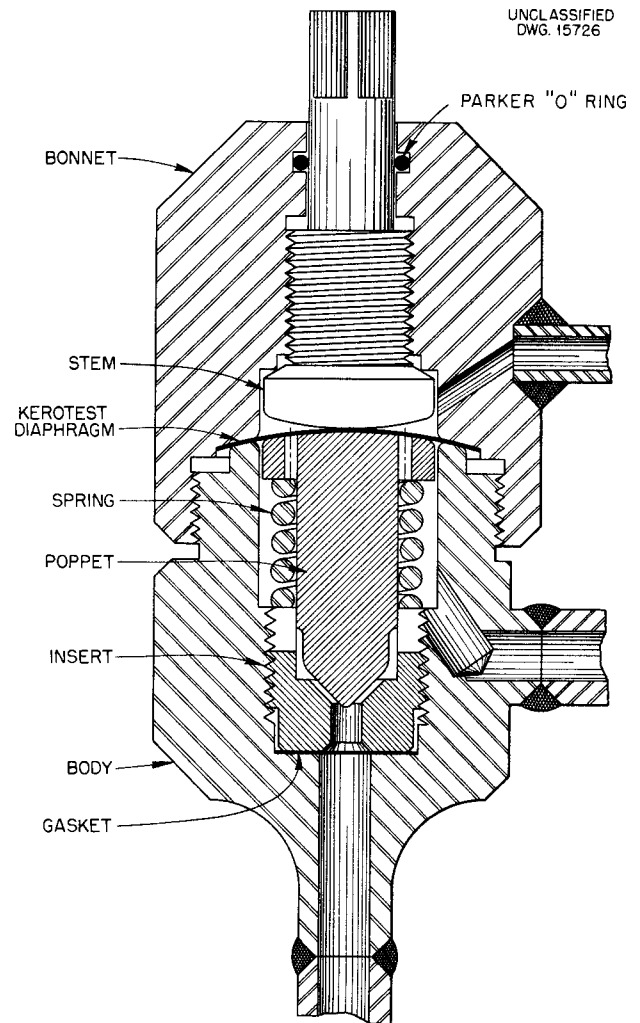


Fig. 12. Conical Poppet Isolation Valve with Core Poppet and Seat of Titanium.

floor and into the unloading port under the lead shield in the hot laboratory. The shield and auxiliary equipment are shown in Fig. 13. The sample is then withdrawn upward into a shielded compartment and transferred to the apparatus by a manipulator and turntable similar to that required for withdrawing the sample from the reactor. Detailed working drawings of this equipment have been prepared and sent to the shop for fabrication.

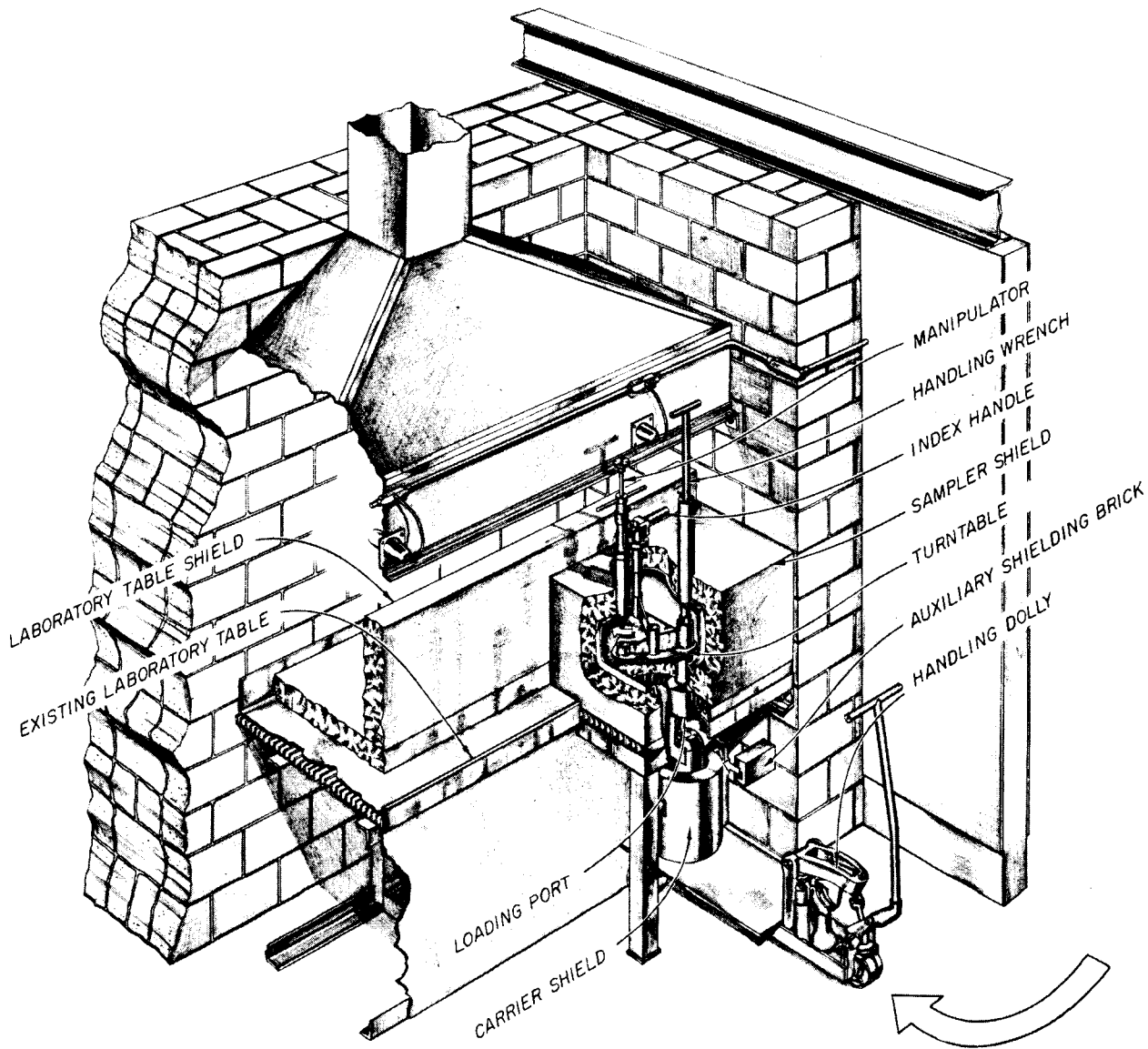


Fig. 13. Fuel Sampler.

**OPERATION OF HRE AT 100°C**

The following factors were considered in a study of the maximum obtainable power and the operating pressure for the HRE if the fuel temperature were limited to 100°C.<sup>(2)</sup>

<sup>(2)</sup> R. van Winkle and F. C. Zapp, *Maximum HRE Power Output and Required Core Pressure for Operation with 100°C Soup*, ORNL CF-52-5-229 (May 22, 1952).

1. The heat removal capacity of the heat exchanger was estimated as a function of the temperature of the steam produced by assuming that the fuel inlet temperature was 100°C and that the water was evaporated under vacuum.

2. Pressure losses in the line between the heat exchanger and the turbine condenser were estimated for

various powers and steam pressures at the heat exchanger.

3. Heat removal by using forced convection of water in the heat exchanger was examined.

4. The core pressure required for the let-down system to pass decomposition gases was estimated.

It was concluded that minor changes to provide 4-in. steam piping through the entire length from the heat exchanger to the turbine condenser would permit the reactor to be operated at a power near 250 kw. The required core pressure was estimated to be between 300 and 400 psi. Forced-convection cooling of the heat exchanger was not considered feasible because the construction is such that most of the water would bypass the tube bundle.

### CONTROLS AND INSTRUMENTATION

W. M. Breazeale, Section Chief  
A. M. Billings      C. A. Mossman  
D. G. Davis        J. E. Owens  
C. G. Heisig        R. H. Powell  
L. P. Inglis        D. S. Toomb  
W. P. Walker

The major portion of the work this quarter was in observing operations, temporarily rearranging circuits for the critical experiments and special tests, and making minor instrument changes. The chief changes in instrumentation were the following: (1) A filter network was added to the period amplifier, which was susceptible to power-line surges. (2) The fuel dump tank level-sensing device, which was sensitive to transient temperature change, was replaced with an element similar to the pressurizer level indicator. (3) A float was placed inside the sight glass on the turbine-condenser hot well and provisions were made for phototube monitoring. If the water level in the hot well rises too high a warning will be transmitted to the operator. On occasion, in the past, the water in the hot well has backed up into the vacuum pump.

### PROCESS INSTRUMENTATION

In the last quarterly report, mention was made of a new coaxial

valve to regulate oxygen flow when the flow is only a few cubic centimeters per minute. This valve is shown in Fig. 14. It consists of a cylinder and a plug made of two materials with different coefficients of thermal expansion. The plug is made of the low-coefficient material, and at ambient temperature has a shrink fit in the cylinder of 0.0005 inch. As the temperature of the valve is raised by the heater windings, the clearance between the plug and cylinder increases, and as a result there is an increase in flow. This arrangement provides a valve which fails (heater power off) closed. A valve with opposite operating characteristics could be provided by exchanging the materials of the cylinder and the plug.

A valve similar to that shown in Fig. 14 was constructed and a limited number of tests have been run. The tests were conducted by welding a thermocouple to the outside wall of the cylinder and automatically controlling the temperature. The results

# HRP QUARTERLY PROGRESS REPORT

UNCLASSIFIED  
DWG. 15727

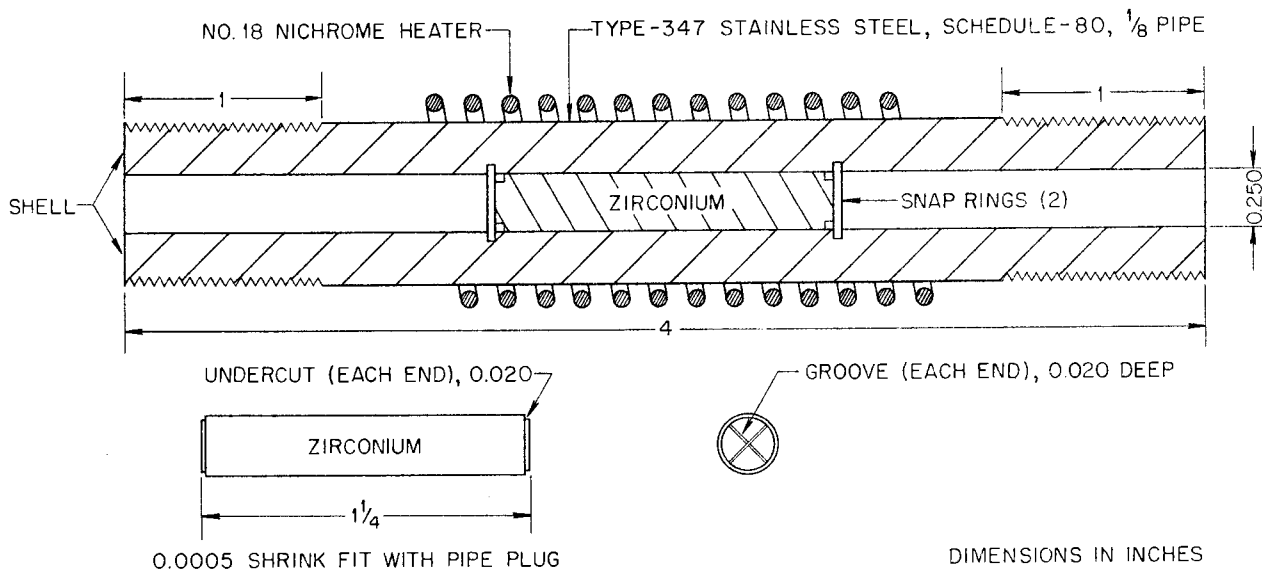


Fig. 14. Thermal Valve for Low Flow Rates.

of these tests are shown in Fig. 15. The time required for the valve to reduce the flow by 63% was found to be 63 seconds.

## CONCENTRATION MEASUREMENT

Effort has been devoted to developing equipment for determining concentration by measuring the absorption of light in the region of a uranyl sulfate absorption band. The absorption spectrum of uranyl sulfate solutions has been determined by the Analytical Chemistry Division.<sup>(1)</sup> This work shows that the usable absorption peak for  $UO_2SO_4 \cdot H_2O$  solutions occurs at 4180 Å at room temperature.

Probably the major problem in the development of a spectrophotometer for this application is the selection of the material for the two cell windows through which the beam of light must pass. The windows must be resistant

to attack by uranyl sulfate solutions at 250°C and must also remain optically stable at 4180 Å when operating for extended periods of time in high neutron and gamma-ray fluxes. Of the materials tested to date, only synthetic sapphires ( $Al_2O_3$ ), spinels ( $MgO \cdot 3.5Al_2O_3$ ), and titania ( $TiO_2$ ) crystals made by Linde Air Products Company show promise of meeting both requirements. In an initial report, English<sup>(2)</sup> shows that synthetic sapphires and titania crystals (rutile) are very resistant to attack by uranyl sulfate solutions at 250°C; the corrosion rates are of the order of 0.2 mpy for titania and 0.7 mpy for synthetic sapphires.

As a rough preliminary check on the radiation stability of synthetic gems, pieces of colorless and golden synthetic sapphires, titania, and ruby were irradiated in a fuel channel of the X-10 graphite reactor for two

(1) Analytical Chemistry Division Quarterly Progress Report for Period Ending September 10, 1951, ORNL-1129, p. 9 and 59 to 61.

(2) J. L. English, *Initial Report on the Corrosion of Fused Titania and Synthetic Sapphire in Uranyl Sulfate Solutions at 250°C*, ORNL CF-52-5-33 (May 3, 1952).

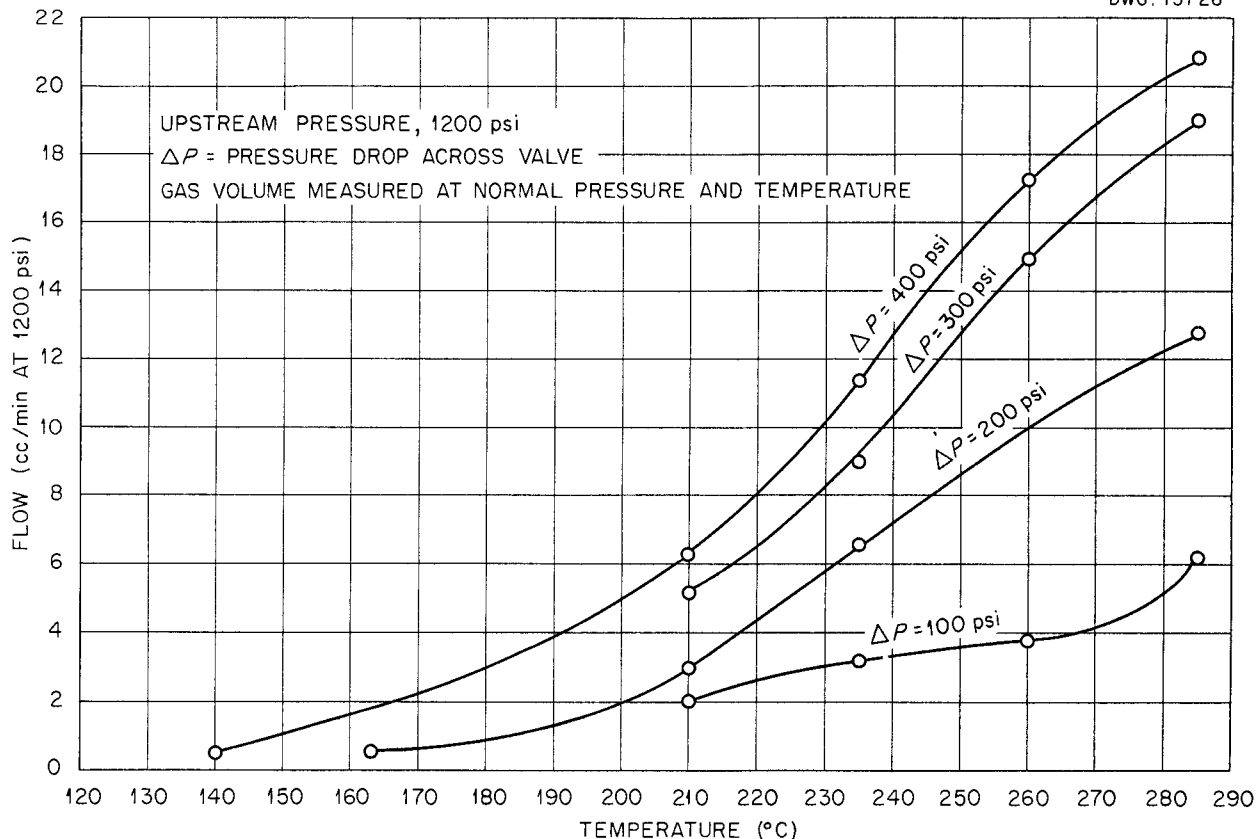


Fig. 15. Flow Curves for Thermal Valve Shown in Fig. 14.

weeks and examined visually. The synthetic, colorless sapphire and titania were not affected sufficiently to exclude them from further consideration. Several 11 by 11 by 5 mm optically polished slabs of spinel, white sapphire, and titania have been received and are being prepared for irradiation in the X-10 graphite reactor to obtain quantitative spectral data on these synthetic gems before and after irradiation, with and without light annealing during irradiation, and at a temperature comparable to that expected in the spectrophotometer cell under development. For these tests the materials will not be in contact with uranyl sulfate solutions. Preliminary irradiation studies of the synthetic ruby and golden sapphires appear to exclude these materials

because of excessive radiation darkening.

The preliminary design of a cell to withstand 250°C at 2000 psig has been completed and a plastic model ordered from the shop. The plastic model is to be used to determine the arrangement and size of the inlet and outlet ports necessary to obtain the shortest possible response time for the instrument.

Calculations have been made which show that gas bubbles in the cell should not be a problem if the solution is kept between 100 and 150°C. This temperature range is further desirable in that it permits the use of stainless steel parts without danger of scaling beyond the filter.

## HRP QUARTERLY PROGRESS REPORT

Investigations of the performance of the Densitrol units described in the last quarterly report are continuing. One low-temperature unit has been installed in the mockup at Y-12 and is awaiting tests.

A second Densitrol unit has been installed in a special laboratory loop. This system is designed so that studies can be made readily of the effect of variations in flow rate, concentration, temperature, gas bubble content, and position of the micro-former. Tests have been conducted at atmospheric pressure. Sodium sulfate solutions of proper concentration to have the same density as  $\text{UO}_2\text{SO}_4$  solutions containing 20 to 40 g of

uranium per liter (that is, a specific gravity of 1.0330 to 1.0530) were used.

The plummet tested, designated stainless steel No. 1, has about 50% greater volume than the glass plummet supplied with the Densitrol and its travel is correspondingly greater. This led to some trouble, which was traced to the fact that the micro-former was being operated in a non-linear region. Heavier weighting chains should remedy this situation.

A temperature change from 50 to 70°C of the nitrogen-pressurized steel plummet mentioned in the last report does not alter the density indication by as much as  $\pm 0.01\%$ . This variation is within specified tolerance.

---

## CORROSION

E. G. Bohlmann, Section Chief

### EXPERIMENTAL CORROSION STUDIES

J. C. Griess     D. J. Sasmor

A mechanism for the corrosion of type 347 stainless steel was presented in a previous quarterly report.<sup>(1)</sup> In brief, the basis for the mechanism was the observation that when stainless steel dissolves in dilute acid solutions, nickelous, ferrous, and chromic ions are initially formed. If an oxidizing agent is present and if the acidity of the solution is not too high, ferric and chromic oxides are precipitated on the surface of the steel and they insulate the steel from the corrosive medium. Consequently, after the initial rapid attack the corrosion rate is greatly reduced.

---

(1) J. C. Griess, *Homogeneous Reactor Project Quarterly Progress Report for Period Ending November 15, 1951*, ORNL-1221, p. 21.

All protective films develop cracks because of various stresses and strains, so it is necessary to have a means for maintaining the films in a continuous state of repair. In the system under consideration the mechanism of film repair is identical to that of film formation, that is, the precipitation of ferric and chromic oxides at the points of film failure. In effect, then, after the oxide coating has been formed, corrosion takes place only where there are cracks or imperfections in the film, that is, at places where steel is exposed to the solution. Therefore a study of the corrosion rate after a film has been formed indirectly shows the frequency and size of imperfections, the efficiency of the healing process, and the solubility of the surface oxides in the solution under consideration. Hence a study of the corrosion process during the initial stages of film formation

combined with a careful analysis of the solution after exposure should give the same type of information as could be obtained by the much longer process of studying the corrosion rate after the protective film has already been formed. The fact that the results reported below showed similar behavior to some of the dynamic tests should be sufficient justification for the use of short-term tests.

The experiments during the past quarter have shown rather conclusively that a protective film can be damaged or its effectiveness reduced by removing chromium oxide from the film by a mechanism involving the oxidation of chromium to the hexavalent state or by dissolving both iron and chromium oxides in their trivalent states in a solution of low pH. From the results below it is apparent that if the corrosion rate of type 347 stainless steel is to be kept low, it will be necessary to suppress the solubility of both iron and chromium oxides.

Studies begun during the last quarter concerning the effect of molybdenum on the corrosion of type 347 stainless steel have been completed. The results presented in the last quarterly report<sup>(2)</sup> indicated that molybdate ions when present in uranyl sulfate solutions containing 300 g of uranium per liter were somewhat effective in reducing the corrosion. The results reported below show that in uranyl sulfate solutions containing 40 g of uranium per liter molybdate has only a very slight inhibitory effect. Although the corrosion rate was not greatly retarded in either case by the presence of molybdate ions, the physical appearance of the oxide films formed

in its presence was greatly different from that of those formed in its absence.

The experimental procedures were essentially the same as those given in the previous quarterly report.<sup>(2)</sup> Some of the experiments were carried out in sealed quartz tubes that contained 5 ml of solution and a corrosion specimen that had a surface area of 8 cm<sup>2</sup>. Other experiments were carried out in American Instrument Company bombs, both with and without quartz liners. In the experiments in which the bombs with quartz liners were used, the corrosion specimen had a surface area of 36 cm<sup>2</sup> and was completely covered by 35 ml of solution. Without the liners, the walls of the bombs served as part of the corrosion specimen. In these cases the surface area of steel exposed to the solution was 116 cm<sup>2</sup> and the volume of solution was 60 ml. When it was desirable to have a particular oxygen pressure, a calculated volume of 30% hydrogen peroxide was added. The thermal decomposition of the peroxide produced the desired oxygen partial pressure. The pH of a uranyl sulfate solution containing a fixed uranium concentration was varied by the addition of uranium trioxide and/or sulfuric acid. All experiments were run at 250°C under static conditions.

**Effect of Oxygen Pressure on the Attack of Type 347 Stainless Steel by Uranyl Sulfate and Sulfuric Acid.** When stainless steel is exposed to uranyl sulfate or dilute sulfuric acid solutions in the absence of an added oxidizing agent the corrosion damage is very extensive. In uranyl sulfate solutions ferrous and nickelous ions are formed with the simultaneous reduction and precipitation of uranium, whereas in sulfuric acid solutions hydrogen gas and ferrous and nickelous ions are formed. In both cases the iron remains as ferrous iron, and

(2) J. C. Griess and D. J. Sasmor, *Homogeneous Reactor Project Quarterly Progress Report for Period Ending March 15, 1952*, ORNL-1280, p. 31.

## HRP QUARTERLY PROGRESS REPORT

hence there is no stifling of corrosion by the precipitation of ferric oxide. Since in both cases it is necessary to have an oxidizing agent present and since oxygen is the one in common usage, it was desirable to know what effect the amount of oxygen in the solution had on the corrosion rate.

The effect of oxygen pressure on the initial stages of corrosion was studied at one concentration both in sulfuric acid and in uranyl sulfate solutions in bombs with quartz liners. In the uranyl sulfate system the uranium concentration was arbitrarily chosen as 300 g per liter of solution; in sulfuric acid solutions the concentration of the sulfuric acid was chosen as 0.039 N. Both of these concentrations were such that the extent of corrosion was appreciable, so analysis of the solutions for corrosion products was not difficult.

The pH of the uranyl sulfate solution containing 300 g of uranium per liter was 1.40 and that of the 0.039 N sulfuric acid was 1.54. The oxygen pressures studied were arbitrarily selected. It should be noted, however, that at an oxygen pressure of 265 psi at 250°C the molar oxygen concentration was 0.044, which was nearly equal to the normality of the sulfuric acid solution. The duration of individual tests was 24 hr and duplicate tests were made under each set of conditions.

The results tabulated in Table 1 show that increasing the oxygen pressure increased the extent of corrosion in the uranyl sulfate system. Table 2 gives the results in the sulfuric acid solutions, and these data indicated the reverse effect, that is, a slightly decreased corrosion rate at the higher oxygen concentrations.

Table 1

EFFECT OF OXYGEN ON THE ATTACK OF TYPE 347 STAINLESS STEEL EXPOSED FOR 24 HR AT 250°C TO URANYL SULFATE SOLUTIONS CONTAINING 300 g OF URANIUM PER LITER (pH = 1.40)

OXYGEN PRESSURE (psi)	OXYGEN IN SOLUTION (ppm)	SOLUTION ANALYSIS AFTER EXPOSURE (ppm)			
		Ni	Mn	Fe	Cr
50	260	57	11	24	11
		59	12	20	11
100	480	149	27	64	107
		118	23	46	82
265	1400	127	24	22	131
		114	21	26	121
500	2600	141	32	88	174
		111	26	31	139

Table 2

EFFECT OF OXYGEN ON THE ATTACK OF TYPE 347 STAINLESS STEEL EXPOSED FOR 24 HR AT 250°C TO 0.039 N SULFURIC ACID SOLUTIONS (pH = 1.54)

OXYGEN PRESSURE (psi)	OXYGEN IN SOLUTION (ppm)	SOLUTION ANALYSIS AFTER EXPOSURE (ppm)			
		Ni	Mn	Fe	Cr
100	480	310	63	8	1
		325	64	8	1
265	1400	298	56	2	1
		309	58	3	1
500	2600	258	54	2	<1
		260	54	2	<1

These experiments were considered a very crude test of the protective value of the oxide films, because the films were formed during the experiment. The experiments were repeated with pretreated specimens and the results are given in Tables 3 and 4.

The very low chromium content in the sulfuric acid solutions was of particular interest (Table 2). Analyses after subsequent exposure of the specimens in uranyl sulfate showed that much of the chromium oxide that was precipitated on the steel during sulfuric acid treatment dissolved in the uranyl sulfate solutions (Table 4). Careful analyses of these solutions showed that at least 90% of the chromium in solution was in the hexavalent state.

In the four tables the manganese concentration in solution has been included to show that the manganese and nickel of the steel dissolved in the same ratio as they were present in the steel. The weight per cent of

nickel in the steel was approximately 10 and that of the manganese was 2. The solution analyses indicated essentially the same ratio of nickel to manganese.

**Effect of Different Acid Solutions on the Attack of Type 347 Stainless Steel.** The proposed mechanism of corrosion implies that the formation of an oxide film is necessary to minimize the corrosion rate. If the film is formed by the hydrolytic precipitation of ferric and chromic oxides, the concentration of acid will be important in determining the rate and extent of hydrolysis. If the iron initially dissolves in the ferrous state, the oxidizing conditions will also be important.

A series of experiments was run in which stainless steel specimens were exposed to different concentrations of either nitric or chromic acids. A similar series was run in various concentrations of sulfuric acid to which oxygen had been added. The oxygen pressure was varied in

# HRP QUARTERLY PROGRESS REPORT

Table 3

ATTACK OF URANYL SULFATE SOLUTIONS CONTAINING 300 g OF URANIUM PER LITER WITH 50 psi OF OXYGEN ON TYPE 347 STAINLESS STEEL SPECIMENS PRETREATED IN URANYL SULFATE SOLUTIONS CONTAINING 300 g OF URANIUM PER LITER AT DIFFERENT OXYGEN PRESSURES\*

Time of Exposure: 24 hr at 250°C

OXYGEN PRESSURE DURING PRETREATMENT (psi)	SOLUTION ANALYSIS AFTER SECOND EXPOSURE (ppm)			
	Ni	Mn	Fe	Cr
50	9	**	15	17
	4	**	20	4
100	15	3	16	30
	4	1	13	16
265	13	2	22	21
	8	1	15	13
500	5	1	20	10
	5	1	14	9

\*Cf., Table 1.

\*\*Solutions not analyzed for manganese.

such a way that at 250°C the molar oxygen concentration in solution was equal to the normality of the acid. In effect, then, the ratio of hydrogen ions to dissolved oxygen molecules was kept equal to unity assuming complete ionization of the sulfuric acid at 250°C. Another series was run with uranyl sulfate solutions containing 300 g of uranium per liter and 50 psi of oxygen. The pH of the uranyl sulfate solutions was varied by the addition of uranium trioxide or sulfuric acid. The addition of oxygen to the uranyl sulfate and sulfuric acid solutions was necessary because they did not contain

oxidizing ions such as were present in the nitric and chromic acid solutions.

All the tests were carried out in quartz tubes and the corrosion specimen in each case had a surface area of 8 cm<sup>2</sup>. Duplicate experiments were run under each set of conditions and in every case the duration of the experiment was 24 hours. Previous experience had indicated that the initial rapid attack was essentially complete during this length of time.

All solutions were analyzed for nickel and some of the solutions were

FOR PERIOD ENDING JULY 1, 1952

Table 4

ATTACK OF URANYL SULFATE SOLUTIONS CONTAINING 300 g OF URANIUM PER LITER WITH 50 psi OF OXYGEN ON TYPE 347 STAINLESS STEEL SPECIMENS PRETREATED IN SULFURIC ACID SOLUTIONS AT DIFFERENT OXYGEN PRESSURES\*

Time of Exposure: 24 hr at 250°C

OXYGEN PRESSURE DURING PRETREATMENT (psi)	SOLUTION ANALYSIS AFTER SECOND EXPOSURE (ppm)			
	Ni	Mn	Fe	Cr
100	69	12	44	200
	74	14	47	209
265	61	13	35	199
	66	16	35	203
500	63	15	35	199
	54	12	40	199

\*Cf., Table 2.

analyzed for chromium and iron. Previous reports<sup>(2,3)</sup> have shown that the nickel concentration is a reliable measure of the total corrosion. Corrosion rates in mils per year could have been calculated from the nickel analyses, but this was not done since the time of exposure was short and the corrosion rates were high.

In chromic and nitric acid solution the room temperature pH values were the same before and after exposure, because the amounts of nickel, iron, and chromium in solution after a run were very small compared with the hydrogen ion concentrations. In sulfuric acid solutions the pH values after exposure were usually one-

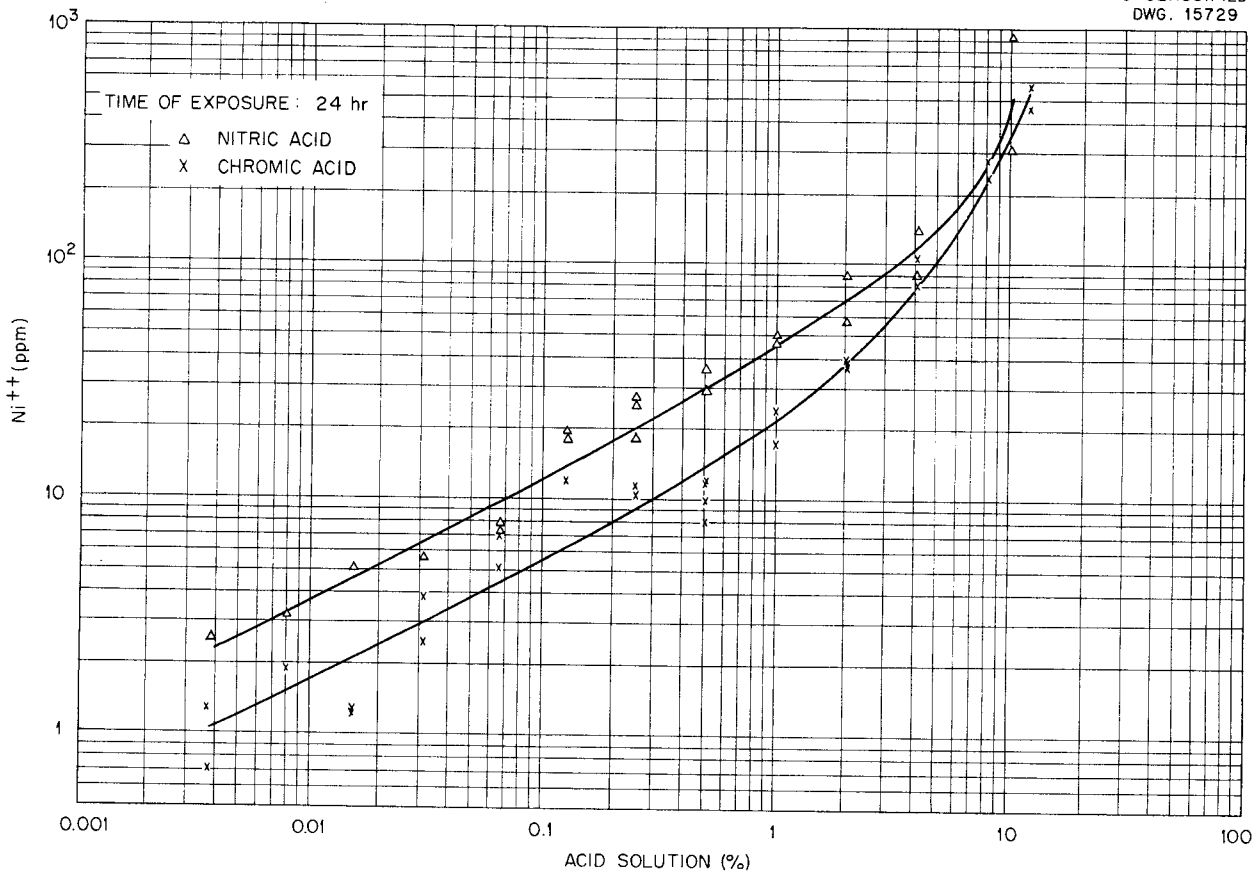
three-tenths of a pH unit higher. This increase in pH could be quantitatively accounted for by the substitution of nickel ions for hydrogen ions.

The results obtained in chromic and nitric acid are shown in Fig. 16; the results obtained in sulfuric acid are shown in Fig. 17; and the results obtained in the uranyl sulfate solutions are shown in Fig. 18. Figure 18 also shows the iron and chromium analysis of the uranyl sulfate solutions. For comparative purposes, the pH of a 0.01% nitric acid solution was 2.79, that of a 0.10% solution was 1.79, and that of a 1.0% solution was 0.79. The pH of a 0.01% chromic acid solution was 2.97, that of a 0.10% solution was 1.98, and that of a 1.0% solution was 1.06.

(3) J. L. English and S. H. Wheeler, *op. cit.*, ORNL-1280, p. 62; also this report.

# HRP QUARTERLY PROGRESS REPORT

UNCLASSIFIED  
DWG. 15729



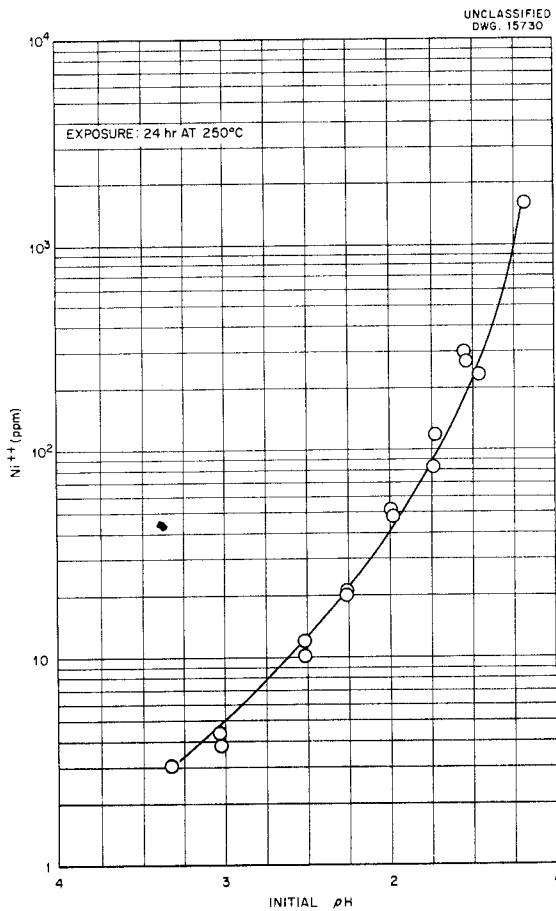
**Fig. 16. Attack on Type 347 Stainless Steel by Different Concentrations of Chromic and Nitric Acids.**

Figure 19 shows a differential plot of the sulfuric, chromic, and nitric acid curves. It can be clearly seen that in sulfuric acid the rapid increase in corrosion began at a pH of about 2.5, whereas in chromic and nitric acids the rapid increase began at a pH of approximately 1.

The rapid increase in corrosion in nitric and chromic acid was associated with a corresponding increase in the iron and chromium concentrations in solution. These data are shown in Table 5. In sulfuric acid solutions this was not the case, and less than 10 ppm of iron and 2 ppm of chromium appeared in solution even at the highest acid concentrations used.

The amounts of iron and chromium in the uranyl sulfate solutions are shown in Fig. 18. Each of the duplicate samples was analyzed for nickel, and one was analyzed for chromium, whereas the other was analyzed for iron.

All the specimens exposed to chromic and nitric acids were then subjected to a uranyl sulfate treatment. In all cases the extent of corrosion in the uranyl sulfate solutions was approximately inversely proportional to the corrosion during the initial treatment. However all the specimens that received treatment in greater than 1% chromic or nitric acid solution had essentially equal corrosion rates, based on the nickel



**Fig. 17. Attack on Type 347 Stainless Steel by Different Concentrations of Sulfuric Acid.**

analyses. The general nature of the corrosion was such that all specimens tended to build up oxide films of approximately equal minimum thicknesses.

It should be pointed out that when steel was pretreated in any concentration of chromium trioxide greater than 0.5%, the resulting film was black. Subsequent exposure of these pretreated steel specimens to uranyl sulfate solutions (300 g of uranium per liter) containing 50 psi of oxygen for 24 hr resulted in a change in the

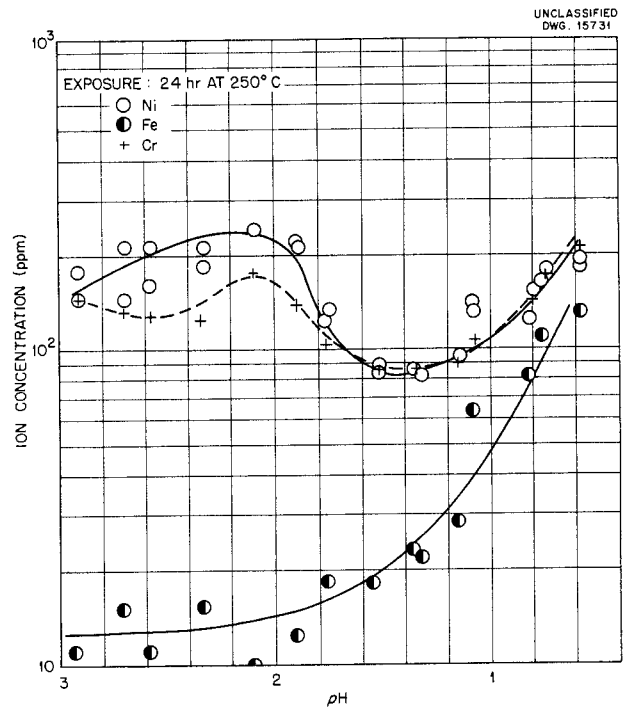


**Fig. 18. Effect of pH on the Corrosiveness of Uranyl Sulfate Solutions (300 g of Uranium per Liter) to Type 347 Stainless Steel.**

color of the specimen from black to tan. Analyses of the uranyl sulfate solutions after exposure to the specimens showed that the chromium concentrations were high and that at least 90% of the chromium was in the hexavalent state. The solution analyses showed low nickel and iron concentrations and indicated that the uranyl sulfate preferentially leached chromium from the oxide film.

The specimens pretreated in nitric acid were also black after a 24-hr treatment. However, subsequent exposure of these specimens to uranyl sulfate did not change their physical appearance, and solution analyses did not reveal high chromium concentrations. The nickel and iron analyses were essentially the same as those obtained from the uranyl sulfate solutions to which the specimens

# HRP QUARTERLY PROGRESS REPORT

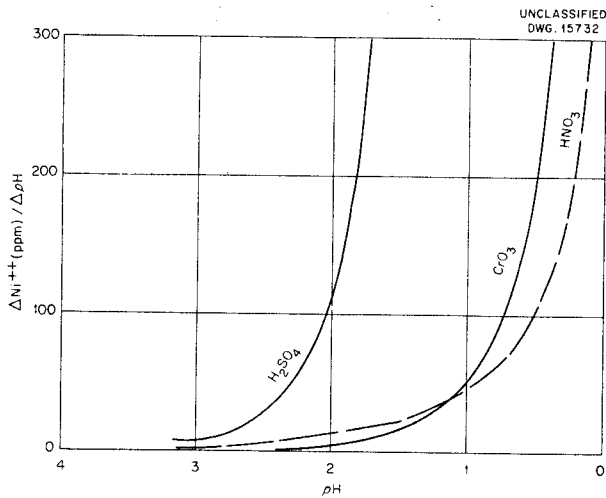


Fig. 19. Differential Plot of Curves Shown in Figs. 16 and 17.

Table 5

## EFFECT OF CHROMIC AND NITRIC ACID CONCENTRATIONS ON THE AMOUNT OF IRON AND CHROMIUM IN SOLUTION

Time of Runs: 24 hr

ACID (wt %)	SOLUTION ANALYSES (ppm)				
	HNO <sub>3</sub>			CrO <sub>3</sub>	
	pH	Fe	Cr	pH	Fe
0.25	1.40	1	2	1.72	
0.50	1.10	1	3	1.42	12
1.0	0.80	1	4	1.06	26
2.0	0.50	2	7	0.79	66
4.0	0.24	12	18	0.50	182
8.0	*			0.22	495
10.0	*	95	23	*	*
12.0	*			*	1260

\*No tests at these concentrations.

prepared in chromic acid had been exposed.

Since the corrosion of type 347 stainless steel by sulfuric acid was not associated with either iron or chromium in solution, it was thought that the physical character of the precipitated iron and chromium oxides might have been such that they did not adhere well to the steel. To determine the differences in iron and chromium oxides hydrolytically precipitated in nitric and sulfuric acids the following experiments were carried out. Into each of four quartz tubes, 5 ml of the following solutions were placed: (1) 0.20 N nitric acid containing 3600 ppm of iron as ferric nitrate, (2) 0.20 N sulfuric acid containing 3600 ppm of iron as ferric sulfate, (3) 0.20 N sulfuric acid containing 1800 ppm of iron and 1800 ppm of chromium as sulfates, and (4) 0.20 N nitric acid containing 1800 ppm of iron and 1800 ppm of chromium as nitrates. All tubes were then sealed and heated at 250°C for 18 hr, during which time the iron and chromium were completely precipitated from solution. An electron micrograph of a portion of the precipitate from each tube was prepared by Willmarth and the results are shown in Figs. 20, 21, 22, and 23. Both the mixed iron and chromium oxides were black. The iron oxide precipitated in the presence of nitric acid was bright red, whereas that precipitated in the presence of sulfuric acid was a much deeper red: x-ray analyses showed both oxides to be identical, that is, ferric oxide.

**Effectiveness of Molybdenum As an Inhibitor.** The initial studies of the inhibitor action of molybdenum (as molybdate) in a system containing type 347 stainless steel were presented in the last quarterly report.<sup>(2)</sup> The corrosion specimens discussed in that

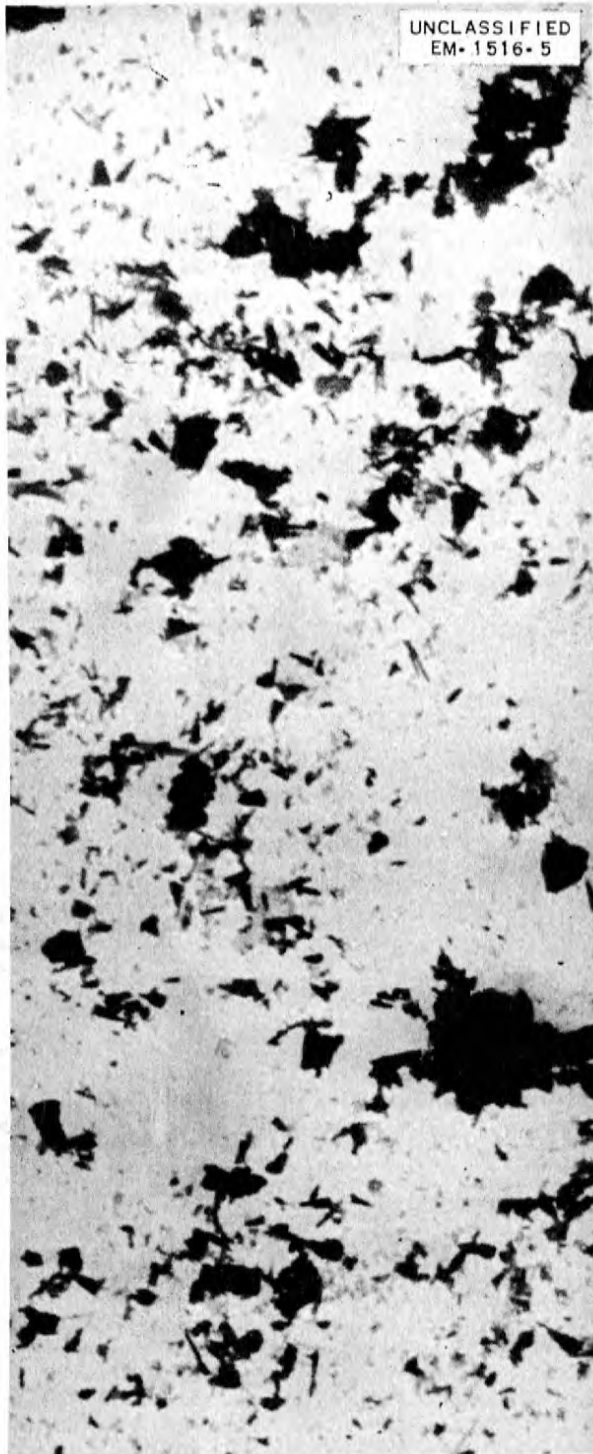


Fig. 20. Ferric Oxide Precipitated at 250°C from a 0.20 N Sulfuric Acid. 5000X.

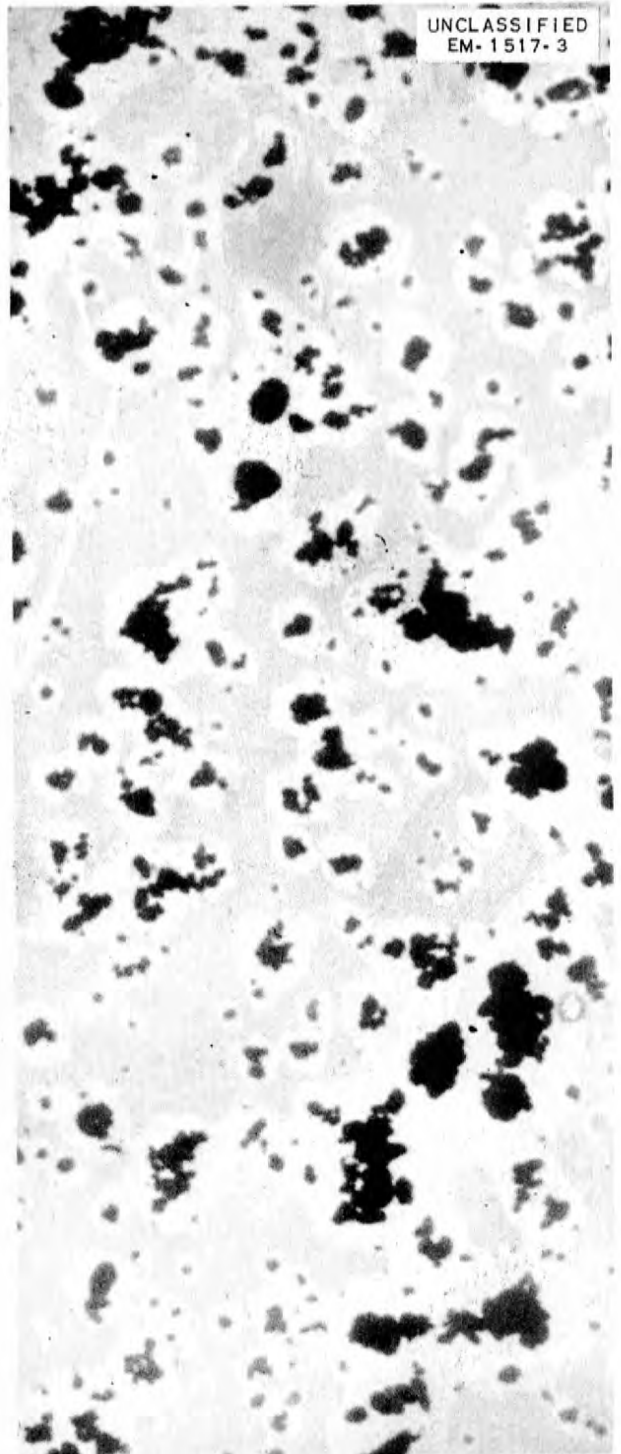


Fig. 21. Ferric Oxide Precipitated at 250°C from a 0.20 N Nitric Acid Solution. 5000X.

HRP QUARTERLY PROGRESS REPORT

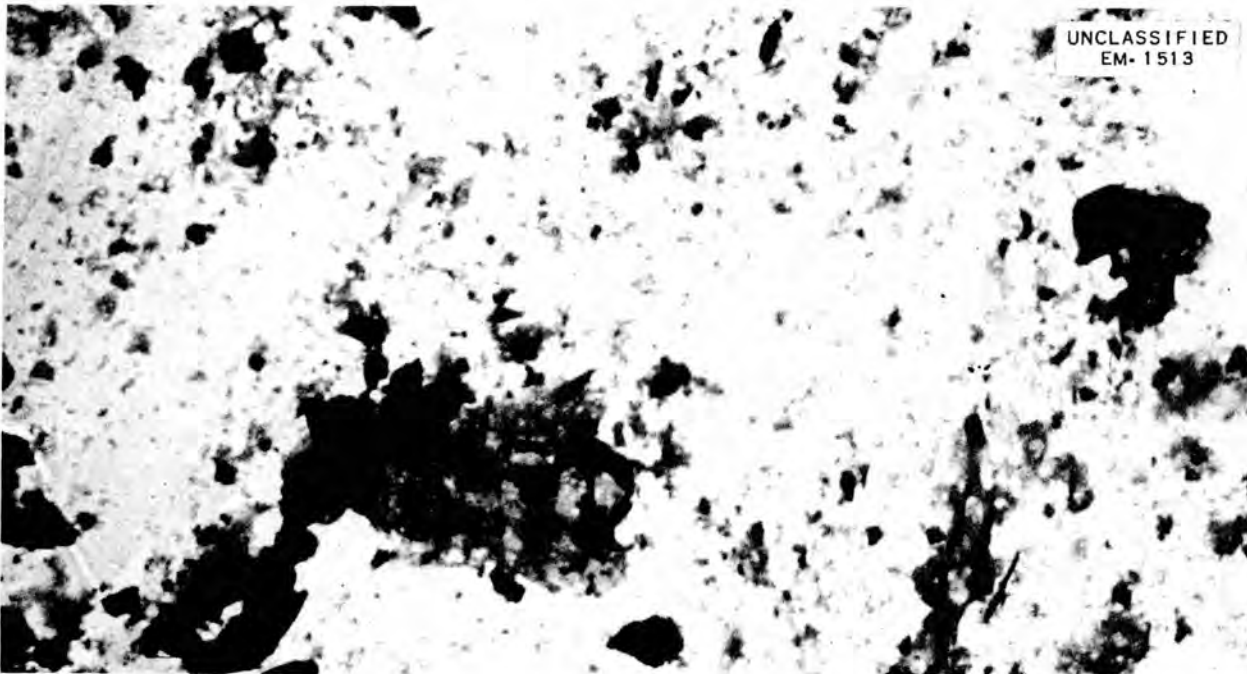


Fig. 22. Mixed Chromic and Ferric Oxides Precipitated at 250°C from a 0.20 N Sulfuric Acid Solution. 5000X.

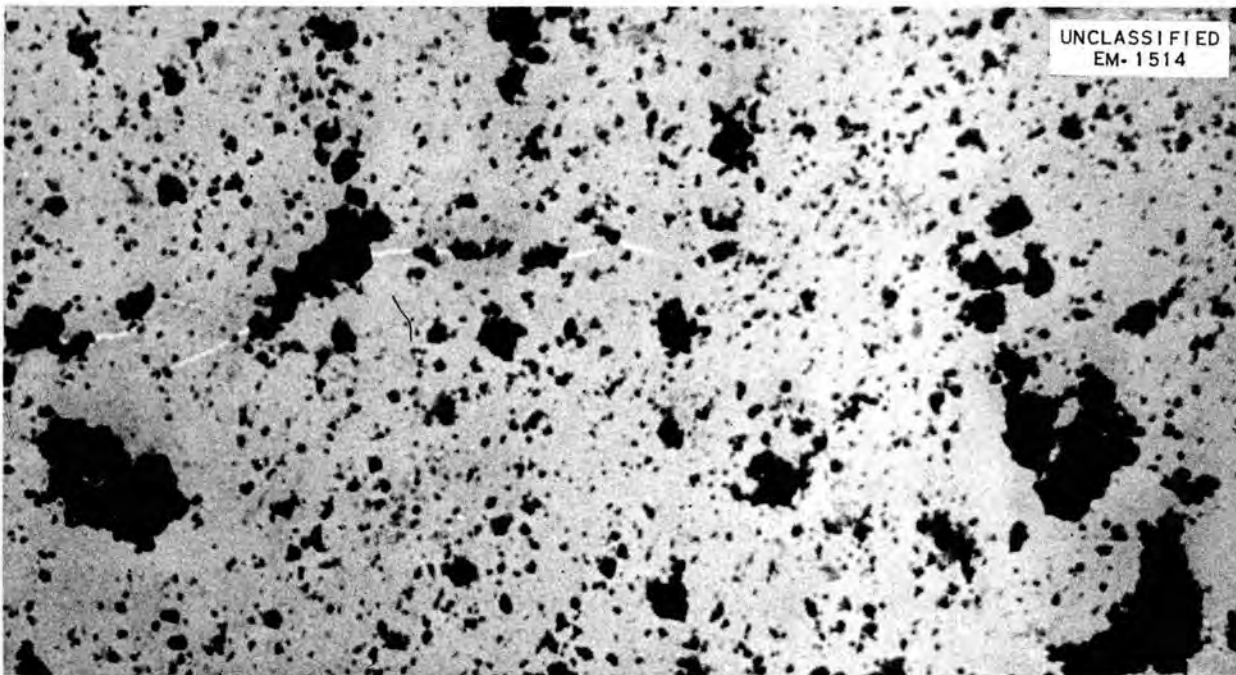


Fig. 23. Mixed Chromic and Ferric Oxides Precipitated at 250°C from a 0.20 N Nitric Acid Solution. 5000X.

report (Table 12) were given to Willmarth for study. (The results will be reported elsewhere.<sup>(4)</sup>) Briefly this study indicated that the films formed in the presence of the molybdenum appear to fit very tightly and follow closely the contours of the substrate metal. The films varied from 0.8 to 1 micron in thickness and in general were thinner and more adherent than films formed by other treatments.

A series of experiments was conducted to determine the effectiveness of molybdenum in reducing the corrosiveness of dilute uranyl sulfate solutions to type 347 stainless steel. In these experiments bombs without liners were used and in all cases the concentration of uranium was 40 g per liter of uranyl sulfate solution. All additions of molybdate were made as molybdic acid and in each case the molybdenum concentration was 160 ppm. All the test solutions, except two, contained uranyl sulfate solutions, and oxygen partial pressures of 100 psi at 250°C were used. The following four types of treatment and exposure were studied: (1) no pretreatment and exposure to solutions containing only uranyl sulfate, (2) no pretreatment and exposure to solutions containing uranyl sulfate and molybdenum, (3) pretreatment in 1% nitric acid containing molybdenum for first 24 hr and then exposure to solutions containing uranyl sulfate and molybdenum, (4) pretreatment in 1% nitric acid for first 24 hr and then exposure to solutions containing only uranyl sulfate. The total time of exposure was 1250 hours. Figure 24 shows the total corrosion including the first 24-hr pretreatment. It is evident that the initial extent of corrosion was different in each case. The corrosion rates appeared to be essentially the same after the initial attack.

**Discussion.** If an oxide coating is formed by hydrolytic precipitation of iron and chromium oxides, the acidity of the solution should be important in determining the rate and extent of hydrolysis. The faster the rate of hydrolysis, the closer the precipitation to the surface and apparently the thinner and more compact the oxide layer that will be formed. Figure 16 showed that this was true. Figure 17, however, indicated that sulfate ions exerted a deleterious effect on the corrosion resistance of the steel. Visual observation of the steel after treatment in sulfuric acid solutions showed a loosely adherent oxide, which is in contrast to the rather compact oxides formed in either chromic or nitric acid solutions. The electron micrographs (Figs. 20 through 23) showed that the oxides of iron and chromium were of considerably different shapes when precipitated in nitric and sulfuric acids. It is probable that this difference was related to the rates of hydrolysis, and if so the electron micrographs indicated that the rate of hydrolysis was slower in the presence of sulfuric acid. Since ferric ions can be complexed by sulfate ions, it is probable that the complexing action of the sulfate ions resulted in a slower rate of hydrolysis in sulfuric acid solutions. It then seems probable that when the steel corroded in sulfuric acid solutions at 250°C in the presence of oxygen, the ferric and chromic ions were complexed to a certain degree and had a chance to diffuse some distance from the surface of the steel before precipitation. That the films were of little value in reducing corrosion was shown by the fact that when these specimens were exposed to uranyl sulfate solutions, the attack was nearly the same as that of untreated steel.

The oxides of iron and chromium precipitated on the surface of the

<sup>(4)</sup>T. E. Willmarth (to be issued).

# HRP QUARTERLY PROGRESS REPORT

UNCLASSIFIED  
DWG. 15733

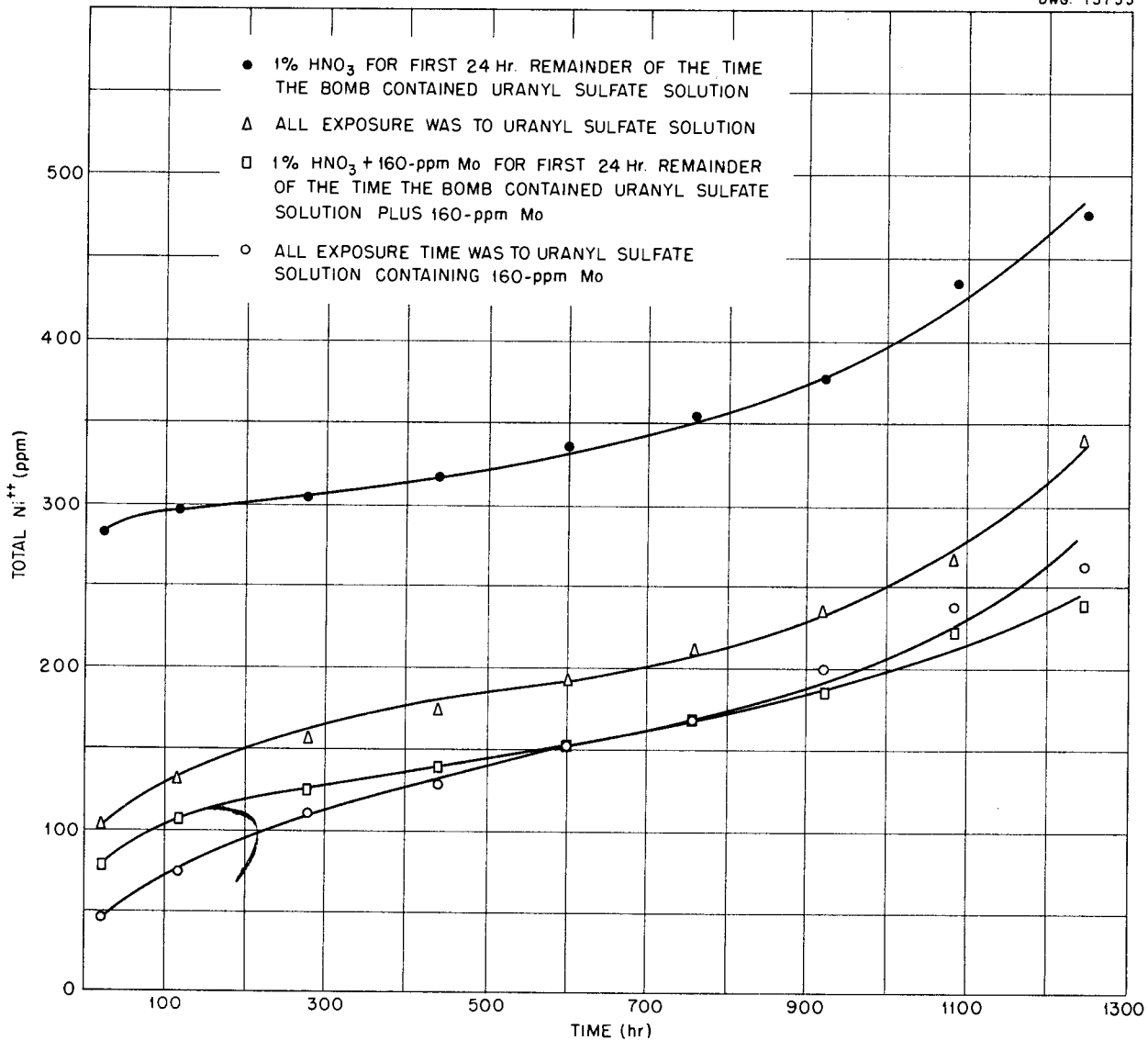


**Fig. 24. Effect of Molybdenum on the Corrosion of Type 347 Stainless Steel by Dilute Uranyl Sulfate Solutions.**

steel during the sulfuric acid treatment were in such a form that the chromic oxide was soluble in uranyl sulfate solutions. The high solubility of the chromium was unexpected since the solubility of chromic oxide in dilute acid was very low. Chemical analysis of the solution, however, showed that at least 90% of the soluble chromium was in the hexavalent

state, which accounted for its ability to remain in solution.

It might be expected that uranyl sulfate solutions would behave in a manner similar to dilute sulfuric acid, but this was not the case. Films formed in uranyl sulfate solutions containing 300 g or less of uranium per liter were compact and

effective in reducing corrosion. In the uranyl sulfate solutions the sulfate ion concentration was very low<sup>(5)</sup> and practically no sulfate ions were available for complexing the iron and chromium. Thus the iron and chromium oxides were precipitated rapidly in close contact with the steel and produced a protective coating.

The effect of oxygen pressure on the corrosion of type 347 stainless steel by uranyl sulfate solutions containing 300 g of uranium per liter was very marked. When the oxygen pressure was 50 psi, the extent of corrosion was low, and correspondingly the chromium concentration in solution was low. At all the higher oxygen pressures the corrosion rates agreed with one another within the limits of error, but the rates were at least twice as high as at the lower pressures. The chromium concentrations in solution at the higher oxygen pressures were also much higher, and again at least 90% of the chromium was in the hexavalent state. The chromium analyses were not sufficiently accurate to determine with certainty whether there was an increase in the chromium concentration when the oxygen pressure was between 100 and 500 psi, but it appeared that the chromium in solution increased slightly as the oxygen pressure increased. At all pressures the iron in solution was approximately constant. A similar difference in corrosion produced by changes in oxygen pressure has been observed in the dynamic tests.<sup>(6)</sup>

Since the uranyl sulfate solutions containing added uranium trioxide had higher pH values than the uranyl sulfate solutions without uranium trioxide, it was expected that the extent

of corrosion would be less. This was not the case; corrosion was greater at a pH of 2.92 than it was at a pH of 1.40. At least part of the reason for the increased corrosion rate could be attributed to the high solubility of chromium. A complete analysis of the valences of the chromium was not made, but analyses in the pH range 2 to 3 revealed that at least 90% of the soluble chromium was in the hexavalent state; at a pH of 0.75 approximately 30% of the chromium was in the hexavalent state. Because the iron concentration in solution was low until the pH of the solution approached one, the high corrosion rate at the high pH values appeared to be primarily due to the solubility of chromium(VI). On the other hand, the high rates at low pH values were associated with the increased solubility of both iron(III) and chromium(III).

The minimums in both the nickel and chromium curves occurred in the pH range 1.4 to 1.6, which is the same range as the pH range of pure uranyl sulfate solutions containing 300 g of uranium per liter. Thus the experiments showed that the addition of either sulfuric acid or uranium trioxide to uranyl sulfate solutions increased the extent of corrosion.

The fact that the addition of uranium trioxide to uranyl sulfate solutions was not beneficial from a corrosion standpoint was confirmed in the dynamic testing program.<sup>(6)</sup> When a uranyl sulfate solution containing added uranium trioxide was circulated in a loop, the corrosion rate was observed to be at least as high as when uranium trioxide was not added. The amount of chromium in solution was found to be high, as in the static tests. Insufficient data have been collected to allow detailed conclusions to be drawn concerning the mechanism of the formation of the hexavalent chromium. Its appearance in solution

<sup>(5)</sup> K. Kraus, private communication.

<sup>(6)</sup> J. Gross, private communication.

## HRP QUARTERLY PROGRESS REPORT

was dependent on the pH, the oxygen concentration, and the presence of uranyl sulfate. Hexavalent chromium was not found in solutions that did not contain uranyl sulfate, except on a few occasions when nitric acid (pH < 0.5) was present. Regardless of the mechanism, the extent of corrosion was directly proportional to the concentrations of iron and chromium in solution.

It has been suggested by Kraus that the addition of excess sulfate ions may reduce the extent of corrosion. Future studies are planned that will include the effects of sulfate ion addition as well as the effect of temperature.

The study of the inhibitor properties of molybdenum in systems containing type 347 stainless steel has been completed. It has been concluded that the effectiveness of molybdenum as an inhibitor was not sufficiently great to warrant further experimental study. While the molybdenum was active in stifling the initial attack, its inhibitory effect was not evident in long-term static tests. Although the presence of molybdenum did not affect long-term corrosion, the physical appearance of these films was greatly different from that of films formed in its absence. The films formed in its presence were blue-black with a high luster. The indications were that these films may have had better mechanical properties than those formed in the absence of molybdenum.

### DYNAMIC CORROSION AND SOLUTION STABILITY

J. H. Gross      H. C. Savage

Seven dynamic test loops are in operation to study the corrosive action and solution stability of uranyl sulfate solution under various operating conditions. These loops are identified as B, C, E, F, H, J, and K.

Loops B and C, which have been rebuilt with new piping containing a large number of tees, ells, and bends, will be used in an effort to evaluate the corrosion rates at points of highly turbulent flow. Loops B and C had previously been cut up for inspection after approximately 5000 and 3000 hr of operation, respectively.<sup>(7)</sup>

An effort has been made during this quarter to find a combination of fuel, container, and operating conditions that will be suitable for reliable service over long periods. The investigation of possible structural materials has been confined principally to the stainless steels because of limitations on the availability of fabricated equipment and specimens of other materials. Experiments in which the test conditions are varied and uranyl sulfate is used as the basic fuel solution have been extended, and experiments at lower temperatures have been run. Of necessity an appreciable fraction of the work has been devoted to attempts to estimate the validity and reproducibility of data obtained with the present equipment.

**Solution Variables.** The solution variables studied have been oxygen, oxygen plus hydrogen, and copper additions, and concentration and temperature.

**Oxygen.** As has been discussed previously,<sup>(8)</sup> a continuously maintained oxygen concentration above 50 ppm appears to protect the uranyl ion against reduction in all cases. An unsuccessful attempt was made to start operation of loop F at 250°C with about 75 ppm of oxygen in uranyl sulfate solution containing 300 g of uranium per liter. Precipitation took

<sup>(7)</sup>H. C. Savage, C. G. Heisig, R. A. Lorenz, D. Schwartz, J. H. Gross, and R. E. Wacker, *op. cit.*, ORNL-1280, p. 40.

<sup>(8)</sup>*Ibid.*, p. 51.

place after about 40 hr, at which time the dissolved oxygen concentration was zero. The question of which phenomenon was causative, disappearance of oxygen or the beginning of reduction, remains unsettled. As previously reported by H. F. McDuffie *et al.*, it is significant that uranium that has been reduced and precipitated can be reoxidized by the introduction of sufficient oxygen at 250°C.

*Oxygen Plus Hydrogen Addition.* Loop A, which had been operating at 250°C with uranyl sulfate solution containing 40 g of uranium per liter plus a gas mixture of hydrogen and oxygen (hydrogen-to-oxygen ratios varying from 2:1 to 6:1), is now being replaced with a new loop. Operation of the loop was suspended after an explosion occurred in the pressure gage lines. The explosion occurred at the moment a dry gas sample was being taken from the gas phase in the top of the pressurizer. Approximately 20 similar samples had been safely taken prior to the explosion. The only damage to the system was the shattering of several pressure gages. A lucite shield in front of the gages was demolished by the explosion and flying gage fragments. Fortunately the protective shielding prevented injury to personnel. Although the circulating loop, pressurizer, and pump were undamaged, the loop was removed from service for examination of corrosion and erosion. The significant results of this examination are presented in a subsequent section of this report on "Flow Tests."

Before the explosion, approximately 400 additional hours of operation with hydrogen-to-oxygen pressure ratios of 2:1 had been accumulated. No effect of the presence of hydrogen on the stability of the solution was found.

*Copper.* The operation of a loop with uranyl sulfate solution containing 40 g of uranium per liter and 6.4 g of copper (as  $\text{CuSO}_4$ ) per liter at 250°C has been extended to a total time of 900 hours. The chemical behavior of the solution remained as described previously.<sup>(8)</sup> Twice when operation was shut down, solid material was found in the specimen holders. This material has been identified by x-ray diffraction as  $3\text{CuO}\cdot\text{SO}_3\cdot 2\text{H}_2\text{O}$ , a basic copper sulfate that is stable at elevated temperatures.<sup>(9)</sup> The hydrolysis of copper(II) probably accounts for the low pH of the fuel solution in this experiment. At the end of 900 hr of operating time the equipment failed due to erosive corrosion at a tee. This failure is discussed in a following section on "Flow Tests." Generalized corrosion attack (calculated from nickel concentration increase) was significantly increased by the presence of the copper sulfate.

*Concentration and Temperature.* Operations have been conducted at 250°C with uranyl sulfate solutions containing 5 g of uranium per liter for 1000 hr, 100 g of uranium per liter for 1000 hr, and 300 g of uranium per liter for 500 hr, in addition to the standard operation with uranyl sulfate solution containing 40 g of uranium per liter. Concentrations of 100 g of uranium per liter have been investigated at 100 and 150°C, and concentrations of 300 g of uranium per liter have been investigated at 100°C. The oxygen concentration used in all of this work has ranged upward from 200 ppm. In no case was there evidence of instability, except for the separation of uranium trioxide.

<sup>(9)</sup>E. Posnjak and G. Tunnel, *Am. J. Sci.* **18**, 1 (1929).

## HRP QUARTERLY PROGRESS REPORT

*Ratio of Uranium to Sulfate in Uranyl Sulfate Solution.* During the test with uranyl sulfate solution containing 5 g of uranium per liter, the equipment was shut down and drained twice. After rinsing, in both instances, a small amount of yellow, crystalline material was recovered from the loop. This material was identified by x-ray diffraction as  $\text{UO}_3 \cdot x\text{H}_2\text{O}$ . Material was recovered initially from the pump volute and on further inspection was found to be deposited also on the pressurizer walls. Throughout the test there had been a small decrease in solution pH and uranium concentration, but these effects were too slight to be attributed positively to the separation of uranium trioxide. An investigation of the uranium-to-sulfate ratio at low uranyl sulfate concentrations is being conducted by Marshall, Gill, and Jones in an effort to clarify these observations (cf., "Solution Chemistry" in Part III of this report).

At the end of a 130-hr run at 250°C with uranyl sulfate solution containing 40 g of uranium per liter in loop J, a small amount of uranium trioxide was found in stagnant regions of the specimen holder. With it was associated a small quantity of uranyl silicate and an appreciable amount of silica dioxide. A small amount of crystalline material was also found in the pressurizer. The concentration of silicon in solution during this run was approximately 40  $\mu\text{g}$  per milliliter of solution.

Silicon had not been observed previously in loops operating under these conditions. In this particular run a cast impeller had been installed in the pump and it is possible that the silica was moulding sand from the cast. Whether or not the presence of silica was responsible for the appearance of uranium trioxide is unknown. Precipitation of a silicate of uranium from  $\text{UO}_2\text{SO}_4$  solutions

contained in quartz at 250°C was observed previously.<sup>(10)</sup>

Studies conducted by Marshall, Gill, and Jones show that appreciable quantities of uranium trioxide can be dissolved in uranyl sulfate solution containing high concentrations of uranium at 250°C with an attendant rise in the pH (measured at room temperature) of the solution. On the hypothesis that hydrogen ion concentration plays a large part in the corrosion reaction, this means of lowering the hydrogen ion concentration provided a possible way of reducing the corrosion. Run F-11 of 130-hr duration was made at 250°C with uranyl sulfate solution containing 270 g of uranium per liter and with the pH adjusted from the normal 1.5 value to a value of 2.8 by uranium trioxide addition. No significant improvement was found over corrosion rates with normal uranyl sulfate solution containing 300 g of uranium per liter.

**Flow Tests.** The geometry and velocity effects on corrosion have been studied in flow tests. All circulating loops have been equipped with sample holders designed for testing numerous samples under various conditions of flow, temperature, and solution composition.

*Geometry and Velocity Effects.* The severity of erosion-assisted attack at sharp corners and in other regions of high turbulence has been described previously,<sup>(7)</sup> and further examples of this type of attack have been found during this period. Figure 25 (furnished by Gray of the Metallurgy Division) is a photograph of the junction of a 1/4-in. bypass line in the main 1 1/2-in. line of loop L. After 900 hr of service at 250°C with uranyl sulfate solution containing 40 g of uranium and 6.4 g of copper per

<sup>(10)</sup>W. L. Marshall, private communication.

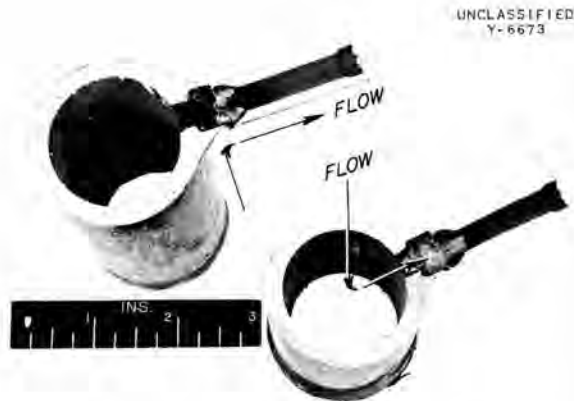


Fig. 25. Rupture in Loop L.

liter of solution, the illustrated rupture occurred at shutdown. Initially a small leak opened at the thinnest portion of the wall, and within 1 min the remaining thin wall tore half way around. This fitting had been made by butt-welding the small pipe to the outside of the large pipe and drilling a 1/4-in. hole through the wall of the large pipe on the axis of the small pipe to make a clean sharp-cornered hole. Flow through the small line was at a velocity of about 50 ft/sec while that in the main line was about 20 ft/sec. Similar pipe arrangements in other loops were examined, and similar attack was found in a loop operated under similar flow conditions with uranyl sulfate containing 300 g of uranium per liter but without copper.

Following a hydrogen-oxygen explosion, loop A was withdrawn from service and a forged tee that had been part of the main flow circuit was sectioned for examination. The fitting had been in service for 2500 hr at 250°C in contact with uranyl sulfate containing 40 g of uranium per liter and usually with hydrogen present, and the bulk solution velocity was 35 to 45 ft/sec. Erosion-assisted attack had taken place downstream from the main flow turn in a manner similar

to that observed in tees made by welding pipe together.<sup>(7)</sup> The attack was smoother, comparatively, and had progressed evenly along the limb of the tee, across the weld, and along the main pipe for a short distance.

In order to make a rough estimate of limitations on the use of conventional pipe configurations, two loops have been built that contain crosses, tees, angles, and bends of various radii, in 1/2-, 1-, and 1 1/2-in. pipe. The fittings used are commercial forgings and locally produced welded-pipe assemblies. These loops replaced loops B and C, and they were put in service at 100°C with uranyl sulfate solution containing 100 g of uranium per liter. At the time of this report, there is indirect evidence that there may be erosion-assisted attack in some of the shapes of 1/2-in. line where the flow rate is 20 ft/sec.

*Sample Holders.* All circulating loops are now equipped with sample holders designed to test numerous specimens under various conditions of flow, temperature, and solution composition. There has not been sufficient experience with the pin and coupon sample holders described in the last quarterly report<sup>(7)</sup> for a discussion of flow effects at this time. However, some design modifications and simplifications have resulted from the tests completed thus far. Also, new holders are being made of titanium to prolong their useful life.

*Materials Tests.* Pin specimens of various stainless steels, titanium, and tantalum have been tested in uranyl sulfate solutions of various concentrations.

*Stainless Steels.* Evaluation of the various available stainless steels by means of the pin specimens<sup>(7)</sup> has

## HRP QUARTERLY PROGRESS REPORT

continued under a number of conditions. Some of the work has involved repetition and duplication in an effort to determine reproducibility of the magnitude of attack on a particular alloy. However it is possible to rank the alloys as to susceptibility to attack under various conditions with the data now available. At 250°C in uranyl sulfate solutions containing 5 to 300 g of uranium per liter, type 321 stainless steel was uniformly the least attacked of the steels tested. Types 347 and 316 stainless steel are not appreciably poorer, except in the presence of copper. At 100 and 150°C, on the other hand, type 309 columbium-stabilized stainless steel occupies the preferred position, and types 347 and 304 stainless steel are only slightly more susceptible to attack. Carpenter 20 stainless steel does not stand up as well as other stainless steels under any of these conditions. Lowering the temperature to 100°C gives a very appreciable lowering of the corrosion rate. Initial data show corrosion rates on stainless steels of less than 0.5 mpy when tested at 100°C in uranyl sulfate solutions containing 100 and 300 g of uranium per liter.

Several experiments have been run with pin specimens insulated from the system by a layer of Teflon tape. No significant differences have been found between these and adjacent un-insulated specimens. Further experiments along this line are being conducted.

*Titanium.* Pin specimens of titanium have been tested during this period at 250°C with uranyl sulfate solution containing 300 g of uranium per liter and with uranyl sulfate solution containing 40 g of uranium and 6.4 g of copper per liter, and at 150°C with uranyl sulfate solution containing 100 g of uranium per liter. No attack has been found under these conditions,

nor has attack on this metal been observed in any previous test. The loop being built to replace loop A will contain a section of titanium pipe and several inserts of titanium to test the effect of hydrogen on corrosion and the metallurgical properties of the metal. Construction of a complete loop and the major portions of a Model 100A pump from titanium is also planned.

*Tantalum.* To test the susceptibility of tantalum to hydrogen embrittlement, two tantalum pins were mounted in a corner of loop A and exposed at 250°C for 460 hr to uranyl sulfate solution containing 40 g of uranium per liter and dissolved hydrogen and oxygen. The specimens showed no flow pattern, but it lost weight corresponding to a corrosion rate of approximately 9 mpy. A simple bend test comparison of exposed and unexposed specimens gave an inconclusive result in regard to hydrogen embrittlement, although there is, perhaps, some evidence of it.

**Westinghouse Model 100A Pump.** The Westinghouse Model 100A pumps used in the test loops have in general given satisfactory service. The most common cause of failure has been leakage of solution through the Inconel diaphragm separating the rotor chamber and the oil-cooled stator windings. Three of the 17 pump diaphragms have either leaked or corroded to the extent that continued service would probably have resulted in leakage. One pump developed a leak after operating for about 1200 hr with uranyl sulfate containing 40 g of uranium per liter. A second pump diaphragm was slightly pitted after operation for a few hundred hours with uranyl sulfate containing 100 g of uranium per liter. This pump was then switched to a loop circulating uranyl sulfate containing 5 g of uranium per liter and developed a leak after about 100 hr of additional

## FOR PERIOD ENDING JULY 1, 1952

operation. The pump used in loop L with uranyl sulfate containing 40 g of uranium and 6.4 g of copper per liter had a badly corroded diaphragm after approximately 1200 hr of operation. The Inconel diaphragms of all other pumps appear to be in good condition even in uranyl sulfate solutions containing up to 300 g of uranium per liter.

Stress corrosion is probably the reason for the apparent wide variation in ability of different diaphragms to resist attack. This is indicated by the pattern of attack in one instance in which the attack was very clearly localized to those portions of the can that were not backed up by the iron core of the stator. Microscopic examination of a section of one of the cans that failed also bore this out.

Three pumps have failed as a result of open windings in the stator. Two of these failures were accounted for by current overloading.

An effort is being made to repair these pumps in laboratory shops. One pump with a leaking diaphragm is being repaired by substituting a sound diaphragm from another pump with a faulty stator. After the removal of the diaphragm, it appeared feasible to rewind the motor and install a new diaphragm. Material for new diaphragms, in which type 321 stainless steel will be substituted for Inconel, has been ordered. The small sacrifice in electrical efficiency brought about by this substitution will be compensated by the better corrosion resistance of the stainless steel. A type 347 stainless steel diaphragm substituted for the Inconel diaphragm in a Model 30A pump produced a 10 to 15% loss in electrical efficiency.

A cast impeller made of type 347 stainless steel was used in one loop.

After 384 hr of operation in uranyl sulfate solutions at 250°C, the cast impeller lost 60 g in weight. Excessive corrosion was noted on the circumference of the front and rear hubs and on the front shroud near the outer edge. A standard, wrought stainless steel impeller sustains very little if any weight loss under similar conditions, although some corrosion is usual on the impeller hubs. On this basis the cast impeller is inferior to the wrought impeller.

A titanium impeller is now being fabricated since titanium continues to exhibit excellent corrosion resistance. A corrosion resistant impeller would virtually eliminate the loss of the pump hydraulic-thrust balance from corrosion at the impeller hubs under the seal rings. Present indications are that 2000 to 3000 hr of operation at 250°C in uranyl sulfate solution containing 40 g of uranium per liter is required to lose thrust balance because of corrosion of the wrought stainless steel impeller hubs.

The Westinghouse Model 100A pump in the HRE system was removed and inspected during the past quarter. All pump parts, including bearings, were in excellent condition. The gasketed flanges on this pump were welded after this inspection to eliminate leakage. No difficulty was encountered in welding, and pump operation was found to be satisfactory afterward.

### STATIC CORROSION STUDIES

J. L. English	H. L. Barker
S. H. Wheeler	R. F. Benson
L. L. Allen	J. W. Brown, Jr.
L. L. Fairchild	

Uranyl Sulfate Corrosion Studies.  
The following phases of the corrosion of type 347 stainless steel in uranyl

## HRP QUARTERLY PROGRESS REPORT

sulfate solutions at 250°C were examined during the past quarter: (1) the effect of uranium and oxygen concentrations on corrosion at 250°C (as a corollary study, the reliability of the dissolved nickel method for the determination of corrosion rates was established by comparison with corrosion rates obtained from measurement of actual defilmed weight losses), (2) the effect of preconditioning type 347 stainless steel surfaces in very dilute solutions of oxygenated uranyl sulfate at 250°C prior to their use in more concentrated solutions at 250°C, and (3) the use of oxygen gas for pretreatment at 250°C to enhance the corrosion resistance of type 347 stainless steel in contact with uranyl sulfate solutions at 250°C.

*Effect of Dissolved Oxygen.* The static corrosion behavior of type 347 stainless steel was investigated in uranyl sulfate solutions containing 100 and 300 g of uranium per liter and with dissolved oxygen ranging from approximately 100 to 2500 ppm at 250°C. The initial phase of the oxygen-uranium concentration studies in uranyl sulfate solutions containing 40 g of uranium per liter and dissolved oxygen of 400 to 3700 ppm at 250°C was reported in the last quarterly progress report.<sup>(3)</sup>

In the work to be described, newly machined type 347 stainless autoclaves were used to contain the solutions and specimens at 250°C. The autoclaves held 150 ml of the test solution at room temperature. The corrosion test specimens were machined from 3.80-cm-dia type 347 stainless steel bar; they were 0.5 cm in thickness and 3.0 cm in diameter. A 0.5-cm-dia hole was drilled in each specimen to permit support by stainless steel hangers in the test solutions. The average surface area was approximately 20 cm<sup>2</sup>. The total surface area of specimen

and autoclave walls immersed in the uranyl sulfate solution was nearly 245 cm<sup>2</sup> after solution expansion at 250°C. The submerged surface area to solution volume ratio at 250°C was 1.6 cm<sup>2</sup> per ml of solution. Type 347 stainless steel wire was used to support the specimens in the solutions. Previous studies indicated little or no galvanic or contact corrosion on test specimens that were coupled directly to the autoclave mass with the wire hangers. The corrosion behavior in these cases was identical with results obtained by using quartz-rod hangers to electrically insulate the specimens from the autoclaves.

The desired dissolved-oxygen concentrations in the test solutions at 250°C were obtained from the thermal decomposition of 35% hydrogen peroxide added in calculated amounts to the solutions at room temperature. The oxygen solubility data were taken from existing information on the solubility of oxygen in water at 250°C and therefore represent only approximations for uranyl sulfate solutions. Table 6 presents a summary of the dissolved-oxygen data assumed for the purpose of this investigation.

Chemical analyses of the two uranyl sulfate solutions are listed in Table 7. The mole ratio of uranium to sulfate indicated slightly acid-deficient solutions in both cases; the deficiency was more pronounced in the solution containing 100 g of uranium per liter.

Duplicate tests were run at each oxygen concentration in the two uranyl sulfate solutions; a total of 16 tests was made. Single specimens were placed in each autoclave. The general test procedure consisted of exposing the specimens at 250°C for weekly periods after which they were scrubbed in distilled water, examined, and

Table 6

**APPROXIMATE DISSOLVED OXYGEN CONTENT IN URANYL SULFATE SOLUTIONS  
CONTAINING 100 AND 300 g OF URANIUM PER LITER AT 250°C**

OXYGEN PARTIAL PRESSURE (psia)	DISSOLVED OXYGEN (ppm)	
	In Solution Containing 100 g of U per liter	In Solution Containing 300 g of U per liter
25	125	100
75	375	300
150	750	600
500	2500	2000

Table 7

**CHEMICAL ANALYSES OF URANYL  
SULFATE TEST SOLUTIONS**

Total U, g/l	97.7	300.5
SO <sub>4</sub> , g/l	38.4	120.6
U-to-SO <sub>4</sub> ratio	1.026	1.005
U(IV), g/l	<0.1	0.1
NH <sub>4</sub> , g/l	<0.1	<0.03
NO <sub>3</sub> , g/l	0.16	0.10
Ni, g/l	<0.001	0.001
Density at 25°C	1.133	1.405
pH (0.1 M solution)	2.75	2.49
pH (lab solution as used)	1.95	1.30

weighed. The initial test solutions, except for make-up, were used throughout the entire test. At the time of specimen examination, 10-ml solution samples were removed from the autoclaves for analytical purposes and replaced with 10-ml volumes of the original uranyl sulfate solution. In each test solution, the final volume was adjusted so that with the addition of the necessary hydrogen peroxide to generate the desired dissolved oxygen content at 250°C the starting volume for each weekly run was always 150 ml. In the solutions with high dissolved-oxygen content, 2000 to 2500 ppm, the hydrogen peroxide addition was 9.0 ml weekly. Thus, during the course of

the tests, the original uranium content of 100 or 300 g per liter of solution was gradually reduced by dilution effects to approximately 75 or 230 g per liter of solution. In all other tests, in which the hydrogen peroxide additions were 0.3, 1.0, and 2.2 ml to produce the desired dissolved-oxygen content at 250°C, the dilution effect on uranium concentration was not nearly so pronounced. The tests were operated for a total of 11 weeks. Nine of the exposure periods were of weekly duration; the final exposure period was of 2 week's duration.

No difficulty was encountered in the operational behavior of the tests during the 11 weeks, with one exception. There were no signs of solution reduction as determined by chemical analyses for uranium (corrected for dilution effect). The exception to satisfactory behavior was the solution containing 300 g of uranium per liter and 100 ppm of dissolved oxygen at 250°C. With these conditions it was not possible to maintain a stable system. Uranium was precipitated from the solutions as oxide and there was severe corrosion attack on the test specimens. This duplicate set of tests was repeated three times with similar results. It was concluded after six failures that

## HRP QUARTERLY PROGRESS REPORT

instability was due to an insufficient amount of dissolved oxygen in solution or the rate of diffusion of oxygen to all parts of the system was too slow.

The physical appearance of the specimens was much the same in all tests. The color of the oxide films ranged from dull, light gray to dark, gray-black. No indications of localized corrosion attack were found even after the oxide films were removed electrolytically. No signs of contact or crevice corrosion were apparent on the specimens in areas contacted by stainless steel hangers.

The specimens were defilmed at 75°C by cathodic treatment in 5 wt % sulfuric acid solution containing 2 ml per liter of an organic inhibitor, Rodine 77 - a product of the American Chemical Paint Co. The rate of metal thickness loss on blank specimens in this operation was 0.001 mil in 3 min, corresponding to a weight loss of 0.025 mg/cm<sup>2</sup>. It was determined from

unexposed specimens that approximately 100 cm<sup>2</sup> of metal surface could be defilmed in the inhibited sulfuric acid solution before depletion of the organic inhibitor resulted in much greater weight losses on the specimens. The final corrosion rates, after defilming, for the duplicate type 347 stainless steel samples are reported in Table 8.

The measured weight changes on the test specimens after removal from the solution and scrubbing in distilled water were uninformative as to the actual extent of corrosion damage. Little, if any, agreement in as-removed weight changes was obtained on duplicate specimens exposed to a similar set of test conditions. Frequently, one specimen of a duplicate set exhibited a weight increase, whereas the companion specimen showed a weight loss. Therefore, since such data were meaningless, the as-removed weight change values are not included in this report.

Table 8

### CORROSION RATES FOR DEFILMED TYPE 347 STAINLESS STEEL EXPOSED TO OXYGENATED URANYL SULFATE SOLUTIONS CONTAINING 100 AND 300 g OF URANIUM PER LITER AT 250°C FOR 11 WEEKS

URANIUM CONCENTRATION (g/l)	OXYGEN PARTIAL PRESSURE (psia)	ESTIMATED DISSOLVED OXYGEN (ppm)	CORROSION RATE (mpy)	
			Specimen 1	Specimen 2
97.7	25	125	0.15	0.17
	75	375	0.21	0.20
	150	750	0.23	0.31
	500	2500	0.23	0.23
300.5	25	100	failed	failed
	75	300	0.26	0.24
	150	600	0.29	0.31
	500	2000	0.28	0.30

FOR PERIOD ENDING JULY 1, 1952

The lack of uniformity in measured weight changes was attributed to the bulk oxide films formed on the specimens during exposure. These films have been identified by x-ray and electron diffraction studies as consisting of  $\alpha\text{-Fe}_2\text{O}_3$  and/or  $\text{Cr}_2\text{O}_3$ .

The corrosion rates showed excellent agreement between duplicate, defilmed specimens. The magnitude of the rates after 11 weeks was well within tolerable corrosion limits. The difference between the corrosiveness of the uranyl sulfate solutions containing 100 and 300 g of uranium per liter on type 347 stainless steel was practically negligible in terms of long-time operation. It was apparent also that the final corrosion rates for 11 weeks in the satisfactorily operated static systems were independent of the dissolved oxygen concentration at 250°C.

For a more complete evaluation of the effects of uranium and oxygen concentrations on the corrosion of type 347 stainless steel at 250°C, the data obtained in the present investigation were compared with corrosion data reported previously for uranyl sulfate solutions containing 40 g of uranium per liter tested for 10.5 weeks at 250°C.<sup>(3)</sup> These data are presented in Table 9. The average corrosion rates for defilmed specimens are reported for the various exposure conditions.

No significant long-time effect of oxygen or uranium concentration on the corrosion of type 347 stainless steel was indicated by the data in Table 9. The slight variations in reported values could be attributed to differences in metal homogeneity, test conditions, etc., rather than to a direct effect of change in oxygen

Table 9

AVERAGE CORROSION RATES FOR DEFILMED TYPE 347 STAINLESS STEEL EXPOSED IN OXYGENATED URANYL SULFATE SOLUTIONS FOR 10.5 TO 11 WEEKS AT 250°C

URANIUM CONCENTRATION (g/l)	APPROX. DISSOLVED OXYGEN (ppm)	CORROSION RATE (mpy)
40.9	400	0.16
	775	0.16
	1275	0.14
	3700	0.22
97.7	125	0.16
	375	0.21
	750	0.27
	2500	0.23
300.5	100	failed
	300	0.25
	600	0.30
	2000	0.29

## HRP QUARTERLY PROGRESS REPORT

and uranium content. Under static conditions at 250°C, the corrosion rates for defilmed type 347 stainless steel exposed in uranyl sulfate solutions containing 40, 100, and 300 g of uranium per liter and dissolved oxygen ranging from 125 to 3700 ppm were thus found to lie within 0.2 to 0.3 mpy after 11 weeks of exposure. The exception to this behavior was the case of the solution containing 300 g of uranium per liter and slightly less dissolved oxygen (100 ppm); stable systems were not obtained with these conditions.

Dissolved nickel concentrations were followed regularly during the operation of the tests for evaluation of corrosion rates and for final comparison with rates determined by defilmed weight-loss measurements on the test specimens. The total, cumulative, dissolved nickel content, corrected for the amount removed weekly in the analytical solution samples and adjustment of starting solution volumes to 150 ml, are reported in Table 10. The dissolved nickel values are included for the duplicate tests to illustrate the

Table 10

CORRECTED, CUMULATIVE, DISSOLVED NICKEL CONTENT IN OXYGENATED URANYL SULFATE SOLUTIONS AT 250°C

EXPOSURE (weeks)	URANIUM CONCENTRATION (g/l)	DISSOLVED NICKEL ( $\mu\text{g/ml}$ )							
		Dissolved Oxygen (ppm)							
		100 to 125		300 to 375		600 to 750		2000 to 2500	
		Speci- men 1	Speci- men 2	Speci- men 1	Speci- men 2	Speci- men 1	Speci- men 2	Speci- men 1	Speci- men 2
0	97.7	<1	<1	<1	<1	<1	<1	<1	<1
1		92	101	106	106	115	140	160	153
2		90	127	107	105	115	154	197	183
3		95	139	112	115	119	168	212	198
4		104	156	122	119	139	192	240	217
5		109	173	129	131	148	221	255	227
6		120	168	136	140	149	232	273	249
7		118	176	137	142	159	242	272	249
8		130	168	151	152	172	251	287	275
9		129	163	148	152	175	246	302	277
11		138		158	170	189	253	307	276
0		300.5			1	1	1	1	1
1				180	200	215	200	185	152
2				197	211	231	211	211	189
3				202	226	249	232	231	225
4				221	236	260	246	252	230
5				246	270	289	253	261	239
6				279	284	299	275	282	265
7				257	283	297	280	286	278
8				281	295	313	300	308	285
9				286	296	324	303	314	300
11				302	315	335	315	329	

degree of reproducibility, or lack thereof, for identical test conditions. A graph of the average dissolved nickel values as a function of exposure time is given in Fig. 26.

Corrosion rates determined by the cumulative, corrected, dissolved nickel values after 1 and 11 weeks of exposure of duplicate specimens are presented in Table 11. In the calculation of corrosion rates by the dissolved nickel method, it was assumed that the average nickel content in the type 347 stainless steel specimens and autoclaves was 10.5 wt %. The reported rates represent attack on approximately 245 cm<sup>2</sup> of surface area, which included the area of the test specimen and the area of the autoclave immersed in the test medium at 250°C. It was assumed also that

corrosion attack was uniform over all surfaces.

Table 12 shows a comparison between the average corrosion rates after 11 weeks as determined by the defilmed weight-loss measurements and the corrected, cumulative, dissolved nickel content in the uranyl sulfate solutions containing 100 and 300 g of uranium per liter at 250°C.

The over-all agreement between the defilmed and dissolved nickel corrosion rates was very good in view of the numerous variables introduced in the two methods of evaluation. More consistent agreement between the two sets of rates was obtained in the solution containing 100 g of uranium per liter than in the solution containing 300 g of uranium per liter.

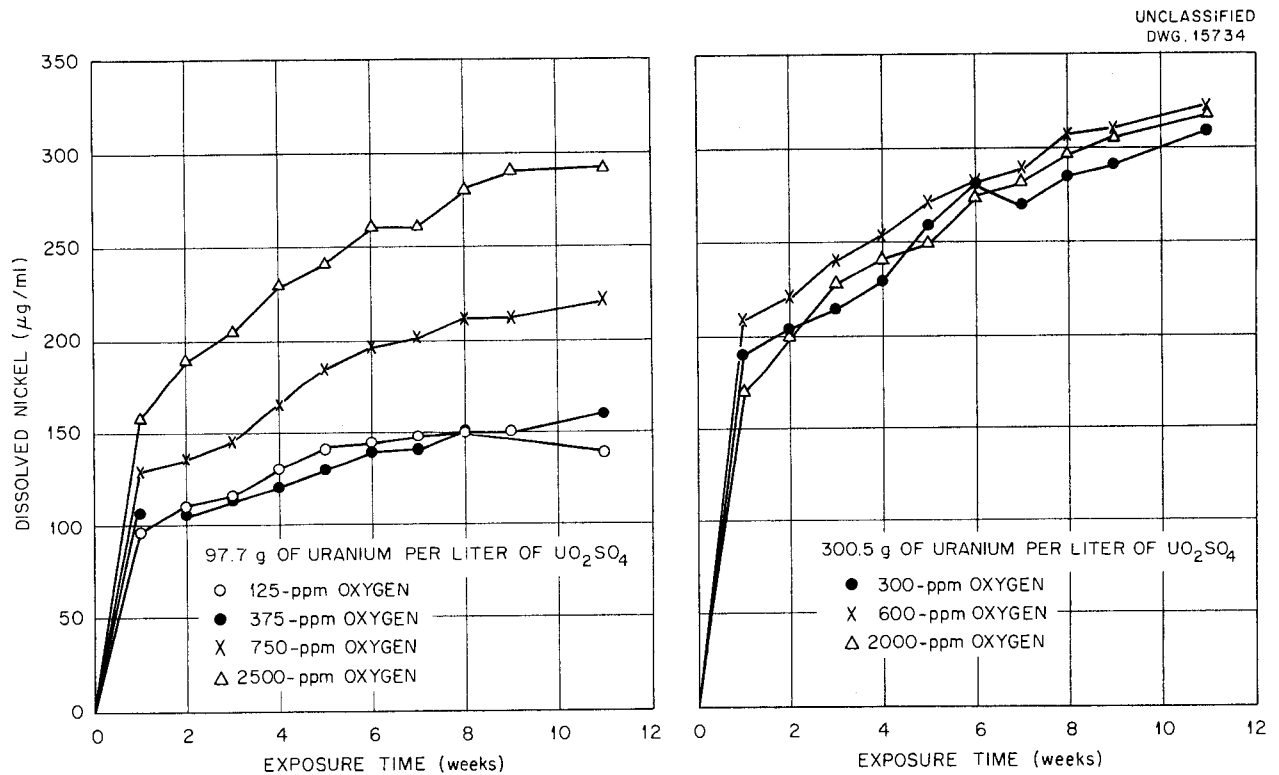


Fig. 26. Corrected, Cumulative, Dissolved Nickel Content of Oxygenated Uranyl Sulfate at 250°C.

# HRP QUARTERLY PROGRESS REPORT

Table 11

**CORROSION RATES ON TYPE 347 STAINLESS STEEL DETERMINED FROM CORRECTED, CUMULATIVE, DISSOLVED NICKEL CONTENT IN OXYGENATED URANYL SULFATE SOLUTIONS AT 250°C**

EXPOSURE (weeks)	URANIUM CONCENTRATION (g/l)	DISSOLVED OXYGEN (ppm)	CORROSION RATE (mpy)	
			Specimen 1	Specimen 2
1	97.7	125	1.36	1.52
11		125	0.19	
1	97.7	375	1.57	1.57
11		375	0.22	0.23
1	97.7	750	1.70	2.07
11		750	0.26	0.34
1	97.7	2500	2.41	2.31
11		2500	0.40	0.36
1	300.5	100	failed	failed
11		100	failed	failed
1	300.5	300	2.66	2.96
11		300	0.41	0.43
1	300.5	600	3.18	2.96
11		600	0.45	0.42
1	300.5	2000	2.77	2.28
11		2000	0.43	

In summation of the results obtained in this series of tests to determine the effect of uranium and oxygen concentrations on the corrosion of type 347 stainless steel, it may be stated that:

1. In static systems, the long-range effect of oxygen and uranium concentrations (on the corrosion of type 347 stainless steel at 250°C), within the limits studied, appears not too significant. Final corrosion rates, determined by defilmed weight losses and dissolved nickel content in solutions containing 40, 100, and 300 g of uranium per liter and 125 to 3700 ppm of dissolved oxygen, were

between 0.15 and 0.45 mpy after 10.5 to 11 weeks of exposure.

2. After short-term exposure of one week, the corrosion rate was increased slightly, from 1.44 to 2.36 mpy (determined by dissolved nickel) as the dissolved oxygen content increased from 125 to 2500 ppm in solutions containing 100 g of uranium per liter. This effect may not be realistic, however, and will require further and more complete examination. There was no such tendency exhibited in the solutions containing 300 g of uranium per liter and increased oxygen content. In general these solutions were slightly more corrosive during

Table 12

**COMPARISON BETWEEN AVERAGE CORROSION RATES ON TYPE 347 STAINLESS STEEL  
DETERMINED BY DEFILMED WEIGHT-LOSS VALUES AND CORRECTED DISSOLVED  
NICKEL CONTENTS IN OXYGENATED URANYL SULFATE SOLUTIONS  
AFTER EXPOSURE FOR 11 WEEKS AT 250°C**

URANIUM CONCENTRATION (g/l)	DISSOLVED OXYGEN (ppm)	CORROSION RATE (mpy)	
		By dissolved nickel	By defilmed weight loss
97.7	125	0.19	0.16
	375	0.23	0.21
	750	0.30	0.27
	2500	0.38	0.23
300.5	100	failed	failed
	300	0.42	0.25
	600	0.44	0.30
	2000	0.43	0.29

the initial week of exposure than the solutions containing 100 g of uranium per liter.

3. The dissolved nickel method for the determination of corrosion rates appears to be reliable when the corrosion attack is definitely of a uniform nature. Very good agreement was obtained by this method in comparison with results reported from defilmed weight-loss measurements.

*Preconditioning in Dilute Uranyl Sulfate Solutions at 250°C.* Since the studies described in the preceding section showed that the corrosion rate of type 347 stainless steel in oxygenated uranyl sulfate solutions at 250°C was quite high initially but decreased markedly thereafter, an attempt was made to limit the magnitude of the initial corrosion attack. The method involved the use of very dilute, oxygenated uranyl sulfate solutions to "condition" the type 347 stainless

steel at 250°C prior to its exposure in more concentrated solutions. The dilute uranyl sulfate solution contained 0.5 g of uranium per liter and 135 ppm of dissolved oxygen produced from the thermal decomposition of hydrogen peroxide that was added to the solution at room temperature.

The type 347 stainless steel test autoclaves were pickled with 10% HNO<sub>3</sub>-4% HF (by weight) at 60°C, scrubbed and washed in distilled water, and then pretreated for 24 hr with 1 wt % HNO<sub>3</sub> at 250°C. The pretreatment was employed to minimize effects of the autoclave surfaces on the corrosion behavior of the test specimens. The machined test specimens, which were 3.0 cm in diameter and 0.5 cm thick, were supported in the test media by means of type 347 stainless steel hangers.

After 48 hr of exposure at 250°C, the dilute uranyl sulfate solutions

## HRP QUARTERLY PROGRESS REPORT

were replaced with solutions containing 40, 100, and 300 g of uranium per liter and the tests operated for a period of seven weeks with dissolved oxygen contents of 100 to 135 ppm at 250°C. The specimens were weighed and examined weekly, and solution samples were withdrawn for uranium and nickel analyses. The oxygen content was maintained by addition of the necessary hydrogen peroxide.

The test specimens were in excellent condition after removal from the dilute uranyl sulfate solutions. The surfaces were covered with lustrous interference colors ranging from golden yellow to red-purple; no bulk oxide films of appreciable thickness were observed. The corrosion rates for the three specimens, as determined from the as-removed weight losses, ranged from 0.08 to 0.18 mpy for 48 hours. The dissolved nickel content did not exceed 1  $\mu\text{g}/\text{ml}$  in any of the solutions, and chemical analyses indicated no reduction in uranium.

The corrosion data for subsequent exposure in uranyl sulfate solutions

containing 40, 100, and 300 g of uranium per liter are reported in Table 13. The corrosion rates are based on the as-removed weight losses, since it was assumed from the appearance of the specimens that the effect of film weight on the over-all weight loss was almost negligible. The weight-loss data for the initial exposure period of 216 hr include weight losses incurred during the 48-hr conditioning treatment.

A steady increase of the dissolved nickel content in the three solutions was observed during the course of the tests. The nickel in the solution containing 40 g of uranium per liter increased from 8 to 16  $\mu\text{g}/\text{ml}$ , from 11 to 30  $\mu\text{g}/\text{ml}$  in the solution containing 100 g of uranium per liter, and from 25 to 51  $\mu\text{g}/\text{ml}$  in the solution containing 300 g of uranium per liter. The total exposure time covered by these increases was seven weeks. It was not possible to calculate corrosion rates by the dissolved nickel content with any degree of accuracy because the amount of nickel contributed to the solutions from the pretreated

Table 13

**CORROSION RATES DETERMINED FROM AS-REMOVED WEIGHT LOSSES ON TYPE 347 STAINLESS STEEL CONDITIONED IN URANYL SULFATE SOLUTION CONTAINING 0.5 g OF URANIUM PER LITER FOR 48 HR AT 250°C AND EXPOSED IN OXYGENATED URANYL SULFATE SOLUTIONS CONTAINING 40, 100, AND 300 g OF URANIUM PER LITER AT 250°C**

CUMULATIVE EXPOSURE (hr)	CORROSION RATE (mpy)		
	Uranium Concentration (g/l)		
	40	100	300
216	0.19	0.20	0.51
384	0.11	0.12	0.30
522	0.08	0.05	0.22
888	0.04	0.05	0.13
1224	0.05	0.04	0.11

FOR PERIOD ENDING JULY 1, 1952

autoclave surfaces was not known. However, to compare the final corrosion rates based on as-removed weight loss measurements with the actual metal consumed in the corrosion reactions, the specimens were electrolytically defilmed at 75°C for 3 min in 5 wt % sulfuric acid containing an organic inhibitor and the weight losses determined. The as-removed weight losses and the weight losses determined by defilming are compared in Table 14.

The agreement in the rates obtained by the two methods was reasonably good. The difference between each set of rates may be interpreted as a relative measure of the oxide film weights. As the uranium concentration was increased from 40 to 300 g/l, the films were thicker and heavier, although in every case the films remained lustrous and metallic gray in color. None of the heavy, dull-appearing, gray-black oxide films such as are generally encountered on unconditioned specimens exposed to similar static test conditions were observed.

A further comparison of the effect of the conditioning treatment in uranyl sulfate solution containing

0.5 g of uranium per liter on the corrosion behavior of type 347 stainless steel at 250°C was made from corrosion data obtained from similar tests not employing the preliminary conditioning treatment. For example, after exposure in a solution containing 40 g of uranium per liter and 400 ppm of dissolved oxygen for 1200 hr at 250°C, the corrosion rate (determined by dissolved nickel) was 0.23 mpy as compared to the defilmed weight-loss rate of 0.08 mpy obtained on a conditioned specimen after 1224 hr at 250°C in a solution containing 40 g of uranium per liter and 135 ppm of dissolved oxygen. A corrosion rate of 0.32 mpy (determined by dissolved nickel) was observed in uranyl sulfate solution containing 100 g of uranium per liter and 125 ppm of dissolved oxygen after 1176 hr at 250°C as compared with the defilmed weight-loss rate of 0.11 mpy on a conditioned specimen after 1224 hr at 250°C in a similar solution.

As reported previously, a stable system was not obtained with a solution containing 300 g of uranium per liter and 100 ppm of dissolved oxygen in a nitric acid-pretreated type 347 stainless steel autoclave at 250°C. However, it was possible to operate a

Table 14

COMPARISON OF CORROSION RATES ON CONDITIONED TYPE 347 STAINLESS STEEL DETERMINED BY AS-REMOVED AND DEFILMED WEIGHT LOSSES AFTER 1224 HR IN OXYGENATED URANYL SULFATE SOLUTIONS AT 250°C

URANIUM CONCENTRATION (g/l)	CORROSION RATE (mpy)	
	As-removed weight loss	Defilmed weight loss
40	0.05	0.08
100	0.04	0.11
300	0.11	0.27

## HRP QUARTERLY PROGRESS REPORT

stable system under these conditions after the type 347 stainless steel was conditioned in dilute, oxygenated uranyl sulfate; the 1224-hr corrosion rate determined by defilmed weight loss was 0.27 mpy.

Additional tests were started with newly machined type 347 stainless steel autoclaves to obtain a further appraisal of the effect of preliminary conditioning on the corrosion behavior of stainless steel in oxygenated uranyl sulfate solutions of various uranium concentrations. The nitric acid pretreatment used in previous tests was eliminated from this series to allow for evaluation of corrosion rates determined over the entire system by dissolved nickel content. Some data are reported for the corrosion of conditioned type 347 stainless steel in uranyl sulfate solution containing 40 g of uranium per liter and an estimated 135 ppm of dissolved oxygen at 250°C.

The conditioning treatment in uranyl sulfate solution containing 0.5 g of uranium per liter and 135 ppm of dissolved oxygen at 250°C was conducted for 24 hr rather than the 48 hr employed previously. The specimen exhibited a lustrous, pale-blue surface after the 24 hr of exposure, and the walls of the stainless steel autoclave were somewhat similar in appearance. The corrosion rate on the specimen, as determined by the as-removed weight loss, was 0.8 mpy; the rate over the entire system, 245-cm<sup>2</sup> surface area, was 1.7 mpy, as calculated from the 24-hr dissolved nickel content of 16 µg/ml. These rates, extrapolated to 0.4 and 0.9 mpy, respectively, for a 48-hr period, were considerably higher than the maximum as-removed weight-loss rate of 0.2 mpy reported previously for a 48-hr exposure period. The difference may be attributed possibly to changes

in test conditions and materials from one set of tests to another.

Nevertheless, the dilute uranyl sulfate solution was replaced with a solution containing 40 g of uranium per liter and 135 ppm of dissolved oxygen at 250°C and the test was run for one week. At the end of the week, a weight increase of 0.22 mg/cm<sup>2</sup> was found for the test specimen. The surfaces were lustrous gray in color as compared to the shiny blue color present after the conditioning treatment. The corrosion rate over the entire system during the one week was calculated from the dissolved nickel content of 10 µg/ml to be 0.13 mpy. The over-all corrosion rate on the system, including the attack incurred during the conditioning treatment, was 0.3 mpy in 216 hr, as determined from the total, cumulative, dissolved nickel content of 26 µg/ml. This was an improvement over the rate obtained from the dissolved nickel content in a uranyl sulfate solution containing 40 g of uranium per liter and 400 ppm of dissolved oxygen; after one week of test, the corrosion rate was 0.6 mpy on a specimen that was not initially conditioned in dilute uranyl sulfate solution.

Based on these preliminary data from static tests, it appears that the use of a preliminary conditioning treatment in very dilute, oxygenated uranyl sulfate solutions at 250°C enhances somewhat the corrosion resistance of type 347 stainless steel when exposed subsequently to more concentrated solutions of oxygenated uranyl sulfate at 250°C. Additional study would be needed to determine whether this inhibitory effect is as realistic as the initial results show. In view of the relatively minor effect indicated, however, further work is not contemplated at this time.

*Pretreatment of Type 347 Stainless Steel in Oxygen at 250°C.* The presence of dissolved oxygen in uranyl sulfate solutions contacting stainless steel at 250°C was found to be necessary to maintain a stable system. It was found also that the use of aqueous solutions of dilute nitric and chromic acids at 250°C for a preliminary conditioning of the stainless steel prior to exposure in uranyl sulfate solutions reduced considerably the oxygen requirements necessary for solution stability in the absence of the pretreatments. The aqueous pretreatment solutions invariably added to the corrosion problem since they mildly attacked stainless steel at temperatures of 250°C and had to be considered in the over-all evaluation of corrosion damage on a metal or alloy exposed subsequently in uranyl sulfate solutions.

In order to eliminate the corrosion attack by acidic pretreatment solutions on stainless steel but still produce a relatively nonreactive surface on the stainless alloy, the practicability of pretreating at 250°C with oxygen gas was considered. Such a pretreatment appeared logical since the role of oxygen in maintaining uranyl sulfate stability is of the utmost importance in untreated stainless steel systems.

The use of enriched oxygen atmospheres was attempted without success during the early phases of the homogeneous reactor static corrosion testing program. In these tests, stainless steel autoclaves and component parts were heated in a box furnace maintained at 250°C. Compressed oxygen gas was introduced into the furnace to enrich the atmosphere. However, autoclaves treated in this manner failed to contain uranyl sulfate solutions satisfactorily at 250°C; solution reduction and

severe corrosion attack were encountered.

Recently, a different technique was employed for the oxygen pretreatment during the operation of small-scale corrosion studies for the boiling reactor. Oxygen gas was used to pressurize a dry, sealed autoclave to 50 psig at room temperature. The autoclave was then heated at 250°C for 24 hr before the uranyl sulfate solution was introduced and the system reheated to 250°C. The results of two preliminary tests are summarized below.

In the first test, designated as Test No. 1-6, a 530-ml total capacity type 347 stainless steel autoclave was pickled for 20 min with 10% HNO<sub>3</sub>-4% HF solution at 60°C. The pickled surfaces were scrubbed thoroughly in distilled water and dried in an oven at 110°C. A machined wafer of type 347 stainless steel was supported in the autoclave with a stainless steel hanger. The autoclave was then sealed and evacuated. The system was pressurized with 50 psig of oxygen gas and heated for 24 hr at 250°C in a tube furnace. After dismantling it was found that the specimen was completely unchanged from its original metallic color and showed no measurable weight change. A 350-ml volume of uranyl sulfate solution containing 39.5 g of uranium per liter was then placed into the autoclave with the test specimen and heated to 250°C. The ratio of submerged surface area to solution volume was 2 cm<sup>2</sup>/ml. During the operation of the test, solution samples were frequently removed for analytical determination of total uranium and nickel content. The results of these analyses are presented in Table 15.

The estimated oxygen content in the system based on the amount of oxygen

# HRP QUARTERLY PROGRESS REPORT

Table 15

## CHEMICAL ANALYSES OF URANYL SULFATE SOLUTIONS TAKEN FROM OXYGEN PRETREATMENT TEST AT 250°C (Test No. 1-6)

EXPOSURE (hr)	SOLUTION pH	TOTAL URANIUM CONCENTRATION (g/l)		DISSOLVED NICKEL (μg/ml)
0	2.38	39.5		1
24	2.39	41.7,	41.8	11
66	2.38	39.5,	39.7	12
138	2.38	38.8,	38.8	20
142*	2.38	39.0,	39.0	22

\*Sample taken after test was stopped and cooled to room temperature.

normally dissolved in 350 ml of uranyl sulfate at room temperature and the quantity contained in 180 cc of free air space above the test solution was estimated to be 65 mg. If this amount of oxygen were assumed to be dissolved in solution at 250°C, the oxygen concentration was 175 ppm. In order to check the dissolved gas content, solution samples were removed after 24 and 138 hr of continuous operation at 250°C. The volume of gas obtained from the 24-hr sample was too small for an accurate gas analysis. The 138-hr sample had a total gas content of 9.9 cc of which 7.5 cc was inert gases and 2.4 cc was oxygen. The 2.4-cc oxygen gas volume was equivalent to a dissolved oxygen content of 180 ppm, which was in excellent agreement with the estimated original dissolved oxygen concentration.

After operation for 142 hr, the test was dismantled and the specimen and solution examined. The specimen showed no signs of corrosion attack except for a light-brown discoloration. All surfaces were extremely lustrous and completely free of bulk oxide films. Corrosion attack had occurred, however, as evidenced by a weight loss of 0.08 mg/cm<sup>2</sup>, which was equivalent

to a corrosion rate of 0.25 mpy after 142 hours. The over-all corrosion rate on the system was determined to be 0.21 mpy by the dissolved nickel concentration of 22 μg/ml. The corrosion rate determined by dissolved nickel after 24 hr at 250°C was 0.9 mpy, which was a marked improvement over the rates of 5 to 9 mpy normally obtained after 24 hr at 250°C in oxygenated uranyl sulfate solutions containing 40 g of uranium per liter.

The rather remarkable behavior of this test prompted the operation of a second test, No. 1-9, in which the system was essentially deoxygenated. The same autoclave was used, and it was pretreated with oxygen gas in a manner similar to that described for the first test. Prior to introducing the uranyl sulfate containing 40 g of uranium per liter, the autoclave was evacuated. The uranyl sulfate solution was deaerated by boiling for 20 min before it was drawn into the evacuated autoclave. These precautions reduced the oxygen content in the system to a fairly insignificant value.

The test system was heated to 250°C, and solution samples were removed frequently because previous

FOR PERIOD ENDING JULY 1, 1952

experience with deaerated solutions at 250°C showed that solution reduction occurred shortly after the operating temperature was reached. The test was operated for 81 hr without any indication of reduction in total uranium content. The results of chemical analyses on the solution samples are reported in Table 16. Unfortunately uranium analyses were not obtained because there was insufficient volume of the sample solutions remaining after dissolved nickel and iron analyses. The final uranium content was 47.8 g/l as compared to the initial value of 39.5. Since no solution loss occurred during the operation of the test, this increase in concentration was attributed entirely to the loss of water during the boiling operation to deaerate the initial solution.

At the end of the test, visual and microscopic examination of the corrosion test specimen showed no effects of the exposure. The surfaces were unchanged from the original metallic

luster; no measurable weight change was found. The final dissolved nickel content of 5 µg/ml was equivalent to a corrosion rate of 0.01 mpy after 81 hours. No dissolved oxygen was found in solution samples removed during the operation of the test. The limit of detection by the analytical method for oxygen was 25 ppm, so it was assumed that the dissolved oxygen content was at least below this amount.

Since uranium analyses were not reported on the solution samples, the autoclave was cleaned with HNO<sub>3</sub>-H<sub>2</sub>O<sub>2</sub> mixtures to dissolve uranium oxides that might have precipitated on the walls of the container. However, analyses for uranium in these solutions showed contents of less than 1 µg/ml, so complete solution stability during the test was indicated.

The test specimen was submitted to the Optical Microscopy section for examination. The corrosion film was stripped from the base metal by immersion in a bromine-methanol

Table 16

CHEMICAL ANALYSES OF URANYL SULFATE SOLUTIONS TAKEN FROM OXYGEN PRETREATMENT TEST AT 250°C (Test No. 1-9)

EXPOSURE (hr)	SOLUTION pH	DISSOLVED NICKEL (µg/ml)	DISSOLVED IRON (µg/ml)
0		1	1
7	2.25	5	18
24	2.38	3	11
29	2.25	3	5
33	2.40	3	4
37	2.40	3	4
53	2.40	3	3
77	2.40	3	5
81*	2.38	4	5

\*Sample taken after test was stopped and cooled to room temperature.

## HRP QUARTERLY PROGRESS REPORT

mixture. The film thickness was less than 300 Å - much thinner than films removed from untreated specimens exposed in oxygenated uranyl sulfate solutions at 250°C. Also, the film was more uniform and continuous than the films removed from untreated specimens. The only discontinuities were areas corresponding to a few minute pit sites observed on the specimen under high magnification before the film was stripped from the metal. Diffraction patterns indicated the film to be amorphous in structure; no definite oxide patterns were determined.

Studies are being continued with the use of oxygen at 250°C for pretreating stainless steel prior to exposure in uranyl sulfate solutions. The use of such a treatment, if proved reliable, for a large reactor system would be difficult. The foremost difficulty would be in maintaining a temperature of 250°C on all component parts contacting uranyl sulfate solution at this temperature. If further study produces as optimistic results

as were obtained in the few preliminary tests, this method of pretreatment may be of much value for conditioning static systems for such purposes as measurement of physical and chemical properties of uranyl sulfate solutions at elevated temperatures, measurement of gas solubilities, etc., where the presence of soluble and insoluble corrosion products, or dissolved oxygen, are not desirable in the test solutions. The use of the oxygen treatment may afford also a means of approach for study of the fundamental corrosion mechanisms involved in the uranyl sulfate-stainless steel system at elevated temperatures.

**Reflector Corrosion Studies.** No new work was undertaken during the past quarter on the corrosion of mild carbon and type 347 stainless steels in distilled water at 200°C, and no further work is contemplated at this time. Detailed information on this work has appeared in previous issues of the Homogeneous Reactor Project Quarterly Progress Reports. A summary report will be issued.

---

### RADIATION STABILITY

H. F. McDuffie, Group Leader

W. E. Hill

G. M. Watson

J. F. Manneschildt

W. C. Yee

F. H. Sweeton

#### LONG-TERM IRRADIATIONS AT HIGH TEMPERATURE AND HIGH FLUX

A sample of uranyl sulfate solution is now in the twelfth week of a long-term irradiation in the high flux of the LITR at horizontal beam hole HB-5. The objectives of this run are:

1. to determine the stability of the solution under radiation similar to that expected in the HRE at a temperature of 250°C (solution

contained in a type 347 stainless steel bomb under excess oxygen pressure),

2. to determine the rate at which the excess oxygen is consumed during irradiation (from which the rate of corrosion of the stainless steel may be inferred),
3. to determine whether, and how much of, this oxidation can be attributed to the presence of radiation.

The type 347 stainless steel bomb has an approximate inside diameter of 3/8 in. and is about 2 3/4 in. in height - the outside dimensions are 5/8 in. and 4 inches. A short thermocouple well fitted into the bottom of the bomb contains two iron-constantan thermocouples cemented in place with silver chloride to ensure good thermal contact. A stainless steel capillary tube connects the bomb to a Baldwin pressure cell outside the reactor. The volume of the bomb is 5.0 ml and its inside surface is 25.5 cm<sup>2</sup>.

The bomb was pretreated with 2% CrO<sub>3</sub> solution at 270°C for 5 hr and then charged with uranyl sulfate, copper sulfate, and hydrogen peroxide. The presence of the copper sulfate was required to bring about recombination of the hydrogen and oxygen at reasonable equilibrium pressures; the hydrogen peroxide was decomposed thermally after the assembly was sealed to produce approximately 64 ml (STP) of oxygen, if excess oxygen pressure was desired. The volume of the solution after peroxide decomposition was 2.50 ml, and its composition (per liter of solution) was as follows:

U <sup>235</sup>	40.9 g
U <sup>235</sup> + U <sup>238</sup>	43.9 g
CuSO <sub>4</sub>	0.0105 moles

The solution under operating conditions at 250°C covers 16 cm<sup>2</sup> of metal surface.

The temperature of the bomb is maintained usually at 250°C to attain a steady equilibrium pressure (gas plus steam plus excess oxygen) of about 1500 psi. During the LITR weekly shutdown, on Tuesdays, the temperature of the bomb is maintained at 250°C to permit all the gases to recombine (since no gas is being

formed) and thus allow a weekly direct measurement of the total pressure exerted by steam and excess oxygen. Once the gases have been recombined the temperature may be shifted to other levels to establish the total pressure exerted by steam and excess oxygen. On Mondays and Wednesdays kinetic data showing rates of approach of the system to equilibrium are obtained by recording pressure changes at temperatures of 210, 230, and 250°C.

The bomb is held in a snug-fitting graphite furnace which, because of its high thermal conductivity, tends to reduce temperature gradients along the bomb. At the normal power level of 1500 kw, the flux inside the bomb has been found (cobalt monitor activation) to be  $3.8 \times 10^{12}$  neutrons/cm<sup>2</sup>·sec. The bomb is about 4½ in. from the side of the reactor assembly and is further separated from the nearest fuel elements by 6 in. of beryllium.

**Solution Stability.** One way of estimating the amount of dissolved uranium in the bomb is to determine the rate of gas production and, assuming all the uranium is in solution, to calculate an apparent *G* value (molecules of hydrogen formed for each 100 ev of energy absorbed). If the uranium has actually started to precipitate, some of the fission energy will be expended in the solid and thus the apparent *G* value is directly related to *K*<sub>1</sub> of the equation

$$dP/dt = K_1 - K_2P,$$

which has been discussed frequently in analyzing previous solution irradiation data. Determinations of the apparent *G* value have been made at various times during the experiment by plotting *dP/dt* as a function of total pressure and extrapolating to a pressure corresponding to only steam

## HRP QUARTERLY PROGRESS REPORT

and excess oxygen. The results, expressed as per cent of the true  $G$  value (1.5) previously determined,<sup>(1)</sup> are given in Fig. 27. No correction for diffusion effects has been attempted, and therefore the results can be expected to be somewhat low. The spread in observed points is not surprising since: (1) the temperature near the bottom of the solution rather than at the vapor-liquid interface is being measured (thus some slight uncertainty is contributed as to the exact pressure of steam plus inert gases) and (2) some extrapolation of the  $dP/dt$  vs.  $P$  data is required in order to arrive at the intercept.

The curve shows a definite trend downward, and, as far as is known, this is a real effect. Whether it is actually due to precipitation, however, will not be known conclusively until the test is terminated and the solution is examined.

(1) J. W. Boyle, J. A. Ghormley, T. H. Handley, C. J. Hochanadel, W. F. Kieffer, A. C. Stewart, and T. J. Sworski, *Chemistry Division Quarterly Progress Report for Period Ending December 31, 1951*, ORNL-1260, p. 93.

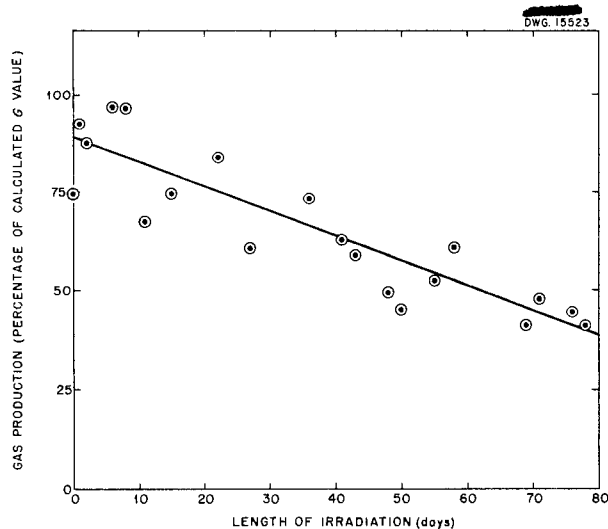


Fig. 27. Gas Production in Long-term Irradiation Experiments at High Flux.

Another method of detecting precipitation is based on the expectation that precipitation will increase the fraction of fission heat liberated near the bottom of the bomb. Readings of thermocouples in the top, middle, and the bottom of the furnace and in the bomb suggest that the average source of heat has shifted downward, but the data are not very self-consistent and are not regarded as being very reliable.

As a result of these considerations it seems possible at this time to say that at least 40% of the original uranium is in solution after 11 weeks of irradiation at an average flux of  $3.5 \times 10^{12}$  (giving a 1% burnup).

**Corrosion In and Out of Radiation.** With reference to the rate of corrosion of stainless steel by uranyl sulfate in the presence of 0.01 M  $\text{CuSO}_4$  and excess oxygen, more definite statements can be made. By attributing the change in the residual pressure observed at the end of the weekly shutdowns to absorption of oxygen by the wall of the bomb, it is possible to calculate the thickness of wall penetration if it is assumed that the effect is uniform over all the surface covered by the solution. Such calculations have been made, and the results are shown in Fig. 28. The over-all corrosion rate found in this manner was 1.3 mpy. The rate after the first two weeks leveled off at 0.8<sub>3</sub> mpy.

Two similar bombs are being heated in the absence of radiation, one pretreated and one not, and both are consuming oxygen corresponding to corrosion rates of 0.2 mpy or less. Thus it appears that most of the corrosion of stainless steel inferred from oxygen consumption in the presence of radiation may be directly connected with the radiation.

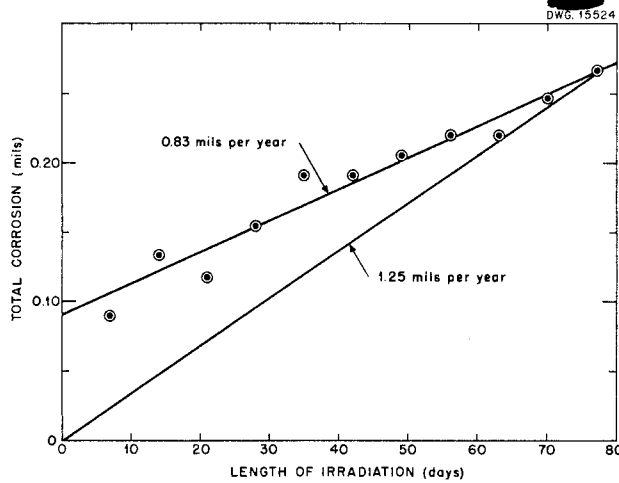


Fig. 28. Corrosion of Type 347 Stainless Steel Calculated from Oxygen Consumption in Long-term Irradiation Experiments at High Flux.

#### KINETICS OF THE DECOMPOSITION OF HYDROGEN PEROXIDE IN URANYL SULFATE SOLUTIONS

Studies of the thermal decomposition of hydrogen peroxide in aqueous solutions have been undertaken because the power level for operating a homogeneous reactor at low temperatures appears to be largely limited by the formation of hydrogen peroxide and consequent precipitation of uranium peroxide.

The differential equation

$$\frac{dC_{H_2O_2}}{dt} = K - k_1 C$$

may be used to express the peroxide concentration at any time in an aqueous homogeneous reactor, where (1)  $K$  is the rate of formation of peroxide, which is assumed to be directly proportional to the power density in the reactor - it appears to be independent of temperature at 250°C or below and may be calculated from the experimental  $G$  value (molecules of  $H_2$  per 100 ev);

(2)  $k_1$  is the specific reaction rate constant for the decomposition of hydrogen peroxide and is strongly dependent on temperature; and (3)  $C$  is the concentration of hydrogen peroxide in the solution at any time. The effects of different levels of the above variables should be known for designing and operating homogeneous reactors. As will be shown in the following sections,  $K$  can be approximated experimentally in the laboratory by controlling the rate of addition of hydrogen peroxide solutions to a system under study;  $k_1$  can be determined by standard kinetic techniques using either dynamic or equilibrium methods; and  $C$  may be determined by equilibrium methods and by observing the concentrations associated with incipient precipitation.

**Determination of Decomposition Rates.** Values for  $k_1$  obtained in 0.0045 to 0.17  $M$  uranyl sulfate solutions at 78°C have been reported previously.<sup>(2)</sup> The rate was observed to be first order with respect to peroxide concentration in the range  $4 \times 10^{-4}$  to  $5 \times 10^{-3} M$  and apparently independent of the uranyl sulfate concentration from 0.0175 to 0.176  $M$ . The pH of these solutions varied from 2.4 to 3.3. There was an apparent slight drop in the rate constant from  $4.8 \times 10^{-4} \text{ sec}^{-1}$  to  $4.2 \times 10^{-4} \text{ sec}^{-1}$  as the concentration of the uranyl sulfate was lowered from 0.0175 to 0.0045  $M$ . Confirmation of the  $4.80 \times 10^{-4} \text{ sec}^{-1}$  value of  $k_1$  has since been obtained at a much higher concentration of uranyl sulfate, 0.75  $M$ . Values of  $k_1$  recently obtained at two other temperatures, 53 and 101°C, are reported in the fourth column of Table 17. It should be noted that different rate constants have been

(2) H. F. McDuffie, J. W. Boyle, E. L. Compere, W. F. Kieffer, M. D. Silverman, and H. H. Stone, *Homogeneous Reactor Project Quarterly Progress Report for Period Ending March 15, 1952*, ORNL-1280, p. 158.

# HRP QUARTERLY PROGRESS REPORT

Table 17

## SPECIFIC REACTION RATE CONSTANTS AND ACTIVATION ENERGIES FOR THE DECOMPOSITION OF HYDROGEN PEROXIDE IN URANYL SULFATE SOLUTIONS

SOLUTION	TEMPERATURE (°C)	$k_1 \times 10^4$ (sec <sup>-1</sup> )	$\Delta E$ (cal)	$A \times 10^{-12}$
1*	53	0.326	25,600	4.49
	78	4.80		
	101	52.4		
2**	53	0.191	25,300	1.62
	78	2.80		
	101	28.7		
3***	53	1.93	23,700	1.52
	78	24.1		
	101	214		

\*Uranyl sulfate solution prepared by the Y-12 production group.

\*\*Uranyl sulfate solution (purer than Solution 1) prepared in the Chemistry Division of ORNL by Lietzke and Griess.

\*\*\*Natural uranium fuel that had been run in the HRE loop for one week at 250°C.

obtained for three different uranyl sulfate solutions. The third group of solutions, which had been run in the HRE loop for one week at 250°C, doubtless possessed impurities that could be expected to give a higher rate constant for the decomposition of hydrogen peroxide. All rate constants in Table 17 were calculated by using the equation

$$\frac{dC_{H_2O_2}}{dt} = -k_1(C_{H_2O_2})$$

The straight line plots of  $\log k_1$  vs.  $1/T$  obtained for all three solutions are shown in Fig. 29. From these data, activation energies for peroxide decomposition may be calculated from the Arrhenius rate equation,

$$k = A e^{-\Delta E/RT}$$

Preliminary values for specific reaction rate constants, activation energies, and frequency factors,  $A$ , are summarized in Table 17. Data for other temperatures may be calculated from the following rate equations:

Solution 1

$$k = 4.49 \times 10^{12} e^{-25,600/RT}$$

Solution 2

$$k = 1.62 \times 10^{12} e^{-25,300/RT}$$

Solution 3

$$k = 1.52 \times 10^{12} e^{-23,700/RT}$$

At the present stage of this investigation it is not known whether the relatively small difference between the activation energies of the first

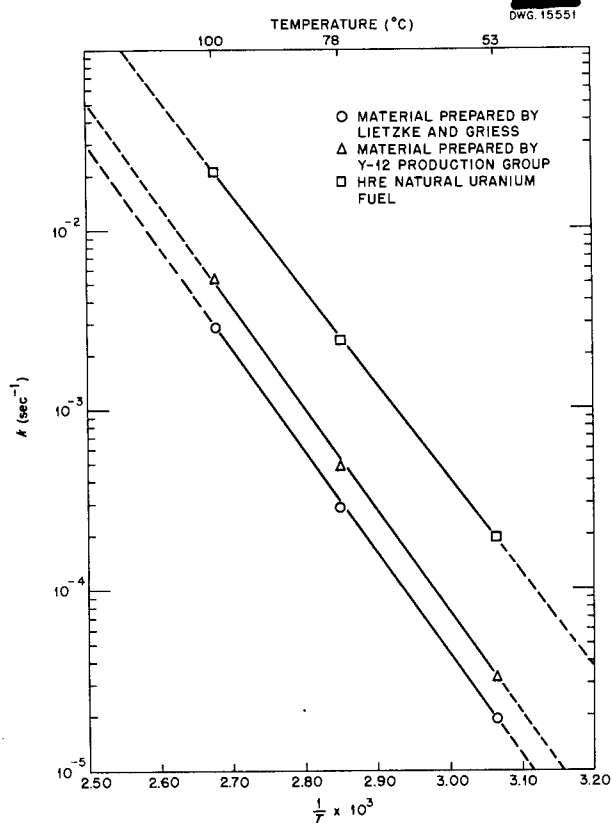


Fig. 29. Specific Reaction Rate Constants for the Decomposition of Hydrogen Peroxide in Uranyl Sulfate Solutions.

two solutions might not be due to experimental errors. The lower activation energy for solution 3 is in line with the larger amounts of impurities contained in this solution.

When definite values for  $K$  are simulated in the laboratory (by the addition of hydrogen peroxide at known rates to a solution of uranyl sulfate), the kinetic equation  $dC/dt = K - k_1C$  may be used to obtain values for  $k_1$ . If the time dependence of  $C$  at constant  $K$  is known adequately, a plot of  $dC/dt$  vs.  $C$  will furnish a straight line with slope of  $-k_1$ . Alternatively, if the value of  $K$  is known and maintained constant throughout an experiment, the concentration of peroxide

will approach a steady-state value ( $C_{ss}$ ) at which point  $dC/dt = 0$  and hence  $K - k_1C_{ss} = 0$ . From this it is seen that  $k_1 = K/C_{ss}$ . Another method for finding  $k_1$  involves plotting the value,  $C_{ss} - C_t$  (the distance away from the steady state), against time on conventional semilogarithmic paper and determining the constant as for any first-order reaction.

Determinations of  $k_1$  have been made for a variety of uranyl sulfate solutions at the boiling point by using the steady-state method. The results of these tests are presented in Table 18. Large differences in values of  $k_1$  are noted. The Y-12 solution was made up from a relatively impure batch of uranyl sulfate and showed a fairly large value of  $k_1$ . By contrast, the Lietzke-Griess material was characterized by low values of  $k_1$ . The deterioration of this solution in successive runs is seen by comparing the  $k_1$  values for runs 8, 9, and 10. Undoubtedly some impurities were introduced that assisted in catalyzing the decomposition of peroxide. If the behavior of the HRE 5A-6A material, which was samples of unenriched fuel that had been run in the HRE loop for one week at 250°C, can be taken as characteristic of that expected from enriched fuel in the reactor, peroxide decomposition will be very rapid. The agreement between the values of  $k_1$  obtained by the two methods (ordinary plot of  $\log C$  vs.  $t$  vs. steady-state method) is apparently excellent, especially in view of the speed of the reactions involved.

**Solubility of Uranyl Peroxide.**

The maximum allowable hydrogen peroxide concentration in solution is limited by the solubility of uranyl peroxide formed according to the equation



**Table 18**  
**DECOMPOSITION OF PEROXIDE IN URANYL SULFATE SOLUTIONS AT 100°C**

RUN NO.	SOLUTION SOURCE	URANIUM CONCENTRATION (g/l)	K (moles/l/min)	C <sub>ss</sub> (moles/l)	k <sub>1</sub> (min <sup>-1</sup> )	PRECIPITATE	T <sub>1/2</sub> (min)	COMMENTS
1	Y-12	8	0.000725 t* 0.00067 c**	0.00122	0.55	no	1.25	
2	Y-12	8	0.00151 t 0.00139 c	0.0022	0.63	yes	1.1	
5	Y-12	40	0.00145 t 0.00096 c	0.00173	0.56	no	1.25	Flask contained type 347 stainless steel turnings
6a	Y-12	40	0.00164	0.00218	0.735	no	0.944	Measurements of C <sub>ss</sub> and K taken at different values of K, with sufficient time allowed for steady state to be reached in each case
b			0.00347	0.00414	0.84	yes?	0.825	
c			0.0057	0.0068	0.8	yes	0.867	
8	Lietzke-Griess	40			0.23	no	3.0	Conventional plot of log C vs. t after one addition of peroxide
9a	Lietzke-Griess	40	0.000298	0.00081	0.37			Measurements of C <sub>ss</sub> and K taken at different values of K, with sufficient time allowed for steady state to be reached in each case
b			0.000312	0.00092	0.34			
c			0.000351	0.00097	0.36			
d			0.000387	0.00110	0.365			
10a	Lietzke-Griess	40	0.000303	0.00060	0.5			Measurements of C <sub>ss</sub> and K taken at different values of K, with sufficient time allowed for steady state to be reached in each case
b			0.000445	0.00113	0.395			
c			0.000396	0.00077	0.515			
d			0.000471	0.00106	0.445	yes		
e			0.000705	0.00131	0.54	yes		
11	HRE	5A-6A	0.0022	0.00126	1.74	no	39 (sec)	This solution had been used in the HRE for runs at 250°C and hence had accumulated impurities that raised the value for k <sub>1</sub>

\* t = titrated.

\*\* c = calculated.

The pH of a dilute solution of uranyl sulfate (0.17 M) is noticeably affected by the addition of hydrogen peroxide. In the case of a concentrated solution (0.85 M), however, very little effect is observed because the solution acts as a buffer. Some equilibrium data, measured at 25°C, are available for this reaction;<sup>(3)</sup> however, there are no data at higher temperatures, nor are there data for the solubility of uranyl peroxide as a function of temperature, especially in uranyl sulfate solutions.

Attempts to obtain solubility data at higher temperatures have met with some measure of success even though changes in peroxide concentration and hydrogen ion concentration become quite rapid. Solubility experiments have been conducted at room temperature (30°C), 78, and 101°C. Analyses for

<sup>(3)</sup> P. F. Grieger and J. W. Gates, Jr., *Uranium Peroxide. Part III. Discussion of the Solubility of Uranium Peroxide in Sulphate Solutions Based on the Uranyl Sulphate Association Hypothesis*, CD-4023 (May 26, 1945).

total peroxide at the point of incipient precipitation of uranyl peroxide were made by titration with ceric sulfate. Hydrogen ion was measured using the Beckman high-temperature electrode with the Model G instrument, with appropriate corrections for the temperature factor. The point of precipitation was determined by visual observation. The data obtained at both low and high concentrations of uranium have been summarized in Table 19.

The main sources of error in these experiments were: (1) detection of formation of the precipitate since it forms very slowly in solution - hence, peroxide concentrations would always be a little high; (2) determination of the hydrogen ion concentration by means of the high-temperature glass electrode. The citrate buffer used for standardization is claimed to have a negligible temperature coefficient up to 70°C; it has been assumed to be negligible in these experiments up to 100°C. Furthermore, no data are

Table 19

## SOLUBILITY OF URANYL PEROXIDE IN URANYL SULFATE SOLUTIONS

TEMPERATURE (°C)	UO <sub>2</sub> SO <sub>4</sub> CONCENTRATION (M)	TOTAL PEROXIDE CONCENTRATION (M)	pH
30	0.16	0.00311	2.32
	0.65	0.00791	1.64
78	0.15	0.00375	2.14
	0.57	0.00685	1.66
	0.71	0.00678	1.59
100	0.112	0.00636	2.09
	0.60	0.0082	1.58
	0.54	0.00914	1.66

## HRP QUARTERLY PROGRESS REPORT

available on the performance of this type of electrode at the temperatures employed. It is estimated that pH values at 78 and 100°C could very easily be in error by 0.1 pH units.

In spite of the rough experimental measurements, some measure of the solubility of uranyl peroxide as a function of temperature has been obtained.

By using the steady-state method in which  $K$  is maintained constant, it is possible to maintain a given peroxide concentration for periods of time long enough to permit sensitive determination of the formation or absence of precipitated  $\text{UO}_4 \cdot 2\text{H}_2\text{O}$ . Preliminary experiments utilizing this technique led to a value of 0.002 to 0.004 moles per liter for the peroxide concentration at saturation in uranyl sulfate solution containing 40 g of uranium per liter at 100°C (based on experiments 6a and 6b in Table 18). This is believed to be a conservative value. The very small amounts of crystalline uranium peroxide observed in experiments 10d and 10e may have been formed as a result of local supersaturation when the entering peroxide was being mixed with the boiling uranyl sulfate solution. Longer steady-state runs with carefully controlled concentrations will be required for more accurate determination of the tolerable level of peroxide.

**Reactor Operation as Governed by Peroxide Decomposition.** The production of hydrogen peroxide in a reactor is considered to be a function of the  $G$  value and the energy input (power density) as expressed by the formula  $K = 0.0052 \times G \times PD$ , where the power density is expressed in kilowatts per liter. For fuel containing 40 g of

uranium per liter,  $G$  is approximately 1.5 and the peroxide formation is  $K = 0.0078 PD$  moles per liter per minute. The tolerable peroxide concentration and the tolerable power density are related by the expression:

$$PD = \frac{C_{ss}}{0.0078} k_1 .$$

By using a value of 1.75 for  $k_1$  (from run 11) and an allowable steady-state peroxide concentration of 0.0039  $M$ , the allowable power density for the HRE at 100°C is calculated to be 0.825 kw/l and the total power of the reactor is 41.25 kw. The accumulation or addition of catalytic materials such as corrosion products or recombination catalysts, the effects of radiation in the presence of dissolved hydrogen, and the conservative values for allowable peroxide will all tend to permit actual reactor operation at higher power levels.

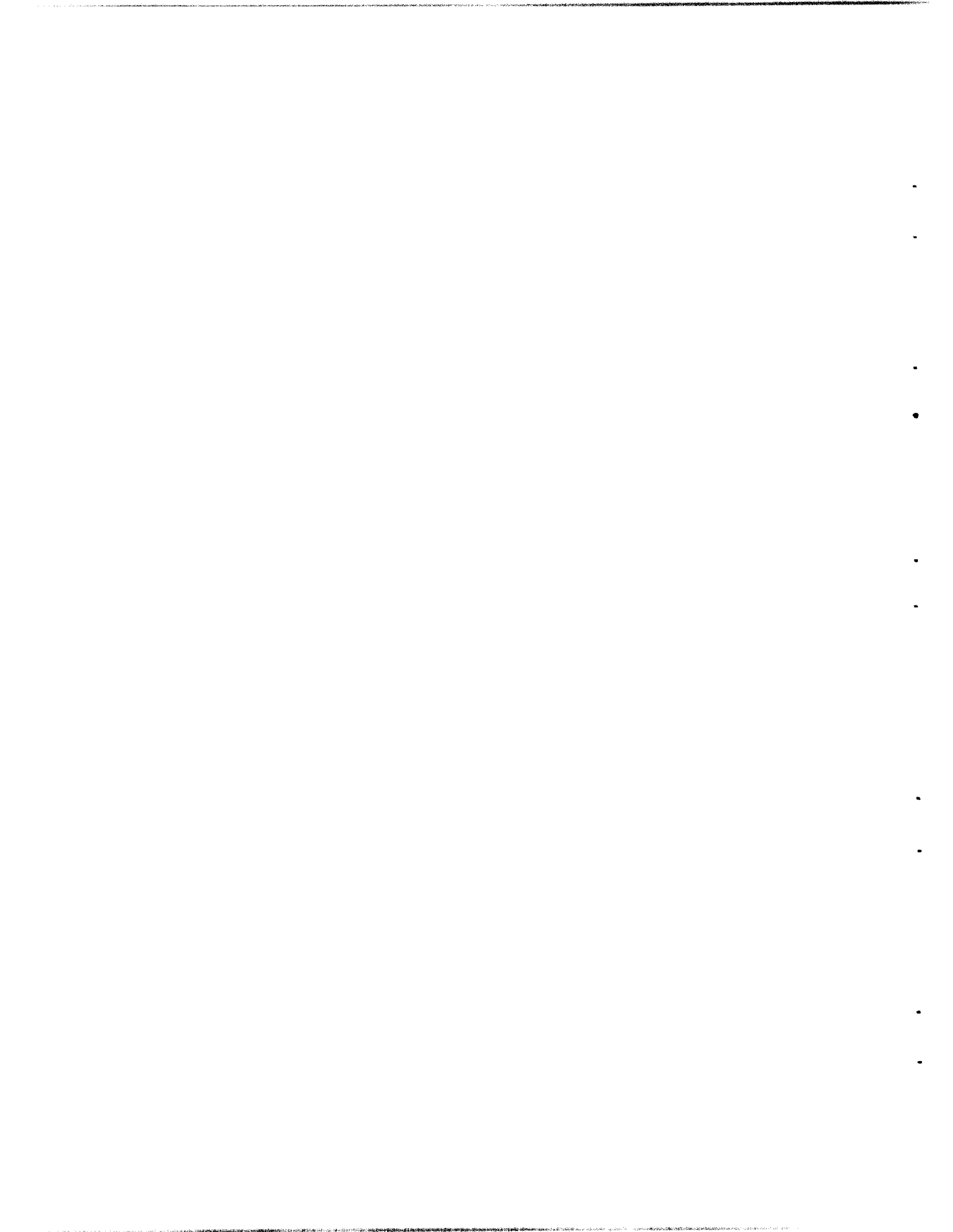
**Plans for Future Work.** Of immediate practical importance is the question of allowable power level for low temperature operation of the HRE. To this end, actual determinations of  $k_1$  for enriched HRE fuel will be carried out following the 250°C critical experiments but prior to operations at substantial power. Additional determinations may be carried out after runs at a low power level to determine whether impurities have been introduced that will allow operation at higher power levels.

Active exploration of remote instrumental methods for determining the peroxide level in uranyl sulfate solutions is already under way. Preliminary work using conductance methods appears encouraging. It is hoped that it will become possible to

FOR PERIOD ENDING JULY 1, 1952

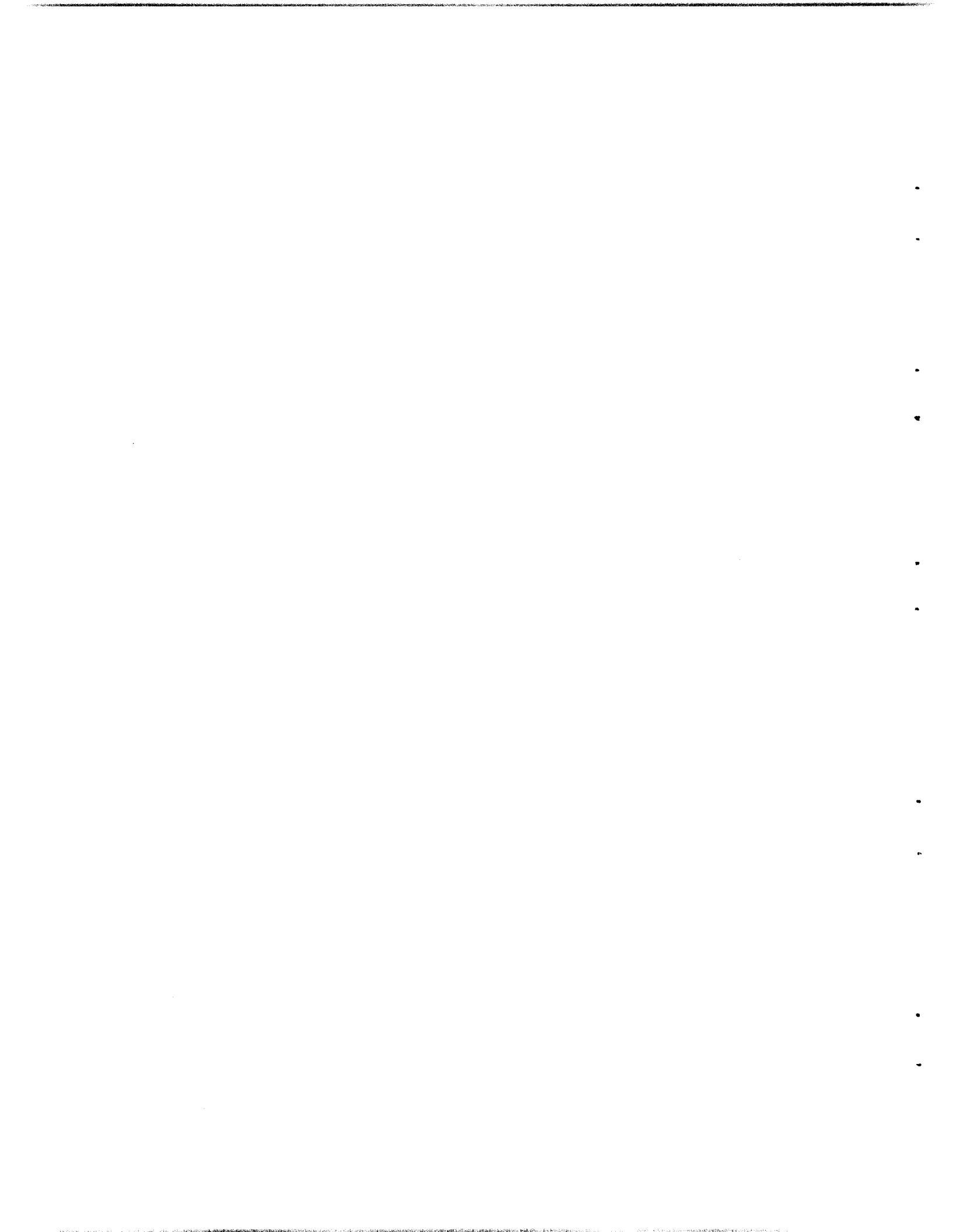
conduct studies of peroxide decomposition without having to take samples of solution from the system - this is almost a necessity for solutions in which the peroxide is decomposing at very rapid rates.

Extension of peroxide decomposition studies to temperatures in the range 100 to 150°C is contemplated. This will depend primarily on the development of rapid instrumental methods of analysis.



**Part II**

**BOILING REACTOR AND SLURRY STUDIES**



## BOILING REACTOR RESEARCH

R. N. Lyon, Section Chief

The current boiling reactor program is designed to provide the necessary information for a broad evaluation of boiling homogeneous reactors in comparison with other types of reactors. To accomplish this three types of studies are under way: (1) individual component and theoretical studies designed to help predict the stability and power output of boiling reactors, or to answer other pertinent questions, (2) experiments with actual boiling reactors to obtain data for answers to complex questions that cannot be answered with assurance or accuracy by synthesis from data of individual experiments, (3) studies of several large-scale, postulated, boiling reactor installations to provide the proper balance between the various theoretical and experimental investigations.

### POWER REMOVAL FROM A BOILING REACTOR

P. C. Zmola

The calculation of the decrement in mean density for a given power output in a boiling reactor that was presented in the previous quarterly report<sup>(1)</sup> and depended upon an idealized circulation pattern has been extended to cases in which 20 and 50% of the rising vapor is entrained in the downcoming region ( $\eta = 0.2$  and  $0.5$ , respectively). This results in a much less favorable, although not impossible, operating condition if the flow resistance of the system can be kept low. The value of the entrainment factor that can be achieved depends upon the nature of steam separation

<sup>(1)</sup>P. C. Zmola, *Homogeneous Reactor Project Quarterly Progress Report for Period Ending March 15, 1952*, ORNL-1280, p. 86.

afforded at the top surface of the unit. At present the steam separation problem is being reviewed by the Babcock and Wilcox Company. Steam generator manufacturers have been successful in separating steam in natural-convection units by utilization of centrifugal separators. In large units, 1500 kw/ft<sup>2</sup> of projected drum surface is attained with final steam moisture of 1/4 to 1/2% and an associated pressure drop of about 0.5 psi. At present it appears that this relatively simple device can be employed in boiling reactors.

One-group (thermal) nuclear calculations are being performed for a bare, cylindrical system to define roughly the limits of density decrement permissible as a function of isotopic enrichment, uranyl sulfate concentration, pressure (temperature), and flow parameters postulated in the circulation studies. About a year ago, in connection with other work, Noderer calculated the change in flux distribution due to a density decrease as a function of radius in the central region of a cylindrical core and found that this change was small for a total density decrement of 10%. It is planned to extend the range of these calculations.

### NUCLEATION BY FISSION FRAGMENTS

R. J. Goldstein

It has been reported that 16°F superheat could be maintained in a uranyl sulfate solution while fission of the uranium was taking place.<sup>(2)</sup> This experiment on the stability of superheated liquid in which fission

<sup>(2)</sup>R. J. Goldstein, *op. cit.*, ORNL-1280, p. 89.

## HRP QUARTERLY PROGRESS REPORT

fragments are present has been changed to give more accurate and definite results. The equipment is to be used in a region of low neutron background rather than in Building 3001 to minimize the possibility of fission during the nonirradiated portion of the test. A polonium-beryllium neutron source will be used when fissions are desired.

Another modification in the technique consists of heating the solution under pressure and then gradually reducing the pressure below the saturation pressure. This will provide more uniform superheating of the sample.

### PHYSICS OF THE TEAPOT REACTOR

P. R. Kasten

A number of calculations have been completed concerning the statics of the proposed Teapot reactor, a cylindrical, boiling type of reactor, 17 1/2 in. in diameter, which has been described in other reports.<sup>(3,4,5)</sup>

**Critical Mass.** The critical mass of the reactor under various operating conditions and with no thimble in the core is given in Fig. 30. An H-to-U<sup>235</sup> ratio exists above which net boiling away of water lowers the critical mass requirements and results in a supercritical assembly if the vapor fraction remains constant. Since it is advisable to avoid the possibility of an unstable situation in an initial experiment, an H-to-U<sup>235</sup> ratio of 400 was chosen. In the calculations, uranium of 93.4% enrichment in U<sup>235</sup> was assumed. Figure 31 gives data concerning

operation under various conditions at this concentration, which corresponds to 58.9 g of U<sup>235</sup> per kilogram of solution (63.1 g of total uranium per kilogram of solution), or 65.3 g of U<sup>235</sup> per kilogram of water.

#### Central Thimble and Control Rod.

It appears desirable to incorporate a vertical thimble along the center axis of the reactor to facilitate (1) insertion of a source for startup, (2) insertion of a control rod for bringing the reactor up to critical and also to power, (3) kinetic experiments in which the rod would be quickly removed from the core region for abrupt reactivity changes, (4) measurements of the vertical flux distribution.

The presence of the thimble and rod will increase the critical mass requirements over those presented in Fig. 30. The size of the rod should also be great enough to make appreciable reactivity changes possible. A rod diameter of 3 cm appears to be a reasonable compromise between minimum rod size and maximum rod effectiveness. The effect on reactivity of this size rod is listed in Table 20, and the effect on critical height is shown in Fig. 32.

**Fission-Product Poisons.** In addition to the poisoning effect of the rod and thimble, some of the fission products have high absorption cross sections and could thus lead to higher critical mass requirements. However, as shown previously,<sup>(5)</sup> operation of the proposed reactor at 250 kw will not lead to enough poisoning to increase the critical mass to any extent.

**Inherent Stability.** An operating reactor that when disturbed tends by itself to approach again an effective multiplication constant of 1 is an inherently stable reactor, if (1) the

<sup>(3)</sup>P. R. Kasten, *Reactor Physics of Teapot. Part I*, ORNL CF-52-6-78, June 5, 1952.

<sup>(4)</sup>P. R. Kasten, *Reactor Physics of Teapot. Part II*, ORNL CF-52-6-118, June 20, 1952.

<sup>(5)</sup>P. R. Kasten, *Reactor Physics of Teapot. Part III*, ORNL CF-52-7-38, July 16, 1952.

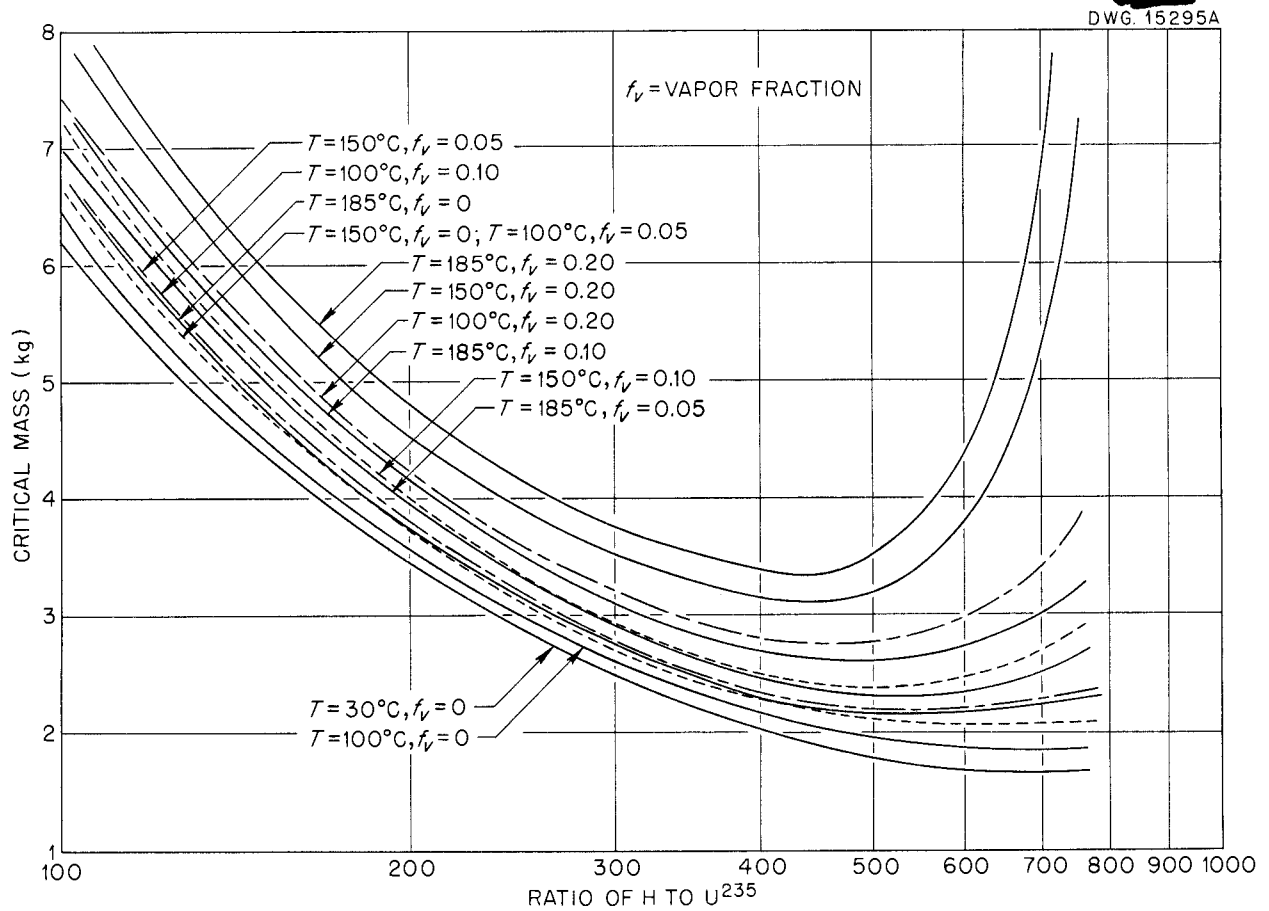


Fig. 30. Critical Mass Required vs. Ratio of H to  $U^{235}$  for a 17½-in.-dia, Cylindrical, Stainless Steel Reactor.

new equilibrium power level and temperature do not exceed safe levels and (2) in reaching the new equilibrium power level a dangerous amount of energy is not produced. In general, the inherent stability results from a reduction in effective reactivity with an increase in thermal energy within the reactor core, but the distribution of this energy may play a very important part in determining the actual reduction in reactivity for a given amount of energy. Thus in a boiling reactor the accumulation of heat in additional vapor in bubbles will have a much more pronounced effect than will the same amount of

heat as sensible heat in the liquid phase.

To study the stability of a boiling reactor, such as the proposed Teapot, the various influences can be studied separately before being combined to determine the over-all effect.

Consider the characteristic two-group equation

$$k_c = (1 + B^2\tau)(1 + B^2L^2) \quad , \quad (1)$$

where

$k_c$  = material multiplication constant required for criticality,

# HRP QUARTERLY PROGRESS REPORT

DWG. 15296A

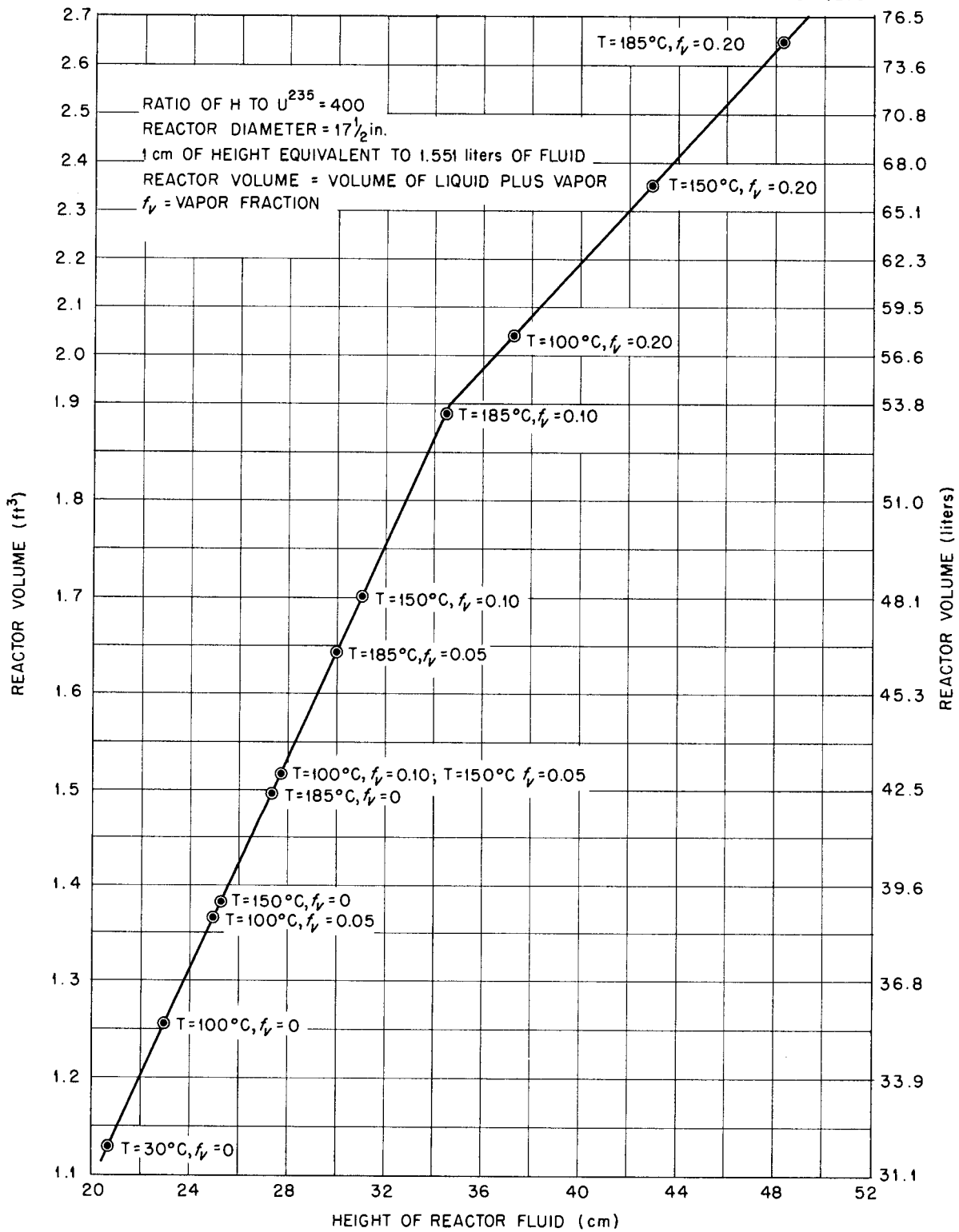


Fig. 31. Data for Conversion of Height of Reactor Fluid to Reactor Volume.

Table 20

$\Delta k_{eff}$  OF 3-cm-dia ROD AND THIMBLE

OPERATING CONDITIONS		$\Delta k_{eff}$		
Temperature (°C)	$f_v^*$	Rod Plus Thimble	Thimble Alone	Rod Alone
100	0	0.080	0.015	0.065
	0.05	0.060	0.015	0.045
	0.10	0.050	0.016	0.034
	0.20	0.038	0.017	0.021
150	0	0.055	0.015	0.040
	0.05	0.048	0.016	0.032
	0.10	0.038	0.017	0.021
	0.20	0.033	0.017	0.016
185	0.0	0.050	0.016	0.034
	0.05	0.042	0.017	0.024
	0.10	0.038	0.017	0.021
	0.20	0.028	0.018	0.010

\*  $f_v$  = vapor fraction.

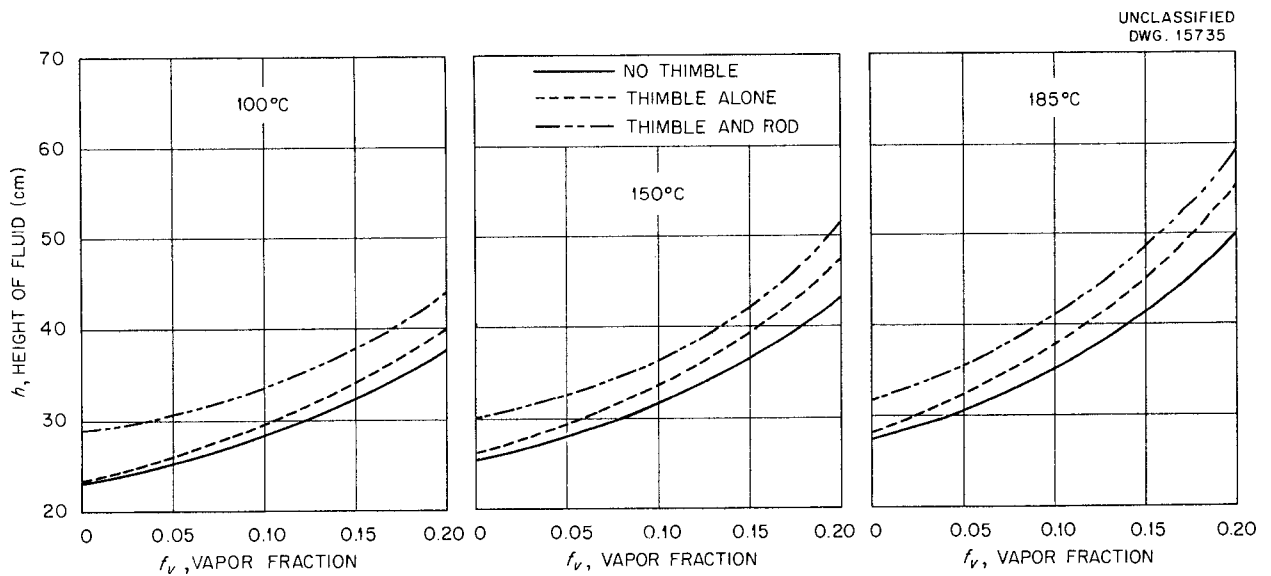


Fig. 32. Effect of Thimble and Rod on Critical Height at Various Operating Conditions.

## HRP QUARTERLY PROGRESS REPORT

$B^2$  = geometric buckling of the reactor ( $\text{cm}^{-2}$ ),

$L^2$  = square of the slowing down length ( $\text{cm}^2$ ),

$\tau$  = Fermi age ( $\text{cm}^2$ ).

$k_c$  can change with the temperature because a temperature change will affect  $B^2$ ,  $L^2$ , and  $\tau$ . Temperature changes have several effects on the reactivity, and thus several temperature coefficients exist (by temperature coefficient is meant the change in  $k_c$  with respect to temperature). As the temperature of the reactor increases, the scattering cross section for water changes. For the Teapot reactor,  $L^2$  is quite small, and since  $\tau$  is not influenced to any degree by the temperature changes expected, the temperature coefficient at constant core density should be small. In fact, for various operating conditions,  $(\partial k_c / \partial T)_\rho$  does not vary greatly from  $1 \times 10^{-4} / ^\circ\text{C}$ .

Another temperature coefficient exists because of the effect of fluid density upon  $k_c$ . Since  $B^2$  and  $L^2$  are both small and both are influenced to the same degree by density changes, Eq. 1 can be written as

$$k_c = 1 + B^2 M^2, \quad (2)$$

where

$$M^2 = L^2 + \tau.$$

Considering only density changes and that the active core region is cylindrically shaped,

$$k_c = 1 + \left[ \left( \frac{\pi}{L} \right)^2 + \left( \frac{2.405}{R} \right)^2 \right] \left( \frac{M_0 \rho_0}{\rho} \right)^2, \quad (3)$$

where

$R$  = equivalent radius of cylinder,

$L$  = equivalent height of cylinder,

$\rho$  = average density of core fluid,

=  $\rho_0$  evaluated under initial conditions.

For a given mass of fuel,  $\rho$  varies inversely with the reactor height; also,  $k_{c0} = 1 + B_0^2 M_0^2$ ; hence

$$k_c = 1 + \frac{k_{c0} - 1}{1 + A} \left[ 1 + A \left( \frac{\rho_0}{\rho} \right)^2 \right], \quad (4)$$

where

$$A = \left( \frac{2.405 L_0}{\pi R} \right)^2,$$

$L_0 = L$  evaluated at initial conditions.

From the above,

$$\left( \frac{\partial k_c}{\partial \rho} \right)_{\rho=\rho_0} = \left( \frac{k_{c0} - 1}{1 + A} \right) A \left( \frac{-2}{\rho} \right) \quad (5)$$

where

$$\rho = \rho_l (1 - f_v) + \rho_v f_v, \quad (6)$$

and

$\rho_l$  = density of core liquid,

$\rho_v$  = density of core vapor,

$f_v$  = vapor fraction in core.

Thus  $\rho$  is a function of both temperature and vapor fraction. The following nomenclature will therefore be employed:

$\left(\frac{\partial k_c(\rho_l)}{\partial T}\right)_{f_v}$  = change in  $k_c$  due to change in temperature, with the temperature influencing only  $\rho_l$ ,

and

$\left(\frac{\partial k_c}{\partial f_v}\right)_T$  = change in  $k_c$  due to change in vapor fraction at constant temperature.

From Eqs. 5 and 6,

$$\left(\frac{\partial k_c(\rho_l)}{\partial T}\right)_{f_v} = 2 \left(\frac{k_{c0} - 1}{1 + A}\right) A \left(-\frac{1}{\rho_l} \frac{\partial \rho_l}{\partial T}\right), \quad (7)$$

and

$$\left(\frac{\partial k_c}{\partial f_v}\right)_T = 2 \left(\frac{k_{c0} - 1}{1 + A}\right) A \left(\frac{1}{1 - f_v}\right), \quad (8)$$

since  $\rho_v f_v$  is comparatively small. The important variables in Eqs. 7 and 8 are plotted in Figs. 33 and 34.

Another temperature coefficient of reactivity exists because of the Xe<sup>135</sup> absorption resonance peak at 0.0863 ev, but because of low temperature and power operation its effect is negligible.

### TEAPOT REACTOR AUXILIARIES

J. D. Roarty

During the past quarter major effort has been directed toward the design of a bellows type of transfer

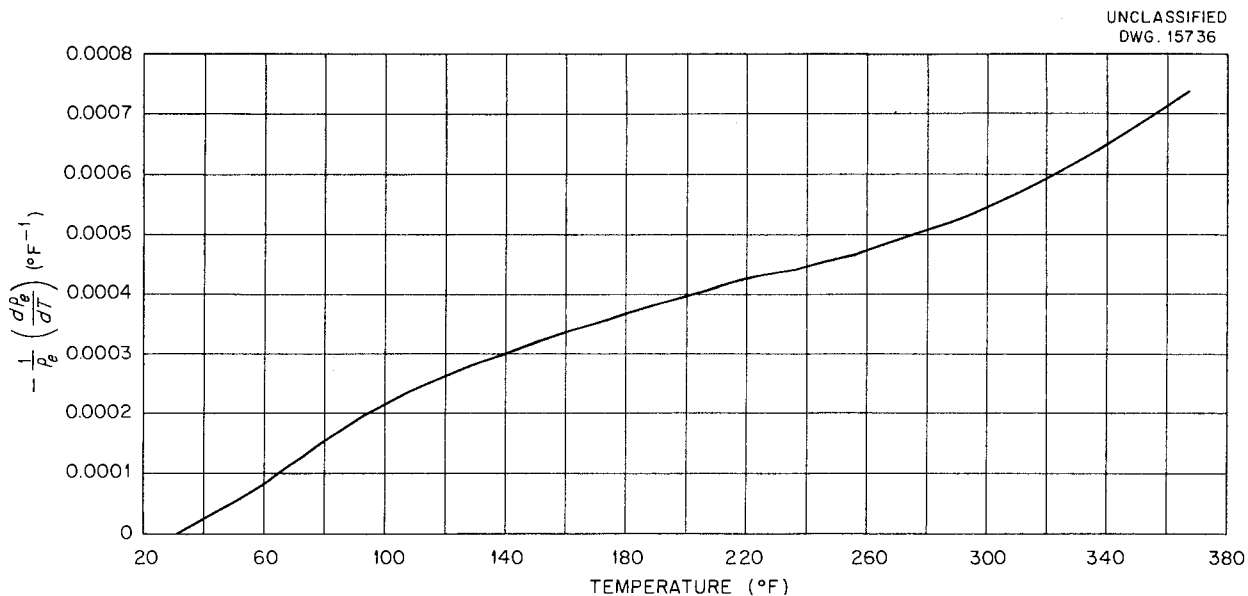


Fig. 33.  $-\frac{1}{\rho_e} \frac{d\rho_e}{dT}$  vs. Temperature Under Saturation Conditions ( $\rho_e$  = density of liquid).

## HRP QUARTERLY PROGRESS REPORT

pump for the Teapot experiment. The design of this pump was described previously.<sup>(6)</sup> The pump will have a capacity of approximately 0.5 gpm, and

it will develop a head by the compression of the active bellows. It will be a manually operated metering pump. Shop drawings are essentially complete.

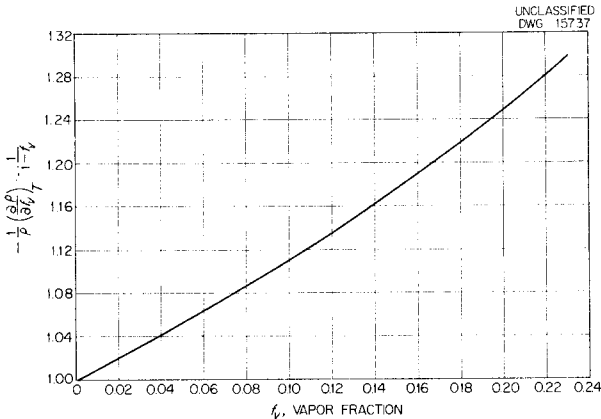


Fig. 34.  $\frac{1}{\rho} \left( \frac{\partial \rho}{\partial f_v} \right)_T = \frac{1}{1 - f_v}$  vs.

Vapor Fraction.

A dump tank assembly for the Teapot experiment has been designed.<sup>(7)</sup> The dump tanks have been specified for an "always-safe" condition. This criterion required that the assembly consist of 4-in. seamless steel pipe, 6 ft long and spaced 15 in. on centers. Each pipe must be shielded from the other pipes by Boral to prevent interaction or neutron exchange. The small diameter is dictated by the possibility of inadvertent flooding of the reactor pit.

<sup>(6)</sup>J. D. Roarty, *Design of a Bellows Type Transfer Pump for the Boiling Homogeneous Reactor*, ORNL CF-52-5-90, May 12, 1952.

<sup>(7)</sup>J. D. Roarty, *Design of Non-Critical Dump Tank Assembly for the Boiling Homogeneous Reactor*, ORNL CF-52-3-211, March 25, 1952.

## SLURRY FUEL STUDIES

### CHEMICAL AND ENGINEERING STUDIES

F. R. Bruce, Section Chief  
J. O. Blomeke            J. P. McBride  
L. E. Morse

The slurry studies described in this report have the objective of developing a suspension containing 250 g of uranium per liter that may be employed as a reactor fuel at 250°C. Requirements of a satisfactory fuel include the following: parasitic neutron losses to the fuel should be less than 10%; it should be readily dispersible after the reactor has operated for its maximum time of 19 days; it should have a high pH to minimize corrosion and a low hardness to minimize erosion; the viscosity should be low to minimize the power

required for pumping; it should have good thermal properties to permit efficient heat removal; it should not foam excessively; and finally, it must permit easy product recovery and must be readily fabricated for reuse.

Previous work in the absence of radiation has shown that  $UO_3$  platelets represent a stable modification under the anticipated conditions of reactor operation and that slurries of this material possess all the requirements for a satisfactory fuel. However, in preliminary experiments, when 93.4% enriched slurries of  $UO_3$  were heated for one week at 250°C, in a neutron flux of  $10^{11}$ , considerable corrosion of the stainless steel container occurred, and the slurry was found to have caked badly. Work in the next

quarter will be concentrated on studying the factors contributing to corrosion and caking.

**UO<sub>3</sub> Chemistry.** A discussion of the three types of crystals formed by digestion of aqueous UO<sub>3</sub>·H<sub>2</sub>O slurries at 250°C was presented in the previous quarterly report. It was found that the method used to prepare the UO<sub>3</sub> had a direct influence on the character of the hydrated crystals obtained after digestion. The UO<sub>3</sub>·H<sub>2</sub>O assumed the form of orthorhombic rods when prepared from uranium peroxide; thin, orthorhombic platelets when prepared from calcined uranyl nitrate; and large, triclinic sheaves (bipyramidal in character) when the rods, platelets, or calcined uranyl nitrate were digested in dilute solutions of uranyl ion. As slurries, the rods were found to have the desirable characteristics of low bulk density, easy dispersibility, and little tendency to cake or pack. The platelets were slightly less satisfactory than the rods from the standpoint of dispersibility, caking, and packing and were somewhat less attractive in that they possessed higher settling rates and settled to greater bulk densities. However, the platelets are considered to be satisfactory fuel material. The bipyramids were considered too large to be of immediate interest to the present slurry program. Each of these crystal habits appeared to be stable, indefinitely, upon standing in water or upon being subjected to mild agitation at 250°C. However, if they were pulverized or broken up mechanically, as might be expected to occur as a result of the fission process or turbulent circulation through a reactor, further digestion invariably resulted in the formation of platelets. On the basis of these observations, it was concluded that the UO<sub>3</sub>·H<sub>2</sub>O present in an aqueous reactor slurry fuel at 250°C would most likely be in the form of the small, platelet crystals.

During the past quarter, experiments designed to further clarify the relationship between rods and platelets were carried out; observations were made on the preparation of UO<sub>3</sub>·½H<sub>2</sub>O and its stability in water above 300°C; and the preparation of pure UO<sub>3</sub> from uranyl acetate was investigated.

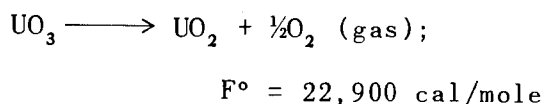
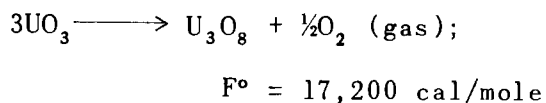
*Relationship Between Rods and Platelets.* Experience has shown that UO<sub>3</sub>·H<sub>2</sub>O crystallizes in the form of orthorhombic rods at 250°C in water when this material is prepared as the decomposition product of UO<sub>4</sub>·2H<sub>2</sub>O. These rod-shaped crystals possess the most favorable slurry characteristics of any UO<sub>3</sub> modification investigated to date. However, any type of attrition process that causes fragmentation of the crystals results in the formation of platelets. Once formed, these platelets have never been successfully converted back to rods. This would seem to indicate that there is something peculiar to the peroxide precipitation step that predetermines the rod-shaped crystal habit - possibly the presence of molecular oxygen produced during peroxide decomposition. However, the nondependence of these systems on external oxygen pressure was indicated when samples of micronized platelets were digested in water at 250°C under 20 to 25 atmospheres of O<sub>2</sub> and under mixtures of O<sub>2</sub> and N<sub>2</sub>. In each of these instances platelets were formed, as had been observed to happen in all previous cases when only steam pressure and air or nitrogen had been present.

It has been suggested that the formation of rods might be traced to the fact that the UO<sub>4</sub>·2H<sub>2</sub>O precipitates in the form of long, hair-like fibers, which, as a result of their geometry, could promote the growth of rods as decomposition to UO<sub>3</sub> occurred. However, this conclusion can be substantiated only indirectly by the lack of conclusive evidence regarding any other type of relationship.

## HRP QUARTERLY PROGRESS REPORT

*Stability of  $UO_3 \cdot H_2O$  at Elevated Temperatures.* In the course of  $UO_3 \cdot H_2O$  crystal growth studies at elevated temperatures, some reduction and caking of the uranium was observed to have occurred in a slurry inadvertently heated for 6 hr at 300 to 350°C. Since no impurities capable of causing this were believed to have been present in the slurry, a question arose as to the stability of  $UO_3$  in water at temperatures in excess of 300°C. Vier<sup>(1)</sup> reported the formation of the hemihydrate when  $UO_3$  was heated at 310 to 350°C in water but did not report any  $UO_3$  instability at those temperatures.

Using the free energy data available in the literature,<sup>(2)</sup> the standard free energies of the two most likely reduction reactions at 350°C were calculated.



(1) D. Vier, *Thermal Stability of Certain Oxide Hydrates in  $H_2O$* , A-1277, May 26, 1944.

(2) I. Kirshenbaum, *Utilization of Heavy Water*, NNES III-4B (1951).

These calculations indicate that reduction at 350°C is quite unlikely.

To explore further the high-temperature stability, a carefully purified  $UO_3 \cdot H_2O$  slurry was prepared and heated at 350°C for 50 hours. The product, a solid closely resembling the  $UO_3 \cdot \frac{1}{2}H_2O$  reported by Vier, was analyzed for reduced uranium and water content. The results of these analyses, together with observations on crystal character of the  $UO_3 \cdot \frac{1}{2}H_2O$  obtained, are presented in Table 21.

No evidence of reduction or caking was obtained. Overdrying of the sample in an oven probably resulted in the moisture content being less than theoretical. On the basis of these data it was concluded that  $UO_3$  is stable in water at 300 to 350°C for an indefinite period of time. This fact is substantiated by lack of reduction in other experiments carried out in this temperature range.

*Preparation of  $UO_3$  from Uranyl Acetate.* The production of pure  $UO_3$  by utilizing a peroxide precipitation step from uranyl nitrate solution is unattractive because of the low bulk density of the peroxide precipitate and the difficulty with which it is washed and filtered. Uranyl acetate,

Table 21

### THERMAL STABILITY OF $UO_3 \cdot H_2O$

Conditions:  $UO_3 \cdot H_2O$  slurry at 350°C for 50 hr in stainless steel autoclave

OBSERVATION	$UO_3 \cdot H_2O$ STARTING MATERIAL	$UO_3 \cdot \frac{1}{2}H_2O$ PRODUCT
$U^{+4}$ (ppm)	50	50
Water content (moles of $H_2O$ per mole of $UO_3$ )	0.83	0.36
Crystal structure	Orthorhombic	Monoclinic*
Crystal habit	Rods, 5 by 30 $\mu$	Imperfect rods, 15 by 60 $\mu$
Color	Yellow	Orange-yellow

\*cf., reference 2 in text.

a water-soluble salt with low thermal stability, was investigated to determine its utility as a starting reagent for the preparation of pure  $\text{UO}_3$ . Table 22 summarizes the results of this investigation.

Direct calcination in air at 360 and 270°C resulted in the formation of  $\text{U}_3\text{O}_8$ . Hydrolysis at 100°C in an open beaker produced a  $\text{UO}_3 \cdot \text{H}_2\text{O}$  that showed a tendency for reduction when heated at 250°C in an autoclave. Precipitation of  $\text{UO}_4 \cdot 2\text{H}_2\text{O}$  from  $\text{UO}_2(\text{Ac})_2$  and subsequent conversion to  $\text{UO}_3 \cdot \text{H}_2\text{O}$  yielded a product identical to that obtained from  $\text{UO}_4 \cdot 2\text{H}_2\text{O}$  precipitated from  $\text{UO}_2(\text{NO}_3)_2$ .

These experiments indicated that a complete separation of acetate radical from the  $\text{UO}_3$  product would be difficult to achieve without causing some reduction of the uranium. The precipitation of  $\text{UO}_4 \cdot 2\text{H}_2\text{O}$  from  $\text{UO}_2(\text{Ac})_2$  solution was somewhat simpler than the corresponding precipitation from  $\text{UO}_2(\text{NO}_3)_2$  since no pH adjustment was required in the former; however, the

peroxide precipitate was equally difficult to process in both cases. It was concluded therefore that  $\text{UO}_2(\text{Ac})_2$  has no significant advantages over  $\text{UO}_2(\text{NO}_3)_2$  as starting material for pure  $\text{UO}_3$  preparation.

*Crystal Growth Measurements.* During the past quarter the rate of growth of particles in  $\text{UO}_3 \cdot \text{H}_2\text{O}$  slurries on being heated at 250°C was investigated. Rods and platelets prepared from  $\text{UO}_4$  and platelets prepared from calcined uranyl nitrate were used in the study. The rate of growth in all cases was rapid during the first 2 hr of heating but decreased markedly as the heating time was extended to 24 hours. In the case of rods and platelets prepared from  $\text{UO}_4$ , the stable particle size was found to be 3.9 and 7.8  $\mu$ , respectively, expressed as equivalent spherical diameter.

The starting material for the crystal growth measurement on rods was  $\text{UO}_3 \cdot 2\text{H}_2\text{O}$  prepared by calcination of well-washed uranium peroxide and subsequent hydration in hot water.  $\text{UO}_3 \cdot \text{H}_2\text{O}$

Table 22  
PREPARATION OF  $\text{UO}_3$  FROM  $\text{UO}_2(\text{C}_2\text{H}_3\text{O}_2)_2$

EXPERIMENT AND CONDITIONS	RESULTS
Calcination in air at 360°C for 16 hr	$\text{U}_3\text{O}_8$ product
Calcination in air at 270°C for 4 hr	$\text{U}_3\text{O}_8$ product
Hydrolysis at 100°C for 15 hr in open beaker	Yellow, irregular $\text{UO}_3 \cdot \text{H}_2\text{O}$ crystals; after autoclaving for 16 hr at 200°C, acquired a greenish tint, analyzed 0.034% $\text{U}^{+4}$
Hydrolyzed in autoclave at 250°C for 16 hr	Yellow, bipyramid crystals of $\text{UO}_3 \cdot \text{H}_2\text{O}$ , analyzed 0.13% $\text{U}^{+4}$
Hydrolyzed in autoclave at 250°C for 64 hr	Greenish, bipyramid crystals of $\text{UO}_3 \cdot \text{H}_2\text{O}$ , analyzed 0.16% $\text{U}^{+4}$
Precipitation of $\text{UO}_4 \cdot 2\text{H}_2\text{O}$ followed by digestion at 250°C	$\text{UO}_3 \cdot \text{H}_2\text{O}$ rods, no $\text{U}^{+4}$ detected

## HRP QUARTERLY PROGRESS REPORT

rods were formed from the dihydrate as the crystal growth studies proceeded at 250°C.

The starting materials for platelet growth studies were prepared in one case by micronizing a sample of rods and in the other by calcination of  $\text{UO}_2(\text{NO}_3)_2$ , followed by washing and hydration to  $\text{UO}_3 \cdot 2\text{H}_2\text{O}$ .  $\text{UO}_3 \cdot \text{H}_2\text{O}$  platelets were formed from both of these samples during heating at 250°C.

The experiments were carried out by heating samples of the slurries at 250°C in sealed quartz tubes in a rocking autoclave for the desired length of time.

Particle size analyses were made by gravitational and centrifugal sedimentation from glycerine-water suspensions of suitable viscosity containing a deflocculant to break up aggregates. In this manner a weight per cent distribution of particles in terms of equivalent spherical diameter was obtained. The average particle size was calculated from the weight distribution in the following manner:

$$S = \frac{6}{100P} \sum \frac{W}{\bar{D}}$$

$$S = \frac{6}{P} \frac{1}{D_{\text{avg}}} \quad (\text{for spherical particles})$$

$$\frac{6}{P} \frac{1}{D_{\text{avg}}} = \frac{6}{100P} \sum \frac{W}{\bar{D}}$$

$$D_{\text{avg}} = \frac{100}{\bar{D}}$$

where

$S$  = surface area of solid

$P$  = density of solid

$W$  = weight per cent of solid between  $D_1$  and  $D_2$

$$\bar{D} = \frac{D_1 + D_2}{2}$$

$D_{\text{avg}}$  = average diameter in microns.

These calculations are quite reliable when  $D_1$  and  $D_2$  are taken over a sufficiently small size interval and the particles are greater than 0.1 micron.

Although this method of analysis probably does not measure true particle sizes, it does yield values that are closely related to the property of interest, that is, how the particles behave on settling from a fluid medium. Moreover, since the data were obtained under consistent conditions, changes in particle size are a measure of the rate of growth. Tables 23, 24, and 25 summarize the results of the investigation.

As the data of Tables 23, 24, and 25 indicate, small  $\text{UO}_3$  particles increase rapidly in size on heating at 250°C in water until a relatively stable particle size is reached after a few hours of heating. In the case of rods, the observed equilibrium particle size was 3.9  $\mu$ ; for platelets prepared from micronized rods, 7.8  $\mu$ ; and the platelets prepared from  $\text{UO}_2(\text{NO}_3)_2$  appeared to have an equilibrium particle size considerably larger than that of the other two.

The observed growth rates may be explained by the various factors governing particle size increase. It is well known that growth by coalescence of small particles is a very rapid process, since two small particles tend to adhere because the surface energies of the particles are decreased by the collision that results in the formation of the larger particle. This type of process may explain rapid

Table 23

PARTICLE SIZE GROWTH IN SLURRIES OF  $UO_3 \cdot H_2O$  RODS UPON HEATING

Conditions: 250 g of uranium per liter; heated in sealed quartz tubes;  
all particle sizes as equivalent spherical diameter

HEATING CONDITIONS	AVERAGE PARTICLE SIZE ( $\mu$ )	2.5 wt % FRACTION UNDER STATED SIZE ( $\mu$ )	10 wt % FRACTION ABOVE STATED SIZE ( $\mu$ )	SOLUBLE URANIUM IN SUPERNATANT (mg/ml)
Unheated slurry	0.5	0.3	1.3	
Heated to 160°C and allowed to cool	2.6	1.0	3.9	0.134
Heated to 250°C and allowed to cool	2.3	1.6	2.7	0.096
Heated at 250°C for 1 hr	3.0	1.6	6.1	0.135
Heated at 250°C for 2 hr	3.1	1.9	4.9	0.210
Heated at 250°C for 4 hr	3.2	1.5	5.3	0.240
Heated at 250°C for 24 hr	3.9	1.8	5.5	0.200

Table 24

PARTICLE SIZE GROWTH IN SLURRIES OF  $UO_3 \cdot H_2O$  PLATELETS  
(PREPARED FROM  $UO_4$ ) UPON HEATING

Conditions: 250 g of uranium per liter; heated in sealed quartz tubes;  
all particle sizes as equivalent spherical diameter

HEATING CONDITIONS	AVERAGE PARTICLE SIZE ( $\mu$ )	2.5 wt % FRACTION UNDER STATED SIZE ( $\mu$ )	10 wt % FRACTION ABOVE STATED SIZE ( $\mu$ )	SOLUBLE URANIUM IN SUPERNATANT (mg/ml)
Unheated slurry	1.8	0.4		
Heated to 160°C and allowed to cool	2.8	0.7	7.4	0.250
Heated to 250°C and allowed to cool	4.2	1.6	10.3	0.310
Heated at 250°C for 1 hr	4.8	1.3	10.4	0.280
Heated at 250°C for 2 hr	6.0	2.5	13.3	0.468
Heated at 250°C for 24 hr	7.8	5.0	14.6	0.625

## HRP QUARTERLY PROGRESS REPORT

Table 25

### PARTICLE SIZE GROWTH IN SLURRIES OF $UO_3 \cdot H_2O$ PLATELETS (PREPARED FROM $UO_2(NO_3)_2$ ) UPON HEATING

Conditions: 250 g of uranium per liter; heated in sealed quartz tubes;  
all particle sizes as equivalent spherical diameter

HEATING CONDITIONS	AVERAGE PARTICLE SIZE ( $\mu$ )	2.5 wt % FRACTION UNDER STATED SIZE ( $\mu$ )	10 wt % FRACTION ABOVE STATED SIZE ( $\mu$ )
Heated 250°C and allowed to cool	2.9	1.1	8.9
Heated at 250°C for 1 hr	5.9	3.1	8.3
Heated at 250°C for 2 hr	7.2	3.2	13.3

growth in the early stages of the experiment when small particles predominate. However, as particle size increases there is less tendency toward this type of process, since the surface energies of the larger particles are much lower. The growth is then controlled by other factors such as solubility, which also decreases with increasing particle size, and rates of diffusion and deposition of the soluble uranium. These factors result in slower growth rates.

In this work soluble uranium, varying from 130 to 625 ppm, was present and may have increased both the rate of particle size growth and the equilibrium particle size.

*Physical Properties of  $UO_3$  Slurries.* Morse spent March 19 to 23 at the laboratory of Professor J. M. Dalla Valle, of Georgia Institute of Technology, investigating methods for determining the surface area of  $UO_3$  powder and the viscosity of  $UO_3$  slurries. Surface area measurements were made by the stearic acid<sup>(3)</sup> and nitrogen adsorption techniques. In the stearic acid

adsorption measurements, changes in stearic acid concentration due to adsorption on the surface of the solid were determined by conductometric titration and by the hydrophil balance, an apparatus that measures the surface areas of stearic acid films on water. Very poor agreement was observed between the stearic acid and nitrogen adsorption methods for determining surface area (Table 26). It is believed that the stearic acid adsorption technique, in its present form, is not applicable to  $UO_3$  powder.

Viscosity determinations were made by measuring the time required for a known volume of slurry to flow through a vertical tube of the proper dimensions. A Saybolt viscosimeter was adapted for this purpose by sealing the tube to the exit nozzle. In this apparatus, only the temperature and concentration could be varied for a given tube. The pressure was fixed by the head of the suspension within the viscosimeter.

Measurements of viscosity as a function of concentration and temperature were made (Fig. 35). The viscosity of the slurry increased with increasing solids concentration and decreased

<sup>(3)</sup>A. S. Russell and C. N. Cochran, *Ind. Eng. Chem.* **42**, 1332 (1950).

Table 26

SURFACE AREA DETERMINATIONS OF  $UO_3 \cdot H_2O$

	SURFACE AREA (sq meters/g)		
	By Stearic Acid Adsorption		By Nitrogen Adsorption*
	Conductometric Titration	Hydrophil Balance	
$UO_3 \cdot H_2O$ (platelets)	0.89	0.08	0.45
$UO_3 \cdot H_2O$ (rods)	2.9	0.14	0.22

\*Measurements made at K-25 Laboratory.

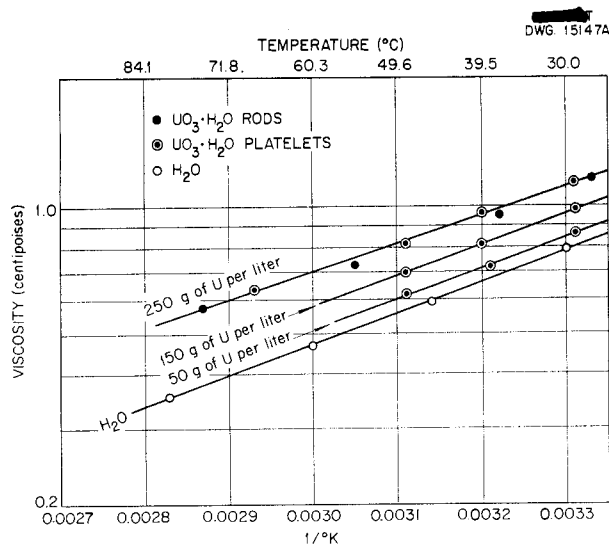


Fig. 35. Viscosity of  $UO_3 \cdot H_2O$  Slurries as a Function of Temperature.

with increasing temperature for a given concentration. The viscosity of a slurry containing 250 g of uranium per liter as  $UO_3 \cdot H_2O$  was greater by 40 to 50% than that of water at the corresponding temperatures. Further, there was no difference in viscosity between the slurries of rods and platelets containing 250 g of uranium per liter.

Plots of the fluidity (reciprocal of viscosity) vs. concentration for fixed temperatures have been made (Fig. 36). The resulting isotherms

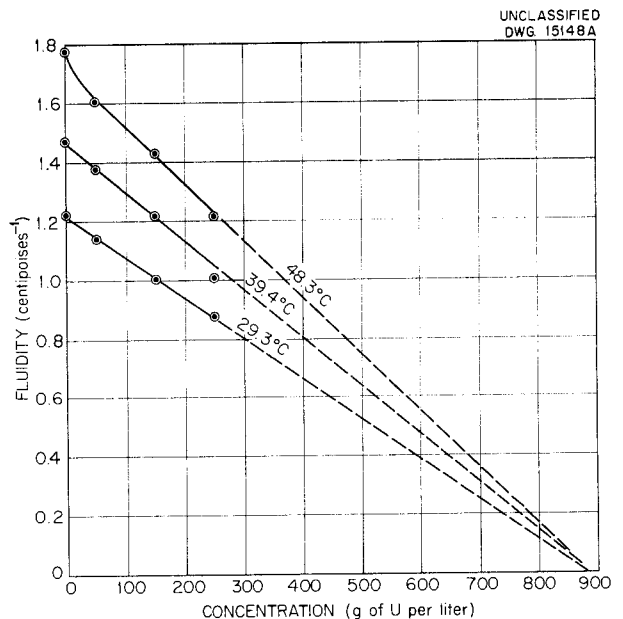


Fig. 36. Fluidity of  $UO_3 \cdot H_2O$  (Platelet) Slurries as a Function of Concentration.

when extrapolated to zero fluidity converge at a concentration of 890 g of uranium per liter. This result is of interest since it appears to be related to the volume occupied by the solid phase of a settled slurry that has been heated over 24 hr at 250°C. It has been found that the settled solids occupy 20 to 30% of the total volume, which is equivalent to a uranium concentration of 1250 to 830 g

## HRP QUARTERLY PROGRESS REPORT

of uranium per liter in the settled-solids volume. Although a linear line has been used to obtain the fluidity intercept, there is no reason to suppose that this is a necessarily true picture. If the isotherm were to approach zero fluidity asymptotically, higher values for the concentration would be obtained. Moreover, variation in the particle size distribution could also affect the results.

**Radiation Chemistry.** The study of the effect of reactor radiation on the properties of uranium oxide slurries has continued with another experiment carried out in hole 12 of the X-10 graphite reactor. Previous experiments have shown that caking was enhanced by radiation.<sup>(4)</sup> In addition, the corrosion of untreated type 347 stainless steel was found to be sufficient to indicate the advisability of using a pretreated steel. The present study was carried out in a chromic acid pretreated bomb. Caking was again pronounced. The pretreatment film was found to be unsatisfactory in that considerable scaling was evident and made difficult any interpretation of corrosion effects directly attributable to chemical attack or radiation damage. Qualitative agreement with the previous studies was observed in the reduction of uranium, the increase in soluble uranium, gas production, and fission-product distribution (Table 27).

The experiment was carried out at three-fourths maximum flux for 144 hr and at an average temperature of 300°C. The sample irradiated was composed of 15 ml of a slurry containing 250 mg of 93.4% enriched uranium per milliliter as uranium trioxide monohydrate rods. It was contained in a type 347 stainless steel bomb equipped with a capillary

tubing and a stirrer with a soft iron core. The stirrer was operated by means of an intermittently activated solenoid placed so as to move the stirrer up and down in the slurry at intervals of 10 seconds. All interior parts of the bomb were pretreated prior to use with 2% chromic acid for 16 hr at 250°C. Temperature was followed by means of a thermocouple attached to the bomb exterior. A control experiment was performed outside the reactor but at 250°C and without stirring.

As in the previous radiation experiments, transfer of the slurry from the radiation bomb to the glass sampling apparatus was incomplete, which indicated that some caking occurred during the experiment. A sufficient fraction of the solid was recovered, however, to demonstrate in a qualitative manner changes that may occur in a slurry during its use as a reactor fuel (Table 27). The caking itself may not at present be considered as directly attributable to radiation damage, since all the variables associated with the experiment have not as yet been thoroughly studied in the absence of radiation.

Considerable sludge, insoluble in 8 N HNO<sub>3</sub>, and probably iron and chromic oxides from the pretreatment film were observed in the final slurry. The sludge contained about 27% of the total fission-product activity produced by the irradiation. Approximately 99% of the remaining activity appeared in the slurry solids and the rest in the supernatant.

Soluble uranium increased in both the control and radiation experiments from 18 mg per liter to 212 and 180 mg per liter, respectively. The final supernatants in both cases contained 49 mg per liter of nitrate ion. A sample of the original solid was found to contain 72 mg per gram of nitrogen.

<sup>(4)</sup>F. R. Bruce, J. O. Blomeke, L. E. Morse, and J. P. McBride, *Homogeneous Reactor Project Quarterly Progress Report for Period Ending March 15, 1952*, ORNL-1280, p. 101-109.

Table 27

## SUMMARY OF REACTOR RADIATION EXPERIMENT 3

OBSERVATION	ORIGINAL SLURRY	CONTROL EXPERIMENT	RADIATION EXPERIMENT
			(flux = $4 \times 10^{11}$ neutrons/cm <sup>2</sup> ·sec)
Material	250 mg of U per ml; 93.4% enriched, UO <sub>3</sub> ·H <sub>2</sub> O rods	10 ml of original slurry	15 ml of original slurry
Duration of experiment (hr)		144	144
Average temperature (°C)		250	300
Recovered volume (ml)		5*	11
Color of slurry	Yellow	Red-brown	Dark gray-green
Uranium recovered (%)			
Original transfer		100	20
Dried cake			30
Uranium in supernatant (mg/ml)	0.018	0.212	0.180
U <sup>4+</sup> in slurry (%)			5
Nitrogen in solid (mg/g)	0.072		
Nitrate in supernatant (mg/ml)	0.035	0.049	
pH	6.7		5.3
Fission-product distribution (%)			
Slurry			72
Supernatant			1
Sludge			27
Corrosion products in supernatant (mg/ml)			
Fe		0.001	0.012
Ni		0.001	0.014
Cr		0.010	0.001
Corrosion products in slurry (wt %)			Total sludge 20 vol % of solid
Fe		1.03	
Ni		0.03	
Cr		1.57	
Equilibrium gas pressure (psia)			2800
Gas composition**			65% H <sub>2</sub> 30% O <sub>2</sub> 1% CO <sub>2</sub> 4% inert material
Approximate G value (ion pairs/100 ev)			0.5
Crystal shape	Rods	Irregular particles	Rods, fragments, and platelets
Average size	2.0 by 5.4 μ		1 μ
Settling rate	Total in 25 min		Total in 2 min

\*About one-half the supernatant had distilled to outside of bomb.

\*\*Analysis performed by W. F. Kieffer.

The increase in soluble uranium may be attributed to the presence of this impurity. The decrease in pH from 6.7 to 5.3 may also be indicative of the increase in uranyl nitrate concentration. Corrosion would likewise be enhanced.

The concentration of substances that could be oxidized by cerate (UO<sub>2</sub>, UO<sub>4</sub>, H<sub>2</sub>O<sub>2</sub>) was equal to 5 mole % of the total uranium. If this is U<sup>4+</sup>, its presence could be explained by the

reduction of the nitrate by radiation and the subsequent reduction of the uranium by the nitrite so produced.

The equilibrium gas pressure, including steam pressure, at 300°C was about 2800 psia. The gas sample removed from the bomb at the end of the irradiation indicated only a slight increase in the hydrogen-to-oxygen ratio (65% H<sub>2</sub> and 30% O<sub>2</sub>) over that to be expected from the radiation decomposition of water. By using the

## HRP QUARTERLY PROGRESS REPORT

initial pressure increase for the first hour of irradiation (1200 psia at 261°C), the estimated gas space of 14.8 ml (bomb volume of 33 ml minus the expanded volume of the slurry), and by assuming no recombination of hydrogen and oxygen, a  $G$  value of 0.4 to 0.5 was calculated. This would indicate that about 30 to 40% of the ionizing activity of the fission fragments is expended in the supernatant, which agrees rather closely with the 28% of the fission activity found outside the slurry solids in the sludge and supernatant. It is also apparent that some process was occurring that allowed the system to reach a rather low steady-state pressure. This process may be the recombination of hydrogen and oxygen promoted by the dissolved uranyl nitrate or by the uranium oxide itself, since pure water alone has only a small effect on the recombination.<sup>(5)</sup> It is also possible that the attainment of the steady-state pressure is the result of a caking process that prevents the majority of the fission fragments from dissipating themselves in the supernatant.

The irradiated material showed the customary particle size degradation and some transformation to platelets. The control run was unusual in its change of color to red-brown and the production of irregular particles. Some of the irregular particles were several hundred microns on a dimension and resembled bipyramids. Since a high concentration of iron and chromium was found in the solid, it appears likely that the observed changes were due in part to a degradation of the pretreatment film and subsequent adsorption of the products on the surface of the particles.

A study of possible pretreatments for use in the radiation bombs and a

(5) H. F. McDuffie, et al., *Chemistry Division Quarterly Progress Report for Period Ending December 31, 1951*, ORNL-1260.

more thorough investigation of the factors contributing to caking and corrosion are planned. In addition, a study of the effect of the slurry itself on the recombination of hydrogen and oxygen will be initiated.

**Slurry Engineering Studies.** Although slurries are generally considered as possible fuels for either the dynamic or boiler type of reactor, which of these types they are better suited for remains uncertain. Consequently, it was felt that some experimental work on the boiling, foaming, and caking properties of slurries, as well as some additional effort on selected pumping problems, was a necessary adjunct to the laboratory developmental program. An experimental, stainless steel boiler, equipped with a 4-kw resistance heater was constructed and a 2-liter-capacity pumping loop was designed. The first experimental boiling run was completed, and some rough calculations were made of the temperature gradient across an idealized slurry particle and its immediate environment in a homogeneous reactor.

**Slurry Boiler.** A sketch of the slurry boiler installation is given in Fig. 37. The boiler is made entirely of heat-treated types 316 and 347 stainless steel. It was designed to operate with 1 liter of slurry at 250°C and 600 psi, with a 100% freeboard allowed above the liquid. It consists of an 18-in. length of 4-in., schedule-80 pipe with a cap welded on the bottom and 4-in.-high pressure flanges at the top. The heat input is supplied by two Calrod heaters of 3- and 1-kw capacity, silver-soldered on the outside on the bottom and around the lower section of the vertical wall. The top heater is wound so that it covers only the section of wall below the liquid level when the boiler is charged with 1 liter of slurry. Three loops of 3/8-in. tubing extend through

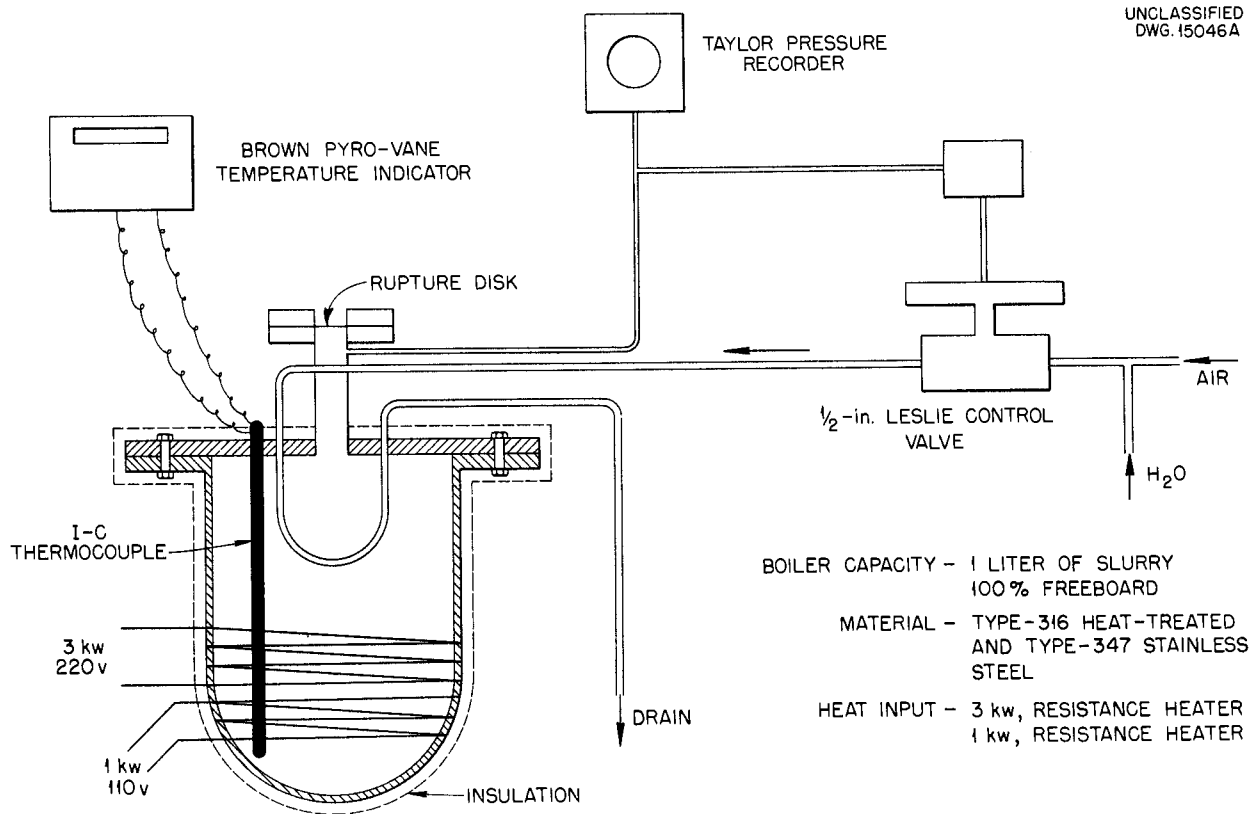


Fig. 37. Slurry Boiler.

the top flange and serve as internal condensers. The coolant inside the coils is water, with air added as a vehicle for flow. The pressure within the boiler is controlled by regulating the rate of water flow within the condenser coils. The water flow is automatically controlled by a Leslie pressure control valve and pilot regulator. A Taylor recorder is used to obtain a continuous record of the pressure within the boiler. The boiler is also equipped with a rupture disk as a safety precaution, and a thermocouple well extends to within 2 1/2 in. of the bottom. The temperature is measured by an iron-constantan thermocouple and a Brown Pyro-Vane indicator. The entire boiler is covered with 2-in.-thick magnesia insulation.

A calibration of the heat losses from the boiler was made by measuring

the energy required to maintain the pressure above 1 liter of water at 565 psig with no coolant circulating through the condenser. This pressure corresponds to the vapor pressure of water at 250°C. The heat loss was found to be 385 w or 1313 Btu/hr; this quantity must be deducted from the total energy input of each run when computing the net heat added to the slurry.

The boiler, together with two small corrosion specimens of types 316 and 347 stainless steel, was given a nitric acid pretreatment prior to the first slurry run. This consisted of allowing a mixture of 20% HNO<sub>3</sub>-3% HF to remain in the boiler at room temperature for 30 minutes. After removing the etching solution, the surfaces were washed and the procedure repeated. Finally, 1500 ml of 1% HNO<sub>3</sub> was added and heated for 16 hr at 250°C. A preliminary UO<sub>3</sub>

## HRP QUARTERLY PROGRESS REPORT

slurry was then introduced, boiled for 8 hr, and removed by washing. The boiler was maintained full of water until the material for the first slurry run was introduced.

Slurry for the first run was prepared from washed, micronized, Mallinckrodt  $\text{UO}_3$  containing 250 g of uranium per liter. After boiling for 4 1/2 hr at  $250^\circ\text{C}$  and a power density of 4.2 kw/liter, the safety disk ruptured prematurely and caused the water to flash evaporate. Analysis of the residual solids showed the  $\text{UO}_3 \cdot \text{H}_2\text{O}$  to be in the form of platelets. The most notable observation made at the conclusion of this short run was that there was no evidence of foaming having occurred. Solids were not found deposited along the walls any higher than the liquid level of the slurry at  $250^\circ\text{C}$ . There was also no change in weight or appearance of the corrosion samples. A second run that utilizes similar oxide and is scheduled to be boiled for a longer period of time is currently under way.

*Heat Transfer Calculations.* Consideration has been given to the thermal environment of a particle of  $\text{UO}_3 \cdot \text{H}_2\text{O}$  suspended as part of a slurry fuel in a homogeneous reactor. Very rough calculations were made to estimate the temperature that the solid particle would attain if the water of suspension was maintained at  $250^\circ\text{C}$ . This question has direct bearing on the chemical form of the slurry under reactor operating conditions. The calculations assumed a reactor power level of 15 kw/liter, a uranium concentration of 250 g per liter of fuel solution, and spherical  $\text{UO}_3 \cdot \text{H}_2\text{O}$  particles 2  $\mu$  in diameter. The heat flux under these conditions would be 38 Btu/hr·ft<sup>2</sup> or  $3.61 \times 10^{-8}$  calories per second per particle. It was found that under such circumstances essentially no temperature gradient

existed within the particle itself. The temperature gradient across a steam film around such a particle is dependent on the thermal resistance of the film. No applicable film coefficient expressing the resistance across a  $\text{UO}_3$ -steam interface is available, but if a value of  $h = 200$  Btu/hr·ft<sup>2</sup>·°F is assumed, a temperature difference of only  $10.5^\circ\text{C}$  would exist between the solid and an enveloping steam film at  $250^\circ\text{C}$ . Such a difference would fall well within the limits of  $\text{UO}_3 \cdot \text{H}_2\text{O}$  stability. It is intended that these calculations be modified as better values of heat transfer data are obtained.

### SLURRY PUMPING STUDIES

R. N. Lyon, Section Chief

A. S. Kitzes                      R. B. Gallaher  
W. Q. Hullings

**Loop Test at  $250^\circ\text{C}$ .** A 100-hr test has been completed of the corrosion-erosion behavior of a circulating slurry containing 78 g of uranium per liter as rod-type  $\text{UO}_3 \cdot \text{H}_2\text{O}$  at  $250^\circ\text{C}$  in a type 347 stainless steel loop equipped with a Westinghouse Model 100A pump. The maximum pipe line velocity of 70 ft/sec occurred in the throat of a venturi. There was no formal pretreatment of the system except cleaning with 3% trisodium phosphate at  $150^\circ\text{C}$  and rinsing until the pH of the effluent was below 7. There was a 24-hr preliminary test with distilled water at  $250^\circ\text{C}$  to check the instruments. The system was pressurized with steam only, so the oxygen in the system was only that associated with air that was trapped when the system was filled or air dissolved in the slurry. During most of the test the pH of the cooled samples was close to 7, perhaps because of the presence of residual trisodium phosphate from the cleaning.

For a 2-hr period during the test the slurry inadvertently was permitted to flow through bearings of the pump with no apparent deleterious effect on the Graphitar bearings or the titanium carbide journals.

After 100 hr of operation, the chromium and nickel measurements on samples taken from the loop were still below 5 ppm, whereas the iron content had risen to about 12 ppm. These results can be considered from only a qualitative standpoint, because the high pH caused most of these elements to occur with the solids in the slurry, rather than with the liquid, and it could not be determined how representative a sample of the solids was obtained.

Examination of the pump impeller, orifice, and test samples in the system showed no visible signs of corrosion or abrasion, other than a shiny film. Figures 38 through 41 are photographs of the impeller and test specimen. The orifice readings showed no drift during operation of the system, which is further evidence that negligible damage occurred to the orifice.

The particles became quite rounded; the rods, which originally were 2 to 3  $\mu$  in diameter and about 15 to 20  $\mu$  in length, became either spherical or ellipsoidal with essentially no change in the diameter. The fragments that were abraded from the rods also became spherical. The abrasion of the particles without apparent abrasion of the loop system lends support to the observation of the Chemical Technology Division that  $UO_3 \cdot H_2O$  rods are much softer than stainless steel.

Measurement of the Graphitar bearings through which slurry flowed for 2 hr showed that wear, if any, was less than 0.0005 in. on the diameter.



UNCLASSIFIED  
PHOTO 10217

**Fig. 38. Front Face of Impeller After Pumping a Slurry Containing 78 g of Uranium per Liter for 100 hr at 250°C. About one-half actual size.**



UNCLASSIFIED  
PHOTO 10218

**Fig. 39. Back Face of Impeller Showing Grooves Cut by Protruding Metal on Back Thrust Pads. Grooves were smoothed out with emery cloth and then exposed to slurry containing 78 g of uranium per liter for 100 hr at 250°C. There was no evidence of erosion. About one-half actual size.**

## HRP QUARTERLY PROGRESS REPORT

A new test at 250°C has been started. In this test a slurry containing about 157 g of uranium per liter as  $UO_3 \cdot H_2O$  will be circulated for 500 hours. Subsequent tests will be made to determine the influence of fission products, oxygen, and other contaminants on the system.

**Thorium Loop Test at 150°C.** A slurry containing 100 g of  $ThO_2$  per liter (88 g of thorium per liter) is



**Fig. 40.** Intake Hub of Impeller After Pumping Slurry Containing 78 g of Uranium per Liter for 100 hr at 250°C. There was no evidence of erosion. Original magnification 10X. Reduced 52%.



**Fig. 41.** Type 304 Stainless Steel Erosion Test Sample After Being Exposed to Slurry Containing 78 g of Uranium per Liter for 100 hr at 250°C. White area is not erosion or corrosion products. Original magnification 2.3X. Reduced 52%.

now being circulated in the 110 to 150°C loop.<sup>(6)</sup> Heat transfer, abrasion, and particle size change will be measured.

A mixture of  $HNO_3$ , HF, and  $Th(NO_3)_4$  will be used to remove residual thorium oxide from the system after draining. The mixture of nitric and hydrofluoric acids is to be used because of the chemical inertness of the oxide with most common reagents. The  $Th(NO_3)_4$  forms a complex with the HF, and tests show that this reduces the attack on the stainless steel system without seriously impairing the action on  $ThO_2$ .

**Bearing Tests with  $UO_3 \cdot H_2O$  Slurry.** The first phase of a test of plain bearings in  $UO_3$  slurries has been completed. A Stellite journal, 1.4995 in. in diameter, was rotated in a 1.502-in.-dia Stellite bearing for 100 hr at 1750 rpm with a radial load of 20 psi. The only lubricant between the surfaces was a slurry containing about 80 g of uranium per liter as rod-type  $UO_3 \cdot H_2O$ . The lubricant was supplied by a small pump. The system was stopped frequently and the surfaces examined for signs of wear or abrasion by means of a profilometer with a sensitivity on the order of 1 microinch. Neither abrasion nor wear was found up to the time the motor of the slurry pump failed and the bearing was forced to run dry for a short time. A new bearing is now under construction at the University of Tennessee. Members of the staff of the university are cooperating in these studies.

**Crystal Growth.** The crystal structure of  $UO_3 \cdot H_2O$  rods did not change when the slurry was autoclaved for less than 72 hr at 250°C in the

<sup>(6)</sup> A. S. Kitzes, R. B. Gallaher, R. V. Bailey, W. Q. Hullings, and C. A. Gifford, *Homogeneous Reactor Project Quarterly Progress Report for Period Ending August 15, 1951*, ORNL-1121, p. 160-161.

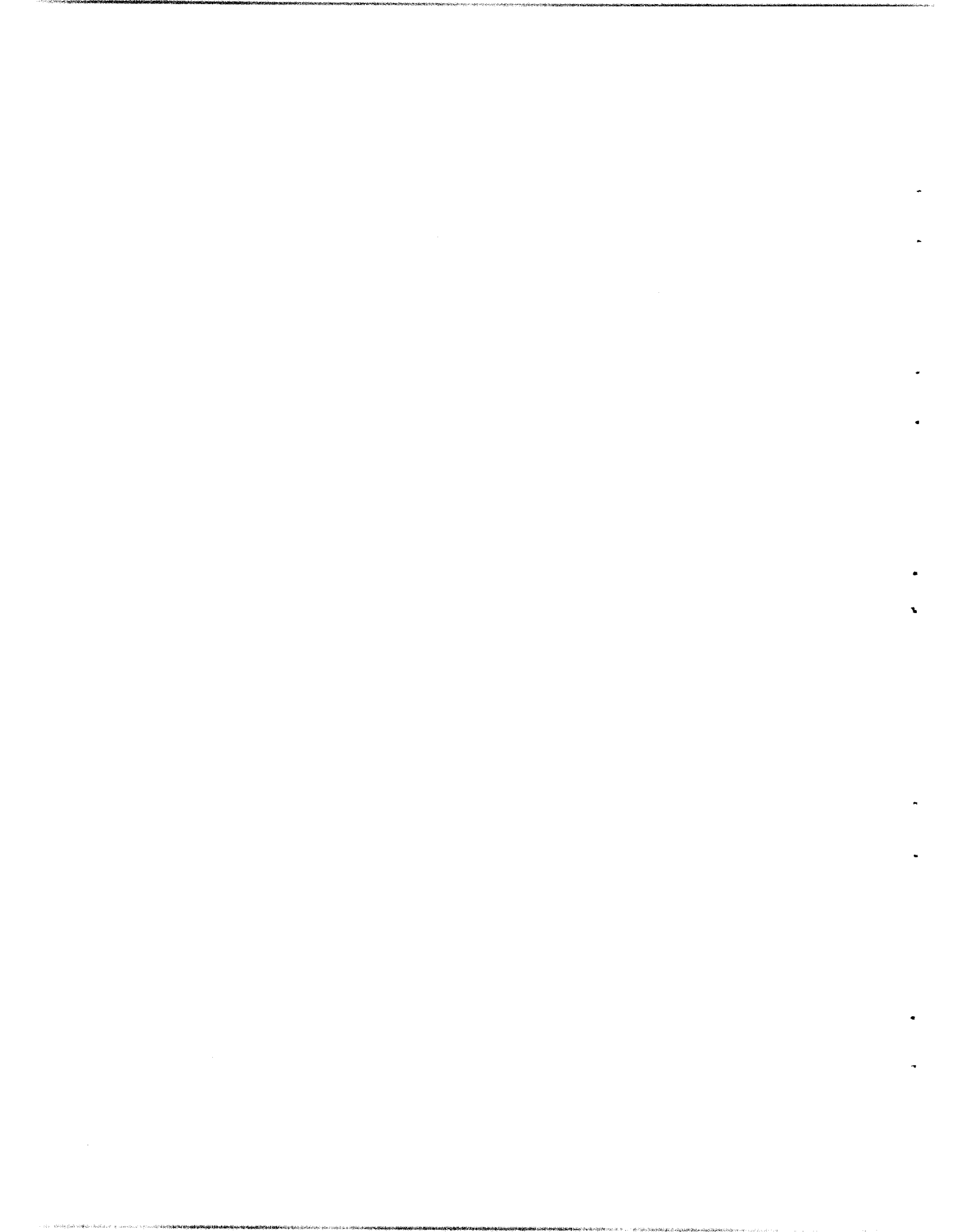
FOR PERIOD ENDING JULY 1, 1952

presence of nitrate ions. Some rhombohedral crystals were found upon microscopic examination of rods autoclaved at 250°C for as much as 72 hr in the presence of 500 ppm of excess nitrate ions as  $\text{KNO}_3$ . Since the chemical analysis and microscopic examination are incomplete, the results cannot yet be interpreted.

Tests are continuing in which the nitrate content is being decreased

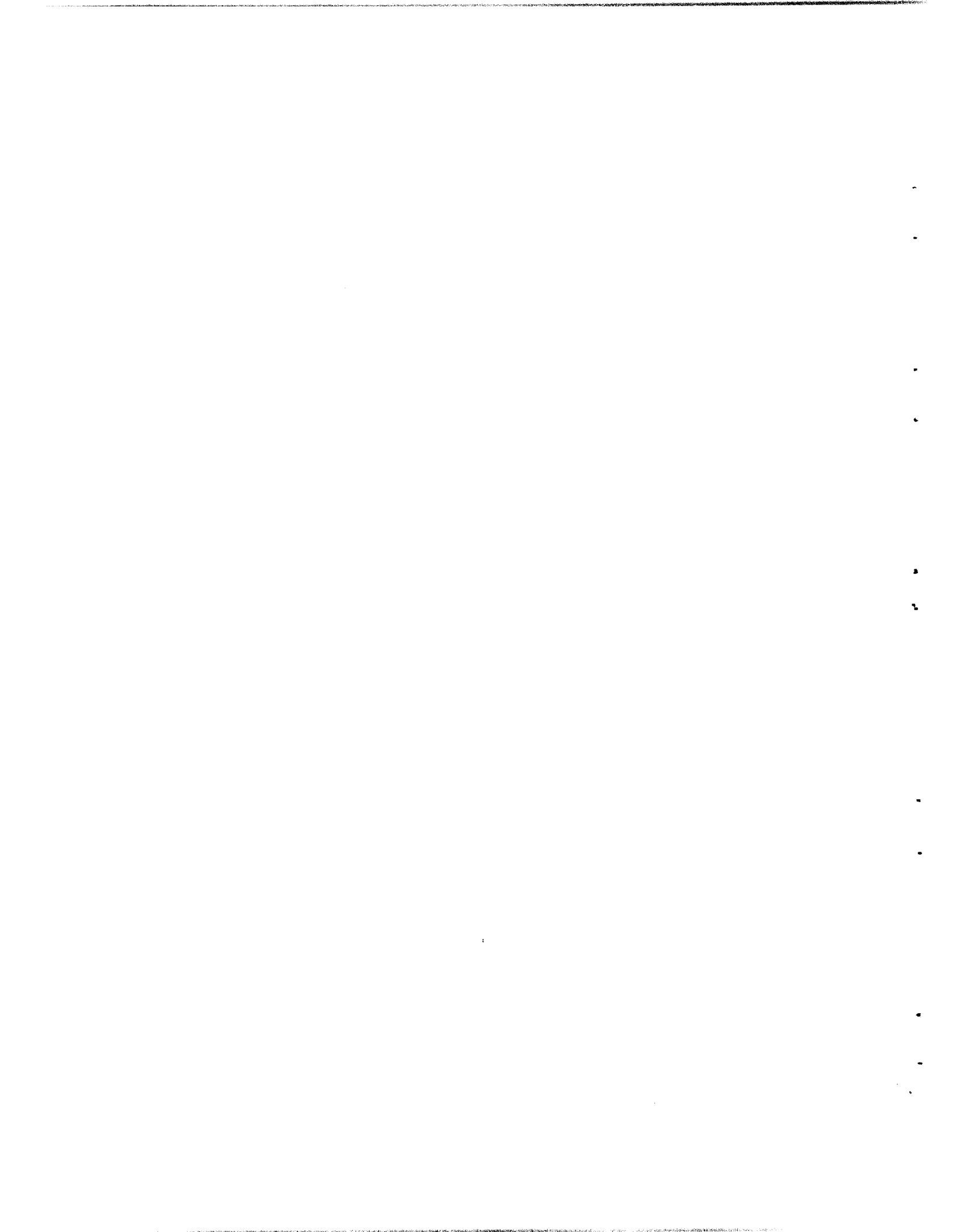
and varying amounts of uranyl ion, as  $\text{UO}_2(\text{NO}_3)_2$ , are added to determine the effect of these ions on the crystal structure of both rods and platelets.

**Criticality Experiments.** The reactor vessel and dump valve for the criticality determination are now being fabricated in the Y-12 shop. This equipment and the instruments will be completed about August 1.



**Part III**

**GENERAL HOMOGENEOUS REACTOR STUDIES**



## ISHR DESIGN

R. B. Briggs, Section Chief  
J. O. Bradfute      P. N. Haubenreich  
R. H. Chapman      M. Tobias  
C. E. Klotz

The basis for selecting a power level, core size, solution circulation rate, and other operating conditions for the ISHR was described in the last quarterly report.<sup>(1)</sup> It was concluded that the power level should be near 50 megawatts, that the core diameter should be 6 ft, and that the fuel (uranyl sulfate in D<sub>2</sub>O) circulation rate should be variable in the range of 5,000 to possibly 20,000 gpm. Curves were presented for the heat production in the reactor vessel, for the penetration of radiation through various shielding combinations, and for the radioactivity induced in the piping by delayed neutrons emitted in the circulating system. Problems incurred in handling the deuterium and oxygen resulting from the radiation decomposition of moderator and the pressures and stresses in equipment resulting from the explosive recombination of the gases were discussed. Information regarding the preliminary flow sheets, layouts of reactor and circulating equipment, design of the core tank and other pieces of equipment, and some of the criticality and control calculations is presented in this report.

Recent corrosion information makes it appear doubtful that a reactor constructed of stainless steel and fueled with uranyl sulfate can be operated at 250°C with the concentration of uranium required for producing plutonium. However, the ISHR is intended to serve as a pilot plant for testing a variety

of fuels under varied operating conditions. Consequently, the conceptual design is proceeding upon the basis that a fuel solution or slurry that can be used at 250°C in stainless steel will be developed. Investigations will be made to show that the same reactor can be used to produce plutonium with uranyl sulfate solutions at lower temperatures. The effect upon the design of lining the equipment with materials more corrosion resistant than stainless steel is being considered.

### FLWSHEETS

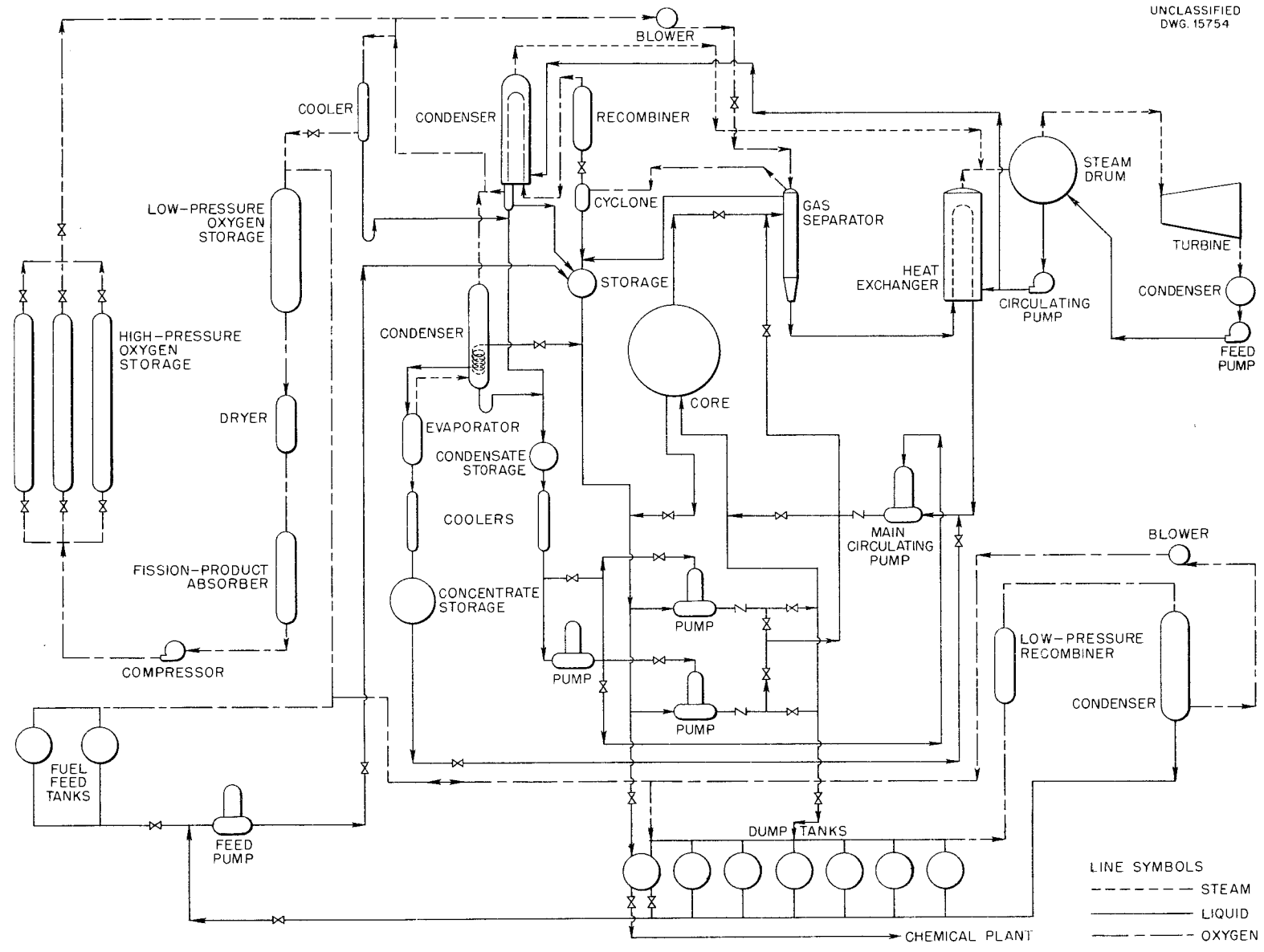
A preliminary flowsheet that shows major equipment items and forms the basis for the conceptual design is presented in Fig. 42. Although similar in many respects to that of the HRE, the flowsheet has modifications intended to eliminate the following features associated with the HRE.

1. The decomposition of H<sub>2</sub>O results in H<sub>2</sub> and O<sub>2</sub> being separated from the fuel solution in the HRE core, which may cause a variable hold-up of explosive gas that could be difficult to control.

2. H<sub>2</sub> and O<sub>2</sub> are recombined at low pressure. The let-down system requires that an appreciable volume of liquid be reduced in pressure with the gas.

3. Because the decomposition gases and some liquid are reduced in pressure continuously, the reactor operation depends upon a steady volume of fuel being returned to the system and the satisfactory operation of a pump discharging against a pressure of 1000 psi.

<sup>(1)</sup> R. B. Briggs, R. E. Aven, J. O. Bradfute, R. H. Chapman, P. N. Haubenreich, C. E. Klotz, and T. H. Pigford, *Homogeneous Reactor Project Quarterly Progress Report for Period Ending March 15, 1952*, ORNL-1280, p. 113.



## FOR PERIOD ENDING JULY 1, 1952

The main circulating system for the ISHR consists of the reactor vessel, an external centrifugal gas separator, a shell-and-tube heat exchanger, and a circulating pump. Separator, exchanger, and pump are shown as single equipment pieces on the flowsheet, although multiple units may be selected for the design.

Oxygen is recirculated at high pressure through the axial void in the gas separator. The decomposition gases are carried by the oxygen from the void through a cyclone separator to remove entrained liquid and into the catalytic recombiner. Hot gases from the recombiner pass into a cooler where the temperature is returned to 250°C and some D<sub>2</sub>O is condensed. A blower is indicated in the flowsheet for recirculating the cooled gas.

The pressure in the reactor is controlled by regulating the pressure in the gas recirculating system. This can be accomplished during steady operation by controlling the temperature of the gases issuing from the cooler. Under abnormal conditions it is possible to reduce the pressure by bleeding gas into a low-pressure reservoir or to increase the pressure by admitting gas from a high-pressure reservoir. Gas from the low-pressure storage is passed through a dryer and a fission-product absorber before being compressed and pumped to the high-pressure storage.

In the present conception the gas separator also serves as a reservoir into which fluid can be ejected from the core if the temperature of the core rises and the fluid expands or from which fluid can be removed if the temperature decreases and the fluid contracts. The changes are taken up as changes in volume of the axial void in the separator. The minimum void volume is regulated by a

baffle that permits excess liquid to overflow into an auxiliary tank. Liquid is pumped continually from the auxiliary tank into the main circulating system so that a contraction in the liquid volume in the separator only results in a temporary enlargement of the void.

Some liquid from the recycle reservoir flows into an evaporator where D<sub>2</sub>O is obtained to supplement that produced in the recombiners for feeding into the rotor cavity of the canned-rotor pumps. This feed is necessary to prevent concentrated uranyl sulfate, or other fuel, from contacting the bearings and the Inconel can. Concentrate from the evaporator is normally returned to the circulating system, but it can be stored when the fuel concentration in the reactor is to be increased. Although an evaporator is shown in the flowsheet, the boiling point of the fuel may be above the temperature at which uranyl sulfate, or another solution, separates into two phases. In this case the light phase would contain so little uranium that it could be withdrawn and used without evaporation.

The heat exchanger in the main circulation system is a vertical, shell-and-tube, forced-circulation boiler. Fuel solution flows through the tubes. Steam generated on the shell side passes into a steam drum where the liquid is separated and returned to the exchanger and the steam is sent to a turbine or condenser.

At present, the pump is considered to be a canned-rotor pump similar in many respects to those used on the WAPD submarine reactor but with greater capacity.

In addition to the high-pressure system there is some equipment that normally operates at low pressure. This includes the dump tanks and the

## HRP QUARTERLY PROGRESS REPORT

fuel feed tanks. Material is transferred from the low-pressure feed tanks to the high-pressure system and must be let down from high to low pressure for chemical processing. Since neither of these operations is continuous, the operation of the high-pressure system does not depend directly upon the operation of any part of the low-pressure system. It does, however, depend upon the leakage through the dump valves being kept small.

A feed pump is shown for transferring liquid from low pressure to high pressure. This pump is not a vital piece of equipment, since the transfer can be accomplished by displacement of the liquid with gas at high pressure.

A relatively small recombiner system is provided for handling the decomposition gases formed in the dump tanks. Oxygen recirculation may not be required if the fuel solutions are permitted to boil. Steam would be the necessary diluent.

### EQUIPMENT LAYOUTS

In serving as a prototype for the large plutonium producers, it is necessary for the equipment in the ISHR to be similar to that visualized for the large reactors. It is desirable to duplicate the equipment where reasonable.

An approach to a layout for the ISHR was begun by preparing a layout of a large-scale machine utilizing the 20,000-gpm pump, heat exchangers, and valves described in the following section on "Engineering Studies of

Components." The result was a circulating system consisting of a reactor surrounded by a number of similar equipment cells. One of the cells attached to the ISHR reactor vessel is shown in Fig. 43. The layout illustrates the most desirable one for the reactor and circulating system, since it involves use of full-scale equipment operating with a flow of 20,000 gpm.

The arrangement shown in Fig. 43 requires a hold-up of about 19,000 liters in the system and is capable of removing 200 megawatts of heat, far in excess of that required for 50-megawatt operation. Figure 44 shows an arrangement in which only one gas separator and one heat exchanger are taken from the typical cell and the pump capacity is reduced to 10,000 gpm. This still involves the use of some full-scale equipment, but since the pipes are smaller the fluid hold-up is less than 12,000 liters. The cost of the installation should be reduced significantly.

Figure 45 shows an alternate arrangement to that shown in Fig. 44. This arrangement shows a reactor and two equipment cells. Each cell contains a 5000-gpm circulating system. The total liquid hold-up is near 12,000 liters. The equipment is one fourth to one half the size of that which would be used in the large reactors and is about the same in size as some of the equipment developed for the submarine reactor. This installation would be more expensive than that shown in Fig. 43 but should operate more reliably.

The three layouts are receiving additional study before a selection is made.

UNCLASSIFIED  
DWG. 15786

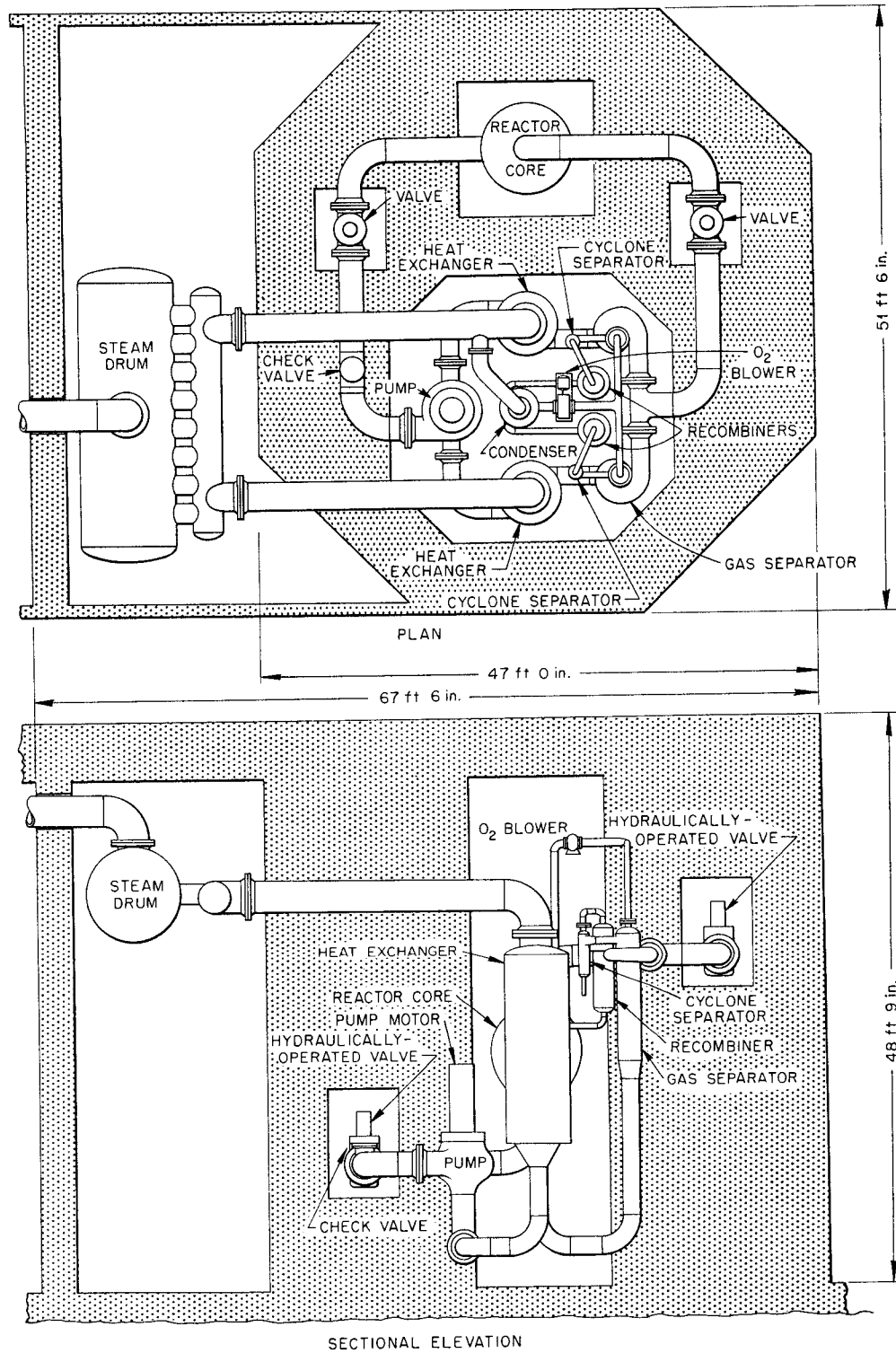


Fig. 43. Intermediate-Scale Homogeneous Reactor 20,000-gpm Circulation System.

UNCLASSIFIED  
DWG. 15738

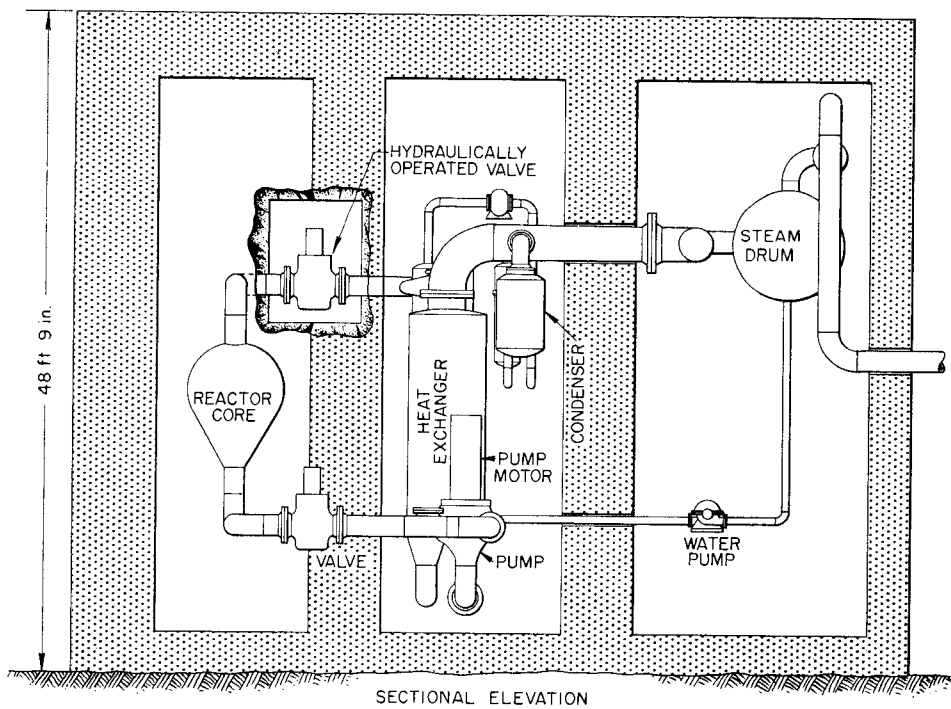
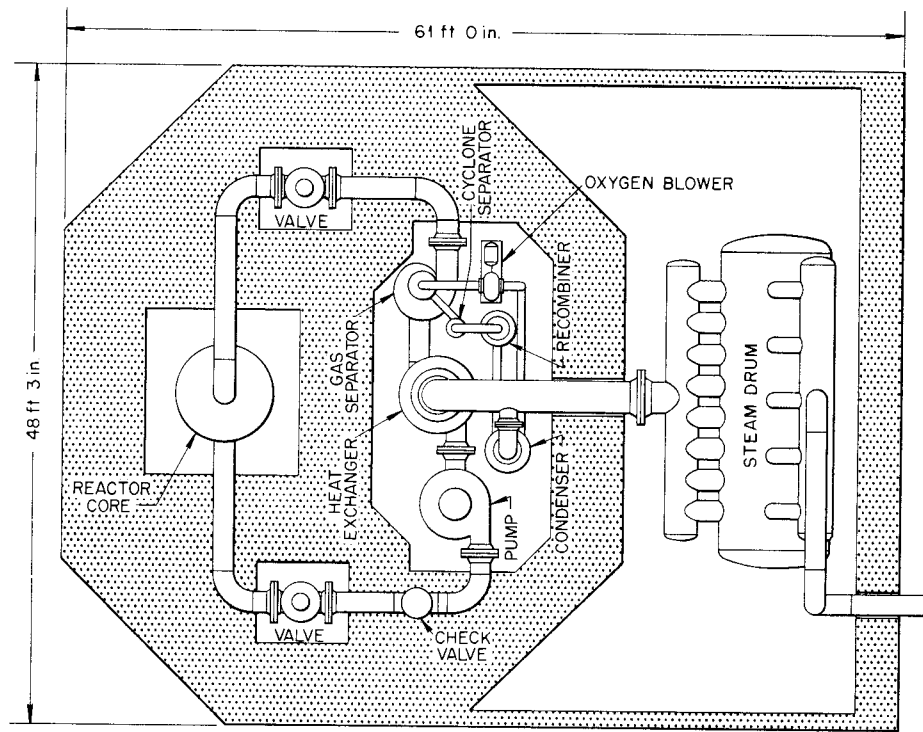


Fig. 44. Intermediate-Scale Homogeneous Reactor 10,000-gpm Circulation System.

UNCLASSIFIED  
DWG. 15739

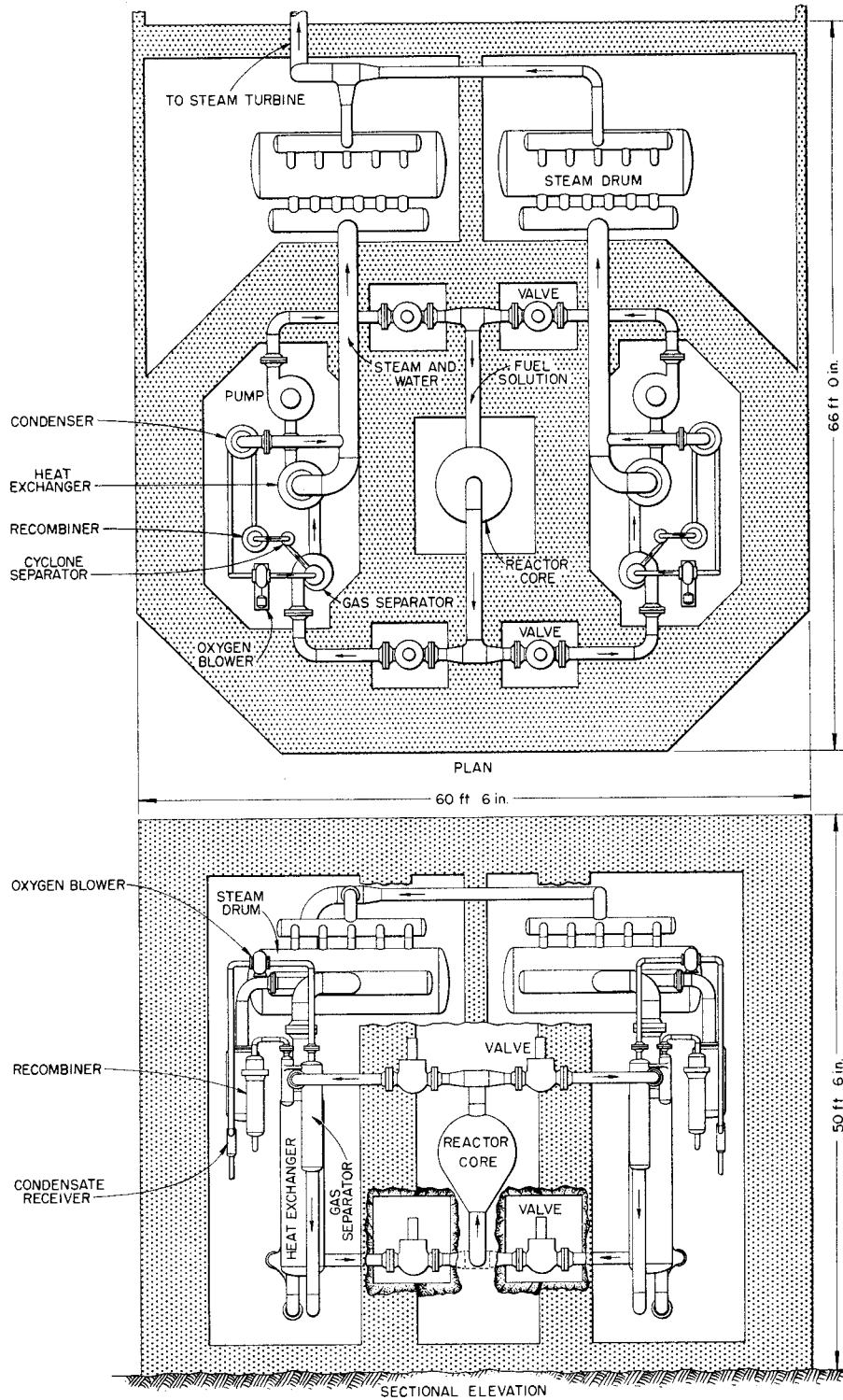


Fig. 45. Intermediate-Scale Homogeneous Reactor Lay-out with Two 5000-gpm Circulation Systems.

# HRP QUARTERLY PROGRESS REPORT

## DESIGN OF REACTOR VESSEL

In the last quarterly report<sup>(2)</sup> a good approximation for the total heat production in the vessel wall surrounding a 6-ft-dia core was reported as

$$H = H_1 e^{-ax} + H_2 e^{-bx} - H_3 e^{-cx}, \quad (1)$$

where  $H$  is the total heat production in  $\text{Mev/cm}^3 \cdot \text{sec}$ ;  $H_1$ ,  $H_2$ ,  $H_3$ ,  $a$ ,  $b$ , and  $c$  are constants evaluated from the heat production curves; and  $x$  is the distance (in centimeters) into the thermal shield.

With the heat production function known, it is possible to calculate the temperature distribution in the reactor shell. Some simplification in the calculations was achieved, with no important error in temperature distribution, by neglecting the curvature of the shell. The temperature of the inner surface was taken as the datum and a condition of no heat flow (perfect insulation) was assumed for the outer surface.

Under these circumstances

$$\begin{aligned}
 T(r) = & + \frac{1}{k} \left\{ \frac{H_1}{a^2} e^{-a(r_i-R)} + \frac{H_2}{b^2} e^{-b(r_i-R)} - \frac{H_3}{c^2} e^{-c(r_i-R)} \right. \\
 & + \left. \left[ \frac{H_1}{a} e^{-a(r_o-R)} + \frac{H_2}{b} e^{-b(r_o-R)} - \frac{H_3}{c} e^{-c(r_o-R)} \right] r_i \right\} \\
 & - \frac{1}{k} \left\{ \frac{H_1}{a^2} e^{-a(r-R)} + \frac{H_2}{b^2} e^{-b(r-R)} - \frac{H_3}{c^2} e^{-c(r-R)} \right. \\
 & + \left. \left[ \frac{H_1}{a} e^{-a(r_o-R)} + \frac{H_2}{b} e^{-b(r_o-R)} - \frac{H_3}{c} e^{-c(r_o-R)} \right] r \right\}, \quad (2)
 \end{aligned}$$

<sup>(2)</sup> *Ibid.*, p. 121-124

where

$T(r)$  = temperature above datum at  $r$ ,

$R$  = outer radius of core,

$r_i$  = inner radius of pressure shell,

= outer radius of core + thickness of thermal shield,

$r_o$  = outer radius of pressure shell,

$k$  = thermal conductivity of metal.

From the boundary conditions it is seen that the temperature is a maximum at the outer surface of the vessel. This produces a maximum tensile stress at the inner surface of the vessel. Timoshenko<sup>(3)</sup> gives the equation for thermal stress at the inner radius of a hollow sphere as

$$\sigma_t = \frac{3\alpha E}{(1-\nu)(r_o^3 - r_i^3)} \int_{r_i}^{r_o} T(r) r^2 dr, \quad (3)$$

<sup>(3)</sup> S. Timoshenko, *Theory of Elasticity*, McGraw-Hill, New York, 1934.

where  $\sigma_t$  is the tangential thermal stress (psi),  $\alpha$  is the linear coefficient of thermal expansion (in./in.·°F),  $E$  is the modulus of elasticity at the operating temperature (psi),  $\nu$  is Poisson's ratio for the material, and  $T(r)$  is defined by Eq. 2.

Carrying out the necessary integration between limits, the thermal stress is given as

and  $P$  is internal pressure, both in psi.

Neglecting the minor stresses due to supports and the like, the stress is essentially the sum of Eqs. 4 and 5. Since the thermal stress is directly proportional to wall thickness and the hoop stress is inversely proportional, their sum must be a minimum for some particular shell thickness and thermal shield thickness.

$$\sigma_t = -\frac{3\alpha E}{k(1-\nu)(r_o^3 - r_i^3)} \left[ \begin{aligned} & + \frac{H_1}{a^3} \left\{ e^{-a(r_i-R)} \left[ r_i^2 + \frac{2r_i}{a} + \frac{2}{a^2} \right] - e^{-a(r_o-R)} \left[ r_o^2 + \frac{2r_o}{a} + \frac{2}{a^2} \right] \right\} \\ & + \frac{H_2}{b^3} \left\{ e^{-b(r_i-R)} \left[ r_i^2 + \frac{2r_i}{b} + \frac{2}{b^2} \right] - e^{-b(r_o-R)} \left[ r_o^2 + \frac{2r_o}{b} + \frac{2}{b^2} \right] \right\} \\ & - \frac{H_3}{c^3} \left\{ e^{-c(r_i-R)} \left[ r_i^2 + \frac{2r_i}{c} + \frac{2}{c^2} \right] - e^{-c(r_o-R)} \left[ r_o^2 + \frac{2r_o}{c} + \frac{2}{c^2} \right] \right\} \\ & + \left[ \frac{H_1 e^{-a(r_o-R)}}{a} + \frac{H_2 e^{-b(r_o-R)}}{b} - \frac{H_3 e^{-c(r_o-R)}}{c} \right] \left[ \frac{r_o^4 - r_i^4}{4} \right] \\ & - \left[ \frac{H_1 e^{-a(r_i-R)}}{a^2} + \frac{H_2 e^{-b(r_i-R)}}{b^2} - \frac{H_3 e^{-c(r_i-R)}}{c^2} + r_i \left( \frac{H_1 e^{-a(r_o-R)}}{a} \right. \right. \\ & \quad \left. \left. + \frac{H_2 e^{-b(r_o-R)}}{b} - \frac{H_3 e^{-c(r_o-R)}}{c} \right) \right] \left[ \frac{r_o^3 - r_i^3}{3} \right] \end{aligned} \right] \quad (4)$$

In addition to the thermal stress given by Eq. 4, there is a hoop stress acting due to the internal pressure. The thin-sphere formula for hoop stress, which uses the mean diameter, is given as

$$\sigma_t = \frac{Pr_i^2}{(r_o - r_i)(r_o + r_i)} \quad (5)$$

where  $\sigma_t$  is tangential pressure stress

The problem is one of calculating the stresses for various shell thicknesses and for various thermal shield thicknesses to find an acceptable combination. This has been done for specific powers of 15 and 75 kw/liter in the core for a carbon steel vessel. The results are presented as a family of curves in Fig. 46. Thermal stresses would be about four times as great in stainless steel vessels.

# HRP QUARTERLY PROGRESS REPORT

DWG. 15740

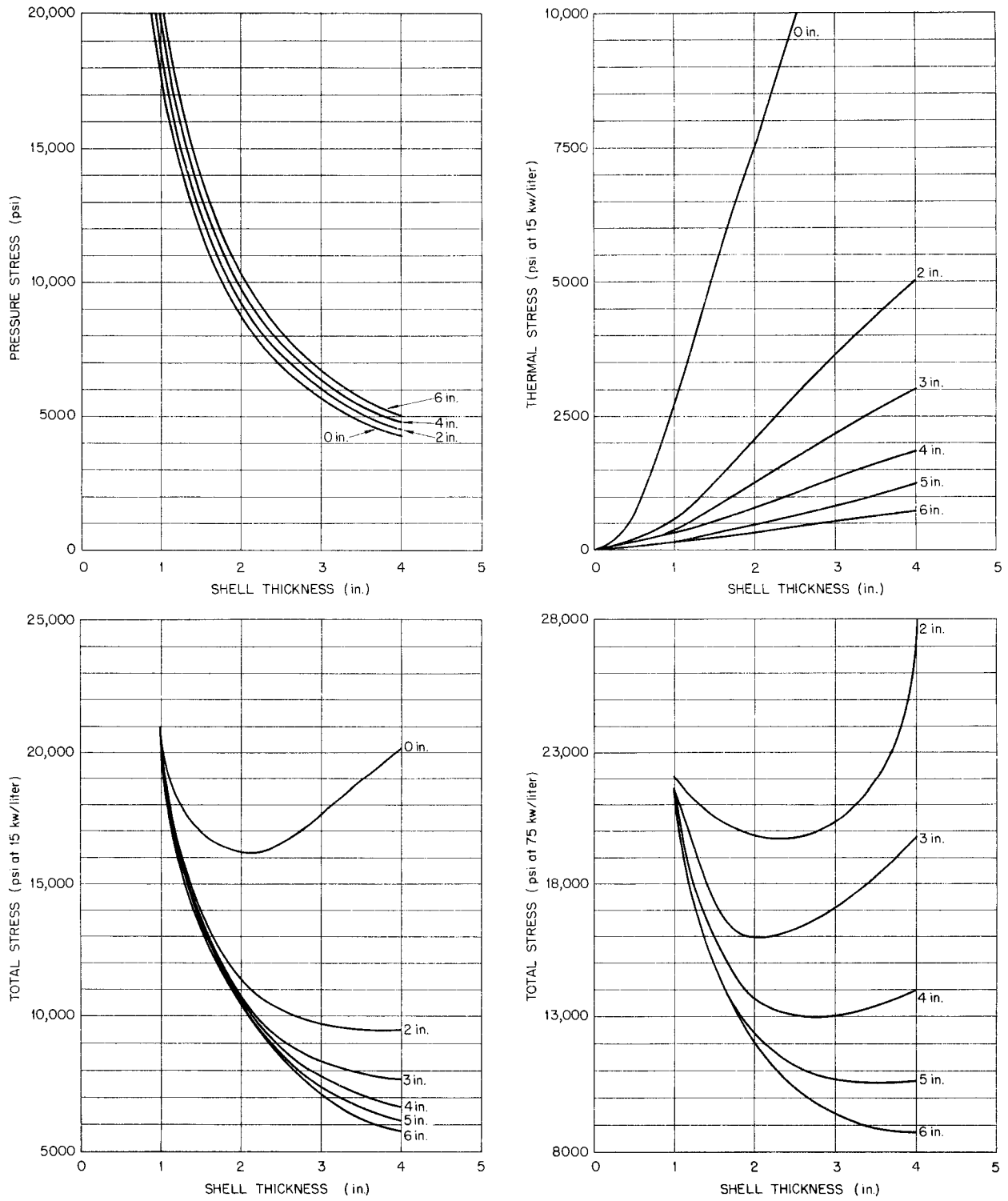


Fig. 46. Stresses in Spherical Pressure Vessel. Thermal shield thickness used as the parameter.

In order to limit the total stress to a maximum of 10,000 psi, thermal shielding must be added. For a 2-in. thermal shield the shell thickness should be 2.75 in., and for a 3-in. thermal shield the shell thickness should be 2.25 in. for 15 kw/liter.

Figure 47 pictures a proposed design for the reactor vessel with a 2.75-in. thermal shield and a wall thickness of 2.50 inches. A pressurized, normal-water cooling system is used to remove the heat from the thermal shield. The inner portion of the thermal shield is made of type 347 stainless steel for corrosion resistance, whereas the remainder of the shield is carbon steel. Linings of materials other than stainless steel are considered reasonable with this type of vessel construction.

#### PUMPS

The problems of pumping solutions for large-scale reactors are discussed at some length in the "Engineering Studies of Components" section of this report. Work on the design of a 20,000-gpm, canned-rotor, circulating pump is in progress at the Allis-Chalmers Mfg. Company. This pump probably could be used in both the 20,000 and the 10,000-gpm circulating systems of Figs. 43 and 44. The 5000-gpm pumps in Fig. 45 could be modifications of the pumps designed for use in the submarine reactor.

The auxiliary circulating pumps shown on the flowsheet are expected to be similar to the 30-gpm and 100 or 150-gpm Westinghouse canned-rotor pumps now being used on the corrosion loops and the HRE. The feed pump will require considerable development, since it will be required to pump solutions and/or slurries at a rate of 5 to 10 gpm against a pressure of 1000 psi. Multistage pumps have

been suggested for this application by the Allis-Chalmers and Byron-Jackson Companies.

#### HEAT EXCHANGER

A general proposal for the main heat exchanger is shown in Fig. 48. The size of the exchanger depends upon whether one unit is required to handle 10,000 gpm or whether two 5000-gpm units are used as in the arrangement of Fig. 45. In principle, the operation is the same. Fuel solution flows through the tubes and steam is generated on the shell side. The U-shaped tubes are stainless steel and are welded into a stainless steel tube sheet. The tube sheet is welded to a stainless steel head that contains the outlet pipes and to a carbon steel shell, thus all-welded construction is provided. Consideration is being given to the use of a double tube sheet with a space between sheets so that leaks that result from welding the tubes into the front sheet can be detected before radioactive fluid enters the steam system.

The size of the exchangers and the number of tubes depend upon the tolerable pressure drop. For a 40-psi drop through the tubes, the 5000-gpm exchanger, capable of removing 50 megawatts of heat when producing 200-psi steam, will be about 17 ft long, 45 in. in diameter, and it is estimated that it will contain 1030 tubes  $\frac{1}{2}$  in. in diameter. An exchanger 19 ft long, 63 in. in diameter, and containing 2060 tubes is required to handle the 10,000-gpm flow and to remove 100 megawatts of heat from 250°C fluid when producing 200-psi steam. To reduce the pressure drop to 20 psi with the same tube diameter requires a 35% increase in the number of tubes. The over-all lengths of the exchangers are decreased by 2 ft. Because of the large size of the

# HRP QUARTERLY PROGRESS REPORT

UNCLASSIFIED  
DWG. TD-4119 A

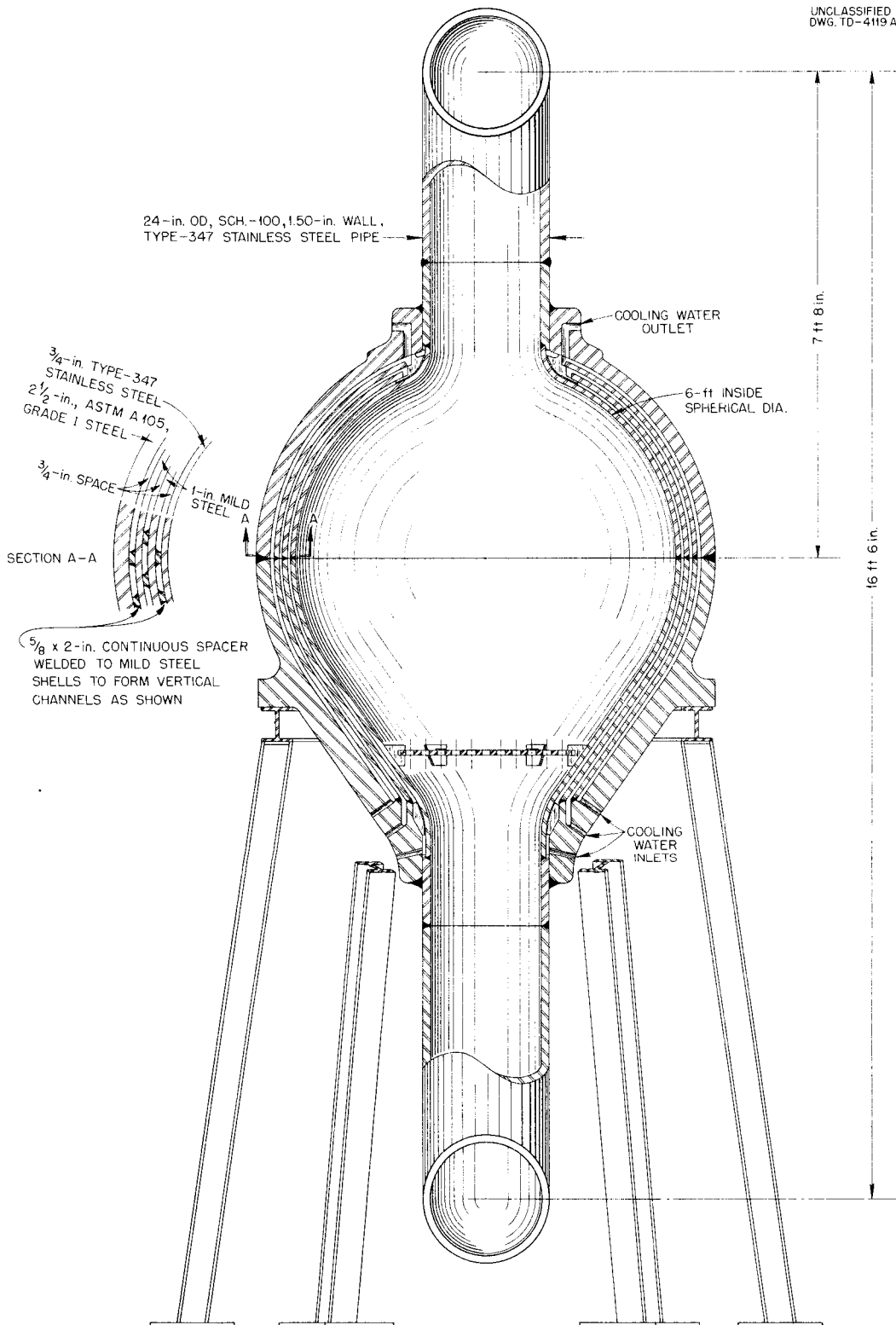


Fig. 47. Proposed ISHR Reactor Vessel.

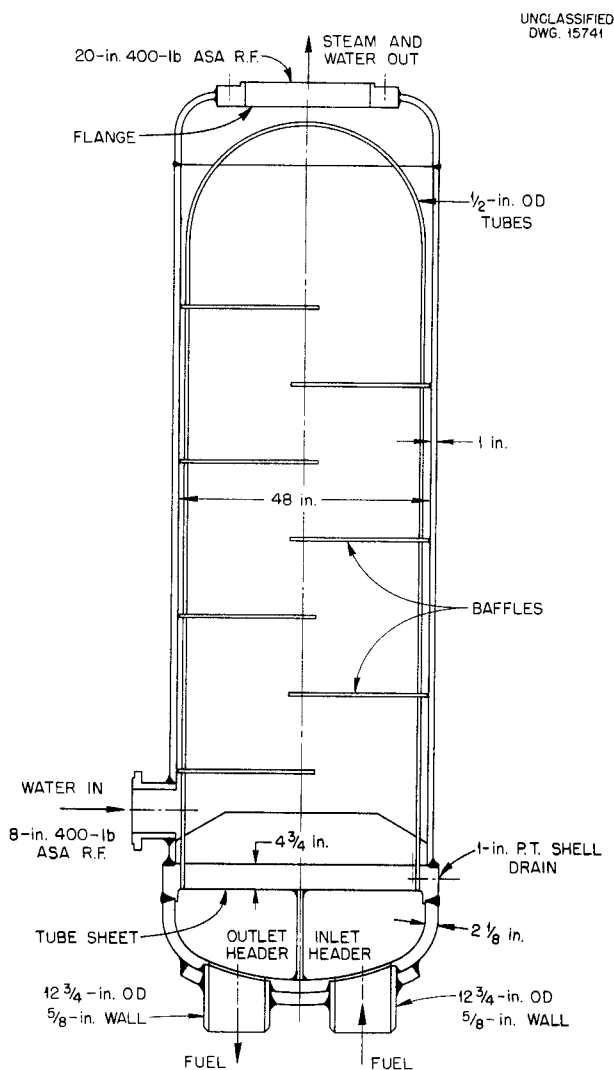


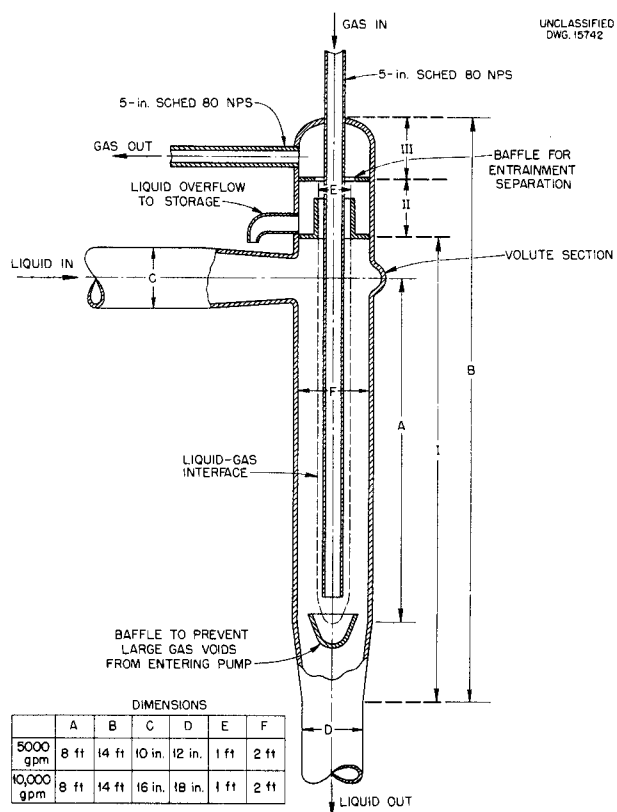
Fig. 48. ISHR Main Heat Exchanger.

tube bundle and the close spacing of tubes, forced convection is required to obtain the necessary circulation of water through the shell.

The descriptions of the exchangers presented here are based upon preliminary design studies by the Lummus Company and maybe changed considerably as more information is developed.

### GAS SEPARATOR

The centrifugal separator proposed for the reactor circulating system is shown in Fig. 49. Liquid from the



DIMENSIONS

	A	B	C	D	E	F
5000 gpm	8 ft	14 ft	10 in.	12 in.	1 ft	2 ft
10,000 gpm	8 ft	14 ft	16 in.	18 in.	1 ft	2 ft

Fig. 49. Proposed Gas Separator for ISHR.

reactor core enters the separator through a volute casing into Section I. The volute casing imparts a large tangential component of velocity to the stream, and the gas bubbles are centrifuged toward the void at the center of the separator. A mixture of oxygen and D<sub>2</sub>O vapor is brought in through the central gas inlet pipe to dilute the gas (D<sub>2</sub>, O<sub>2</sub>, and D<sub>2</sub>O) that is released at the liquid-gas interface of the vortex void. In this way the deuterium concentration is reduced to 1 or 2 mole %, which is far below the explosive limit.

Excess liquid in the system is spilled over into Section II and returned to the dump tanks or other receivers. Gas that has been separated continues through Section II into Section III and is released through the gas outlet pipe into a cyclone

## HRP QUARTERLY PROGRESS REPORT

liquid-particle separator that immediately follows.

Separation of the gas is essentially complete in the first 4 ft of Section I, but the additional length provides a safety factor and a larger void volume for expanding liquid. The baffle near the liquid discharge has been provided to define the length of the vortex void. The pressure drop of the liquid through the separator has been computed to be about 3 psi and the pressure drop from the liquid inlet to the gas outlet 4 to 5 psi.

### HIGH-PRESSURE RECOMBINER SYSTEM

The design of the high-pressure recombiner system has not progressed sufficiently to give a firm description of the system or equipment. Some of the information developed is presented here to give an indication of equipment size.

In the current design gas will be circulated through each separator at a rate of approximately 350 cfm. This gas will contain 45 mole %  $O_2$  and 55 mole %  $D_2O$  vapor. Deuterium equivalent to half of that produced by 50-megawatt operation results in a  $D_2$  concentration of 1 mole % in the gas leaving the separators, in the arrangements of Figs. 43 and 45, when both cells are operating.

The gas passes into a cyclone separator, 12 in. in diameter by 42 in. long, in which particles 10  $\mu$  or larger are removed. Following the cyclone is a catalytic recombiner packed with alumina pellets containing 0.3% platinum or possibly palladium. The pellets are 1/8 in. long by 1/8 in. in diameter and are packed between two concentric, cylindrical screens to form a tubular bed 5 in. in inside diameter, 3 in. thick, and 5 ft long. The catalyst bed is installed in a 7-ft long, 16-in. pipe through a

flanged opening. Gas flows into the bed through the axial opening and leaves the recombiner through the annulus between the bed and the pipe wall.

The temperature of the gas increases 72°C as it flows through the catalyst. It is cooled to 250°C again in a tubular heat exchanger similar in many respects to the main heat exchanger but smaller. Gas flows inside the tubes, and steam is generated on the shell side. The exchanger contains 128 U-tubes 3/4 in. wide and about 12 ft long. The over-all length of the shell is 6 ft and the diameter is 42 inches. The exchanger is mounted vertically, but the gas is cooled during about three fourths of its travel through the tubes; therefore condensation occurs only in the downward pass.

Following the cooler is a blower that returns the gas to the separator. The blower must be totally enclosed and may require a canned rotor similar to that used on the pumps. The pressure rise across the blower will be near 6 psi. The power consumed in each blower will be about 12 hp.

### CRITICALITY CALCULATIONS FOR REACTOR

The method used for calculating critical enrichments and concentrations in the ISHR is described in LA-524.<sup>(4)</sup> This method, which is an approximate solution of the two-group equations, has been used at Los Alamos and in the HRE criticality calculations with good results.<sup>(5)</sup> Comparison with other methods shows that the LA-524 method

<sup>(4)</sup>R. P. Feynman and T. A. Welton, *Calculations of Critical Masses Including the Effect of the Distribution of Neutron Energies*, LA-524 (Jan. 21, 1947).

<sup>(5)</sup>T. A. Welton, H. T. Williams, L. H. Thacker, and P. M. Wood, *Homogeneous Reactor Project Quarterly Progress Report for Period Ending August 15, 1951*, ORNL-1121, p. 84.

is quite accurate in the case of the HRE, a water-moderated, water-reflected, low-concentration reactor.<sup>(6)</sup> The ISHR is larger, the fuel may be more concentrated, and instead of a water reflector there is a thick steel shell around the core. Despite these differences it is believed that a reasonable approximation of criticality requirements can be obtained for the ISHR by this method.

The most difficult effect to calculate is that of the steel "reflector." The assumption of similar transport properties in core and reflector does not hold true in this case. Accurate values for diffusion constants for steel are not known and must be calculated from cross-section data. In the present design for the reactor vessel, water circulates in passages between the steel shells. Presumably this would reduce the effectiveness of the steel as a reflector, since fast neutrons will be slowed down in the water and absorbed in the steel. In view of the approximate nature of the method as applied to this reactor, no attempt was made to take the water into account.

Table 28 gives the macroscopic two-group constants used. Values for  $D_2O$  are based upon information previously reported.<sup>(7)</sup> Constants for type 347 stainless steel were calculated from cross sections given in *Science and Engineering of Nuclear Power, General Electric Chart of the Nuclides*, and from ANP cross-section data.

For  $UO_2SO_4-D_2O$  solutions,  $L^2$  is corrected for the presence of uranium and sulfur:

(6) L. C. Biedenharn and P. M. Wood, *Homogeneous Reactor Project Quarterly Progress Report for Period Ending November 15, 1951*, ORNL-1221, p. 81.

(7) N. F. Lansing and L. C. Noderer, *Critical Calculations for Homogeneous Low-Enrichment  $UO_2SO_4-D_2O$  Systems*, ORNL CF-50-11-41 (Nov. 13, 1950).

$$L^2 = \frac{L^2(D_2O) \Sigma_a(D_2O)}{[\Sigma_a(U) + \Sigma_a(S) + \Sigma_a(D_2O)] F^2}$$

where  $F$  is the volume fraction of  $D_2O$  in the solution.

Table 28  
TWO-GROUP CONSTANTS AT 250°C

	$D_1$ (cm)	$\tau$ (cm <sup>2</sup> )	$D_2$ (cm)	$L^2$ (cm <sup>2</sup> )
Type 347 stainless steel	0.496	99.4	0.324	1.77
$D_2O$	1.42	196.4	1.26	35,438

The results that follow are based upon a spherical steel shell 6 ft in inside diameter and 5 1/4 in. thick (the over-all thickness of the core tank, thermal shields, and pressure vessel). Figure 50 shows critical enrichment as a function of concentration for various temperatures from 100 to 250°C. Figure 51 is a plot of

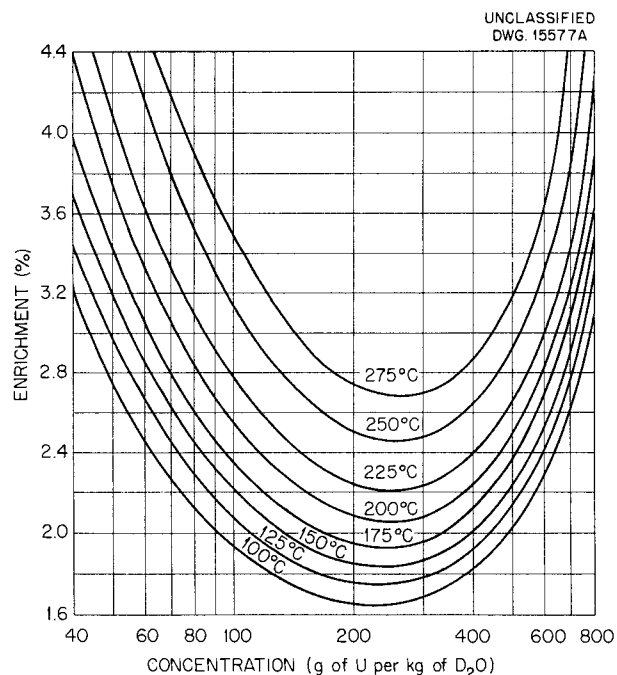
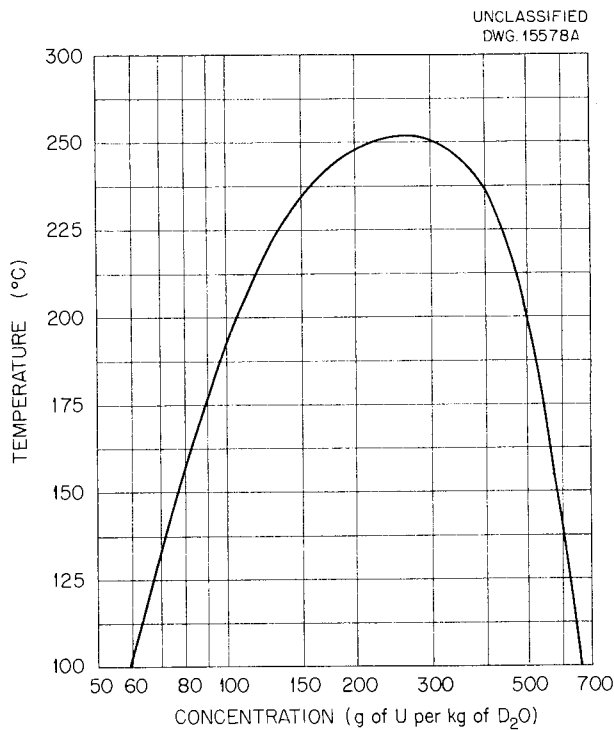


Fig. 50. Critical Enrichment vs. Concentration.

# HRP QUARTERLY PROGRESS REPORT



**Fig. 51. Critical Temperature vs. Concentration for 2.48% Enrichment.**

the critical temperature as a function of concentration when the enrichment is that necessary for criticality at 250°C with a concentration of 250 g of uranium per liter of solution. Large changes in fuel concentration are required to achieve small changes in reactivity (or operating temperature). This increases the stability of the reactor but makes control by adjusting concentration less attractive for normal operation.

## CRITICALITY CALCULATIONS FOR DUMP TANKS

Critical concentrations and enrichments were calculated for dump tanks of various sizes by a method essentially the same as that used for the core criticality calculations.<sup>(8)</sup> For these calculations the following assumptions were made: (1) the tanks

<sup>(8)</sup>T. A. Welton, *Simplified Two-Group Calculation for Reflected Homogeneous Thermal Reactors*, ORSORT Lectures, March 1952.

are infinite cylinders in an infinite water reflector, separated by sufficient distance so that one cylinder has no effect upon another; (2) the fuel is  $UO_3$  slurry in a normal or heavy water moderator; (3) the atomic ratio of fuel to moderator is sufficiently small that in the core the *transport* properties, that is, diffusion coefficient and scattering cross section, are the same as for pure moderator; (4) the Fermi age is the same as for moderator only; (5) the thermal diffusion length is corrected for the uranium in the tank; and (6) the temperature of tank and reflector is 80°C. The results of the calculations are given in Table 29 and Fig. 52.

**Table 29**

**TWO-GROUP CONSTANTS AT 80°C**

	$D_1$ (cm)	$\tau$ (cm <sup>2</sup> )	$D_2$ (cm)	$L^2$ (cm <sup>2</sup> )
H <sub>2</sub> O	1.174	34.82	0.1741	8.612
D <sub>2</sub> O	1.158	126.8	0.9550	17,915

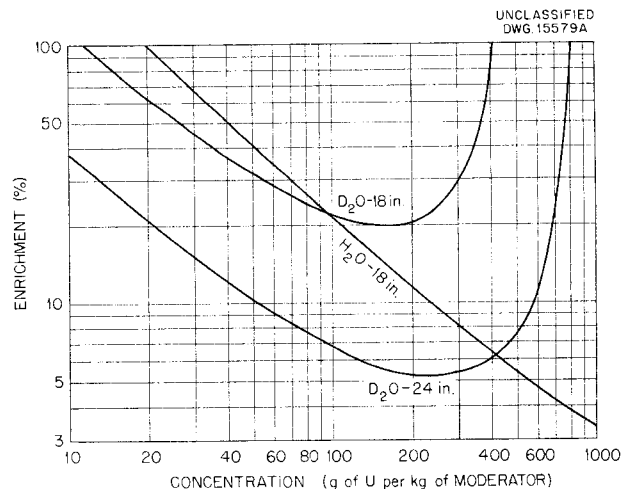


**Fig. 52. Dump Tank Criticality.**

## POWER AND PRESSURE SURGES

An initial evaluation of the safety of the reactor can be obtained by estimating maximum power and pressure

FOR PERIOD ENDING JULY 1, 1952

increases that occur as a result of instantaneous increases in reactivity. The equations used and methods of solving the equations have been reported in previous HRP quarterly reports and by Sangren.<sup>(9)</sup> These calculations have been made for the ISHR operating at a specific power of 15 kw/liter at 100 and 250°C with various concentrations of uranium of critical enrichment. In addition, two locations of gas separator (void into which the liquid expands) were considered. One was 40 ft from the core, the distance shown in Figs. 43, 44, and 45, and the second location was 8 ft from the core, a convenient

minimum distance. Calculations were based upon the change in reactivity that occurs as a result of a 2.5% change in the density of the fuel solution in the core. Such a change in density might occur as a result of substituting fuel solution for the voids in the core or an instantaneous change in temperature of 11°C at 250°C or 18°C at 100°C.

Results of the calculations made with the short-formula solutions of the equations are presented in Table 30. The pressure rise is considered to be within a factor of 2 of that calculated by more exact methods. Indications are that the pressure rises may not be serious even with the gas separator 40 ft from the core.

<sup>(9)</sup>W. C. Sangren, *Kinetic Calculations for Homogeneous Reactors*, ORNL-1205 (April 1, 1952).

Table 30

POWER AND PRESSURE RISES RESULTING FROM 2.5% INSTANTANEOUS CHANGE IN DENSITY OF CORE

URANIUM CONCENTRATION (g/l)	AT 100°C					AT 250°C				
	$\Delta k$	$P/P_0^*$	$P/P_0^{**}$	$\Delta P^*$ (psi)	$\Delta P^{**}$ (psi)	$\Delta k$	$P/P_0^*$	$P/P_0^{**}$	$\Delta P^*$ (psi)	$\Delta P^{**}$ (psi)
1.4						0.0283	35	30	18	3
50	0.0199	29	28	8	2	0.0221	38	32	21	4
100	0.0163	29	28	8	2	0.0187	39	32	23	4
250	0.0112	27	26	8	2	0.0136	44	34	30	5
500	0.0085	27	26	9	2	0.0100	64	40	53	7

\*Separator 40 ft from core.

\*\*Separator 8 ft from core.

# HRP QUARTERLY PROGRESS REPORT

## ENGINEERING STUDIES OF COMPONENTS

C. B. Graham, Section Chief

J. S. Culver	J. I. Lang	P. N. Stevens
J. A. Hafford	L. B. Lesem	D. Taylor
C. W. Keller	W. L. Ross	R. H. Wilson
R. J. Kedl	I. Spiewak	C. D. Zerby

### 4000-gpm PUMP TEST LOOP

The 4000-gpm Byron Jackson pump and approximately 10% of the major components of the test loop and auxiliary equipment have been received, and all major items of equipment are on order. Completion of delivery of all material for the loop is anticipated by November 1952.

### HRP MAIN CIRCULATING PUMPS

Three pump manufacturing companies have shown an active interest in the program to develop pumps for large-scale homogeneous reactors. The Allis-Chalmers Mfg. Co. is under contract to design and possibly fabricate a 20,000-gpm, totally enclosed, canned-rotor pump. A similar contract is in the final stages of negotiation with the Worthington Corporation. Proposals for a program to develop a satisfactory shaft seal applicable to a standard type of high-suction-pressure pump are being discussed with the Byron Jackson Company.

#### Allis-Chalmers Pump Development.

The Allis-Chalmers Mfg. Co. has completed the preliminary design and engineering studies (phase I) of the totally enclosed, centrifugal pump. Work on the final design (phase II) of the pump is well under way.

A comparison of pumps of several synchronous speeds for 20,000 gpm capacity has been made in the last quarterly report.<sup>(1)</sup> The pertinent

<sup>(1)</sup>C. B. Graham et al., *Homogeneous Reactor Project Quarterly Progress Report for Period Ending March 15, 1952*, ORNL-1280, p. 138.

data of the comparison demonstrated that a 1200-rpm synchronous-speed machine had reasonable relative fluid velocities and the best over-all (pump and motor) efficiency of the four speeds that were compared. The low relative fluid velocities would be desirable from the standpoint of corrosion-erosion or mechanical erosion if an aqueous slurry is used.

Allis-Chalmers is designing a 1200-rpm synchronous pump with a capacity of 20,000 gpm to develop a head of 160 ft of 1.5 (and lower) specific-gravity fluid. The pump is a canned-rotor, totally enclosed type that has a metallic diaphragm to seal the motor stator from high-pressure fluid. The canned rotor, which includes a metal-sealed armature, rotates submerged in the high-pressure fluid. The fluid fills what would normally be the air gap in a standard motor. Pump bearings to support and align the rotating parts are of the hydraulic-pressurized, fluid-piston type that have either an auxiliary impeller attached to the rotating shaft or an external source to supply pressurized water to the bearings. There are two radial bearings and one thrust bearing. The thrust bearing will take loads in two directions. One radial bearing is located near the top of the rotating shaft and the other one is located between the armature and pump impeller.

The pump will be positioned so that the shaft will be vertical, with the pump impeller at the bottom and the motor at the top. The fluid-filled motor and bearings chamber of the pump will be isolated from the impeller

## FOR PERIOD ENDING JULY 1, 1952

and volute by a close-clearance labyrinth. By injecting uncontaminated water into the motor and bearings chamber and continuously flushing through the labyrinth into the pump volute, the corrosion on the motor and bearing parts should be reduced considerably. The flush volume would be small enough to make dilution of the pumped fluid insignificant (in the order of 1 gpm through the labyrinth to 20,000 gpm through the pump).

The present design for the Allis-Chalmers pump provides a built-in cooler to keep the bearing and motor chamber water at about 150°F. The upper radial-bearing water supply and drain will be cooled in tubing conduits to the upper bearing. The tubing will lie in an annular channel in the pump casing or outside the casing within a low-pressure cooling jacket. Low-pressure cooling water will be circulated in the casing annular channels or in the jacket.

The pump power will be supplied by a 440-v, 6-pole (1200-rpm synchronous speed) induction motor. The stator, which is sealed from the high-pressure fluid by the metal diaphragm, has hollow conductors. Motor cooling water will flow through the hollow channels in the conductors and remove the heat developed in the conductor. This method of removing the heat is similar to an induction heating coil in which the source of power is often a copper tube coil with water flowing through the tubing. In the stator the conductors are the major source of heat and the motor cooling water will remove the heat close to its source. The conductor insulation will not be subjected to high temperatures. At present, Allis-Chalmers plans to use Formica, grade FF-55, and mica with silicone varnish binder for the slot insulation of the stator conductors. Mica and glass-fiber tape with a

silicone binder will be used for insulation of the conductor end turns.

Construction of the pump casing enclosing the volute and impeller of the pump will not be easy. The major diameter of the casing will be approximately 5 ft. The casing and volute are irregular and asymmetrical in all planes. No two vertical sections through the casing will be identical. The suction pressure will be approximately 1000 psi, and therefore heavy wall sections will be required. However, several equipment fabricating companies have investigated the construction of the pump casing. Each of three companies has studied a different method of fabrication, and each reports that the construction is feasible and can be accomplished by present shop techniques and equipment. Lebanon Steel Foundry has studied the casing construction by casting with type 347 stainless steel. The Midvale Company investigated construction by machining and welding heavy plate sections. The Lukenweld Division of Lukens Steel Company investigated construction by forged, formed, and welded fabrication of type 347 stainless steel. The last two methods will produce a welded, wrought stainless steel casing, whereas the first method results in a cast structure. The present limited information on the corrosion of materials by HRP fuel solution indicates that wrought stainless steels are superior to cast stainless steels. Hence, the wrought construction will probably be the preferred method of fabrication.

**Worthington Corporation Pump Development.** The Worthington Corporation has done some preliminary work on the design of a 20,000-gpm centrifugal pump, although complete agreement has not been reached on the contract to design, develop, and fabricate the special pump. Negotiations to complete the agreement are

## HRP QUARTERLY PROGRESS REPORT

in the final stages, and the contract should be negotiated before July 1952.

Unlike the Allis-Chalmers design, the Worthington Corporation's pump design incorporates a more conventional high-suction-pressure pump driven by a standard electric motor. Worthington's preliminary design and engineering studies have produced a bearing-pressure breakdown design that utilizes an injection pump to introduce a small volume of uncontaminated water into an annulus formed by the drive shaft and a sleeve bearing. The layout of the pump unit would show the pump casing containing the impeller followed by a bearing-pressure breakdown around the drive shaft that is, in turn, followed by an atmospheric-pressure shaft seal. External to the shaft seal is a heavy thrust bearing and the standard motor. The unique, uncertain, and highly specialized element of the Worthington design is the method of breaking the pressure down along the power drive shaft between the pump and motor. This pressure breakdown must operate against a working pressure of approximately 1000 psi, and it must prevent external leakage of the pumped fluid. Also, the breakdown unit should provide a bearing surface so that the radial load that the pumping impeller puts on the drive shaft will be balanced and the shaft aligned to maintain alignment of the impeller to the casing. Hence, the high-pressure breakdown becomes a combination sleeve-type bearing-pressure breakdown. Further, the bearing breakdown must provide trouble-free, continuous operation, since it is desirable to hold maintenance and outage time to the very minimum on the HRP equipment.

The uncontaminated water injected into the bearing breakdown will be at a pressure substantially higher than the pressure in the pump casing. Consequently, a portion of the injected water will flow along the bearing

toward the impeller and prevent leakage of the reactor fluid into the bearing. The remainder of the injected water will flow along the close-clearance bearing annulus away from the pump. The pressure of the injected water will be reduced to atmospheric pressure by the fluid frictional resistance of the close-clearance annulus. The atmospheric-pressure water will be retained by a rotating, mechanical shaft seal and flow back to the sump of the injection pump. The shaft seal will be about 5 ft from the pumped reactor fuel fluid, and there will be stainless steel, heavy water (most likely), and reactor shielding to shield the organic plastic or rubber materials that conventional mechanical shaft seals utilize to function properly.

To determine whether the selection of bearing materials and seal design is adequate and whether the system will function properly, two bearing breakdown tests units will be built and tested by Worthington. The Worthington contract requires that they prove the feasibility of the bearing breakdown unit before work on the final design and fabrication of the pump unit is started.

**Byron Jackson Company Shaft Seal Development.** The Byron Jackson Company has made proposals to initiate a research and developmental program for a satisfactory high-pressure mechanical shaft seal that can be installed on a conventional pump. This development is expected to be long-range, but if it is successful it will result in a pump that utilizes conventional bearings and motor and operates at higher efficiency.

This program would consist of ascertaining the best mechanical shaft seal design and the suitable construction materials for the service requirements of a pump in a homogeneous

## FOR PERIOD ENDING JULY 1, 1952

reactor. The work will involve considerable designing and experimental testing to attain the objectives. In contrast to the Worthington pump unit that utilizes a mechanical shaft seal at atmospheric pressure, located about 5 ft from the pumped fuel fluid, the Byron Jackson mechanical shaft seal will be required to establish and maintain a high pressure (in the order of 1000 psi) relatively close to the pumped fuel fluid where radiation is high. Consequently, the mechanical shaft seal cannot be of a conventional type with standard materials of construction such as organic plastics or elastomers.

The following design criteria and service requirements were specified for the mechanical shaft seal, to aid Byron Jackson in making the proposals for a developmental program.

1. The seal should be suitable for use on a 20,000-gpm pump with external bearings that pumps a corrosive water solution with properties similar to water:

- a. normal suction pressure, 1000 psi,
- b. suction pressure capable of pressure increase of 500 psi for a short duration,
- c. shaft speed, 1200 or 1800 rpm.

2. The seal should be backed by a second seal or other means for preventing loss of fluid in case the main seal fails.

3. Clean heavy water may be supplied to the seal to prevent corrosive solution from coming in contact with seal parts:

- a. small inleakage (say about 1 gpm) to the pump is permissible,

b. leakage to the atmosphere must be very low (a few drops per day).

4. No adjustment or replacement of the seal after operation should be required, since this would be difficult if not impossible.

5. Seal parts should be made of corrosion and radiation resistant materials and should be cooled to less than 100°F to minimize corrosion. The following materials are corrosion resistant and suitable for operation in dilute water solution: austenitic stainless steels, tantalum, titanium, Stellite No. 98M2, Stellite No. 3, Stellite No. 6, StarJmetal, graphite, Graphitar No. 14, silver-filled graphite, Inconel, Worthite, and Elgilloy. Unsatisfactory materials include: rubber, synthetic rubbers, organic plastics, leather, asbestos, and, in general, the metals and alloys not listed above.

### FUEL FEED PUMP DEVELOPMENT

Large-scale homogeneous reactors will require fuel feed pumps. The pulsafeeder pumps used in the HRE probably will not be suitable because of capacity and other limitations. A multistage centrifugal pump will probably be the preferred type, since it is anticipated that future homogeneous reactors will operate at around 1000-psi pressure. The centrifugal pump must be a multistage unit to develop the required high heads (slightly higher than 1000 psi) in order to inject fuel fluid into a pressurized reactor or a high-pressure dump tank. The head requirement is similar to that of the HRE; hence, if a high-head centrifugal pump could be developed in a reasonably short time it might provide an alternate pump to replace the pulsafeeder pumps in the HRE. Discussions with pump manufacturing

## HRP QUARTERLY PROGRESS REPORT

companies regarding a feed pump have been conducted with dual application of the pump as a service requirement.

The tentative service requirements and design criteria specified for the fuel feed pump are as follows:

1. capacity, 10 gpm, must be able to throttle to approximately 1 to 2 gpm and maintain stable flow,
2. head, 1050 to 1100 psi at discharge, with fluid of specific gravity 1.0,
3. fluid temperature, approximately 170°F,
4. fluid specific gravity, may vary from 1.0 to 1.5,
5. approximately 3 ft of positive suction head above atmosphere available for 2-gpm application, with more available for 10-gpm operation,
6. fluid saturated with  $H_2$  and  $O_2$  or slightly supersaturated at at pump suction,
7. fluid capable of generating a small amount of  $H_2$  and  $O_2$  during the time it flows to and through the pump,
8. fluid, a corrosive aqueous solution or an aqueous slurry,
9. no external leakage permissible.

Three pump manufacturing companies have been contacted regarding the design, development and fabrication of the feed pump. A preliminary proposal to design and fabricate a totally enclosed, canned-rotor (motor arrangement similar to the one described under "Main Circulating Pump") feed

pump has been received from the Allis-Chalmers Mfg. Co. Their preliminary design of the centrifugal pump features 30 stages and pressurized, fluid-piston-type bearings.

The Byron Jackson Company has built a 22-stage, 10-gpm centrifugal pump for boiler feed water service. An alteration of this pump to replace some materials and provide a leak-proof driving design may render it suitable for homogeneous reactor feed pump service. A proposal to design and fabricate a feed pump is expected from Byron Jackson by July 1952. Also, the Ingersoll-Rand Company may be interested in designing and fabricating a feed pump suitable for homogeneous reactor service.

### ISOLATION VALVES

Recently negotiations were started with the Crane Company of Chicago to obtain an agreement whereby they would make a predesign study of the 20-in. isolation valves required in the external circulating systems of a large homogeneous reactor.

The purpose of the study is to establish fundamental design concepts and feasibility of one or more special valves for use in a system containing an aqueous solution and in a system containing a slurry.

It is essential that these large valves be as trouble-free as possible since the continuous operation of a large homogeneous reactor is dependent on them for isolation of units if failure occurs in any equipment in the external circulating system.

For purposes of guiding the pre-design study, the following tentative specifications were submitted to the Crane Company.

## FOR PERIOD ENDING JULY 1, 1952

### *General Valve Requirements*

1. The valves shall be of a size suitable for installation in a 20-in., schedule-100, pipe line.

2. The valves shall be operated by remote means.

3. The valves shall be of the shut-off type operated to a fully open or closed position.

4. The valves shall be capable of being operated freely from either a normally closed or normally open position after extended lengths of time in the normal position.

5. All parts subject to failure shall be replaceable by remote means with relative ease and without the necessity of removing the valve housing from the pipe line.

6. The valves shall be capable of operating in the pipe line system where the contained fluid has the following characteristics:

- a. 482°F temperature,
- b. 1,000 psi pressure,
- c. 25 ft/sec velocity,
- d. contain up to 3.5% by volume explosive gas and steam.

7. The maximum design stress for wet surfaces of the valves shall be 10,000 psi under all operating conditions.

8. When the valves are closed, there shall be no leakage of the system fluid across the valves with a 1,000-psi differential pressure imposed across the valves. Very small inleakage of uncontaminated, injected water through the valve seat is permissible.

9. There shall be no external leakage of the system fluid throughout its life expectancy. The life expectancy is estimated to be 500 cycles of trouble-free operation over a ten-year period, without maintenance.

10. The valves shall be capable of operation with approximately 25- to 50-psi pressure drop at the closed and partially open positions unless large check valves are used.

11. Means shall be provided by which any gas or steam trapped in the valves from the system fluid can be removed during operation. Means shall also be provided for flushing system fluid from the mechanism prior to removal.

### *Additional Requirements for Valve to Operate in Aqueous Solution*

1. The following fluid characteristics will be considered part of item 8 above when the valves are for use with aqueous solution:

- a. pH of 1.35,
- b. specific gravity of 1.2,
- c. highly corrosive.

2. The materials of construction that will be in contact with the solution and can be tentatively considered are given below in the relative order in which they resist the corrosive action of the solution - the first material has the best resistance:

- a. titanium,
- b. 3 to 5% tin-zirconium alloy,
- c. tantalum (hydrogen embrittlement may rule this out),
- d. austenitic stainless steel.

## HRP QUARTERLY PROGRESS REPORT

### *Additional Requirements for Valve to Operate in Aqueous Slurry*

1. The following fluid characteristics will be considered part of item 8 of the general requirements when the valves are for use with aqueous slurry:

- a. pH of 6 to 7,
- b. particle size, 1 to 15 microns,
- c. approximately  $2.7 \times 10^5$  particles per cubic centimeter,
- d. particle hardness, 2.5 Mohs,
- e. general abrasive action of slurry negligible,
- f. specific gravity of 1.2,
- g. slurry will not settle appreciably if mildly agitated.

2. Means shall be provided for removal of any trapped particles of slurry from the valve.

3. The materials of construction that will be in contact with the slurry and can be tentatively considered are given below:

- a. austenitic stainless steel,
- b. the Stellites,
- c. titanium,
- d. zirconium,
- e. other metals suitable for use in 482°F water are likely to be satisfactory but they must be checked individually.

### LARGE HEAT EXCHANGERS

As mentioned in previous reports, the heat removal system of a 2000-megawatt reactor might consist of ten

200-megawatt heat exchangers. The Lummus Co. has predesigned an exchanger to remove this amount of heat from 20,000 gpm of fuel solution. Their design appears feasible and within the scope of industrial practice.

The Lummus Co. design and several alternates have been studied at ORNL, with the result that one alternate and several variations of the Lummus Co. design appear attractive for further study. The suggestion has been made that the Lummus Co. and the Combustion Engineering Superheater, Inc., jointly make a study of the several designs for ORNL, and a proposal covering this work is expected in the near future.

### CORE DEVELOPMENT STUDIES

The HRE core flow pattern and dimensions cannot be scaled up to larger reactor sizes directly because of the excessive liquid velocities and pressure drop that would result. Further development is in progress to determine new parameters for the design of reactor cores for intermediate- and industrial-scale homogeneous reactors.

The most favorable geometry from the nuclear standpoint is that of a sphere, which also has the engineering advantage of minimum thickness for the walls of the vessel. There must be adequate heat removal from all points to prevent local overheating and nuclear instability. The gas produced from water decomposition must be removed in a reasonable time so that it does not have an excessive effect on reactivity. In addition, there are the normal problems of pressure drop, corrosion, and economy in construction that must be met.

The investigation is being carried out by examining small models of possible reactors; the information

obtained in this manner will then be used to design and build the 8-ft sphere, which will approximately represent an intermediate-scale core vessel, and its associated equipment. The 8-ft sphere tests will provide data, some of which cannot be obtained on a small scale, for the final design of large-scale reactor vessels.

Two general types of configuration are being considered. The first is a core with tangential inlets and with outlets at the poles. In this configuration, the fluid has a rotating motion, which is an aid to gas removal from the core. The second geometry gives straight-through flow and includes designs in which the liquid has little or no rotation.

In comparing the two types of vessels contemplated, the rotating-flow type appears advantageous for gas removal, but straight-through flow can be accomplished with a lower pressure drop. The latter can probably be made to produce a definite, favorable temperature pattern more easily, whereas the temperature distribution in the former is relatively fixed and has not yet been proved satisfactory.

#### Small-Scale Rotating-Flow Models.

An investigation of pressure drop through a 12-in. sphere with four 2-in. tangential inlets and two 2-in. polar outlets was described previously.<sup>(2)</sup> The data obtained with this model are substantially in agreement with the results obtained with other models at the University of Tennessee. The university work covers spheres with one and two inlets.

The data for cases of three and four inlets<sup>(2)</sup> indicate that the pressure drop from inlet to outlet, with all inlets of the same diameter and inlet velocity constant, is

<sup>(2)</sup> *Ibid.*, p. 144.

approximately proportional to the number of inlets.

Further insight into the pressure drop problem has been provided by a velocity study made with pitot tubes in the 12-in. sphere. Figure 53 shows the tangential velocity distribution near the outer wall of the sphere for various operating conditions. The abscissa is radial position divided by the sphere radius and the ordinate is tangential velocity divided by average inlet velocity. The pitot tube is assumed to have a coefficient of unity, which is a reasonable assumption for the type of tube employed. The accuracy of the data is believed to be within 10%.

The center line of the inlet pipe corresponds to an  $r/R$  of 0.838. For one inlet, the tangential velocity of liquid in the sphere at this radius is seen to be greater than that of liquid in the pipe near the inlet, and it falls off rapidly as the inlet jet dissipates to a value considerably below the inlet velocity. At an  $r/R$  of 0.6, the tangential velocity appears to be reasonably constant around the sphere. For the curves that represent multiple inlets, there is a gradual increase of tangential velocity as the number of inlets is increased.

Table 31 illustrates how the increased velocity affects the pressure drop. If the flow pattern in the sphere were independent of the number of inlets used, the over-all pressure drop would be dependent only on the square of the tangential velocity taken at a point near the inlet. Columns 4 and 5 of Table 31 offer a comparison of the square of the observed velocity at  $r/R = 0.6$  and the over-all observed pressure drop; column 6 shows that there is fairly good agreement. The deviations are caused by small differences in flow

# HRP QUARTERLY PROGRESS REPORT

UNCLASSIFIED  
DWG. 15743

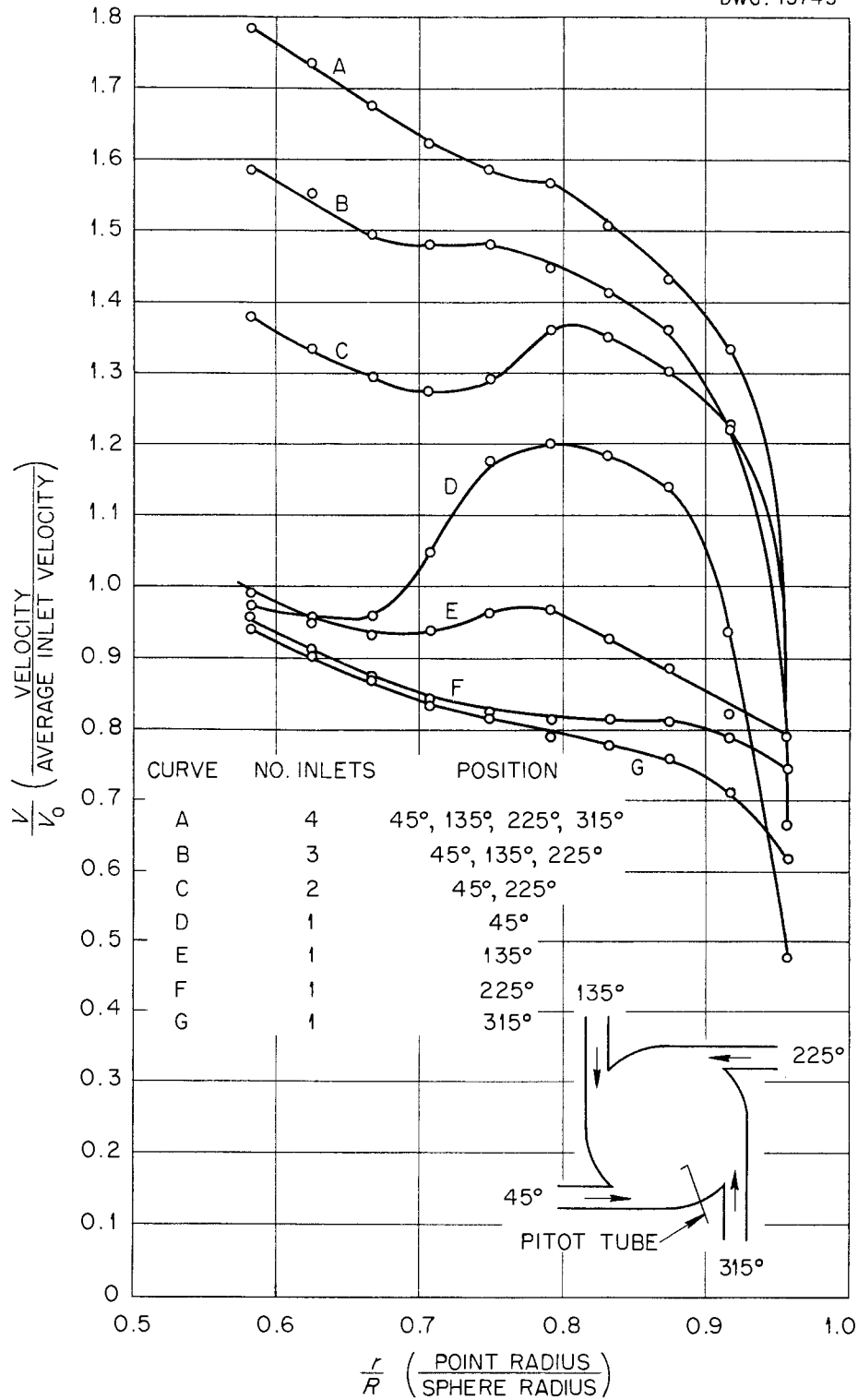


Fig. 53. Effect of Number of Inlets on Velocity in a 12-in. Sphere.

FOR PERIOD ENDING JULY 1, 1952

pattern that become more marked as the number of inlets increases. It is believed that a reasonable explanation for this deviation is that the tangential velocity distribution comes closer to a free vortex by a small amount as the number of inlets is increased.

Figure 54 is a tangential velocity traverse at the equator. In this case, one inlet was used with an average pipe velocity of 6.3 ft/sec and a flow rate of 58 gpm. It is believed that the curvature of the flow lines near the center of the sphere can cause considerable error in the static pressure reading of the pitot. Furthermore, the disturbance of flow by the pitot is estimated to be 17% near the center of the sphere and 8% at the outlet radius.

The confidence that can be placed on the data of Fig. 54 is much less than in the case of Fig. 53. However, there is the characteristic almost-free vortex found in HRE models<sup>(3)</sup> and the almost-forced vortex at the center. The dividing line is near the radius of the outlet pipe.

<sup>(3)</sup> Homogeneous Reactor Experiment Report for the Quarter Ending February 28, 1950, ORNL-630.

The equation describing the "free" portion of the vortex is:

$$v = 4.16 \frac{r}{R} - 0.813$$

where  $v$  is tangential velocity in ft/sec,  $r$  is radius to the point under consideration, and  $R$  is radius of the sphere, with  $r$  and  $R$  in consistent units. The pressure drop predicted from inlet to outlet by using this equation is 73 in. H<sub>2</sub>O. The observed pressure drop is 105 in. H<sub>2</sub>O. Extrapolating the observed points to the outer wall of the sphere and assuming a true free vortex in the sphere gives a theoretical pressure drop of 120 in. H<sub>2</sub>O. Inasmuch as the latter value is closer to the experimental evidence, and also since the errors in pitot readings are such that velocity readings are abnormally reduced near the center, it is reasonable to infer that the true velocity distribution is between a free vortex and that described in the above equation.

Pressure drops were recorded for various types of outlet pipes. A 1-in.-ID insert was mounted in an outlet pipe. Three variations were

Table 31

EFFECT OF VELOCITY NEAR THE WALL ON THE PRESSURE DROP IN A SPHERE

NUMBER OF INLETS	$V/V_0$ AT $r/R = 0.6^*$	RELATIVE $V/V_0$	RELATIVE $(V/V_0)^2$	RELATIVE OVER-ALL PRESSURE DROP	DEVIATION (%)
1	0.965	1.00	1.00	1.00	0
2	1.355	1.404	1.97	2.07	4.8
3	1.574	1.631	2.66	2.93	9.2
4	1.764	1.828	3.34	4.07	17.9

\*  $\frac{V}{V_0} = \frac{\text{tangential velocity at } r}{\text{average velocity in inlet pipe}}$

$\frac{r}{R} = \frac{\text{point radius}}{\text{sphere radius}}$

# HRP QUARTERLY PROGRESS REPORT

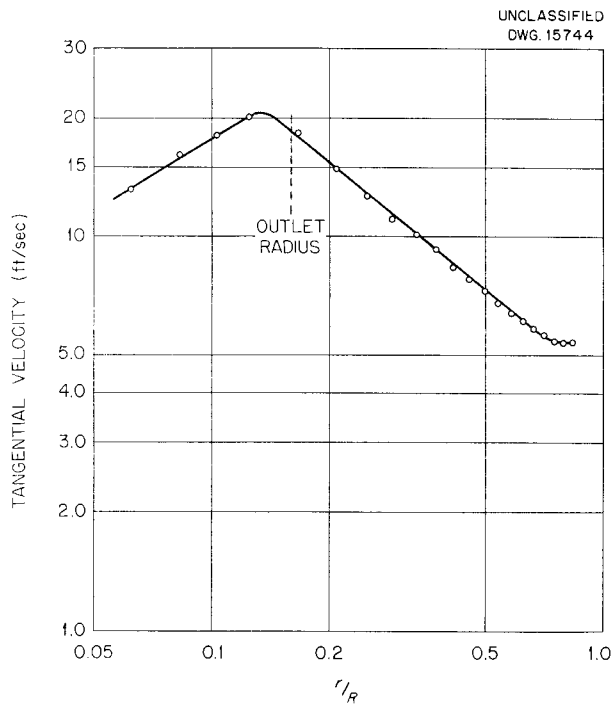


**Fig. 54. Tangential Velocity in 12-in. Sphere with One Inlet.** Flow conditions: 58 gpm; inlet velocity, 6.3 ft/sec.

tried, including a sharp outlet, a rounded outlet, and an outlet that was sharp but extended 1 in. into the sphere. These spheres are shown in Fig. 55. Pressure drops for the sharp and rounded outlets were very nearly the same, but the pressure drop for the inserted outlet was 20% higher. The conclusion is that from a pressure-drop standpoint, either rounded or sharp corners are satisfactory. The rounded corner is somewhat preferable from the standpoint of corrosion.

Further work planned with the 12-in. sphere includes additional checks of the University of Tennessee pressure-drop correlation for varying inlet size; further pitot tube work, if it continues to be fruitful; and the testing of an outlet insert that would extend far into the sphere and have a radical effect on the flow distribution.

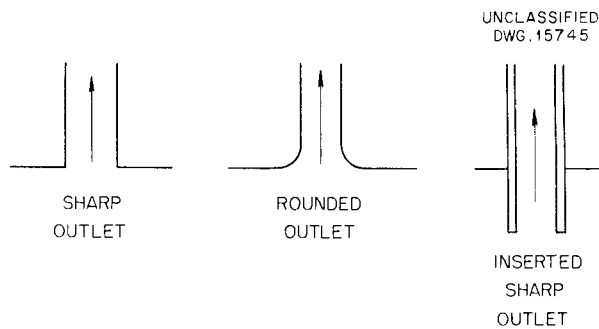


**Fig. 55. Sphere Outlets.**

**Intermediate-Scale Rotating-Flow Models.** A 50,000-gpm loop is being constructed for studying the flow characteristics of an 8-ft sphere. The first sphere will have two tangential inlets of 24-in. pipe and two 30-in. polar outlets. A detailed experimental program has been outlined, and preliminary preparations for the tests are being made.

The main components of the system are eight centrifugal pumps in parallel, the sphere, and two 10,000-gal holdup tanks in parallel. Valves are provided at the pumps and between the sphere and the holdup tanks.

According to current shop estimates, the system should be ready for operation in September 1952. An initial testing period of roughly one month will provide preliminary information for ISHR design work. A more detailed examination will then be carried out that will include work on pressure drop, velocity distribution and direction, residence time of liquid, and gas and liquid mixing.

Considerable preliminary refinement of techniques is required to facilitate later work on the sphere itself. This type of work is already well under way. A simple procedure for estimating liquid residence time, which involves an acid-base reaction in the sphere, has been demonstrated in an 18-in.

model. Salt injection to study mixing and flow pattern has been investigated, and preliminary indications show promise. Also, studies are being made of lighting and other difficulties that arise in the use of photographic analysis in a large tank. Pitot tubes and other possible flow meters are being purchased or constructed for trial runs on small equipment.

#### Small-Scale Straight-through Models.

A preliminary model study carried out in a 12-in. cylindrical section was described previously.<sup>(4)</sup> Further study is planned of a number of designs that are scaled to the best current visualization of a 15-ft core operating at 1000 to 2000 megawatts. The factors to be examined in these models are flow pattern and gas removal, and, if those factors are promising, pressure drop.

Figures 56, 57, 58, and 59 are schematic sketches of models of the mixing-type reactor core arrangements. The entrances are all in the form of sizable jets that produce quite turbulent conditions throughout the sphere and lead to a fairly uniform temperature distribution in a reactor. Figure 56 is a model with 19 entrance jets distributed in the southern hemisphere, and one large outlet at the opposite end. Figure 57 is a model with six jets at the equator and outlets at the poles. Figure 58 is a model with the same entrance jets as in Fig. 56, but the exits are annuli surrounding the inlets. The model shown in Fig. 59 has a single entrance and four exits located in the same hemisphere.

A second type of straight-through reactor utilizes "slug" flow. In this case, the fluid is injected in such a manner that turbulence is minimized, and the flow from inlet

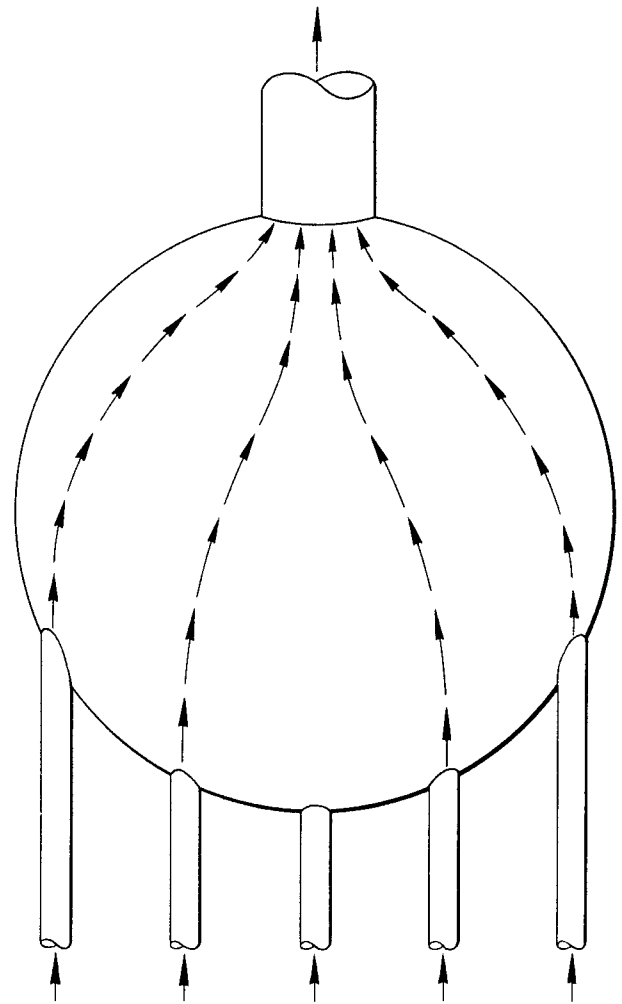
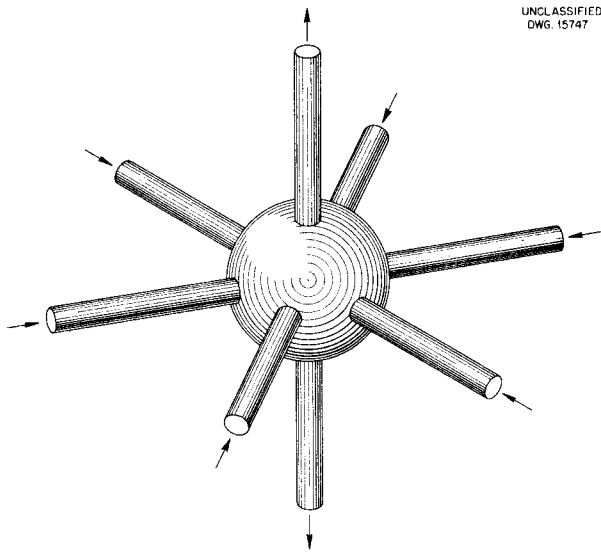


Fig. 56. Multijet Sphere Model with One Northern Outlet.

to outlet is smooth. The temperature distribution consists of a gradient from inlet to outlet. In the ideal case, more liquid flows through the high-power-density regions than flows through the low-power-density regions, and as a result there is a uniform temperature over any given horizontal plane. The advantage of this type of core is that there is a lower pressure drop than in the mixing type of core and a lower concentration of uranium because of the lower average temperature. The difficulty may be in

<sup>(4)</sup>Graham et al., *op. cit.*, ORNL-1280, p. 149.

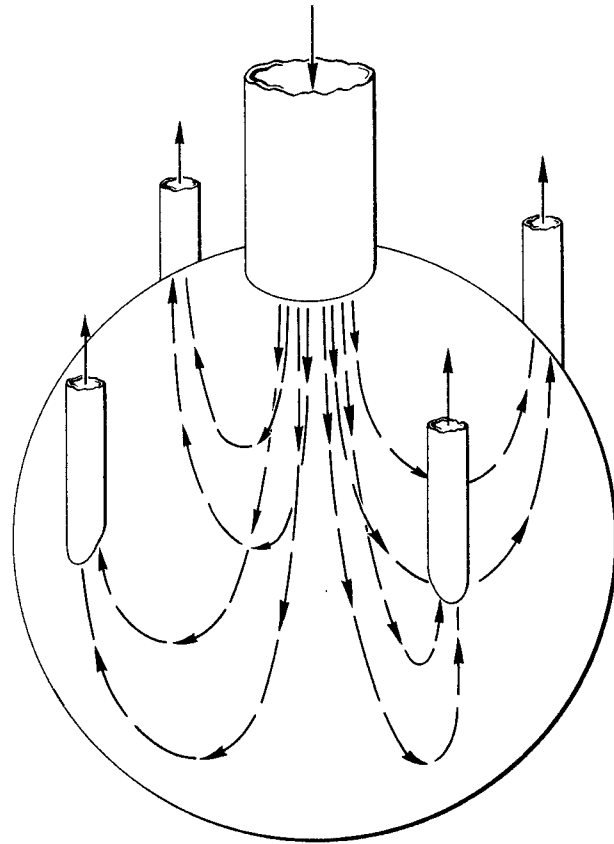
HRP QUARTERLY PROGRESS REPORT



UNCLASSIFIED  
DWG. 15747

UNCLASSIFIED  
DWG. 15749

**Fig. 57. Sphere Model with Six Radial Equatorial Inlets and Two Axial Outlets.**



UNCLASSIFIED  
DWG. 15748

**Fig. 59. Sphere Model with One Axial Inlet and Four Axial Outlets.**

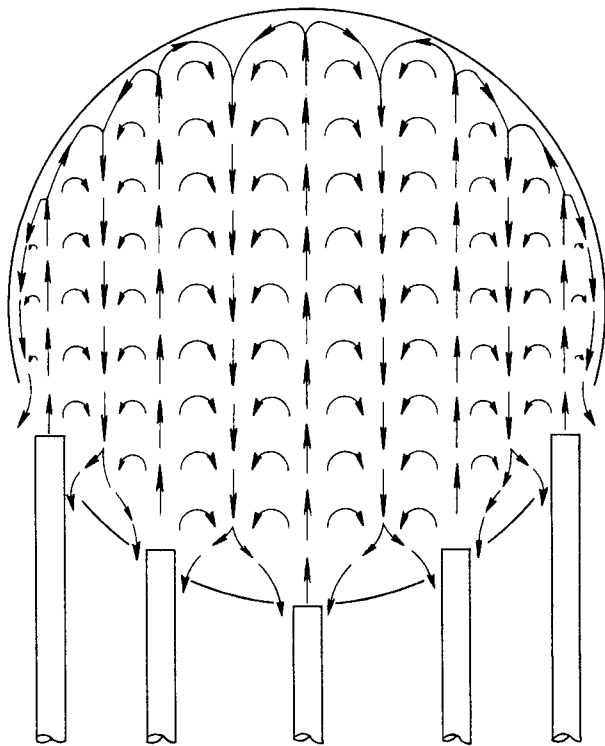


**Fig. 58. Multijet Sphere Model with Annular Outlets.**

the formation of stagnant zones. Figure 60 is a slug-flow model with small entrance jets provided by a perforated plate at the bottom of the sphere and a single outlet at the top. Figure 61 is a model with vanes in the entrance section to create rotation that will stabilize the slug flow. This type of construction should aid in gas removal because of the centrifugal force created by rotation.

Figure 62 is a hybrid of straight-through and rotating-flow cores. The amount of fluid entering in the two tangential inlets is of the same order of magnitude as that in the two inlets directed at the center of the sphere. It is hoped that this model

UNCLASSIFIED  
DWG. 15750

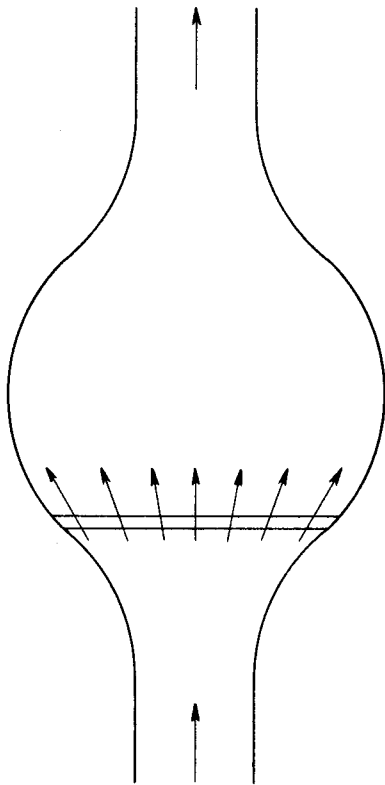


Fig. 60. Sphere Model with Axial Inlet and Outlet and Perforated Plate for Distributing Flow.

will have the gas removal advantages of the rotating-flow core with a considerable reduction in pressure drop.

Further study of these spherical models is required before a good evaluation of straight-through flow can be made.

**Intermediate-Scale Straight-through Models.** If a straight-through geometry appears promising on the basis of small-scale tests, an 8-ft core model will be constructed for operation in the 50,000-gpm loop. Two steel hemispheres have been ordered for this purpose.

UNCLASSIFIED  
DWG. 15751

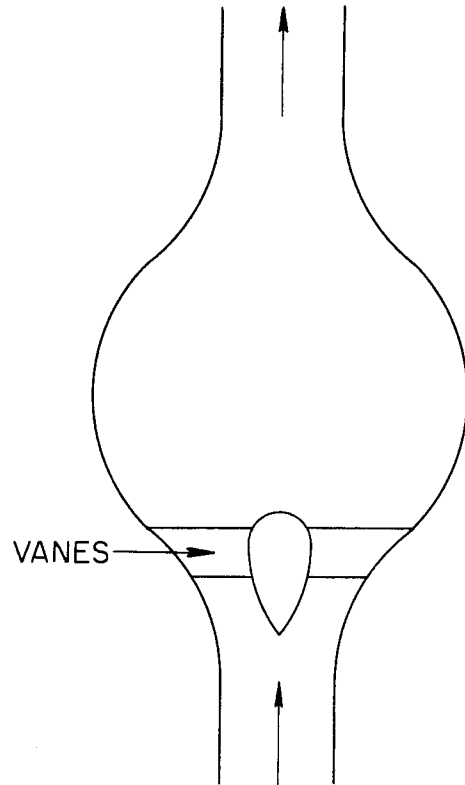


Fig. 61. Sphere Model with Axial Inlet and Outlet and a Vane System for Creating Rotation of the Fluid.

#### GAS SEPARATORS

If a rotational flow pattern is used in the intermediate-scale reactor, gas will probably be removed from a vortex at the core outlets, or in the outlet pipes close to the core. This will be tested in the 50,000-gpm rotating-flow model described previously.

If the gas removal is shown to be incomplete, or if a straight-through core is selected for the ISHR, gas must be removed in the external system. According to the available

# HRP QUARTERLY PROGRESS REPORT

UNCLASSIFIED  
DWG. 15752

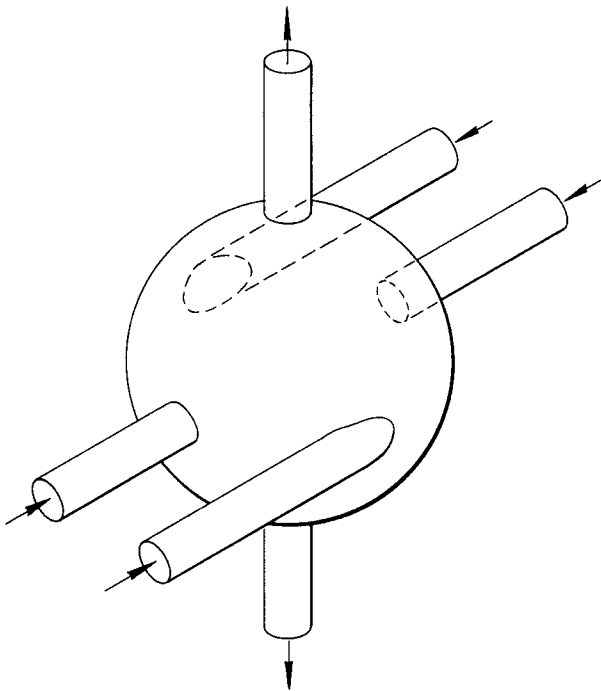


**Fig. 62. Sphere Model with Two Tangential Inlets, Two Radial Inlets, and Two Axial Outlets.**

information, the best way to accomplish the external gas removal is in a pipe gas separator, where the liquid is made to spin and the gas is removed from a central gas void. The model shown in Fig. 63 is being assembled. This unit is capable of handling 500 gpm, which is five times the HRE flow rate. The rotation is produced in the vane section, after which a vortex forms. The rotational energy is recovered in the volute, and thus the pressure drop across the separator is reduced. Gas is removed from a small tube at the volute end of the separator. Provision is made for the measurement of separating efficiency, pressure drop, and rotational velocity.

The unit can be reversed so that the volute produces the rotation and the vanes effect the energy recovery. This will allow comparison of the two techniques for obtaining rotation.

UNCLASSIFIED  
DWG. 15753

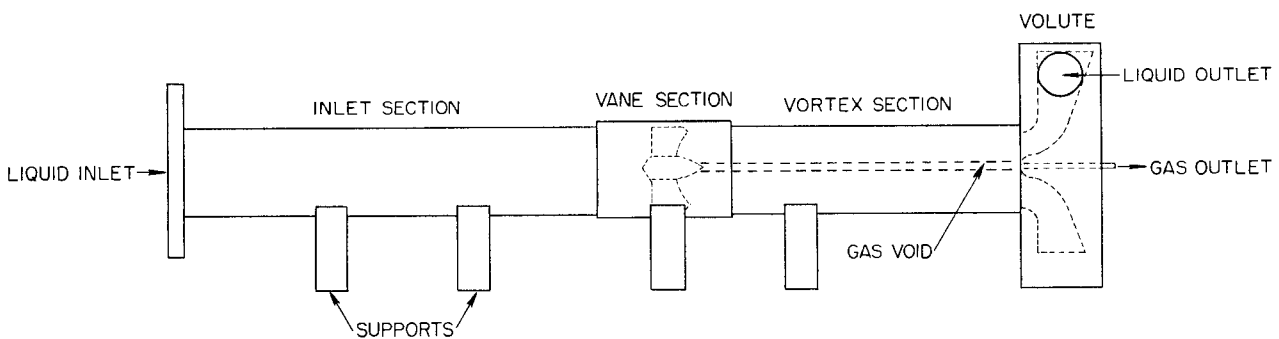


**Fig. 63. Test Model of Pipe Gas Separator.**

## FUNDAMENTAL RADIATION CHEMISTRY STUDIES

H. F. McDuffie, Group Leader  
 J. W. Boyle                      W. F. Kieffer  
 E. L. Compere                    H. H. Stone

## GAS PRODUCTION FROM URANIUM SOLUTIONS

**Uranyl Nitrate.** G values for gas production from uranyl nitrate solutions have been determined under conditions similar to those used for the studies of uranyl sulfate<sup>(1)</sup> and uranyl fluoride.<sup>(2)</sup> The data indicate that at low uranium concentrations G for H<sub>2</sub> gas production is the same as that for comparable sulfate or fluoride solutions. At higher uranium concentrations, nitrate solutions have lower G(H<sub>2</sub>) than either of the other uranyl solutions. The results are compared in Table 32.

The ratio of hydrogen to oxygen present in the ampoules containing

(1) J. W. Boyle, J. A. Ghormley, T. H. Handley, C. J. Hochanadel, W. F. Kieffer, A. C. Stewart, and T. J. Sworski, *Chemistry Division Quarterly Progress Report for Period Ending December 31, 1951*, ORNL-1260, p. 89.

(2) H. F. McDuffie, J. W. Boyle, and W. F. Kieffer, *Chemistry Division Quarterly Progress Report for Period Ending March 31, 1952*, ORNL-1285 (in press).

irradiated solutions of high concentration UO<sub>2</sub>(NO<sub>3</sub>)<sub>2</sub> suggests that the nitrate may be decomposed by pile radiations (Table 33). The gas analysis data for the more dilute solutions of UO<sub>2</sub>(NO<sub>3</sub>)<sub>2</sub> are similar to those found in all analyses of irradiated uranyl sulfate and fluoride solutions. The small amount of N<sub>2</sub> (appearing as inert gas by the combustion technique used for gas analysis) is undoubtedly due to residual air, which is very difficult to outgas from ampoules and solutions before irradiation. The data for the more concentrated nitrate solutions show marked contrast to the results for solutions of comparable concentration containing other anions. The oxygen present is far in excess of the O<sub>2</sub>:H<sub>2</sub> ratio of 1:2 to be expected if only water were decomposed. The identity of the large amounts of N<sub>2</sub> was confirmed by spectroscopic examination.

**Uraneous Sulfate.** A solution of uraneous sulfate containing 40 mg of

Table 32

G VALUES FOR H<sub>2</sub> PRODUCTION FROM AQUEOUS URANYL SOLUTIONS  
 IRRADIATED IN THE X-10 GRAPHITE REACTOR AT 120°C

TOTAL U (mg/ml)	U <sup>235</sup> (mg/ml)	RATIO OF FISSION ENERGY TO TOTAL ENERGY	G (moles H <sub>2</sub> /100 ev)		
			UO <sub>2</sub> (NO <sub>3</sub> ) <sub>2</sub>	UO <sub>2</sub> SO <sub>4</sub>	UO <sub>2</sub> F <sub>2</sub>
4.24	3.95	0.959	1.63	1.63	1.66
42.3	39.4	0.995	1.50	1.51	1.58
318.1	2.29	0.932	0.6*	0.8**	1.0**
420.1	36.9	0.994	0.55	0.78	1.00

\* Value calculated from data of an exploratory study by J. W. Boyle and T. H. Handley, June 1951.

\*\* Values estimated graphically from data for other concentrations and enrichments.

# HRP QUARTERLY PROGRESS REPORT

**Table 33**

**GASES PRODUCED ON PILE IRRADIATION OF URANYL NITRATE**

CONCENTRATION OF $UO_2(NO_3)_2$ SOLUTION		COMPOSITION OF GASES PRODUCED BY PILE IRRADIATION		
Total U (mg/ml)	$U^{235}$ (mg/ml)	$H_2$ (%)	$O_2$ (%)	$N_2$ (%)
4.2	3.95	71	25	4
42.3	39.4	68	30	2
318.1	2.3	25	27	48
420	36.9	38	34	28

uranium (93% enrichment) per milliliter was prepared from the corresponding solution of uranyl sulfate. The calculated amount of concentrated sulfuric acid to supply the additional sulfate ions needed was added to the uranyl sulfate solution and the mixture treated with zinc amalgam. Air was bubbled through the decanted solution for 5 min to ensure the oxidation of any uranium(III) formed by the reduction process. The resulting solution showed almost no precipitation of uranium(IV) as the hydroxide at room temperature, and it oxidized slowly. Most of the samples were irradiated when the uranium(IV)-to-uranium(VI) ratio was about 4.0. No attempt was made to remove the zinc sulfate present in the solutions as a product of the uranyl reduction. Silica ampoules were prepared and degassed by the same method as that used for the uranyl solution studies.<sup>(1)</sup> A temperature not exceeding 30°C was maintained during irradiation by placing the ampoules in water-filled plastic tubes and by holding the temperature of the Hole 12 cooling water to 30°C. After the ampoules were opened and the gas analyzed in the usual manner, samples of the solution were submitted for uranium analysis. From the resulting uranium(IV)-to-uranium(VI) ratio, the amount of oxidation of uranium(IV) to

uranium(VI) during irradiation could be calculated. The data are presented in Fig. 64. It can be seen that the oxygen gas yields are very low but that the amount of uranium(IV) converted to uranium(VI) accounts very satisfactorily for these low yields.

The G for hydrogen gas production in this system is 1.50. This is in excellent agreement with the value for uranyl sulfate and indicates that the process by which  $H_2$  molecules are formed in a fissioning solution is not affected by the presence of the easily oxidized uranium(IV) ions. The low oxygen yield suggests that either the dissolved oxygen or some substance

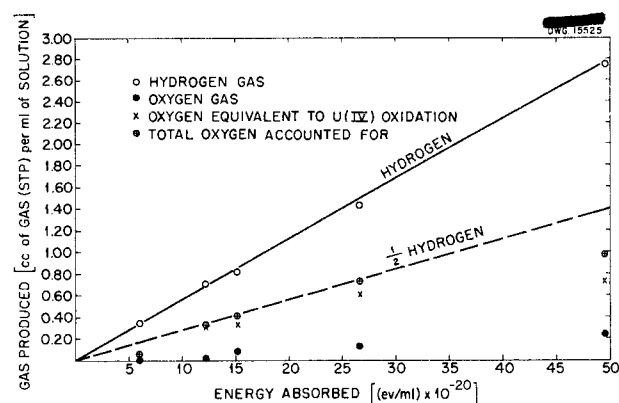


**Fig. 64. Gas Production in  $U(SO_4)_2$  Solutions Irradiated in the X-10 Graphite Reactor at 30°C.**

## FOR PERIOD ENDING JULY 1, 1952

intermediate in its formation reacts with the available uranium(IV) in solution. The fact that some oxygen gas is formed, even in the presence of sufficient uranium(IV) to completely remove it, probably can be explained by the escape of some of the oxygen into the gas phase before it has opportunity to react. This hypothesis was tested by irradiating two ampoules filled with solution to leave no gas space. The data indicate that when the ampoules were filled to leave the gas-to-liquid volume ratio approximately 1.0, the gaseous oxygen found in the products was 17.2% of the stoichiometric amount. In ampoules where the gas-to-liquid volume ratio was nearly zero, the oxygen gas found was only 2.2% of the calculated total amount. Analysis of the resulting solutions indicated that uranium(IV) oxidation had occurred to account for the remaining 97.8% of the oxygen.

Investigations of the effect of increased uranium concentrations on the gas yields for uranous sulfate solutions are under way. Preliminary results indicate that a lowering of  $G(H_2)$  occurs as has been reported for uranyl solutions.

### CATALYTIC SOLUTION RECOMBINATION OF HYDROGEN AND OXYGEN AT 100°C

Efforts during the current period have largely been concerned with exploratory work seeking a suitable catalyst for the solution recombination of hydrogen and oxygen at 100°C. Such a catalyst is desirable because of the interest in operating the HRE in this temperature range. Copper sulfate, which has been shown to be effective as a recombination catalyst at 250°C, is not significantly active at 100°C because of the high temperature coefficient of the catalytic reaction.

No dissolved catalyst has been found that is effective at 100°C, but the platinum group metals appear to be promising catalysts in suspended and, possibly, in colloidal form.

Experiments were carried out in 30-ml bombs of type 347 stainless steel attached for pressure measurement to a Baldwin strain gage equipped with a Brown recorder. The bombs were placed in an aluminum-block-heater thermostat that could be rocked 58 times a minute. When heating to a new temperature the bombs were not rocked to avoid forcing liquid from the bombs into the dead space of the lines and strain gage. Except as noted, all experiments were carried out using uranyl sulfate solutions containing 40 g of uranium per liter. Ordinarily 600 psi of hydrogen and 300 psi of oxygen were charged to the bombs.

A uranyl sulfate solution was prepared to contain the major fission products in concentrations expected after one month's operation of a reactor at a power density of 50 kw/liter and with no gas removal.<sup>(3)</sup> The following elements were included: Ce, Nd, Zr, Cs, Mo, Ru, Ba, Sr, La, Pr, Nb, Rb, and Rh. The rhodium was inadvertently present at ten times the calculated reactor concentration. While four of these bombs were being heated without shaking, an explosion occurred in one at about 200°C, and the other bombs also showed very rapid pressure drops due to recombination. On recharging with gas, high catalytic activity was found at 100°C. A fine, black precipitate was centrifuged from the solution taken from the bombs, and the supernatant liquid showed much lower catalysis. Rhodium and ruthenium were shown to be the catalytically

<sup>(3)</sup>J. S. Gill and W. L. Marshall, *Homogeneous Reactor Project Quarterly Progress Report for Period Ending March 15, 1952*, ORNL-1280, p. 175.

## HRP QUARTERLY PROGRESS REPORT

active substances by separate tests on the various fission-product elements.

The bombs proper retained a considerable degree of catalytic activity. This was not removed by a 30-min treatment with 3% HF-20% HNO<sub>3</sub> solution, nor by a 3-min treatment with concentrated HCl, but it was slowly removed by repeated runs with uranyl sulfate solution at 250°C and with regular gas pressures.

All observations of explosions in these experiments are consistent with the view that a catalyst particle on the wall in contact with the gas is heated and dried by the accelerating recombination reaction and then ignites the mixture.

**Catalysis by Rhodium.** A rhodium sulfate-uranyl sulfate solution containing 600 ppm Rh gave a first-order solution rate constant at 100°C of 130 hr<sup>-1</sup> at 1000 psi of 2H<sub>2</sub>:O<sub>2</sub>. The order of the reaction has not yet been established with respect to rhodium, hydrogen, or oxygen. After the run the washed bombs catalyzed recombination strongly, which indicated a wall deposit. This has been the general experience with rhodium solutions, and, because such a deposit renders a bomb useless until cleaned, it has hampered operations.

**Catalysis by Ruthenium.** A uranyl sulfate solution containing 600 ppm Ru gave a first-order solution rate constant of 3.4 hr<sup>-1</sup> at 100°C and 1000 psi of 2H<sub>2</sub>:O<sub>2</sub> gas. The bomb did not retain a significant degree of catalytic activity.

**Catalysis by Palladium.** A colloidal hydrosol of palladium stabilized by sodium protalbinat was available. This was tested at 50 ppm Pd in the absence of uranyl sulfate. The first-order solution rate constant at 100°C

and 900 psi of 2H<sub>2</sub>:O<sub>2</sub> gas was 80 hr<sup>-1</sup>. Suspensions of reduced palladium in uranyl sulfate solutions are being prepared for testing.

**Catalysis by Osmium.** A solution of 1 g of osmium tetroxide in 1 liter of water was prepared. On heating with 900 psi of 2H<sub>2</sub>:O<sub>2</sub> gas, the gas mixture exploded. The bomb was catalytically active after removal of the solution.

**Catalysis by Platinum.** An Adams platinum dioxide catalyst<sup>(4)</sup> was prepared by fusion of ammonium chloroplatinate with sodium nitrate. This catalyst (approximately 800 ppm Pt in UO<sub>2</sub>SO<sub>4</sub>) gave a first-order solution rate constant of 100 hr<sup>-1</sup> at 100°C and 600 psi of 2H<sub>2</sub>:O<sub>2</sub> gas. Reduction was expected to be effected by the hydrogen gas. Because an active wall deposit was obtained, which possibly indicated some dissolving of the platinum dioxide before reduction, it is believed more desirable to reduce the platinum before combining with the uranyl sulfate. Experiments of this type are under way.

Auric chloride showed no catalytic activity. Iridium metal has been obtained and will be converted to a form suitable for testing.

The order of the catalyzed reaction with respect to the gases has not been determined. Although the rate is expressed above as first order, this has been done because of ease of visualization and comparability of results and does not imply any particular order for the reaction. Recombination rates required for practical use of a solution catalyst in the HRE at 100°C are estimated to be 100 to 2000 hr<sup>-1</sup>. Thus it appears that practical recombination rates

---

<sup>(4)</sup> *Organic Syntheses*, Coll. Vol. I, p. 463.

may be achieved with suspended or colloidal catalysts of the platinum group metals.

Experiments on stabilization of noble metal colloidal solutions by various inorganic colloids (hydrous titanium dioxide, silicon dioxide, ferric oxide, and others) have been initiated. Although temperature, radiation, and the presence of salts such as uranyl sulfate do not promote stability, the possibility of using a colloidal catalyst will be explored because of the relatively greater efficiency of this form.

#### EFFECTS OF RADIATION ON CORROSION

The work of the HRP radiation chemistry group has been brought to the point where solution stability is no longer the overriding problem and where it is now possible to begin studies of corrosion in the presence of radiation. As seen in the preceding section, one approach to this problem involves the measurement of oxygen consumption in and out of radiation. Static bombs are used to contain the solution.

Severe dynamic corrosion in some systems has been disclosed by the operation of test loops at temperatures of 150 to 250°C in the absence of radiation. Testing in the presence of radiation imposes certain constraints as to apparatus size, duration of experiments, safety, and amounts of fissionable material that may reasonably be utilized. From a chemical point of view it is more important to determine the effects of changes in controllable variables over as great ranges as possible than it is to put together some system and see how long it will run. Consequently, it has become of interest to develop an accelerated dynamic test that is useful both in and out of radiation.

A review of the literature has led to the conclusion that the dynamic corrosion in the loops was caused by the impingement of turbulent solution upon the protective film and ultimate removal or destruction of the film. The subsequent rapid attempt of the solution to reform a protective film oxidizes the next layer of metal which is immediately removed by the impingement of the solution. Thus, in the dynamic system, the rate of pitting may be a function of the ability of the solution to oxidize fresh stainless steel surfaces. It is believed that any method of testing that leads to impingement of metal upon solution will give similar results. Several possible small-scale dynamic tests have been evolved that may prove useful either in or out of radiation. These tests are described in the following, and the ultimate choice as to use by the radiation chemistry group of the HRP will be governed by two factors:

1. whether the test can be scaled down in size to fit in pile facilities, and
2. whether the test can be carried out in a very short period of time and thus permit surveys of a variety of environmental conditions and the possible use of materials (in the test apparatus) that are not very resistant to radiation.

**Whirligig Test.** If a shaft is caused to generate a conical surface (by use of a motor, face plate, off-center bearing, and two universal joints) but is kept from turning by clamping the universal joint furthest from the face plate, a container attached to the shaft will describe a circle. If that container is partially filled with liquid, the motion of the liquid will be similar to that obtained by swirling a glass

## HRP QUARTERLY PROGRESS REPORT

partially filled with water. Such an apparatus has been constructed and equipped with a thick-walled, cylindrical, glass container. Operation with approximately 1-in. offset and a speed of 600 rpm has been observed by using a stroboscope. The inside liquid was observed to form a clean wave front that traveled around the inside of the container at the same angular velocity as that given to the supporting shaft.

The container mounted on the supporting shaft can be any of several types. The two most interesting are the cylinder and the torus. A torus can be constructed of tubing or standard pipe joints and thus simulates expected mechanical conditions.

**Connecting Rod.** If the supporting shaft for the container is caused to move as a connecting rod in a piston-type engine, a point on the rod will describe an ellipse. The approach to uniform circular motion is probably good enough to be useful in driving liquid around a torus or around the inside wall of a cylinder much as in the whirligig test.

**Magnetostrictor Test.** Corrosion studies have been carried out at other laboratories<sup>(5)</sup> with metal specimens in contact with the test liquid and attached to the end of a nickel tube that is vibrated by magnetostriction. The vibration imparted to the specimen was sufficient to cause rapid erosion-corrosion.

**Test Using Audio Speaker Drive.** If vibration in the audio range

<sup>(5)</sup> S. L. Kerr, *Trans. Am. Soc. Metals* 59, 373 (1937).

(5,000 to 10,000 cps) is sufficient to cause dynamic corrosion, it should be possible to attach the specimen to a drive such as is used to move a speaker cone. Two companies that manufacture vibration testing equipment (Calidyne Co. and M B Manufacturing Co.) have been contacted to see whether components of their equipment might possibly be of use in our testing program. At present it seems likely that this approach will be very promising.

**Jet Impingement Test.** A very successful jet impingement test has been described in the literature<sup>(6,7)</sup> but this test appears to have little chance of being scaled down to the size required. Consideration has been given to the possibility of forming a jet of high-pressure liquid and causing it to impinge upon a fixed plate by using gas pressure in excess of steam pressure to force the liquid to move. The extent of corrosion would be determined by examination of the plate.

In the near future a decision will be made as to which of the tests, if any, should be investigated intensively. Following the decision, it is expected that evaluation of uranyl sulfate and uranyl fluoride under various conditions of temperature, concentration, and excess oxygen or hydrogen-oxygen pressure would be attempted.

<sup>(6)</sup> J. M. Mousson, *Trans. Am. Soc. Metals* 59, p. 399 (1937).

<sup>(7)</sup> C. R. Soderberg, *Mech. Eng.* 57, p. 165 (1935).

## SOLUTION CHEMISTRY

W. L. Marshall, Group Leader

R. D. Brown	E. V. Jones
H. O. Day, Jr.	M. H. Lietzke
J. S. Gill	K. S. Warren

H. W. Wright

PLUTONIUM SOLUBILITY IN  $\text{UO}_3\text{-H}_3\text{PO}_4\text{-H}_2\text{O}$  SOLUTIONS

H. W. Wright

The ratio of  $\text{PO}_4$  to U necessary to maintain a stable solution of  $\text{UO}_3\text{-H}_3\text{PO}_4\text{-H}_2\text{O}$  at  $250^\circ\text{C}$  is about 5.2 for a 1.26 M uranium concentration.<sup>(1)</sup> The solubility ratio,  $\text{PO}_4:\text{U}$ , increases both as a function of temperature between 100 and  $300^\circ\text{C}$  and as an inverse function of uranium concentration.<sup>(2,3)</sup> The purpose of this work was to determine the effect of excess  $\text{H}_3\text{PO}_4$  on the stabilization of plutonium in solution. Plutonium(IV) has been shown to undergo hydrolysis precipitation above  $100^\circ\text{C}$  in both  $\text{UO}_2\text{SO}_4\text{-H}_2\text{O}$  and  $\text{UO}_2\text{F}_2\text{-H}_2\text{O}$  systems.<sup>(4,5)</sup> The first experiment in a silica tube was carried out at  $140^\circ\text{C}$  for 140 hr with a 1.05 M U-12.1 M  $\text{H}_3\text{PO}_4$  solution containing 2 g of plutonium(IV) per liter. No precipitation of plutonium occurred. The next experiment was made with a 0.454 M U-3.1 M  $\text{H}_3\text{PO}_4$  solution containing 2 g of plutonium(IV) per liter. After 7 hr at  $200^\circ\text{C}$  the entire solution formed a gel that reliquified only after remaining at

$25^\circ\text{C}$  for several days. Similar results were obtained with experiments at  $175^\circ\text{C}$ .

Enough phosphate can be added to stabilize plutonium in a uranyl phosphate solution. However, this amount of phosphate will, in all probability, be more with respect to cross section to achieve the same objective than is necessary for a  $\text{UO}_2\text{SO}_4\text{-H}_2\text{O}$  system containing a slight excess of  $\text{H}_2\text{SO}_4$ .<sup>(5)</sup>

## INFLUENCE OF RADIATION ON THE VALENCE OF PLUTONIUM

K. S. Warren

An investigation has been started on the effect of  $\text{Co}^{60}$ -emitted gamma radiation and inpile radiation on the stability of the III and VI valence states of plutonium as sulfate. In one experiment uranyl sulfate was also present to the extent of 88.5 g per liter of solution. It was found that the tendency of plutonium(III) and plutonium(VI) to return to plutonium(IV) was greatly enhanced by the presence of the two types of radiation.

**Gamma-Ray Bombardment of Plutonium Solutions.** Samples of plutonium(III) and plutonium(VI) were prepared by electrolyzing plutonium(IV) sulfate in a glass cell by using platinum electrodes, without stirring, and a current density of 0.55 ma per square centimeter of electrode surface. Portions of the electrolyte were removed from the anode and cathode compartments and sealed in 5-mm pyrex

(1) J. S. Gill, W. L. Marshall, and H. W. Wright, *Homogeneous Reactor Project Quarterly Progress Report for Period Ending August 15, 1951*, ORNL-1121, p. 120.

(2) J. S. Gill and H. W. Wright, *Homogeneous Reactor Project Quarterly Progress Report for Period Ending May 15, 1951*, ORNL-1057, p. 112.

(3) B. J. Thamer, *The Solubility of Uranium in Possible Fuels for Homogeneous Reactors*, Paper presented at Second Fluid Fuels Development Conference, Oak Ridge, 1952.

(4) K. S. Warren and H. W. Wright, *Homogeneous Reactor Project Quarterly Progress Report for Period Ending March 15, 1952*, ORNL-1280, p. 173.

(5) W. Tomlin, *op. cit.*, ORNL-1121, p. 178.

## HRP QUARTERLY PROGRESS REPORT

glass tubes. A  $\text{Co}^{60}$  gamma-ray source was provided in the canal of Building 3001. This source emitted about 720,000 r/hr at the particular location. After periods of exposure, which varied from 67 to 127 hr, suitable dilution of the samples was made, and plutonium determinations were carried out by two methods that permitted a comparison of the oxidized and reduced states of plutonium. Similar determinations were also made simultaneously on control samples, that is, portions of the original solution that had not been irradiated. The results are given in Table 34. These data indicate that  $\text{Co}^{60}$ -emitted radiation (roughly 1.2 Mev) speeds up considerably the reactions in neutral solutions that result in bringing the VI or III valence states of plutonium back to the more stable IV state (on standing and without other added reagent). This is also true in the presence of uranyl ion.

**Inpile Irradiation of Plutonium Solutions.** A sample of plutonium solution was removed from the desired compartment of the electrolysis cell and suitably diluted, and 3.0 ml of the diluted solution was transferred to a silica tube. The tube was evacuated after freezing the solution and then sealed. The system was surrounded by a protective aluminum jacket and placed in water-cooled Hole 12 in the X-10 graphite reactor for overnight exposure. The tube was then removed from the reactor and allowed to decay to a safe level before opening and analyzing the contents. The use of the Beckman, or other, spectrophotometer was not feasible because of the low plutonium concentrations (0.1 mg per milliliter of solution, or less) necessary because of gas-pressure hazards in a closed system. It was necessary therefore to use chemical methods in ascertaining valence states. Besides the lanthanum fluoride coprecipitation method which

Table 34

VALENCE CHANGES IN GAMMA-IRRADIATED SOLUTIONS

TIME OF IRRADIATION (hr)	ORIGINAL STATE OF PLUTONIUM	METHOD OF ANALYSIS	VALENCE CHANGE AFTER IRRADIATION	
			Control Sample*	Irradiated Sample
67	Oxidized (VI)	Beckman spectrophotometer	Considerable Pu(VI) retained	Pu(VI) completely removed
127	Oxidized (VI)	Beckman spectrophotometer	Considerable Pu(VI) retained	Pu(VI) completely removed
68	Oxidized** (VI)	$\text{LaF}_3$ coprecipitation	50% Pu(VI) present	0% Pu(VI) present
116	Oxidized** (VI)	$\text{LaF}_3$ coprecipitation	35% Pu(VI) present	0% Pu(VI) present
67	Reduced (III)	Beckman spectrophotometer	Pu(III) retained	Pu(III) removed
127	Reduced (III)	Beckman spectrophotometer	Pu(III) retained	Pu(III) removed

\* Retained after standing at room conditions for the same length of time as required for the irradiation of the test sample.

\*\* 264 g of uranium (as the sulfate) present per liter of solution.

is standard for distinguishing quantitatively between plutonium(VI) and the lower valence states, an anion-exchange resin (Dowex A-1) was tried. The latter would retain valences higher than III, and this method was used satisfactorily for separating plutonium(III) and plutonium(IV). The results are given in Table 35. The data indicate that plutonium in the VI state is rapidly reduced to the tetravalent condition by inpile radiation, whether in the presence of uranyl ion or not. Conversely, data obtained in connection with neutron-irradiated plutonium(III) have shown that it is rapidly oxidized to the IV state by the conditions prevailing during inpile irradiation of aqueous solutions.

#### CONDUCTIVITY OF URANYL SULFATE IN AQUEOUS SOLUTION

R. D. Brown

The previous report<sup>(6)</sup> contained data on the conductivity of uranyl sulfate and uranyl fluoride in aqueous solution over wide concentration ranges and at various specific temperatures in the range 0 to 90°C. Additional data obtained at 125°C for

<sup>(6)</sup>R. D. Brown, *op. cit.*, ORNL-1280, p. 183.

uranyl sulfate are presented in Table 36.

Recent efforts have been directed towards the measurement of the conductivity of uranyl sulfate in aqueous solutions at 200 and 250°C. This work has been hampered by difficulties encountered in constructing a conductivity cell that will withstand the high pressures encountered at these temperatures and by the fact that uranyl sulfate solution shows a corrosive action on the materials used for the cells. Some of the cells designed and constructed are described in the following.

One bomb type of cell, made of type 347 stainless steel, contained a silica conductivity chamber with a pyrex cover through which the electrode leads were passed. The leads and electrodes were of platinum, and entry into the bomb was made through pressure fittings with soapstone glands. This cell gave erratic results because of leakage across the lead wires, which were in contact with water vapor inside the cell.

A second bomb was constructed to hold a small pressure cell made of heavy-wall pyrex tubing. The solution

Table 35

#### VALENCE CHANGES IN INPILE-IRRADIATED SOLUTIONS

ORIGINAL STATE OF PLUTONIUM	TIME OF IRRADIATION (hr)	METHOD OF ANALYSIS	VALENCE CHANGE AFTER IRRADIATION	
			Control Solution	Irradiated Solution
Oxidized	16	LaF <sub>3</sub> coprecipitation	Pu(VI): 0.08 mg/ml	0.009 mg/ml
Oxidized*	8	LaF <sub>3</sub> coprecipitation	Pu(VI): 0.10 mg/ml	0.000 mg/ml
Reduced	18	Dowex A-1 ion exchange	Pu(III): 0.018 mg/ml	0.000065 mg/ml

\*89 g of uranium (as the sulfate) present per liter of solution.

## HRP QUARTERLY PROGRESS REPORT

**Table 36**  
**CONDUCTIVITY OF URANYL SULFATE**  
**SOLUTIONS AT 125 AND 200°C**

CONCENTRATION (eq./l)	EQUIVALENT CONDUCTANCE (ohms <sup>-1</sup> .cm <sup>2</sup> )	
	At 125°C	At 200°C
4.66	10.07	
2.52	18.00	20.60
1.00	26.78	33.38
0.50		39.82
0.10	42.08	55.0
0.05	48.6	66.09
0.01	81.4	105.4
0.005	110.4	124.8
0.001	236	
0.0005	320	
0.0001	600	

was sealed inside the cell and the cell placed inside the bomb. A nitrogen pressure approximating the vapor pressure of water at the operating temperature was then admitted to the bomb. Electrical connection to the outside was made through conventional pressure fittings with soapstone glands. This cell gave fairly reliable results at 200°C in the more concentrated (>0.001 N) solutions. The data in Table 36 were obtained with this cell. The data at 200°C are considered reliable to ±5%.

It was shown, however, that considerable solution of the pyrex glass took place at this temperature. This was done in two ways - the conductivity of a solution was measured at room temperature before and after use in the conductivity cell. A sample so used ( $C = 0.001 N$ ) had an equivalent conductivity of approximately 110 ohms<sup>-1</sup>.cm<sup>2</sup> at 25°C. After being held in the cell for 2 hr at 200°C it was removed, cooled to 25°C, and the

conductivity again measured. The conductivity was then found to be approximately 130 ohms<sup>-1</sup>.cm<sup>2</sup>. A sample of 0.1 N UO<sub>2</sub>SO<sub>4</sub> was held in the bath for a period of 16 to 18 hr and then removed, and a spectrographic determination of boron was obtained. The solution was found to contain 8.2 μg of boron per milliliter, which showed considerable solution of the pyrex glass.

The first bomb cell was then modified. The platinum leads were painted with Teflon paint baked on at 250°C. This bomb cell could be fitted with either a silica or pyrex lining and tests were made with each. These cells also gave erratic results either because of vapor contact with the type 347 stainless steel or because of the solution of the silica or pyrex in the uranyl sulfate solution. Again this bomb was modified. A Teflon rod (4 cm in diameter) was hollowed out to form a cell with a tight-fitting Teflon cap through which the electrode leads were passed. These leads were coated with Teflon paint and access from the exterior was made through conventional fittings. This cell gave reasonably good data with concentrations above 0.1 N, but the conductivity of dilute solutions increased rapidly when held in this cell for an appreciable length of time. This cell was also tested with pure water. It was filled at 25°C, where  $k_{H_2O}$  was known to be  $5 \times 10^{-6}$ , and after 2 hr in the bath at 250°C the bomb was removed and allowed to cool to room temperature. The value of  $k_{H_2O}$  was then found to be about  $8 \times 10^{-5}$ .

**Conductometric Titration.** Information was desired concerning the variation in conductivity of uranyl sulfate solutions containing an excess of uranium as UO<sub>3</sub>. Solid UO<sub>3</sub> was added to a stock solution of 1.25 M UO<sub>2</sub>SO<sub>4</sub> to give a solution with

a  $U:SO_4^{=}$  ratio of 1.2:1. The solution thus prepared was 1.5 M in U and 1.25 M in  $SO_4^{=}$ , neglecting the slight volume increase due to the addition of  $UO_3$ . From this solution, others of the concentrations given in Table 37 were prepared. The conductivities of these solutions were measured at 25°C, and standard sulfuric acid was added in measured amounts until the sulfate concentration was greater than that of the uranium. Clearly defined end points were obtained in all cases by plotting the conductivity (reciprocal of the bridge reading,  $1/R$ ) vs. milliliters of standard acid added. These plots are shown in Figs. 65 and 66.

A tabulation of the data is given in Table 38. The equivalent conductivity in each case is in good agreement with that obtained in previous work.

It is concluded that uranyl oxide ( $UO_3$ ) behaves as a weak base in aqueous solution and shows a strong buffering action, as indicated by the small change in conductivity upon addition of sulfuric acid until the stoichiometric end point is reached. This is

Table 37

SOLUTIONS PREPARED FOR CONDUCTIVITY MEASUREMENTS

SOLUTION NO.	URANIUM CONCENTRATION (M)	SULFATE CONCENTRATION (M)
1(stock)	1.5	1.25
2	0.7	0.625
3	0.30	0.25
4	0.15	0.125
5	0.075	0.0625
6	0.0075	0.00625

of interest in consideration of corrosion. It appears probable that since there is little difference in conductivity between the 1.2:1 and the 1:1 U to  $SO_4$  solutions the corrosion effect of the two should be approximately the same.

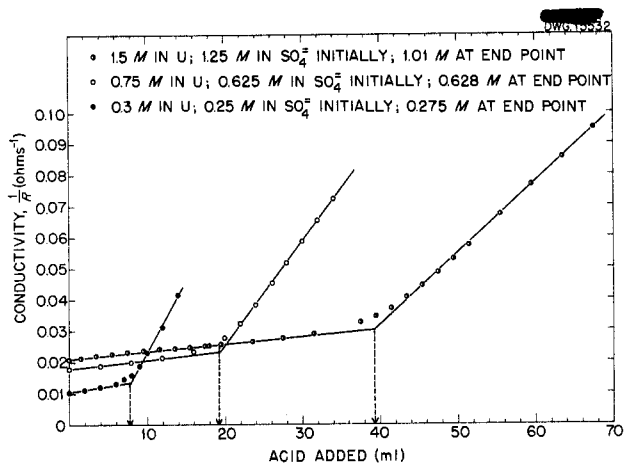


Fig. 65. Conductometric Titration of  $UO_3$  in  $UO_2SO_4$  Solution with 1.281 N  $H_2SO_4$ . Cell constant, 0.501.

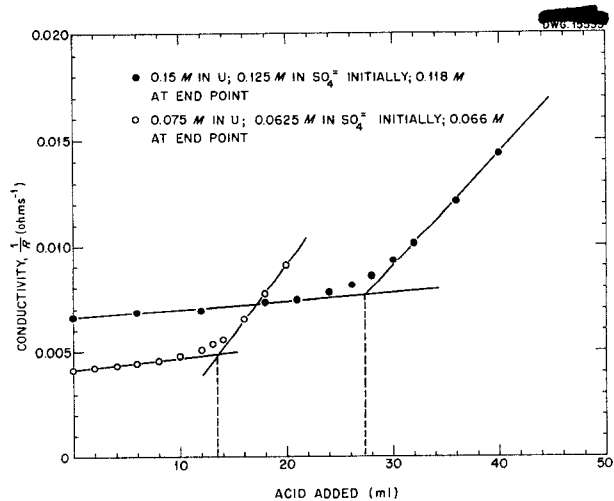


Fig. 66. Conductometric Titration of  $UO_3$  in  $UO_3SO_4$  Solution with 0.180 N  $H_2SO_4$ . Cell constant, 0.501.

# HRP QUARTERLY PROGRESS REPORT

Table 38

## CONDUCTOMETRIC TITRATION OF $UO_2SO_4$ SOLUTION CONTAINING EXCESS $UO_3$

SOLUTION NO.	URANIUM (eq./l)	URANIUM AT END POINT (eq./l)	1/R	K*	EQUIVALENT CONDUCTANCE ( $ohm^{-1} \cdot cm^2$ )
1	3.0	2.02	0.0345	0.0173	8.5
2	1.5	1.26	0.0267	0.0134	10.6
3	0.6	0.556	0.0155	0.00775	13.9
4	0.3	0.236	0.0084	0.0042	17.8
5	0.15	0.132	0.0054	0.0027	20.4
6	0.015	0.0110	0.0012	0.0006	56.8

\* Cell constant = 0.501.

### VAPOR PRESSURES OF AQUEOUS URANYL SULFATE SOLUTIONS

H. O. Day, Jr.

The vapor pressures of saturated uranyl sulfate solutions were determined by using a compound manometer apparatus. The temperature range covered was 50 to 100°C. About 15 readings were taken at each temperature and the results were averaged.

The solid phase of uranyl sulfate froze the stirrer in the pressure vessel shortly after the determinations were started, and as a result equilibrium was attained very slowly. Any errors in the measurements can most likely be attributed to this factor. Table 39 presents the experimental data. The values at 50 and 60°C are apparently in error, probably because of not attaining equilibrium. It is planned to repeat the measurements at some future date.

In order to obtain more accurate data at temperatures below 100°C, a differential vapor pressure apparatus has been built. It is hoped that the data will prove accurate enough to enable precise activity coefficients to be calculated.

This apparatus consists of two glass vessels of about 50-ml capacity connected by separate glass tubing to a glass U-tube. The glass vessels connect to the tubing by means of standard-taper ground-glass joints. The glass U-tube was filled with dibutylphthalate as a manometer fluid, and the entire U-tube was thermostated at  $103.38 \pm 0.09^\circ C$ . Dibutylphthalate has a vapor pressure of about 0.061 mm Hg at this temperature and an experimentally determined density of  $0.9792 g/cm^3$ . The sensitivity of the vapor pressure measurements is therefore increased by a factor of over 13.5 as compared with mercury manometer measurements. The dibutylphthalate was loaded into the manometer under vacuum to remove air. Stopcocks are provided in the glass lines to close off the manometer from the rest of the system. The two glass lines leading from the pressure vessels to the manometer have stopcock connections leading to a high vacuum line and also a reservoir of water that has been freed from air by sublimation of ice at low temperature under a vacuum. The sublimation was repeated about a dozen times. The reservoir also has a stopcock for isolating it from the high-vacuum line.

Table 39

## VAPOR PRESSURES OF SATURATED URANYL SULFATE SOLUTIONS

TEMPERATURE (°C)	MOLALITY OF $\text{UO}_2\text{SO}_4$ AT SATURATION*	VAPOR PRESSURE DEPRESSION (mm Hg)	RELATIVE MOLAL VAPOR PRESSURE LOWERING $(P_0 - P)/P_0M$
50	4.333	14.10 ± 0.10	0.0351 <sub>7</sub>
60	4.457	23.69 ± 0.05	0.0355 <sub>7</sub>
70	4.602	34.65 ± 0.05	0.0322 <sub>2</sub>
80	4.769	51.68 ± 0.15	0.0305 <sub>1</sub>
90	4.963	73.09 ± 0.32	0.0280 <sub>0</sub>
100	5.187	106.20 ± 0.13	0.0269 <sub>4</sub>

\*C. H. Secoy, *J. Am. Chem. Soc.* **70**, 3450 (1948).

The connecting tubing from the pressure vessels to the manometer is wound with nichrome wire to allow heating to prevent condensation of water in the tubing when the pressure vessels are above room temperature. The pressure vessels were thermostated in a vigorously stirred bath of glycerol-water. The temperature of this bath was measured with a platinum resistance thermometer and controlled by means of a nickel resistance element in conjunction with a Leeds and Northrup duration-adjustment type of control. This control was excellent except at 90 and 100°C, at which temperatures the thermometer showed variations of ±0.02°C. (Temperatures of 25 to 30°C were attained by use of a water-cooled copper cooling coil.)

Each pressure vessel contained a small, glass-enclosed, iron magnet. By moving another magnet nearby, the contents of the vessels were amply stirred to allow equilibrium to be more quickly attained.

The technique used in a determination of vapor pressure was to weigh accurately finely powdered uranyl

sulfate into one of the pressure vessels. The vessel was attached to the system and evacuated. Air-free water was distilled onto the solid uranyl sulfate and the uranyl sulfate dissolved. The solution was then frozen and the vessel again evacuated. The contents of the vessel were then allowed to thaw under a vacuum. This process of alternately freezing and melting under vacuum was repeated several times to ensure complete removal of air. Pure air-free water was distilled into the second vessel. The vessels were then immersed in the thermostat by raising the thermostat bath. The thermostat was then heated to the desired temperature and the difference in vapor pressure of the solution and the pure water was observed on the manometer.

After completion of the pressure measurements the thermostat bath was lowered and the uranyl sulfate solution frozen by means of a dry ice-acetone bath. The pressure vessel was then removed from the line and quickly capped. The contents were then allowed to thaw. After reaching room temperature the vessel and its

## HRP QUARTERLY PROGRESS REPORT

contents were accurately weighed. Since this weighing allowed the total mass of water to be known, the concentration of the uranyl sulfate solution could then be calculated at each temperature. Correction for the mass of water present as vapor in the connecting lines and manometer was made. So far measurements have been made from 25 to 100°C for concentrations of about 0.6 and 2.1  $m$   $UO_2SO_4$ .

After the vapor pressures of the 2.1  $m$   $UO_2SO_4$  solution were measured it was noticed that the uranyl sulfate appeared discolored and had an odor similar to butyl alcohol (the odor was probably due to this substance). The conclusion reached was that the dibutylphthalate had very slowly hydrolyzed. Whether the mechanism of this hydrolysis was a vapor-phase hydrolysis in the manometer or whether a small amount of the ester distilled into the pressure vessel and there hydrolyzed is not known. This hydrolysis would be bound to affect both the pressure measurements and the concentration measurements. The exact extent of this effect is unknown. The hydrolysis process could be minimized by making measurements more quickly and by keeping the stopcocks in the line closed except during measurements. However, it was felt that finding a more suitable manometer fluid would be the best solution.

Two possible manometer fluids are *m*-diphenylbenzene and tri-*p*-cresyl phosphate. Experimental determination of their densities at  $103.38 \pm 0.09^\circ C$  gave  $1.03157 \pm 0.00010$  g/cm<sup>3</sup> for *m*-diphenylbenzene and  $1.1087 \pm 0.00005$  g/cm<sup>3</sup> for tri-*p*-cresyl phosphate. The diphenylbenzene would therefore make a slightly more sensitive manometer fluid. However, the vapor

pressure of this substance is roughly four times that of dibutylphthalate, whereas the vapor pressure of tri-*p*-cresyl phosphate is 0.3 of a micron at  $103.38^\circ C$ . From this aspect the tri-*p*-cresyl phosphate would be better. The tri-*p*-cresyl phosphate is, however, an ester and might possibly hydrolyze as did the dibutylphthalate. This possibility would not exist if *m*-diphenylbenzene were used as the fluid. Therefore *m*-diphenylbenzene was chosen as the manometer fluid for the present. Measurements of the vapor pressure of uranyl sulfate solutions will determine whether this substance is satisfactory.

Results of the measurements already made with dibutylphthalate as the manometer fluid are given in Tables 40 and 41. The solid uranyl sulfate that was used to make up the solution had been analyzed for uranyl sulfate content (difference is water of hydration). The value taken was the mean of the analyses. This means that there is a definite uncertainty in the concentrations of uranyl sulfate as reported. The concentrations of the solutions vary from temperature to temperature because of the loss of varying amounts of water to the vapor phase. To show this variation in concentration the actual concentrations recorded are carried to more significant figures than the accuracy of the analysis warrants. In Table 40 the uncertainty due to analysis errors is  $\pm 0.0002$  in molality and  $\pm 0.000003_5$  in mole fraction. In Table 41 the uncertainty due to analysis errors is  $\pm 0.0010$  in molality and  $\pm 0.00001_7$  in mole fraction. This refers to errors of analysis of the original uranyl sulfate and does not take into account errors due to hydrolysis of dibutylphthalate.

FOR PERIOD ENDING JULY 1, 1952

Table 40

VAPOR PRESSURES OF 0.592 *m* UO<sub>2</sub>SO<sub>4</sub>-H<sub>2</sub>O SOLUTIONS

TEMPERATURE (°C)	MOLALITY OF UO <sub>2</sub> SO <sub>4</sub>	MOLE FRACTION OF UO <sub>2</sub> SO <sub>4</sub>	Δ <i>P</i> (mm Hg)
25	0.59172	0.010548 <sub>0</sub>	0.233
30	0.59173 <sub>6</sub>	0.010548 <sub>3</sub>	0.300
35	0.59175	0.010548 <sub>5</sub>	0.392
40	0.59176 <sub>4</sub>	0.010548 <sub>8</sub>	0.511
45	0.59178	0.010549 <sub>0</sub>	0.675
50	0.59180 <sub>1</sub>	0.010549 <sub>4</sub>	0.884
60	0.59188 <sub>4</sub>	0.010550 <sub>9</sub>	1.443
70	0.59198 <sub>2</sub>	0.010552 <sub>6</sub>	2.164
80	0.59211 <sub>7</sub>	0.010555	3.107
90	0.59230	0.010558 <sub>2</sub>	4.166
100	0.59253 <sub>1</sub>	0.010562 <sub>3</sub>	5.699

Table 41

VAPOR PRESSURES OF 2.09 *m* UO<sub>2</sub>SO<sub>4</sub>-H<sub>2</sub>O SOLUTIONS

TEMPERATURE (°C)	MOLALITY OF UO <sub>2</sub> SO <sub>4</sub>	MOLE FRACTION OF UO <sub>2</sub> SO <sub>4</sub>	Δ <i>P</i> (mm Hg)
25	2.08967	0.0362816	0.749
30	2.08972	0.0362824	1.051
35	2.08977	0.0362833	1.377
40	2.08984	0.0362844	1.830
45	2.08993	0.0362859	2.384
50	2.09003	0.0362876	3.068
60	2.09032	0.0362925	4.916
70	2.09071	0.0362990	7.591
80	2.09122	0.0363075	11.909
90	2.09189	0.0363187	16.900
100	2.09273	0.0363328	23.587

# HRP QUARTERLY PROGRESS REPORT

## SOLUBILITY OF SILVER SULFATE IN 1.26 M AND 0.126 M URANYL SULFATE

E. V. Jones

The solubility of silver sulfate in 1.26 M and in 0.126 M  $\text{UO}_2\text{SO}_4$  has been studied by the silica tube method previously described;<sup>(7)</sup> the temperature coefficient of solubility is positive. The study in 0.126 M  $\text{UO}_2\text{SO}_4$  was limited to temperatures below 140°C because a reversible reaction occurred at about that temperature and yielded a reddish solid phase that is being investigated.

The data are given in Table 42 and are plotted in Fig. 67 along with the data of Seidell and Zemel<sup>(8)</sup> for the solubility of silver sulfate in water. If the logarithm of solubility is plotted against  $1/T$  (°A) the resultant slopes above 100°C give  $\Delta H_{\text{soln}}$  for the solid phases of +1.1, +2.3, and +3.7 kcal/mole in water, 0.126 M, and 1.26 M  $\text{UO}_2\text{SO}_4$ , respectively.

Table 42

### SOLUBILITY OF SILVER SULFATE IN URANYL SULFATE SOLUTIONS

IN 1.26 M $\text{UO}_2\text{SO}_4$		IN 0.126 M $\text{UO}_2\text{SO}_4$	
Temperature (°C)	$\text{Ag}_2\text{SO}_4$ (wt %)	Temperature (°C)	$\text{Ag}_2\text{SO}_4$ (wt %)
42.5	1.54	36.0	1.04
52.0	2.36	54.0	1.46
84.6	3.63	83.3	2.18
106.5	5.38	107.8	2.72
131.4	7.43	127.4	3.01
161.6	9.89	140.0	A red product formed
174.3	11.01		
197.1	12.82		
214.9	14.14		
237.5	15.75		
259.1	17.25		

(7) C. H. Secoy, *J. Am. Chem. Soc.* **72**, 3343 (1950).

(8) B. Zemel, *op. cit.*, ORNL-1057, p. 117.

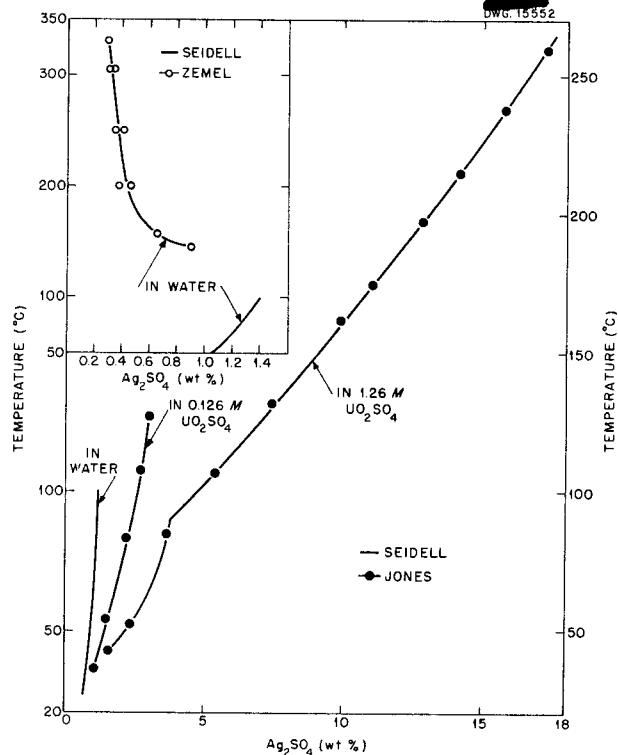


Fig. 67. Solubility of  $\text{Ag}_2\text{SO}_4$  in 1.26 and 0.126 M  $\text{UO}_2\text{SO}_4$  and in water.

### SOLUBILITY OF BARIUM SULFATE IN URANYL SULFATE SOLUTIONS AT 250°C

E. V. Jones J. S. Gill

Solubility data have been determined for barium sulfate in  $\text{H}_2\text{O}$  and in  $\text{UO}_2\text{SO}_4\text{-H}_2\text{O}$  solutions at 250°C by the filter-bomb method described in a previous report.<sup>(9)</sup> Zemel has obtained similar data for barium sulfate solubility in water as a function of temperature.<sup>(10)</sup> The two sets of data in water at 250°C disagree by a factor of approximately 10. No explanation of this difference is available at present.

The experimental data are given in Table 43. If these data are plotted

(9) C. H. Secoy, *Homogeneous Reactor Experiment Quarterly Progress Report for Period Ending August 31, 1950*, ORNL-826, p. 78.

(10) B. Zemel, *Homogeneous Reactor Experiment Quarterly Progress Report for Period Ending February 28, 1951*, ORNL-990, p. 105.

logarithmically against the square root of the molarity of the uranyl sulfate solution a straight line results, as shown by Fig. 68. This type of plot is similar to the Debye-Hückel characteristics in very dilute solution, namely, plots of the square root of the ionic strength vs. the log of the solubility. This increase in barium sulfate solubility is rather striking. For example, barium sulfate is 42 times more soluble in a 1.0 M  $UO_2SO_4$  solution than in water. The large solubility increase of most of the fission products in uranyl sulfate solution has been pointed out in previous quarterly reports.<sup>(11)</sup>

**Table 43**  
**SOLUBILITY OF BARIUM SULFATE IN URANYL SULFATE SOLUTION AT 250°C**

MOLARITY OF $UO_2SO_4$	MOLAR SOLUBILITY OF $BaSO_4 \times 10^5$
0.000	0.53
0.125	1.46
0.313	3.32
0.625	8.95
0.775	10.34
1.00	17.40
1.15	22.42
1.25	37.35

**SOLUBILITY OF URANIUM TRIOXIDE IN URANYL SULFATE SOLUTIONS AT 250°C**

J. S. Gill      E. V. Jones  
W. L. Marshall

Experimental data on the solubility of uranium trioxide above 100°C in uranyl sulfate solutions containing 20, 30, and 40 g of uranium per liter have been given in previous reports.<sup>(12,13)</sup>

These data were obtained in silica tubes by the synthetic method and indicated a solubility ratio for U to  $SO_4$  at 250°C of about 1.04. The data were erratic; therefore a more complete investigation was started beginning first at 25 and 100°C. The solubility of a uranium trioxide hydrate, which appears by analysis to be  $UO_3 \cdot \frac{1}{2}H_2O$ , in uranyl sulfate was

(11) E. V. Jones, *Homogeneous Reactor Experiment Quarterly Progress Report for Period Ending November 15, 1951*, ORNL-1221, p. 99.

(12) W. L. Marshall, J. S. Gill, and C. H. Secoy, *Chemistry Division Quarterly Progress Report for Period Ending March 31, 1950*, ORNL-685, p. 32.

(13) W. L. Marshall and J. S. Gill, *Chemistry Division Quarterly Progress Report for Period Ending December 31, 1950*, ORNL-1036, p. 13.

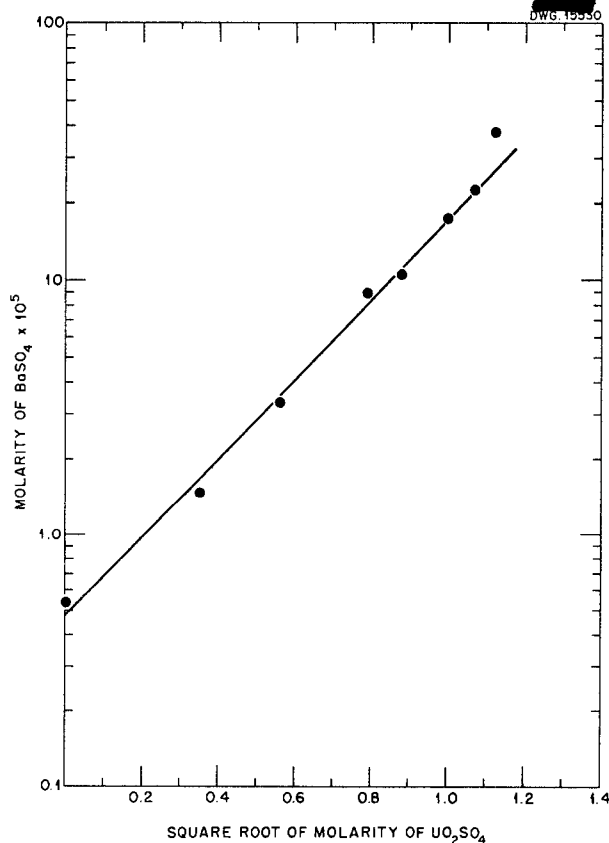


**Fig. 68. Solubility of  $BaSO_4$  in  $UO_2SO_4-H_2O$ .**

## HRP QUARTERLY PROGRESS REPORT

determined from low concentrations to above 50 wt % uranium in the uranyl sulfate solution, and solubility ratios of 1.40 and 1.36 at 25 and 100°C, respectively, were obtained.<sup>(14)</sup> This investigation was discontinued since, at that time, information about the low concentration solution required for the HRE was most urgent.

The consideration of different uranium concentrations for fuel media for production reactors and the development of a filter-bomb apparatus for filtering a solution from the solid phase at the equilibration temperature have supplied a motive for a further study of this system.

The apparatus in its present form has evolved from apparatus devised by Zemel and Stoughton of the Chemistry Division. Briefly, the titanium apparatus consists of two sections containing a sintered-platinum filter disk in the middle. The solution is equilibrated in the lower end of the unit either by rocking or by a magnetic mixer, depending on which of two types of apparatus is used. Thermostating is accomplished either by aluminum heating blocks or by a liquid salt bath. The solution is filtered from the solid phase by inverting the filter-bomb unit and cooling the lower end. Analyses are made for sulfate and uranium.

The solubility data given in Figs. 69 and 70 and in Table 44 show excess solubility of uranium trioxide in uranyl sulfate solutions at 250°C. The scatter of the data in Fig. 70 was probably the result of analytical difficulty at these low concentrations. The solid phase has been identified as a uranium trioxide hydrate. Analytical data indicated  $\text{UO}_3 \cdot \frac{1}{2}\text{H}_2\text{O}$  rather than

$\text{UO}_3 \cdot \text{H}_2\text{O}$  or  $\text{UO}_3 \cdot 2\text{H}_2\text{O}$ . The structure is the platelet type observed by Blomeke in his study of  $\text{UO}_3\text{-H}_2\text{O}$  slurries at 250°C.<sup>(15)</sup> Some of the uranium trioxide crystals in equilibration with  $\text{UO}_3\text{-UO}_2\text{SO}_4$  solutions are as much

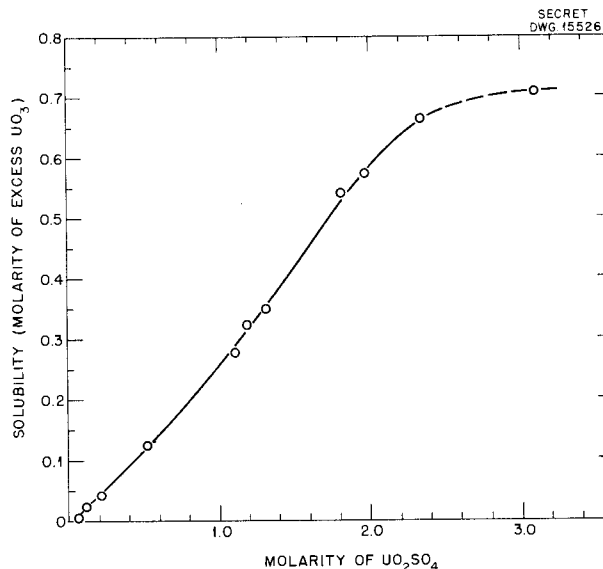


Fig. 69. Solubility of  $\text{UO}_3$  in  $\text{UO}_2\text{SO}_4\text{-H}_2\text{O}$  at 250°C. Molarity based on room temperature densities.

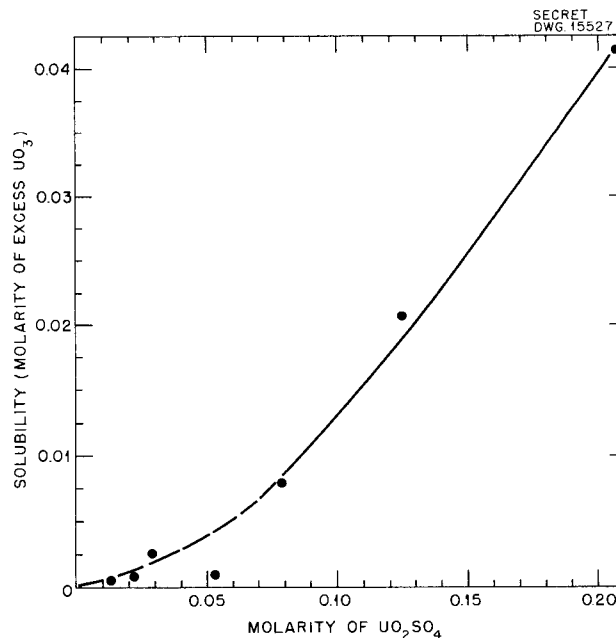


Fig. 70. Solubility of  $\text{UO}_3$  in  $\text{UO}_2\text{SO}_4\text{-H}_2\text{O}$  Solutions in Dilute Concentrations at 250°C.

(14) W. L. Marshall and J. S. Gill, *op. cit.*, ORNL-990, p. 134.

(15) F. R. Bruce, J. O. Blomeke, L. E. Morse, and J. P. McBride, *op. cit.*, ORNL-1221, p. 128.

Table 44

SOLUBILITY AND OTHER CHARACTERISTICS OF URANIUM TRIOXIDE IN  $UO_2SO_4-H_2O$  SOLUTIONS AT 250°C

Molarity based on room temperature densities

SAMPLE NO.	MIXING TIME AT 250°C (hr)	TOTAL URANIUM (M)	SO <sub>4</sub> (M)	URANIUM TRIOXIDE EXCESS SOLUBILITY (M)	TOTAL MOLE RATIO UO <sub>3</sub> :SO <sub>4</sub>	pH (at 25°C)	TEMPERATURE OF APPEARANCE OF TWO LIQUID PHASES (°C)
1	72	0.0134	0.0127	0.0004	1.06	3.80	
2	48	0.0228	0.0220	0.0008	1.04	3.40	
3	168	0.0323	0.0298	0.0025	1.08	3.50	
4	75	0.0525	0.0518	0.0007	1.01	3.31	
5	75	0.0869	0.079	0.0079	1.10	3.52	
6	78	0.1458	0.1251	0.0207	1.17	3.32	
7	48	0.2472	0.2059	0.0413	1.20	3.41	292.8 (?)
8	17	0.6529	0.5317	0.1212	1.23	3.20	271.5
9	78	1.381	1.106	0.275	1.25	2.90	265.7
10	78	1.506	1.185	0.321	1.27	2.91	
11	72	1.657	1.308	0.349	1.27	2.84	
12	17	2.352	1.812	0.540	1.30	2.66	267.5
13	36	2.542	1.970	0.572	1.29	2.65	
14	48	3.002	2.341	0.661	1.28	2.52	270.0
15	78	3.805	3.096	0.709	1.23	1.91	

FOR PERIOD ENDING JULY 1, 1952

## HRP QUARTERLY PROGRESS REPORT

as 3 mm on an edge, even though the original uranium trioxide is finely powdered.

In Fig. 71, the ratio  $UO_3$  to  $SO_4$  is plotted as a function of total uranium concentration. The solubility ratio decrease in dilute solution is apparent. For a time, it was thought that the ratio would decrease below 1.0 at concentrations below 10 g of uranium per liter, but judging from an inspection of Fig. 70, this does not appear to occur.

Synthetic solutions with the solubility ratios mentioned previously were rocked at 250°C for 72 hr in silica tubes. A slight, orange-yellow precipitate appeared after 24 hr and increased slowly during the remaining 48 hours. Upon cooling the tubes a rather abundant amount of the same orange-yellow precipitate appeared. The precipitate has been identified as uranyl silicate, which was observed previously in the study of  $UO_2F_2-H_2O$  in silica tubes.<sup>(16)</sup> It is believed now that the erratic nature of the data reported for uranyl sulfate solutions containing 20, 30, and 40 g of uranium per liter was caused by the silicate, which previously was not suspected to occur in the uranyl sulfate system in silica tubes.

The acidity data for the saturated solutions are given in Fig. 72 and compared with uranyl sulfate solutions containing a stoichiometric amount of sulfate. All acidities were determined at 25°C. The higher pH of the uranium trioxide saturated solution may account for the increased dissolution of silica into the solution, since silicon dioxide is known to be more soluble in alkaline media.

<sup>(16)</sup>W. L. Marshall and J. S. Gill, *Chemistry Division Quarterly Progress Report for Period Ending September 30, 1950*, ORNL-870, p. 25.

A similar solubility study at 175°C is in progress on the sulfate system. Future plans are first to make a similar study on the system  $UO_3-UO_2F_2-H_2O$  at 250 and 175°C, and then to attempt to define completely both the  $UO_3-UO_2SO_4-H_2O$  and fluoride systems at 250°C and lower temperatures.

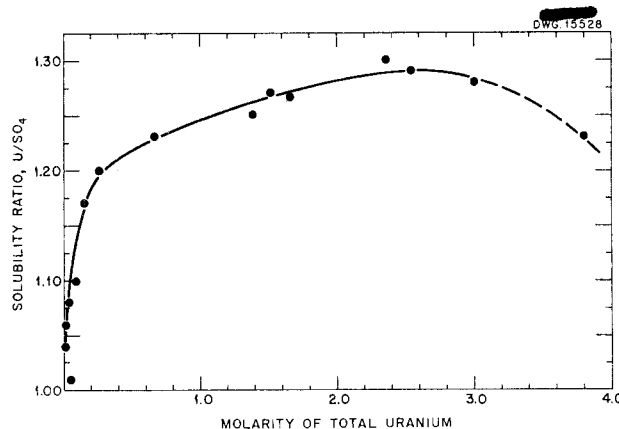


Fig. 71. Solubility Ratio of U to  $SO_4$  in  $UO_3-H_2SO_4-H_2O$  Solutions at 250°C.

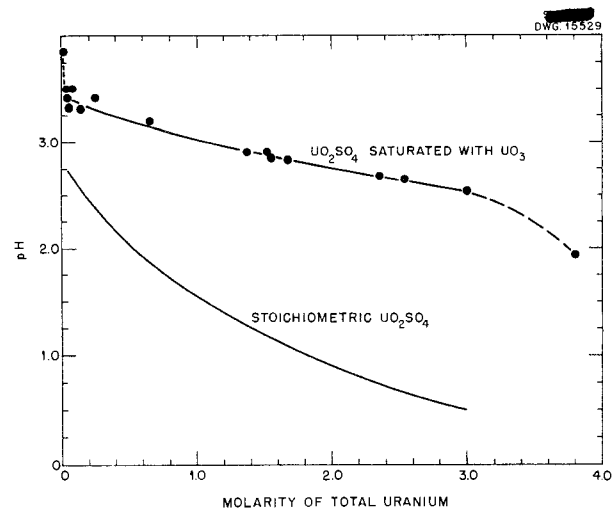


Fig. 72. Acidity of  $UO_2SO_4$  Solutions Saturated with  $UO_3$  at 250°C. Acidities measured at 25°C.

FURTHER STUDIES OF TWO-LIQUID PHASE  
TEMPERATURES FOR  $UO_3-UO_2SO_4-H_2O$   
SYSTEMS

E. V. Jones

The two-liquid phase transition temperatures were determined for uranyl sulfate solutions of various concentrations by use of the method previously described.<sup>(7)</sup> The U-to- $SO_4$  ratios were made 1.20 and 1.10 by adding  $UO_3$ .

One system with a U-to- $SO_4$  ratio of 1.20, including constant 0.02 M uranyl nitrate, was studied. The data are given in Tables 45, 46, and 47 and are plotted in Fig. 73 together with the curve for the Lietzke-Griess stoichiometric solution. As was previously observed, adding uranium trioxide lowered the two-liquid phase temperatures. It is interesting to note that the curves for  $U/SO_4 = 1.10$  and for  $U/SO_4 = 1.20$ , including 0.02 M  $UO_2(NO_3)_2$ , are almost identical.

Table 45

TWO-LIQUID PHASE TEMPERATURES FOR  
 $UO_3-UO_2SO_4-H_2O$  SOLUTIONS

$U/SO_4 = 1.10$

TEMPERATURE (°C)	TOTAL URANIUM (wt %)
291	7.14
282	9.23
281	11.19
279	15.63
279	19.51
279	25.93
279	31.04
279	35.20
283	38.65
290	40.69

EXPERIMENTS WITH HIGH-TEMPERATURE  
ELECTRODES

M. H. Lietzke

The work, previously described,<sup>(17)</sup> to develop a high-temperature reference electrode is being continued. Considerable difficulty has been experienced in setting up a Pb,  $PbSO_4$  electrode that, in combination with a Ag,  $Ag_2SO_4$  or Hg,  $Hg_2SO_4$  electrode, will give a potential that agrees with the value calculated from thermodynamic data. Although amalgams and sulfuric acid of different concentrations have been tried, the cell potentials that were measured with the lead electrodes combined with a Ag,  $Ag_2SO_4$  electrode have been at least 15 mv low. Both the Ag,  $Ag_2SO_4$  and Hg,  $Hg_2SO_4$  electrodes, however, seem to function properly and can be used as high-temperature reference electrodes in dilute  $H_2SO_4$ .

<sup>(17)</sup> M. H. Lietzke, *op. cit.*, ORNL-1280, p. 199.

Table 46

TWO-LIQUID PHASE TEMPERATURES FOR  
 $UO_3-UO_2SO_4-H_2O$  SOLUTIONS

$U/SO_4 = 1.20$

TEMPERATURE (°C)	TOTAL URANIUM (wt %)
Above 338	1.40
Above 322	2.76
290	6.55
281	12.07
277	16.78
278	24.39
277	30.28
277	34.97
279	38.80
286	41.98
290	44.03

# HRP QUARTERLY PROGRESS REPORT

Table 47

**TWO-LIQUID PHASE TEMPERATURES FOR  $UO_3$ - $UO_2SO_4$ - $H_2O$  SOLUTIONS CONTAINING  $0.02 M UO_2(NO_3)_2$**   
 $U/SO_4 = 1.20$

TEMPERATURE (°C)	TOTAL URANIUM (wt %)
293	6.52
279	12.02
280	16.72
279	30.20
279	34.89
283	40.38
293	44.24

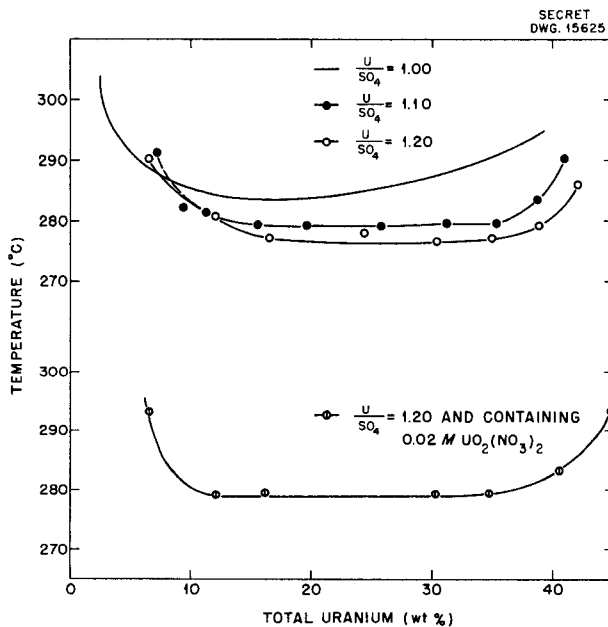


Fig. 73. Two-Liquid Phase Temperature Curves for the  $UO_3$ - $UO_2SO_4$ - $H_2O$  System.

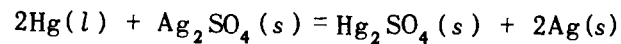
solutions. Also, the  $Ag, Ag_2SO_4$  electrode can be used as a reference electrode in  $UO_2SO_4$  solution.

Experiments at temperatures from 25 to 70°C indicated that the  $Ag, Ag_2SO_4$  and  $Hg, Hg_2SO_4$  electrodes in  $H_2SO_4$  must be allowed to stand several days before equilibrium potentials are ob-

tained. Over the temperature range indicated, the slope of the potential vs. temperature plot is -0.345 mv/deg. Since  $dE/dT = \Delta S/nF$ , the value of  $\Delta S$  for the cell reaction can be calculated. From the slope,

$$\Delta S = \frac{2(96,500)(-0.345)}{(4.1833)(1000)} = -16.2 \text{ e.u.}$$

This corresponds to the average value of  $\Delta S$  for the reaction



over the temperature range 25 to 70°C. The value for  $\Delta S$  computed from individual entropies given in Latimer's tables<sup>(18)</sup> is -16.4 e.u. Therefore the two values are in very good agreement, and the electrodes seem to be functioning properly. In future work the high-temperature behavior of these electrodes will be studied, and the value of  $\Delta S$  for the cell reaction will be obtained as a function of temperature.

A series of experiments has been performed in which the potential of the passive film produced on stainless steel by 1%  $HNO_3$  was measured against the  $Ag, Ag_2SO_4$  electrode in 0.13 f  $UO_2SO_4$  solution. As long as the film was intact and the uranyl sulfate solution was unreduced, the potential of the film was positive or, at most, 50 to 100 mv negative with respect to the  $Ag, Ag_2SO_4$  electrode. However, when the film went bad and the uranyl sulfate solution was reduced, the potential of the steel vs. the  $Ag, Ag_2SO_4$  electrode was -200 to -400 millivolts. Thus it was easy to discern when the change occurred, since the latter shift in potential was rather abrupt. These experiments demonstrated the use of the  $Ag, Ag_2SO_4$  electrode as a reference electrode in  $UO_2SO_4$  solution at high temperature.

(18) W. M. Latimer, *Oxidation Potentials* (new edition to be published soon).

STATIC CORROSION TESTS OF ALTERNATE SYSTEMS

E. G. Bohlmann, Section Chief  
J. L. English S. H. Wheeler

CORROSION OF TITANIUM IN  
URANYL SULFATE SOLUTIONS

Static corrosion tests are in operation to determine the long-time effect of exposure in uranyl sulfate solutions at 250°C on the tensile properties of commercial titanium metal. The tensile test specimens were machined from 1.270-cm-dia, hot-rolled and annealed, titanium bar supplied by the Allegheny Ludlum Steel Co. Duplicate specimens have been exposed in uranyl sulfate solutions containing 40 and 300 g of uranium per liter for 20 weeks at 250°C. The sulfate solutions were pressurized with approximately 150 psia of oxygen obtained from the thermal decomposition of calculated quantities of hydrogen peroxide added at room temperature.

The tests were run in type 347 stainless steel autoclaves that were pickled in 10% HNO<sub>3</sub>-4% HF solution at 60°C before the start of the experiments. The volume of uranyl sulfate solution used in each autoclave was 150 ml. No attempt was made to insulate the titanium test bars from the containers. The bars and solutions were examined every two weeks, at which time 10 ml of solution was removed from each test for analytical purposes and the hydrogen peroxide content necessary to generate the desired oxygen partial pressure was renewed. The tests will operate for a period of 24 weeks, after which time they will be subjected to a tensile test. The values obtained on the specimens will be compared with tensile-strength properties of unexposed titanium test bars.

Corrosion data were collected on the specimens during the course of the

tests. The bars exposed to uranyl sulfate containing 40 g of uranium per liter exhibited an extremely lustrous, pale-blue color. One specimen showed a cumulative weight increase after 20 weeks of 0.017 mg/cm<sup>2</sup>; the duplicate sample lost 0.006 mg/cm<sup>2</sup> during this time. No other visible signs of corrosion damage were evident. An estimate of the extent of corrosion attack on the type 347 stainless steel autoclave was made from the cumulative dissolved nickel content (31 ppm) in the sulfate solution. Assuming the stainless steel to contain an average of 10.5% nickel, the corrosion rate on the autoclave was 0.03 mpy at the end of 20 weeks. This rate, of course, assumes that corrosion attack was uniform on all surfaces.

The tensile bars exposed in the uranyl sulfate solution containing 300 g of uranium per liter were a shiny, pale-violet color. No other indications of the effect of exposure were apparent. The cumulative weight losses on the specimens after 20 weeks were identical, that is, 0.054 mg/cm<sup>2</sup>, which corresponds to a rather insignificant corrosion rate of 0.01 mpy. The corrosion rate on the walls of the stainless steel container after 20 weeks was calculated from the dissolved nickel content of 170 ppm to be 0.2 mpy.

URANYL FLUORIDE CORROSION STUDIES

Work continued during the past quarter on the study of uranyl fluoride systems at temperatures of 100 and 250°C. The solutions contained 40, 100, and 300 g of uranium per liter. The results of various investigations appear in the following paragraphs.

## HRP QUARTERLY PROGRESS REPORT

The effect of uranium and oxygen concentration on the corrosion of type 347 stainless steel at 250°C was examined. These tests were duplicates of the uranyl sulfate tests described in a previous section of this report. Uranyl fluoride solutions containing 100 and 300 g of uranium per liter were contained in newly machined, type 347 stainless steel autoclaves. The oxygen partial pressures included in the tests were 25, 75, 150, and 500 psia at 250°C. These partial pressures resulted from the addition of hydrogen peroxide to the solutions at room temperature in amounts estimated to produce the desired oxygen pressures at 250°C by decomposition of the peroxide. The hydrogen peroxide supply was renewed weekly.

A solution volume of 150 ml of the fluoride was used for each test. Duplicate tests were operated for each set of test conditions. The total exposure period was 11 weeks.

The estimated dissolved oxygen content at 250°C with the various oxygen partial pressures are reported in Table 48 for the two uranyl fluoride

solutions. The uranium concentrations in grams per liter of solution and the pH of the solutions at the start of the tests are also given in Table 48.

As in the case of the uranyl sulfate corrosion tests, the type 347 stainless steel test specimens were characterized by the formation of bulk oxide films that ranged from light gray to dull black in color after 11 weeks of exposure. The as-removed weights of these specimens were of little value for determining the real extent of corrosion damage. It was observed also at the completion of the tests that the cumulative dissolved nickel content in the fluoride solutions was not a reliable criterion for evaluation of corrosion attack. There was no consistent agreement between corrosion rates obtained from the defilmed weight losses and the rates determined by the dissolved nickel method. The latter rates were considerably lower in magnitude, in most cases, than the rates calculated from the defilmed weight losses. The defilming technique used on the specimens consisted of cathodic cleaning in 5 wt % sulfuric acid containing an organic inhibitor at 75°C.

Table 48

ESTIMATED DISSOLVED OXYGEN CONTENT PRODUCED BY THE DECOMPOSITION OF HYDROGEN PEROXIDE AT 250°C IN URANYL FLUORIDE SOLUTIONS

	URANYL FLUORIDE SOLUTION	
	Solution 1	Solution 2
Initial pH	2.76	2.21
Actual uranium (g/l)	98.3	307.5
Dissolved oxygen (ppm)		
at 25 psia	125	100
at 75 psia	400	330
at 150 psia	800	660
at 500 psia	2700	2200

FOR PERIOD ENDING JULY 1, 1952

The time required for defilming was usually 3 minutes. A comparison between the corrosion rates calculated by defilmed weight losses and final dissolved nickel concentrations appears in Table 49.

In only two cases, 98.3 g of uranium per liter with 400 and 800 ppm of dissolved oxygen, was there any semblance of agreement in the values obtained by the two methods, that is, the solutions containing 400 and 800 ppm of dissolved oxygen and 98.3 g of uranium per liter. Correlation was extremely poor in the majority of tests. This could be attributed to the nickel solubility behavior.

Several facts were apparent from the corrosion rates determined by the defilmed weight losses. In the solutions containing 98.3 g of uranium per liter, the minimum corrosion rates were obtained in the presence of dissolved oxygen concentrations between 400 and 800 ppm. Rates were higher

by a factor of 2 in the solutions with 125 ppm of dissolved oxygen and higher by a factor of nearly 9 in the solutions with 2700 ppm of dissolved oxygen. The intensity of corrosion attack by the solutions containing 307.5 g of uranium per liter was noticeably suppressed as the dissolved oxygen content was increased from 100 to 2200 ppm. The reduction in the 11-week corrosion rate was from an average value of 16.6 mpy in the lower oxygen range to an average of 0.7 mpy with approximately 2200 ppm of oxygen present in the solutions.

The comparative corrosiveness of uranyl sulfate and uranyl fluoride solutions containing 100 and 300 g of uranium per liter at 250°C with various dissolved oxygen concentrations is shown in Table 50. The test conditions were identical for each medium and corrosion rates were determined from the average defilmed weight losses on type 347 stainless steel specimens after 11 weeks.

Table 49

A COMPARISON BETWEEN DEFILMED AND CUMULATIVE DISSOLVED NICKEL CORROSION RATES ON TYPE 347 STAINLESS STEEL EXPOSED IN OXYGENATED URANYL FLUORIDE SOLUTIONS AT 250°C FOR 11 WEEKS

URANIUM (g/l)	DISSOLVED OXYGEN (ppm)	CORROSION RATE (mpy)			
		By weight loss		By dissolved nickel	
		Specimen 1	Specimen 2	Specimen 1	Specimen 2
98.3	125	0.48	0.62	0.10	0.09
	400	0.21	0.42	0.22	0.12
	800	0.12	0.32	0.37	0.33
	2700	1.76	2.70	0.49	0.46
307.5	100	15.33	17.87	3.08	3.00
	330	6.70	7.32	0.57	0.81
	660	2.13	2.27	0.62	0.68
	2200	0.66	0.77	1.16	0.90

# HRP QUARTERLY PROGRESS REPORT

**Table 50**

**AVERAGE CORROSION RATES DETERMINED BY DEFILMED WEIGHT LOSSES ON TYPE 347 STAINLESS STEEL EXPOSED 11 WEEKS IN OXYGENATED URANYL SULFATE AND FLUORIDE SOLUTIONS AT 250°C**

APPROXIMATE URANIUM CONTENT (g/l)	DISSOLVED OXYGEN (ppm)	CORROSION RATE (mpy)	
		In UO <sub>2</sub> SO <sub>4</sub>	In UO <sub>2</sub> F <sub>2</sub>
100	125	0.16	0.55
	375 to 400	0.21	0.32
	750 to 800	0.28	0.22
	2500 to 2700	0.23	2.23
300	100		16.60
	300 to 330	0.25	7.01
	600 to 660	0.30	2.20
	2000 to 2200	0.29	0.72

With the exception of the solutions containing 100 g of uranium per liter with 375 to 800 ppm of dissolved oxygen, the uranyl fluoride solutions appeared more corrosive than the sulfate solutions by a factor of 3 to 30, depending upon the specific static test conditions. This comparison does not include the solutions containing 300 g of uranium per liter with low oxygen content, since a stable system could not be maintained in the sulfate solutions with these conditions.

Welded specimens of type 347 stainless steel to types 304, 309 niobium-stabilized, and 316 stainless steels were prepared for exposure in uranyl fluoride solution containing 40 g of uranium per liter with an estimated dissolved oxygen content of 800 ppm at 250°C. Hydrogen peroxide additions to the test solutions were used to generate the desired oxygen concentration. The welds were made by a heliarc process with niobium-stabi-

lized, type 347 stainless steel, weld rod for joining the dissimilar alloys. Close examination of the weld and adjacent areas was made weekly. After 12 weeks, there were no signs of preferential or intergranular corrosion attack on any of the stainless steels.

A study was made with similar types of welded specimens to determine the degree of nobility of the individual stainless alloys under conditions in which reduction of the uranyl fluoride solutions took place. Uranyl fluoride solutions containing 300 g of uranium per liter and no source of excess oxygen were used in the tests. After one week at 250°C, during which time solution reduction occurred, it was found that types 304 and 316 stainless steels welded to type 347 stainless steel underwent severe preferential attack, whereas type 347 stainless steel was preferentially attacked when welded to type 309 niobium-stabilized stainless steel.

## FOR PERIOD ENDING JULY 1, 1952

Miscellaneous corrosion studies with uranyl fluoride solutions are summarized in the following:

1. Wrought and sand-cast specimens of type 347 stainless steel were exposed in uranyl fluoride solutions containing 40 g of uranium per liter at boiling temperature for a period of 11 weeks. The corrosion resistance of the wrought specimen was slightly superior to that of cast type 347 stainless steel. The final corrosion rate on the wrought specimen was 0.03 mpy as compared with a rate of 0.13 mpy for the sand-cast material.

2. The corrosion rate for Stellite 98M2 bearing material was slightly less than 1 mpy after 12 weeks in uranyl fluoride solution containing 40 g of uranium per liter at 100°C. The corrosion resistance of this material was determined also in uranyl fluoride solutions containing 300 g of uranium per liter at 100°C with and without aeration. Deaeration did not materially affect the corrosion resistance; the corrosion rate in the oxygen-deficient system was 26.4 mpy after 7.7 weeks

as compared with a rate of 21.8 mpy for the same period of time in an aerated solution.

3. An effect of aeration was found in the case of Inconel exposed in uranyl fluoride solutions containing 300 g of uranium per liter at boiling temperature. Without aeration, the corrosion rate was 25.6 mpy for eight weeks as compared with 82.5 mpy in air-aerated solutions for a similar period. In uranyl sulfate solutions containing 300 g of uranium per liter at boiling temperature, the effect of aeration was not very pronounced on the corrosion of Inconel. With aeration, a corrosion rate of 0.5 mpy was observed after eight weeks; in the absence of aeration, the corrosion rate was 1.2 mpy in eight weeks.

4. Nickel, D nickel and Monel were found completely unsatisfactory for use in uranyl fluoride solutions containing 300 g of uranium per liter with approximately 2200 ppm of dissolved oxygen (by hydrogen peroxide decomposition) at 250°C. The specimens exhibited heavy weight gains and severe pitting attack after one week of test.

---

### METALLURGY

E. C. Miller, Group Leader  
W. J. Leonard      A. R. Olsen  
W. J. Fretague      F. J. Lambert  
R. G. Berggren

In the preceding quarterly report<sup>(1)</sup> the metallurgical problems of the project were reviewed and the proposed program was outlined. Progress since then on some phases of the work has been limited because of lack of manpower, but additional technical personnel have been assigned to the

project and the work is now being accelerated.

### CORROSION METALLURGY

A. R. Olsen, REED

Metallurgical assistance was provided for the corrosion studies. Details of sample preparation are

<sup>(1)</sup>E. C. Miller and A. R. Olsen, *Homogeneous Reactor Project Quarterly Progress Report for Period Ending March 15, 1952*, ORNL-1280, p. 203-208.

## HRP QUARTERLY PROGRESS REPORT

described in the report of the corrosion group (cf., "Dynamic Corrosion and Solution Stability," this report).

### SPECIFICATIONS AND FABRICATION

W. J. Leonard      A. R. Olsen

Because of the encouraging welding data, reported in the last quarterly report, and the progress on titanium riveting, a program was established to develop techniques for assembly of a titanium impeller for a Westinghouse Model 100A pump.

The test assemblies shown in Fig. 74 were designed to compare riveting and welding that might be used on the impeller. Riveting was first attempted by Bomar of the Metallurgy Division by furnace heating the parts and attempting to transfer them to the hydraulic press quickly enough to perform the upsetting before the material cooled below the minimum forging temperature of 1300°F. Difficulties were encountered because of the rapid cooling of the rivet end to be upset when it came in contact with the cold press head. It was then decided to heat the rivets by resistance heating while in the press. Four

riveted assemblies were made by using a small, portable, spot welder attached to the heads of the hydraulic press. The resulting assemblies provided the mechanical test data reported in Table 51. More controlled tests using the recently installed spot-welding machine for both heating and pressing are planned.

The welding test assemblies were fabricated in the dry box under the direction of Patriarca of the Metallurgy Division. All welds were made in a highly pure helium atmosphere (99.99%) with a current of  $48 \pm 2$  amp at 12 volts. The initial pass was a fusion pass of the RC-70 base material, whereas the remaining passes were made with the addition of Ti-75A welding rod (the only kind available). In both the riveting and the welding tests, the assemblies were machined from a 1-in.-thick plate of titanium, type RC-70, with a reported carbon content of 0.23%.

The data reported in Table 51 are encouraging. It appears that a titanium impeller can be fabricated with either welded or riveted fastenings provided the imposed load in operation is purely tensile. Certain reservations must be made with reference to the specific application, however, since a straight tensile test does not simulate the dynamic stressing of a pump impeller. In the impeller, the fastenings will probably be subjected to shearing stresses, repetitive stress reversals, and some shock loading. In addition, the available materials for impeller fabrication, although of type RC-70 titanium, have carbon analyses of 0.32 and 0.3%. Experience reported in the literature indicates that welds in material containing more than 0.25% carbon will probably be brittle.

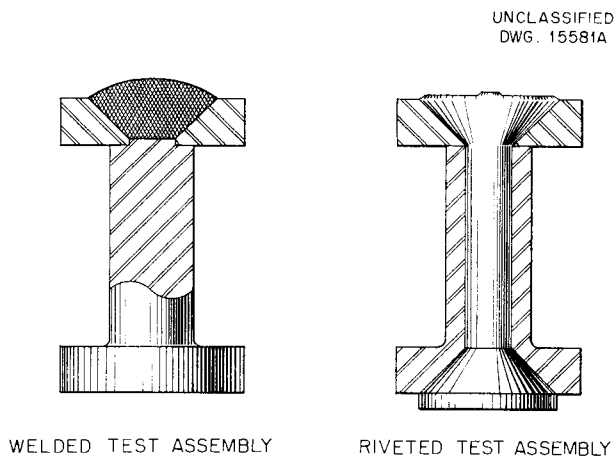


Fig. 74. Sectional Views of Riveted and Welded Titanium Test Assemblies.

It thus appears that the most satisfactory assembly procedure for

Table 51

TENSILE TESTS ON BOTH RIVETED AND WELDED ASSEMBLIES  
SIMULATING PUMP IMPELLER FABRICATION

TEST NO.	TEST TYPE	MAXIMUM LOAD (lb)	ELONGATION (%)	LOCATION OF FRACTURE
1	Rivet	2450	18	Approximately in the center of the rivet
2	Rivet	2700	18	Approximately in the center of the rivet
3	Rivet	2600	18	Approximately in the center of the rivet
4	Rivet	2400	18	Approximately in the center of the rivet
5	Weld	3500		Immediately below the end plate
6*	Weld	6260		Immediately below the end plate
7	Weld	8260		Immediately below the end plate
8	Weld	7600		Immediately below the end plate
9	Weld	8300		Immediately below the end plate

\*Unlike the other welded samples this assembly had the 1/32-in.-high 5/32-in.-dia plateau removed before welding.

use with the available material is riveting. However, the weld strengths are such that, at an admittedly greater risk (considering the material available), an all-welded impeller of reduced cost is a definite possibility.

PROPERTIES OF TITANIUM

W. J. Fretague

The program for determining the properties of titanium includes:

1. transition-temperature studies of arc-melted iodide titanium and commercially pure titanium type 75A,

2. studies of the effect of hydrogen on the impact properties of the material,
3. exposure of impact specimens to conditions encountered in dynamic corrosion test loops prior to impact testing,
4. exposure of impact specimens in static corrosion test apparatus with and without radiation prior to impact testing.

**Transition Temperature Investigations.** In investigating the transition temperature of titanium, impact specimens, 0.204 in. dia by 10 3/4 in. long, notched every inch of their

## HRP QUARTERLY PROGRESS REPORT

length to a depth of 0.020 in. will be used. This type of specimen permits ten individual or impact breaks on each specimen and, from the standpoint of economy of specimen material, represents the optimum specimen size employed to date. It is identical with the specimen used by the Solid State group for irradiated materials. This permits the use of the impact testing equipment developed by the Solid State Division.

In the impact testing equipment the specimen is clamped vertically in the specimen vise with the center of the specimen notch even with the top surface of the vise. A suitable liquid medium is used to cool the specimen while in the vise. The liquid level is maintained so the specimen notch is immersed at all times. A Leeds & Northrup, Micromax, Model C, indicator and controller, used in conjunction with a bank of infrared lamps, permits accurate control and measurement of the testing temperature in the range from approximately - 200°C to + 200°C. When the transition temperatures of the arc-melted swaged and annealed iodide titanium and the swaged and annealed titanium type 75A have been determined, impact specimens of both varieties of titanium will be heated in a hydrogen atmosphere and the amount of hydrogen absorbed measured. These specimens will be impact tested to determine the effect of hydrogen on the transition temperature. In conjunction with this portion of the program, specimens of arc-melted iodide titanium and titanium type 75A (swaged and annealed) will be vacuum annealed to remove hydrogen prior to impact testing. The effect of hydrogen removal on the transition temperature will be investigated. Specimens to which hydrogen will be added by making the specimen the cathode in an electrolytic cell will also be tested. Various electrolytes

will be employed and the effect of hydrogen addition by the various methods on the transition temperature will be noted.

Titanium impact specimens (principally type 75A) will be exposed in dynamic corrosion test loops prior to impact testing. It is hoped that valuable information on the effects of temperature, solution concentrations, solution velocity, oxygen and hydrogen gas content of solution, etc., on the impact properties of titanium will be obtained.

Static corrosion tests in various media will be made on impact specimens of titanium prior to impact testing. Eventually inpile corrosion tests are planned, but the initial specimens will not be subjected to radiation.

**Preparation of Materials for Impact Specimens.** A 50-g melt of iodide titanium has been prepared and swaged to 0.243-in. dia rod. There is sufficient material for one 0.204-in.-dia by 10 3/4-in.-long impact specimen. Two 1 5/8-in. pieces of this material have been submitted to the x-ray laboratory for determination of the textures obtained by swaging, and by swaging and annealing (vacuum annealed at 500°C for 1 hr and furnace cooled).

Approximately 2 ft of 1-in.-dia titanium type 75A bar (Item No. 24, heat No. L782, annealed and pickled) was cold swaged to 0.238-in.-dia rod. A 5-in.-long piece of this same material was cut off the original bar prior to swaging to be used for rolling tests. Sufficient swaged material for thirty-six 10 3/4-in.-long impact specimens was obtained. These rods will be sand blasted, to remove any scale picked up during swaging, pickled, and vacuum annealed at approximately 500°C for 1 hr and furnace cooled. A similar annealing treatment

## FOR PERIOD ENDING JULY 1, 1952

will be performed on the swaged iodide-titanium rod. After annealing, the rods will be submitted to the Research Shops for machining in 0.204-in.-dia by 10 3/4-in. long impact specimens. These specimens will be available for the experiments outlined.

### NONDESTRUCTIVE TESTING

F. J. Lambert, Y-12

The nondestructive testing group of the Y-12 Research Engineering Department received a reflectoscope during this quarter and is training personnel in its use and application.

Two Audigages have been purchased, and delivery will be made in the latter part of June. One instrument operates in a high-frequency range and will be used on heavy gage materials in an effort to determine the progress of corrosion. The other instrument, which will operate at a lower frequency range, will be better suited for lighter gage material.

A Zyglo testing unit has been purchased and delivery is expected in July. The Zyglo unit will be installed in the Y-12 Machine Shop and operated by the nondestructive testing group to reveal surface defects on heat-treated parts, welds, forgings, and castings.

During the month of May, visits were made to the Bureau of Mines Stations at Amarillo, Texas, and College Park, Maryland, to obtain

information on the welding of titanium. As a result of these visits, specially constructed dry boxes are being fabricated for titanium welding.

Radiographic services have continued as usual during this quarter.

### RADIATION DAMAGE STUDIES

J. C. Wilson      R. G. Berggren, SSD

Work has progressed in the study of the effect of irradiation on the impact strength of materials of interest in the HRP.

A sample of normalized SAE 1040 steel has been irradiated in a donut hole of the X-10 graphite reactor for a period of four weeks, and a second sample of normalized SAE 1040 steel is now being irradiated in the same position for a period of nine weeks. Samples of normalized SAE 1040 steel and type 304 ELC stainless steel are being prepared for irradiation in the LITR. These will probably be exposed in a vertical beryllium piece in the LITR.

Impact testing of the steel samples now available is awaiting completion of revisions to the remotely controlled impact machine. Revisions to the machine include an improved specimen clamp and facilities for conducting the tests at temperatures ranging from approximately -200°C to +200°C. These revisions are about three-fourths completed and trial runs are expected to be started in three weeks.

# HRP QUARTERLY PROGRESS REPORT

## CHEMICAL PROCESSING

F. R. Bruce, Section Chief  
D. E. Ferguson, R. G. Mansfield  
G. I. Cathers, W. E. Tomlin

The development of chemical processing for a plutonium-producing reactor using uranyl sulfate as the fuel solution has progressed to the point of obtaining a reliable tributyl phosphate extraction flowsheet. The effort this past quarter has been directed toward improving this flowsheet, evaluating fluoride distillation as an alternate method of uranium decontamination, and further studying the chemical behavior of plutonium in a uranyl sulfate solution in a reactor.

### PLUTONIUM CHEMISTRY

In order to establish the optimum method of chemical processing for an aqueous-solution, homogeneous, plutonium producing reactor, it is necessary to know the chemical behavior of plutonium in such a reactor. The present data indicate that in a reactor using uranyl sulfate solution as the fuel and operating at either 250 or 100°C there will be precipitation of plutonium. It is the purpose of this study to establish the amount of plutonium that will remain in solution in the reactor under operating conditions, to determine what will happen to the plutonium that does not remain in solution, and to seek methods of controlling the chemical behavior of plutonium in the reactor.

It has been previously reported that the solubility of tetravalent plutonium in 1 M  $\text{UO}_2\text{SO}_4$  is only 0.003 mg/ml at 250°C. When a solution of uranyl sulfate containing more than this concentration of tetravalent plutonium is heated to 250°C, the plutonium precipitates as  $\text{PuO}_2$ . This precipitation is essentially complete

in 12 hours. It has also been reported that a partial pressure of oxygen of 200 psi will stabilize the soluble hexavalent plutonium in uranyl sulfate solution at 250°C but that in the absence of oxygen, hexavalent plutonium is rapidly reduced to the insoluble tetravalent state. It was also found that a partial pressure of oxygen would not reverse the precipitation of tetravalent plutonium.

**Effect of Varying Oxygen Pressure on the Behavior of Hexavalent Plutonium at 250°C.** The results of experiments conducted at 250°C indicate that hexavalent plutonium in 1 M uranyl sulfate solution is stabilized by partial pressures of oxygen as low as 40 psi. At 20 psi, the results are contradictory. In one experiment at 20 psi, hexavalent plutonium was almost completely reduced, whereas in a duplicate experiment the amount of hexavalent plutonium reduced was not different from that observed at higher oxygen pressures (Table 52). These results were obtained by heating 5-ml portions of a 1 M uranyl sulfate solution in pyrex tubes with a capillary opening for 48 hr in an autoclave under various oxygen pressures.

**Effect of Plutonium Concentration on the Behavior of Plutonium in 1 M Uranyl Sulfate Solutions.** The results of experiments conducted at various plutonium concentrations indicate that an equilibrium exists between hexavalent plutonium and tetravalent plutonium in solution. When 1 M uranyl sulfate solutions containing more than 0.1 mg of plutonium(VI) per milliliter were heated for 48 hr under 200 psi of oxygen, the hexavalent plutonium was

Table 52

## EFFECT OF OXYGEN PRESSURE ON THE BEHAVIOR OF PLUTONIUM AT 250°C

Starting solution: 1 M UO<sub>2</sub>SO<sub>4</sub>

Solutions kept at 250°C for 48 hr under indicated oxygen pressures

OXYGEN PRESSURE (psi)	CONDITIONS	Pu(VI) (%)	Pu(IV) (%)	WEIGHT OF Pu(VI) IN SOLUTION (mg)
200	Before heating	79	21	0.984
	After heating	97	3	0.780
100	Before heating	93	7	1.133
	After heating	97	3	0.798
40	Before heating	88	12	1.047
	After heating	92	8	0.540
20	Before heating	84	16	1.041
	After heating	95	5	0.541
20	Before heating	61	39	0.719
	After heating	77	23	0.080

observed to be partly reduced. Under the same conditions, but with an initial plutonium(VI) concentration of 0.05 mg/ml, significant oxidation of plutonium(IV) to plutonium(VI) was observed. In all cases the final ratio of hexavalent to tetravalent plutonium (Table 53) was about 33:1.

Experiments with longer heating periods will be required to establish the exact equilibrium concentrations; however, based on present data the final concentrations under the above conditions will be 0.003 mg of plutonium(IV) and about 0.10 mg of plutonium(VI) per milliliter.

**Solubility of Tetravalent Plutonium in 1 M Uranyl Sulfate Solution at 100°C.**  
The solubility of tetravalent plutonium in 1 M uranyl sulfate at 100°C was

found to be about 0.010 mg/ml, compared with 0.003 mg/ml at 250°C. The rate of hydrolysis and precipitation of plutonium(IV) is slower at 100°C than at 250°C. The reaction is essentially complete in 12 hr at 250°C and was observed to be only 90% complete at the end of 48 hr at 100°C.

**Adsorption of Plutonium on Stainless Steel.** It was found that as much as 1.7 mg of plutonium per square inch of type 347 stainless steel will be adsorbed at 250°C from 1 M uranyl sulfate solution containing approximately 0.24 mg of plutonium per milliliter. The following procedure was used to determine plutonium adsorption in a reactor.

A solution containing 0.24 mg of plutonium per milliliter in 1 M UO<sub>2</sub>SO<sub>4</sub>

# HRP QUARTERLY PROGRESS REPORT

Table 53

## EFFECT OF PLUTONIUM CONCENTRATION ON PLUTONIUM BEHAVIOR IN 1 M URANYL SULFATE SOLUTION

Temperature: 250°C  
 Heating time: 48 hr  
 Oxygen pressure: 200 psi

CONDITIONS	CONCENTRATION OF Pu(VI) (mg/ml)	CONCENTRATION OF Pu(IV) (mg/ml)	Pu(VI) (%)	Pu(IV) (%)
Before heating	0.475	0.514	48	52
After heating	0.313	0.010	97	3
Before heating	0.275	0.311	47	53
After heating	0.157	0.005	97	3
Before heating	0.176	0.198	47	53
After heating	0.127	0.004	97	3
Before heating	0.087	0.102	46	54
After heating	0.067	0.002	97	3
Before heating	0.040	0.058	41	59
After heating	0.061	0.001	98	2

was prepared. The plutonium was 90% Pu(VI)-10% Pu(IV). Five milliliters of the solution was placed in a series of tubes, each of which contained a piece of pretreated type 347 stainless steel. The steel was pretreated by heating for 24 hr at 250°C in a 1 M UO<sub>2</sub>SO<sub>4</sub> solution under a pressure of 200 psi of oxygen. The tubes were placed in an autoclave under an oxygen pressure of 200 psi and heated to 250°C for 48 hours. At the end of the heating period the steel was removed and rinsed with distilled water. The steel was then dissolved in aqua regia, and after centrifuging the residue was treated twice with ammonium hexanitrate cerate in 6 N nitric acid.

An adsorption value of 1.7 mg of plutonium per square inch of steel was obtained from the amount of plutonium contained in these solutions and the area of the steel. This amount of adsorption would result in 175 g of plutonium being held up on the surface of a 15-ft-dia spherical core.

### SOLVENT EXTRACTION

Solvent extraction studies this quarter have been limited to a study of the extraction of neptunium by tributyl phosphate under Purex process conditions, scouting experiments to evaluate alternate solvents, and a study of radiation decomposition of

the solvent mixture proposed for homogeneous chemical processing by tributyl phosphate extraction.

**Extraction of Neptunium by Tributyl Phosphate.** It has been reported that a cooling period of at least 45 days was necessary to obtain adequate decontamination of uranium and plutonium by TBP extraction from  $\text{Np}^{239}$  activity. Based on more recent distribution data, adequate separation from neptunium may be obtained after only 35 days of cooling.

In making this study of neptunium extraction, the behavior of the various stable oxidation states of neptunium in the Purex process has been investigated. Countercurrent batch extractions simulating Purex 1A column conditions were carried out first with feed solutions containing  $\text{Np}^{239}$  tracer prepared by neutron irradiation of normal uranium trioxide. A thenoyl trifluoroacetone extraction method was used to isolate neptunium. Since results of extraction experiments carried out with this tracer material were somewhat erratic, it was thought that a trace of TTA might be carried along with the tracer. To eliminate the possibility of such impurities,  $\text{Np}^{239}$  tracer was prepared by irradiating uranium that contained only 0.03%  $\text{U}^{235}$ . This material was used without chemical separation in the following studies.

*Behavior of Neptunium(VI) and Neptunium(IV) in the Purex Process.* Feed solutions containing neptunium tracer at an activity level of about  $10^7$  beta counts/min/ml were prepared. In one solution the neptunium was reduced to the IV state by addition of ferrous sulfamate to a final concentration of 0.05 M; in the other the VI state was produced by addition of potassium dichromate in slight excess. Results of the extraction experiments

showed that the neptunium was completely extracted by TBP-Amsco when present in these oxidation states. Since it was desired to put the neptunium in a nonextractable form, no further work was done on the IV or VI valence forms.

*Neptunium(V).* Neptunium(V) is the most stable form of the element in aqueous nitric acid solution. The pentavalent state is produced instantaneously by reduction of the hexavalent state with nitrite. It is also possible to prepare neptunium(V) by oxidizing the tetravalent state with nitrite in nitrate solutions, but this may not be effective in a sulfate system.

It was found that under flowsheet conditions a decontamination factor of 100 for neptunium could be obtained from neptunium(V) in the Purex 1A column. When uranium was omitted from the feed, which would simulate second plutonium cycle conditions, the neptunium(V) decontamination factor dropped to 13. The addition of nitrite to the 1A scrub solution also lowered the neptunium(V) decontamination factor from 100 to 25. This is in agreement with previously reported data in that a definite correlation existed between the presence of nitrite and the extraction by TBP of pentavalent neptunium from nitric acid solutions.

To investigate the behavior of neptunium(V) in the Purex process, feed solutions that contained neptunium tracer in the pentavalent state were prepared. The tracer solution was treated separately from the bulk of the feed, the neptunium being oxidized by addition of a slight excess of potassium permanganate (measured by persistence of a faint pink color for 15 min after heating the oxidant with tracer solution to 70 to 80°C for 1/2 hr). Addition of sodium nitrite to the tracer to a final concentration of

## HRP QUARTERLY PROGRESS REPORT

0.1 M reduced the neptunium to the pentavalent state. Feed solutions were then spiked with this tracer and put through 100 equilibrations in batch countercurrent runs simulating Purex 1A column conditions, with the difference that in some runs no uranium was present, and in others sodium nitrite was present in the scrub solution at a concentration of 0.05 M.

The results tabulated in Table 54 show that only a small fraction of the neptunium is extracted by TBP when the element is present in the pentavalent state. The presence of uranium in the feed appeared to decrease the extractability of neptunium(V).

The feed solution had a final activity level of  $10^6$  to  $10^7$  gross beta counts/min/ml, and the neptunium distribution throughout the system was determined by gross beta activities, since the tracer was prepared from nearly pure  $U^{238}$ . Neptunium beta activity, however, was also determined on the AP, AF, and AW solutions, since the uranium interfered in the AP solution, and the accumulated fission products interfered in the AW solution.

Table 54

### DECONTAMINATION FACTOR FOR NEPTUNIUM(V) IN THE PUREX 1A COLUMN

Standard Purex 1A flowsheet except where indicated

Batch countercurrent run for 100 equilibrations

RUN CONDITIONS	DECONTAMINATION FACTORS FOR NEPTUNIUM(V)
Standard Purex flowsheet	95
Standard Purex flowsheet	95
0.05 N $NaNO_3$ in scrub solution	25
No uranium in feed solution	13

**Dibutyl Butylphosphonate as an Extractant for Uranium from Uranyl Sulfate Solutions.** The results of a single equal-volume extraction of irradiated uranyl sulfate solution with dibutyl butylphosphonate (0.5 M solution in Amsco) are shown in Table 55. The uranium distribution coefficient under these conditions is about a factor of 3 higher than that for the TBP-Amsco extraction in which the uranyl sulfate is 3 M in  $HNO_3$ .

**Radiation Damage on Solvent Extraction.** A series of experiments has been started to study the susceptibility of TBP mixtures to radiation damage. Although certain impurities are known to affect solvent extraction processes employing TBP, there is very little evidence that shows the relation between radiation damage and formation of impurities that might affect process performance. Some experiments carried out with an electron beam in a Van de Graaff machine tended to show some effect on plutonium extraction and the stripping of fission products, but

Table 55

### EXTRACTION OF URANIUM FROM IRRADIATED URANYL SULFATE SOLUTION BY DIBUTYL BUTYLPHOSPHONATE

Conditions: One equal-volume equilibration

Solvent: 0.5 M dibutyl butylphosphonate in Amsco

Aqueous feed: 1.0 N  $HNO_3$ , 17 mg of irradiated uranium per milliliter

ELEMENT OR ACTIVITY	DISTRIBUTION COEFFICIENT, O/A
U	40
Gross $\beta$	0.03
Ru $\beta$	0.04
Np $\beta$	0.1
Total rare earth $\beta$	0.02

FOR PERIOD ENDING JULY 1, 1952

further work is necessary before a definite conclusion can be reached about the limitation imposed by radiation damage on solvent extraction processing.

Preliminary tests of solvent damage are being carried out in 6000 r/min/ml gamma radiation from a  $\text{Co}^{60}$  source. These results will be correlated on an energy basis (assuming approximately 100 ergs of absorption per roentgen) with those already secured with the Van de Graaff and with chemical tests now being developed. If justified by the results, further experiments will be carried out with the Chemistry Division's Van de Graaff, since much higher rates of energy dissipation can be secured in this type of irradiation. Consideration is also being given to the use of short-cooled dissolver solution to duplicate the conditions reached in actual chemical processing. The high activity of fission-product material, staying predominantly in the aqueous phase, may require some investigation of the interfacial surface conditions in actual chemical extraction. Tests with the  $\text{Co}^{60}$  source or a Van de Graaff will be basic in that any solvent change will be related to actual energy absorption within the organic phase.

A tracer chemical test for irradiated samples has been developed for the preliminary work to check on whether the extraction or stripping of plutonium or fission products is affected. By comparison of irradiated and control samples it will be possible to detect changes in the solvent that are capable of affecting tracer amounts of plutonium or fission product. Higher burnup irradiations may be made later if findings indicate that certain impurities build up in the solvent despite a cyclic washing process.

#### ECONOMIC COMPARISON OF $\text{UF}_6$ DISTILLATION AND TBP EXTRACTION FOR PROCESSING URANYL SULFATE FUEL

The results of an economic study indicate that uranium hexafluoride distillation compares favorably with tributyl phosphate extraction as a method of decontaminating uranium from a uranyl sulfate solution reactor. The saving indicated for dry fluoride processing is about one dollar per gram of plutonium produced. This conclusion is based on a comparatively untested dry fluoride flowsheet and is valid only insofar as the assumptions made in drawing up the flowsheet are realistic. However, the dry fluoride method of decontaminating uranium from a homogeneous plutonium producer appears attractive enough to warrant a comprehensive study to establish its desirability compared with the solvent extraction method. The basis of this economic comparison was 0.6 ton of uranium per day as 1.0 M  $\text{UO}_2\text{SO}_4$  in heavy water containing no plutonium. It was assumed that the plutonium would be removed continuously from the reactor and that the method of plutonium decontamination would be the same for either process.

The TBP extraction process was described in the last quarterly report. The fluoride distillation process consists of drying the uranyl sulfate to remove  $\text{D}_2\text{O}$ , roasting to  $\text{U}_3\text{O}_8$ , fluorinating to  $\text{UF}_6$  with  $\text{F}_2$  in  $\text{BrF}_3$ , and fractionating in two columns to produce decontaminated  $\text{UF}_6$ .

Table 56 summarizes the operating costs for these two processes. Labor costs were estimated to be the same for both processes, but chemical costs for fluoride distillation are more than twice those for TBP extraction because of the cost of fluorine, which

Table 56

## SUMMARY OF OPERATING COSTS FOR PROCESSING URANYL SULFATE SOLUTIONS

Basis: 0.6 ton of uranium per day as 1.0 M  $\text{UO}_2\text{SO}_4$  in  $\text{D}_2\text{O}$ , 2000 g of plutonium per day removed before  $\text{D}_2\text{O}$  recovery. Costs for plutonium processing site development, plant protection, and similar items not included

ITEM	METHOD OF EVALUATION	YEARLY COST	
		Fluoride Distillation	TBP Extraction
Labor	\$11,000/man/year	\$660,000	\$660,000
Chemical costs	Estimated from market prices	200,000	95,000
Utilities	Estimated from plant requirements	25,000	75,000
Maintenance	20% of equipment cost	70,000	117,000
Analytical service	\$5.00 per analysis	300,000	400,000
Amortization	16% of plant cost per year	670,000	840,000
Conversion of $\text{UNH}$ to $\text{UF}_6$	\$0.80/lb of uranium		320,000
Total cost per year		\$1,930,000	\$2,510,000
Cost per gram of Pu		\$3.20	\$4.20

was taken as \$0.80/lb. The analytical costs for fluoride distillation were estimated to be less than for TBP extraction because of the numerous feed analyses required for the extraction process. Utilities, maintenance, and amortization were estimated to be less for fluoride distillation, since this process requires smaller equipment. In addition, to make the processes equivalent, it is necessary to add \$0.80/lb of uranium to the solvent extraction process cost for the conversion of uranyl nitrate from

this process to uranium hexafluoride for recycling to an isotopic enrichment plant.

The total costs of uranium decontamination were \$3.20 per gram of plutonium for fluoride distillation and \$4.20/g for solvent extraction. It should be emphasized that these costs do not include plutonium decontamination or such items as site development and plant protection, and for this reason they do not represent the total cost of chemical processing.